Modelling and Control of Large Horizontal Axis Wind Power Plants

Mattsson, Sven Erik

1984

Document Version:
Publisher's PDF, also known as Version of record

Modelling and Control of Large Horizontal Axis Wind Power Plants

Sven Erik Mattsson

MODELLING AND CONTROL
OF LARGE HORIZONTAL AXIS WIND POWER PLANTS

av

SVEN ERIK MATTSSON

Civ ing, Mlm

Akademisk avhandling som för avläggande av teknologie doktorsexamen vid Tekniska fakulteten vid Universitetet i Lund kommer att offentligen försvaras i sal M:A, Lunds Tekniska Högskola, torsdagen den 28 februari 1985, kl. 10.15.

Organization
LUND UNIVERSITY
Department of Automatic Control
Box 118
S 221 00 Lund, Sweden

Document name
DOCTORAL DISSERTATION

Date of issue December 1984

CODEN: LUTFD2/(TFRT-1026)/1-176/(1984)

Author(s)
Sven Erik Mattsson

Sponsoring organization
The National Swedish Board for Energy Source Development (NE) and Sydkraft AB

Title and subtitle

Modelling and Control of Large Horizontal Axis Wind Power Plants

Abstract

In order to make wind power competitive in a large utility grid it is important that the wind power plants are cheap and reliable. It is a nontrivial problem to choose the best design. The objective of this thesis is to give a global picture of the control problem of large horizontal axis wind power plants.

The system dynamics and the wind characteristics are discussed and explained. An account of the fundamental properties of horizontal axis wind power plants are given. A modular simulation model is presented. Measured data are analysed and models are identified which show good agreement with models derived from first principles.

After the analysis of the system dynamics, control is considered. The control objectives are discussed. The possibilities of compensating for wind speed variations are investigated. Basic factors such as control authority and measurements as well as interaction between process design and control design are discussed. A design procedure for pitch angle control is proposed. It is based on the LQG framework and considers wind properties and measurement noise explicitly.

Key words

Wind power, Modelling, Simulation, Identification, Control Design.

Classification system and/or index terms (if any)

Supplementary bibliographical information

Language English

ISSN and key title

ISBN

Recipient's notes

Number of pages 176

Price

Security classification

Distribution by (name and address)

Signature Sven Erik Mattsson Date December 12th, 1984

Organization	Document name
LUND UNIVERSITY Department of Automatic Control Box 118 S 221 00 Lund, Sweden	DOCTORAL DISSERTATION
	Date of issue December 1984
	CODEN: LUTFD2/(TFRT-1026)/1-176/(1984)
Author(s) Sven Erik Mattsson	Sponsoring organization The National Swedish Board for Energy Source Development (NE) and Sydkraft AB

Title and subtitle

Modelling and Control of Large Horizontal Axis Wind Power Plants

Abstract

In order to make wind power competitive in a large utility grid it is important that the wind power plants are cheap and reliable. It is a nontrivial problem to choose the best design. The objective of this thesis is to give a global picture of the control problem of large horizontal axis wind power plants.

The system dynamics and the wind characteristics are discussed and explained. An account of the fundamental properties of horizontal axis wind power plants are given. A modular simulation model is presented. Measured data are analysed and models are identified which show good agreement with models derived from first principles.

After the analysis of the system dynamics, control is considered. The control objectives are discussed. The possibilities of compensating for wind speed variations are investigated. Basic factors such as control authority and measurements as well as interaction between process design and control design are discussed. A design procedure for pitch angle control is proposed. It is based on the LQG framework and considers wind properties and measurement noise explicitly.

Key words

Wind power, Modelling, Simulation, Identification, Control Design.

Classification system and/or index terms (if any)

Supplementary bibliographical information	Language English
ISSN and key title	ISBN
Recipient's notes	Number of pages 176 / Security classification / Price

Distribution by (name and address)

TABLE OF CONTENTS

I
S
V

1. INTRODUCTION

This thesis considers control of large horizontal axis wind power plants connected to large utility grids. The objective is to give a global picture of the control problem. The following questions are investigated:

1. Which properties and limitations are fundamental and common to all horizontal axis wind turbines?
2. Which properties and limitations are design dependent?
3. Which properties can be influenced by control system design?
4. What are the control objectives and is it possible to fulfil them?

There are a number of different types of horizontal axis wind turbines in operation and more are under construction. A survey is given in Koeppl (1982). The characteristics of the MOD-2, the WTS-3, the WTS 75 and the Growian I are referenced in the discussion. A listing of their basic characteristics is given in Appendix A.

The thesis is organized as follows. The dynamics of horizontal axis wind power plants is analysed and explained in Chapter 2. First, simple physical models are considered in order to explain the basic dynamics. Then higher order dynamics of the different parts of the plant is considered. A modular simulation model is presented in Appendix B. When modelling, it is important to know the purpose of the model. Our purpose is control design. The wind is a source of both joy and sorrow. This power source cannot be controlled in any way and it is the major source of disturbances. It is a basic control objective to compensate for the large, rapid and random variations in the wind. Thus Chapter 2 concludes with models for design of compensators for the wind variations. The characteristics of the wind are considered in Chapter 3. Measurements from the WTS-3 are analysed in Chapter 4. Different models are identified and compared with physical models. Control is considered in Chapter 5. First, the control objectives are discussed. Then the possibilities to compensate for the wind speed variations are investigated. Basic factors like control authority and measurements as well as interaction between process design and control design are discussed. The results of the investigation are summarized in Chapter 6.

2. SYSTEM DYNAMICS

A suitable characterization of the system dynamics of horizontal axis wind power plants should tell how energy is transferred from the wind to the utility grid. For reasons of safety it is also necessary to consider the structural dynamics. A characterization of the system dynamics can be given in different ways. A modular simulation model is presented in Appendix B. In this chapter a more analytical presentation is given in order to explain the dynamics.

Several modes of operation can be identified: startup mode, power generation mode, shutdown mode and emergency modes. In the startup mode the turbine is accelerated and the generator is connected to the utility grid. In the power generation mode power is extracted from the wind and transferred to the utility grid. In the shutdown mode the generator is disconnected and the turbine is decelerated. The system is in an emergency mode if malfunctions have been detected. In an emergency mode backup systems are invoked to provide for a safe shutdown. The power generation mode will be of principal consideration here. A plant will hopefully operate in this mode during the major part of its lifetime. This mode has the most difficult and the most interesting control problems.

A wind power plant may be viewed as consisting of an aerodynamical part and an electrical part, which are connected by a drive train. The aerodynamical part is influenced by the wind and consists of the wind turbine, the nacelle and the tower. The electrical part is connected to the utility grid and consists of the generator. The drive train which connects the turbine and generator consists of shafts and gearboxes.

The basic wind characteristics are summarized in Section 2.1. A more detailed discussion is given in Chapter 3. The investigation of the system dynamics starts in Section 2.2 by considering simple models in order to understand the behaviour of wind turbine generators. Higher order dynamics and the validity of the simple models for the aerodynamical part are discussed in Section 2.3 and for the electrical part in Section 2.4. The dynamics of interest in designing compensators for wind speed variations is summarized in Section 2.5.

2.1 Basic Wind Characteristics

It is convenient to view the wind speed sensed by the wind turbine as consisting of one quasi-constant part and one varying part. The quasi-constant part represents the mean wind speed over 10 minutes and the varying part the turbulence. The mean wind speed over the turbine is important, but also the spatial variation induces important variations in the driving aerodynamical torque.

Most wind models use the concepts of a stochastic process. An introduction on stochastic processes satisfactory for our purposes is given in Åström (1970). For clarity some definitions are listed below.

Some Stochastic Concepts

The concept of spectral density (power spectrum) is important. Unfortunately, different definitions are used in the literature. The placement of the factor 2π in the Fourier transform varies. We will use the following definition. Let $r(\tau)$ be the covariance function of a continuous time, weakly stationary stochastic process. Then $r(\tau)$ and the spectral density $\phi(\omega)$ are related as

$$\begin{cases} \phi(\omega) = \dfrac{1}{2\pi} \displaystyle\int_{-\infty}^{\infty} e^{-i\omega\tau}\, r(\tau)\, d\tau \\ r(\tau) = \displaystyle\int_{-\infty}^{\infty} e^{i\omega\tau}\, \phi(\omega)\, d\omega \end{cases} \tag{2.1}$$

The concept of white noise is a useful idealization. White noise has constant spectral density; i.e. $\phi(\omega)$ = constant. If $\phi(\omega) = c/(2\pi)$, we have formally that white noise has the covariance function $r(\tau) = c\delta(\tau)$, where $\delta(\tau)$ is the Dirac delta function. The parameter c is in the following called the noise intensity.

Mean Wind Speed over the Turbine Area

Let the mean wind speed U_0 over the turbine be the sum of $\bar{U}_0$ and ΔU_0, where $\bar{U}_0$ is the mean of U_0. A simple and useful model for ΔU_0 is given by

$$\Delta\dot{U}_0 = -\Delta U_0/T_w + \sigma_w\sqrt{2/(r_w T_w)}\; w \tag{2.2}$$

where w is Gaussian white noise with zero mean and the noise intensity r_w. The time constant T_w is of the order of 5 - 30 seconds and the standard deviation σ_w

of ΔU_0 is in the order of 5 - 20% of $\bar{U}_0$. Model (2.2) gives the spectral density ϕ_{U0} of ΔU_0 as

$$\phi_{U0}(\omega) = \sigma_w^2 \cdot \frac{1}{\pi} \cdot \frac{T_w}{1 + \omega^2 T_w^2} \qquad (2.3)$$

Effects of Spatial Variations

The spatial variation of the wind speed over the turbine area causes nonnegligible fluctuations in the driving aerodynamical torque. Let the rotational frequency of the turbine be P. If the turbine has two blades these fluctuations appear in the spectrum as narrow-band spikes at integer multiples of 2P. The most significant fluctuation is that at 2P. For a fixed blade angle the amplitude of the 2P variation in the driving aerodynamical torque typically is 10 - 30% of the rated turbine torque. There are also spikes at odd integer multiples of P, but they are much smaller. There are three major sources of these spikes. Firstly, the mean wind speed varies with altitude (wind profile). Secondly, the tower blocks the airflow for a rotating blade when it passes the tower. Thirdly, the turbulence contributes also to these fluctuations. The blades chop across the eddies and experience them as high frequency fluctuations.

2.2 Basic System Dynamics

In this section simple models are considered in order to understand the behaviour of horizontal axis wind power plants. Higher order dynamics and the validity of the simple models are discussed in Sections 2.3 and 2.4.

The dynamics of the drive train with the large turbine and the electrical coupling to the grid give a wind power plant its basic dynamic characteristics.

The equation of motion for the turbine is

$$J_t \ddot{\psi} = T - T_s \qquad (2.4)$$

where ψ is the angular position of the turbine and J_t is the turbine inertia. The torque T is the driving aerodynamical torque and T_s is the reaction torque from

the shaft. The equation of motion for the generator is

$$J_g \ddot{\theta}_m = T_m - T_e - T_{el} \tag{2.5}$$

where θ_m is the angular position of the generator rotor and J_g is the rotor inertia. The torque T_m is the mechanical torque driving the generator rotor, T_e is the developed electrical torque and T_{el} represents electrical torque losses in the generator. The drive train from the turbine to the generator usually has a step up gear. The inertia of the drive train can be neglected. The important features are the gearing and the torsional compliance. We can consider the shaft between the gearbox and the generator as being rigid and thereby transform all the compliance of the drive train to the shaft between the turbine and the gearbox. If the step up ratio of the gear is N_g then

$$T_m = T_s/N_g \tag{2.6}$$

and the torsion γ of the drive train is

$$\gamma = \psi - \theta_m/N_g \tag{2.7}$$

The compliance of the drive train can be represented by a spring coefficient K_s and a damping coefficient D_s, which gives

$$T_s = K_s\gamma + D_s\dot{\gamma} \tag{2.8}$$

The models for the torques T_e and T_{el} depend on the generator type and are discussed further in this section. In proceeding it is convenient to make some simple transformations and relate the description to the electrical system. To facilitate comparisons between different wind power systems and also to other kinds of power systems, it is convenient to introduce a base T_B for the torques as $T_B = S_B/\omega_0$, where S_B is the rated apparent power of the generator and ω_0 is the synchronous electrical angular frequency. There may be an upgearing between the mechanical rotational speed of the generator and the electrical angular frequency, so that the rated generator speed $\dot{\theta}_{m0} = \omega_0/N_e$. The gear ratio N_e is for example p/2 for a synchronous generator with p generator poles.

Introduce

$$\begin{cases} \psi_e = N_g N_e \psi & \theta = N_e \theta_m \\ t_a = T/(N_g N_e)/T_B & t_m = T_m/N_e/T_B \\ t_e = T_e/N_e/T_B & t_{el} = T_{el}/N_e/T_B \\ j_t = J_t/(N_g N_e)^2/T_B & j_g = J_g/N_e^2/T_B \\ k_s = K_s/(N_g N_e)^2/T_B & d_s = D_s/(N_g N_e)^2/T_B \end{cases} \tag{2.9}$$

and

$$\gamma_e = \psi_e - \theta \tag{2.10}$$

then the equations of motion can be written as

$$\begin{cases} j_t \ddot{\psi}_e = t_a - k_s \gamma_e - d_s \dot{\gamma}_e \\ j_g \ddot{\theta} = k_s \gamma_e + d_s \dot{\gamma}_e - t_e - t_{el} \end{cases} \tag{2.11}$$

The generated power P_e is given by

$$P_e = \omega_{bus} t_e S_B \tag{2.12}$$

where ω_{bus} is the angular frequency of the bus. Some numerical values are given in Table 2.1. When discussing the electrical torque it is convenient to introduce the angle δ defined as

$$\delta = \theta - \theta_{bus} \tag{2.13}$$

where $\dot{\theta}_{bus} = \omega_{bus}$.

Table 2.1: Numerical values for some wind power systems.

Wind power system	j_t [s^2/rad]	j_g [s^2/rad]	k_s [1/rad]	d_s [s/rad]
MOD-2	0.083	0.0028	0.065	0.005
WTS-3	0.033	0.0038	0.050	0.020
WTS 75	0.067	0.0035	6.2	*)

*) The value is small, but not known.

The driving aerodynamical torque T is a nonlinear function of the pitch angle, the oncoming wind and the turbine speed. Turning of the blades or parts of them around their longitudinal axes thus modifying the pitch angle makes it possible to control the power generation. The properties of T are discussed in Section 2.3. The aerodynamical damping is low, because the blades are designed to give maximum power and minimum losses. For the WTS-3 the aerodynamical damping coefficient $-\partial t_a/\partial \dot{\psi}_e$ is 0.002 s/rad at 14 m/s and increases to 0.01 s/rad at 26 m/s. Compare with the damping coefficient d_s which is 0.02 s/rad. The aerodynamical damping of the turbine oscillation will for simplicity be neglected in this section.

Turbine Inertia

Hinrichsen (1981) points out that the per unit turbine inertia j_t is very high because

1. The low energy density of wind leads to a large rotor diameter.
2. The tip speed/wind speed ratio must lie within a narrow range to achieve good efficiency. This leads to turbine speeds between 15 and 50 rpm.

The per unit inertia j_t of a typical wind power plant is about ten times greater than the per unit inertia of typical hydro or steam turbines.

Synchronous Generator

The MOD-2 and the WTS-3 have a synchronous generator with four poles. The dynamics of synchronous generators is discussed in Section 2.4. Here a simple but useful model for the electrical torque will be given. Assume that the generator is connected to an infinite bus. Linearized models for the electrical torques are then given by

$$\begin{cases} \Delta t_e = k_e \Delta\delta \\ \Delta t_{el} = d_e \Delta\dot{\delta} \end{cases} \tag{2.14}$$

where Δ denotes deviation from a stationary operating point. The assumption of infinite bus implies that $\omega_{bus} = \omega_0 = \text{constant}$, which means that $\Delta\theta = \Delta\delta$. The electrical coupling given by $\Delta t_e + \Delta t_{el}$ is equivalent to a mechanical coupling consisting of a spring and a damper.

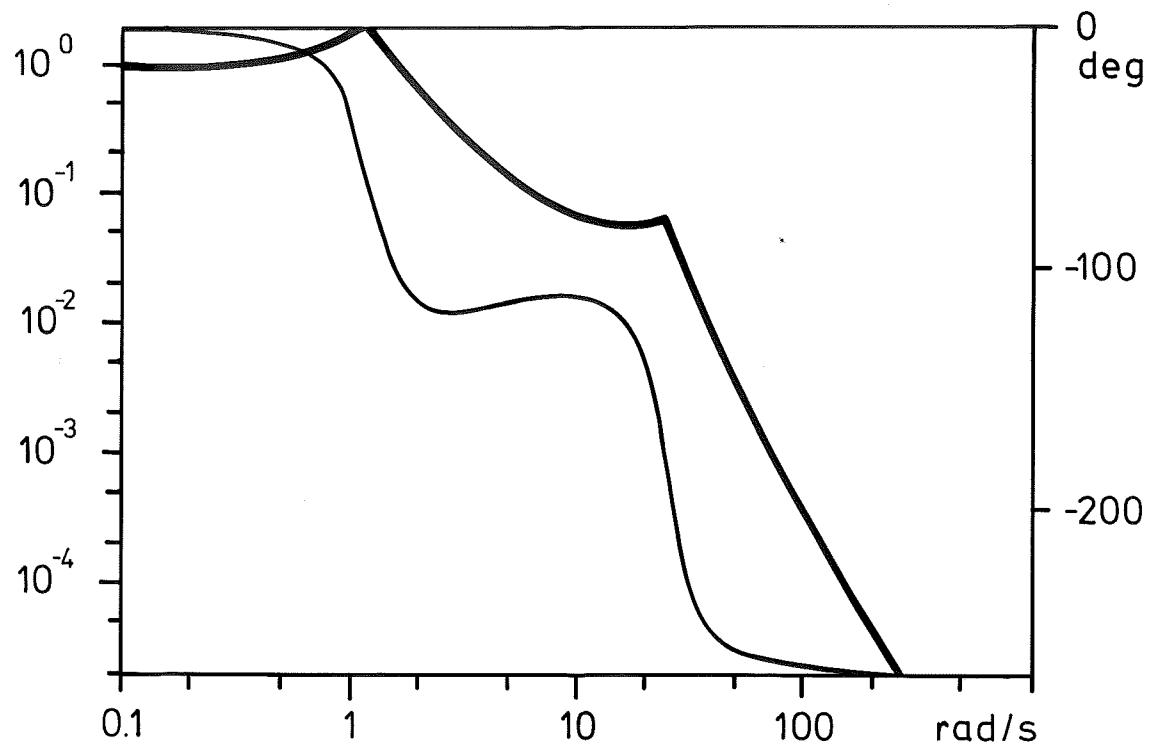

Figure 2.1: Bode plot of the transfer function (2.16) from Δt_a to Δt_e for the WTS-3.

The models (2.11), (2.13) and (2.14) give the characteristic polynomial P(s)

$$P(s) = j_t j_g s^4 + [j_t(d_s+d_e)+j_g d_s]s^3 + [j_t(k_s+k_e)+j_g k_s+d_s d_e]s^2 + [d_s k_e+k_s d_e]s + k_s k_e \qquad (2.15)$$

In the frequency domain Δt_e, $\Delta\gamma_e$, $\Delta\psi_e$ and $\Delta\theta$ are given by

$$\Delta t_e(s) = \frac{k_e(d_s s+k_s)}{P(s)} \Delta t_a(s) \qquad (2.16)$$

$$\Delta\gamma_e(s) = \frac{j_g s^2+ d_e s + k_e}{P(s)} \Delta t_a(s) \qquad (2.17)$$

$$\Delta\psi_e(s) = \frac{j_g s^2+ (d_s+d_e)s + k_s+k_e}{P(s)} \Delta t_a(s) \qquad (2.18)$$

$$\Delta\theta(s) = \frac{d_s s + k_s}{P(s)} \Delta t_a(s) \qquad (2.19)$$

With k_e = 2.3 rad^{-1} and d_e = 0.017 s/rad, the characteristic polynomial (2.15) gives for the WTS-3 poles in -0.3 ± 1.2i and -4.8 ± 24i. The mode associated with the first pole pair has the lowest natural frequency. The mode will be referenced as the first torsional mode. Its natural frequency is 1.2 rad/s (= 0.47 P) and its relative damping is 0.25. The mode is approximately turbine oscillations against the electrical system. The mode associated with the pole pair -4.8 ± 24i will be referenced as the second torsional mode. Its natural frequency is 25 rad/s (= 9.5 P) and its relative damping is 0.20. This mode is approximately generator oscillations against the synchronous power system. Note that more than half of the damping of the second mode is due to d_s, since the damping of the drive train and the electrical coupling for this mode work in parallel. The MOD-2 has the same modes and their natural frequencies are 0.88 rad/s and 26 rad/s (Hinrichsen and Nolan (1980)).

The first torsional mode is also called the soft shaft mode. This mode is important. It gives the MOD-2 and the WTS-3 their basic dynamic characteristics. It is excited by the wind and blade angle changes. It has low damping. However, the soft shaft also has its merits. Figure 2.1 shows that the large turbine and the soft shaft act as a low pass filter. Rapid wind variations are prevented from going through the system into the utility grid. This filtering effect is important. As pointed out in Section 2.1 the variations in the wind speed over the turbine disc cause significant fluctuations with frequencies being multiples of 2P (5.2 rad/s). Figure 2.1 shows that these disturbances are attenuated drastically by the soft shaft.

The soft shaft also prevents small electrical disturbances like frequency-, voltage- and impedance fluctuations in the utility grid from influencing the turbine. The angle δ is at normal operation typically 20 - 30° and to keep the synchronism it must be within ±90°. For the WTS-3 the torsion γ_e of the drive train is about 1000° at rated operation. Thus small electrical disturbances do not have the possibility to build up any significant shaft torques.

For a wind turbine system with a soft shaft, mechanical compliance is much greater than electrical compliance. This implies that shaft torque amplification during electrical switching and faults is less severe than in conventional turbine generators. Bracing of generator windings, not strength of shafts, is the limitation during electrical disturbances. The soft shaft also reduces the accuracy required

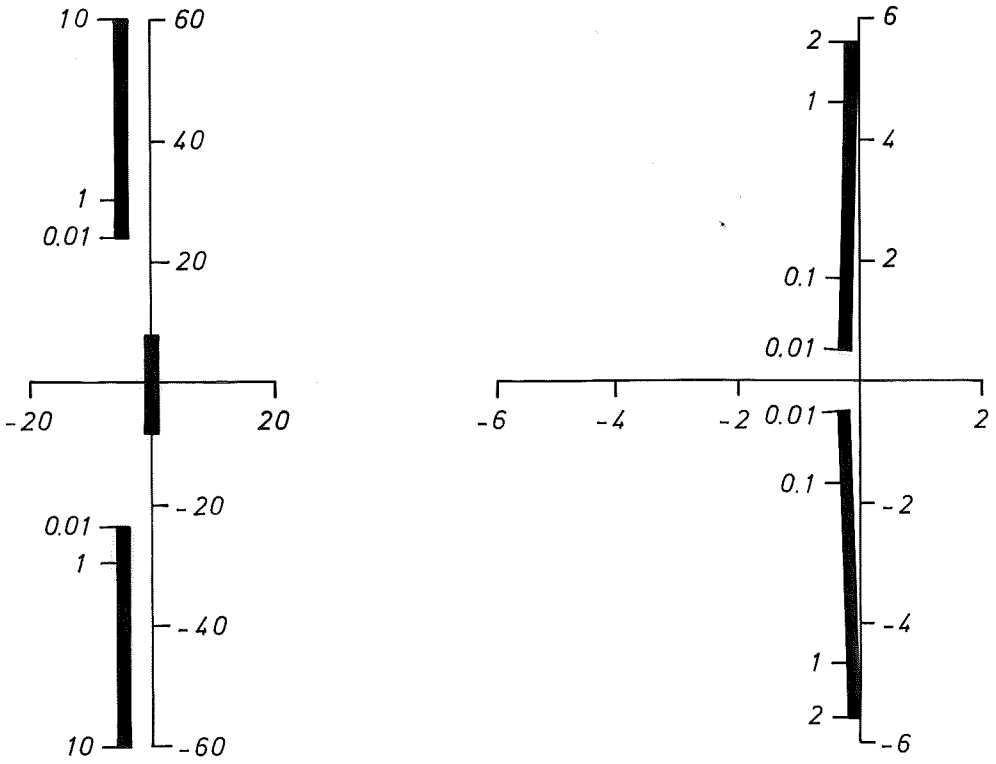

Figure 2.2: Root-locus of (2.15) with respect to k_s [rad^{-1}] for the WTS-3.

for matching voltage, speed and phase angle during synchronization. The study by Hinrichsen and Nolan (1980) shows that a well designed wind turbine generator with a soft shaft will perform equally well in single and multi-machine applications, since turbine and generator are transiently decoupled by the soft shaft.

The second mode is of great importance for the generator control. It dominates the response to small and rapid electrical disturbances. In conventional turbine generators this is generally the lowest mode and the only one considered.

In the models discussed above the inertia of the gearbox is neglected. For the MOD-2, the WTS-3 and the WTS 75 the per unit inertia of the gearbox is less than 0.0003 s^2/rad. Hinrichsen and Nolan (1980) report that for the MOD-2 there is a natural mode in which the rotating part of the gearbox oscillates through the high speed shaft against the generator rotor with 550 rad/s. They state that this mode can be neglected because it is hard to excite it. Simulations made by ASEA (1980) show that this is also the case for the WTS-3.

Table 2.1 shows that the coupling between the turbine and the generator is 100 times stiffer for the WTS 75 than for the MOD-2 and the WTS-3. The MOD-2 and the WTS-3 have deliberately designed soft drive trains. The MOD-2 has a quill shaft. The planetary gearbox of the WTS-3 is not rigidly mounted, but it is suspended with springs and hydraulic dampers, which is equivalent to a torsionally soft shaft. Figure 2.2 shows the root-locus with respect to k_s for the WTS-3. For $k_s = 5$ rad^{-1} the WTS-3 would have poles in -0.14 ± 6.7i and -5 ± 45i which means that there would be no filtering effect for the 2P (5.2 rad/s) disturbances.

Induction Generator

The WTS 75 wind power system has an induction generator with four poles. An induction generator influences the first torsional mode in a more complex way than a synchronous generator. Statically the electrical torque Δt_e is proportional to $\Delta\dot{\delta}$, with the mechanical interpretation of the coupling to the grid being a damper. However, dynamically the situation is somewhat more complex. All electrical time constants cannot be neglected. The electrical torque Δt_e can be modelled as (linearized around a stationary operating point)

$$T_{te}\Delta\dot{t}_e + \Delta t_e = d_{te}\Delta\dot{\delta} \qquad (2.20)$$

The time constant T_{te} and the static gain d_{te} vary with the operating point and they are typically halved when produced power is increased from zero to the rated. They also depend on the generator resistances and inductances. Typical values are T_{te} = 0.1 - 0.2 s and d_{te} = 0.1 - 0.4 s/rad. The electrical torque t_{el} is neglected.

The models (2.11) and (2.20) give the characteristic polynomial P(s) (the integrator giving $\Delta\theta$ is excluded)

$$P(s) = j_t j_g T_{te} s^4 + [j_t j_g + (j_t + j_g) d_s T_{te}] s^3 + [j_t d_{te} + (j_t + j_g)(d_s + k_s T_{te})] s^2$$
$$+ [(j_t + j_g) k_s + d_s d_{te}] s + k_s d_{te} \qquad (2.21)$$

In the frequency domain Δt_e, $\Delta\gamma_e$, $\Delta\dot{\psi}_e$ and $\Delta\dot{\theta}$ are given by

$$\Delta t_e(s) = \frac{d_{te}(d_s s + k_s)}{P(s)} \Delta t_a(s) \qquad (2.22)$$

$$\Delta\gamma_e(s) = \frac{j_g T_{te} s^2 + j_g s + d_{te}}{P(s)} \Delta t_a(s) \qquad (2.23)$$

$$s\Delta\psi_e(s) = \frac{j_g T_{te} s^3 + (j_g + d_s T_{te}) s^2 + (d_s + k_s T_{te} + d_{te}) s + k_s}{P(s)} \Delta t_a(s) \qquad (2.24)$$

$$s\Delta\theta(s) = \frac{d_s T_{te} s^2 + (T_{te} k_s + d_s) s + k_s}{P(s)} \Delta t_a(s) \qquad (2.25)$$

Figures 2.3 - 2.5 show the root-locus with respect to k_s for some pairs of T_{te} and d_{te}. The damping coefficient d_s of the drive train is set to zero to illustrate the damping effects of the induction generator. The figures show that the damping of the pole pair with the greater modulus then becomes very low for large k_s. For a stiff drive train the mode associated with this pole pair is approximately the oscillation of the generator against the drive train. The damping of the drive train is thus important for this mode. The natural frequency for a stiff drive train is high compared to electrical time constant T_{te} and the coupling to the grid becomes less important.

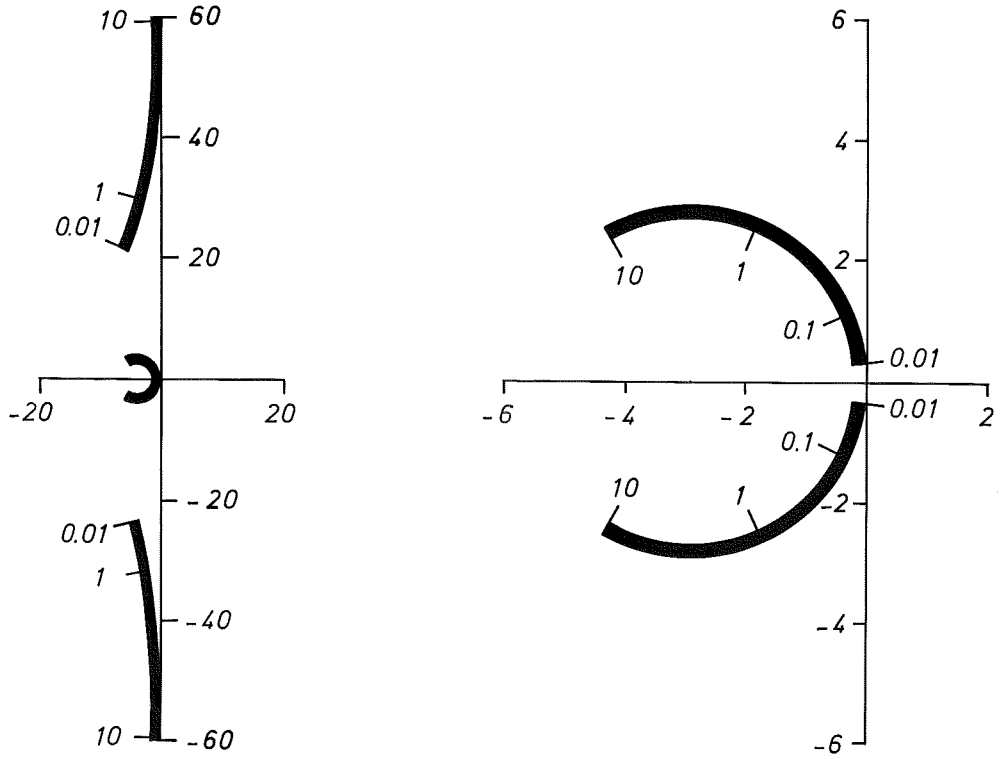

Figure 2.3: Root-locus of (2.21) with respect to k_s [rad^{-1}] for the WTS 75 when d_{te} = 0.2 s/rad, T_{te} = 0.1 s and d_s = 0.

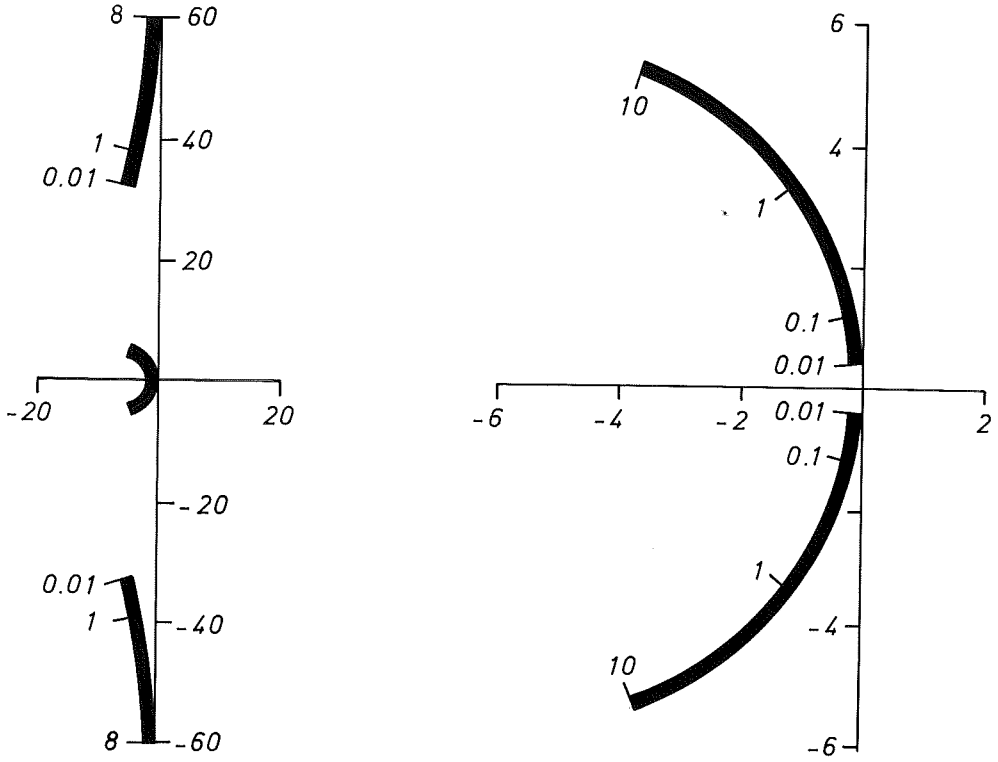

Figure 2.4: Root-locus of (2.21) with respect to k_s [rad^{-1}] for the WTS 75 when d_{te} = 0.4 s/rad, T_{te} = 0.1 s and d_s = 0.

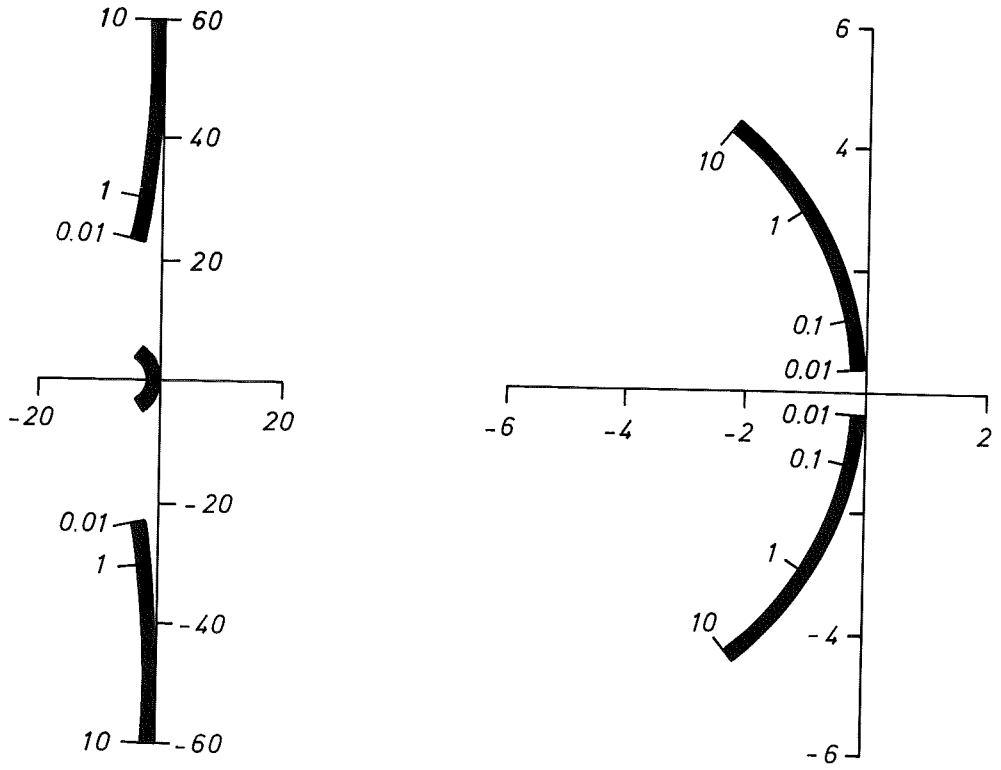

Figure 2.5: Root-locus of (2.21) with respect to k_s [rad^{-1}] for the WTS 75 when d_{te} = 0.4 s/rad, T_{te} = 0.2 s and d_s = 0.

The two branches closest to origin in Figures 2.3 - 2.5 show that also when an induction generator is used there is a basic complex pole pair. Consider now this basic pole pair. The relative damping is low when the shaft is soft but increases with increasing k_s. The difference between the root-loci in Figures 2.4 and 2.5 is that they are calculated for different time constants T_{te}. The pole pairs lie on the same arc in both figures. If the shaft is soft they are almost identical. If the shaft is stiff the pole pair moves moves closer to origin with increasing T_{te}. The difference between the root-loci in Figures 2.3 and 2.4 is that they are calculated for different d_{te}. The figures show that the pole pair moves from origin and the relative damping decreases with increasing d_{te}.

Other Generator Systems

The generators of the MOD-2, the WTS-3 and the WTS 75 have four poles and gearboxes are used to step-up the turbine speed. However, the gearbox is an expensive part, typically amounting to 7 - 10% of the costs for a delivered unit. Nygren, Grop and Pettersson (1981) suggest a low speed generator with 216 poles. This means that j_g is in the magnitude of 10^{-7} s^2/rad. The pole pair of the first torsional mode is insensitive to this decrease of j_g. Then the simple model gives poles with a modulus greater than 60.

When a synchronous generator or an induction generator is used the turbine must operate at an almost constant speed and the possibilities of controlling generated power at the generator are negligible. Pitch angle control is the only means of controlling generated power for these systems. Thyristors can be used to control the power output if the difference between the power input at the turbine and the power output to the grid can be absorbed elsewhere. The large turbine inertia can be used as an energy storage, if the turbine speed is allowed to vary. The electrical system must supply the electrical power to the network at power system frequency, but to obtain this it is not necessary to operate the turbine with constant speed. A frequency converter can be used to give the power output from a generator operating with variable speed a constant frequency. For example, Brown Boveri (Schweickardt and Suchanek (1982)) has such systems for wind power plants. The generator speed is typically allowed to vary in the range 4 - 130% of synchronous speed. The system contains a synchronous generator, a static frequency converter and a power transformer. Raina and Malik (1983) suggest a system with an induction generator, a rectifier and an inverter. The induction machine is excited by a capacitor across each of

its terminals. The voltage at the machine terminals are kept constant by a thyristor controlled inductor.

Another approach is to use a variable frequency exciter and to control this in such a way that power output from the generator has constant frequency. The Growian I has a generator of this type. It is a doubly-fed generator and the generator speed is allowed to vary ±15% of synchronous speed. Leonhard (1979) describes the control scheme in the following way

> "Since it is based on the magnitude and direction of a flux vector, established by direct or indirect measurement, it is called field-oriented control. The magnitude, frequency and phase of the input currents (in this case the rotor currents) are generated in such as to give the rotor MMF-vector a prescribed orientation in relation to the main flux vector (which itself is a function of the rotor currents). The longitudinal component of the rotor current vector changes the terminal voltage, hence the reactive power, and through a substantial lag the magnitude of the main flux; the quadrature component of the rotor current vector immediately affects the torque and active power."

2.3 Aerodynamical Part

A wind turbine is a complex construction with several degrees of mechanical freedom. The rotation of the turbine around its axis is the main motion. The rotation of the nacelle and the turbine around the axis of the tower is called yawing. The blades may or may not move out of plane of rotation depending on how they are attached to the turbine shaft. To allow pitch control, the blades or parts of them can be turned around their longitudinal axes.

A survey of rigid body and elastic body motions is given below and the equations of motion are given in Appendix B.1. The structural dynamics and stability of wind power plants are thoroughly considered in Stoddard (1978).

Torque and Thrust

The driving aerodynamical torque T and the thrust F acting on the turbine can be obtained by applying static and two-dimensional airfoil theory. The driving aerodynamical torque acting on a blade at the distance s from the rotor axis can, neglecting profile drag, be expressed as

$$\begin{cases} dT_i = 0.5\ \varrho_a s\ c\ \{U_d^2+s^2\dot{\psi}^2\}\ (\sin\alpha)\ C_L(\alpha+\beta)\ ds \\ \\ \alpha = \arctan U_d/(s\dot{\psi}) \end{cases} \qquad (2.26)$$

where ϱ_a is the density of air and c the local chord length. The variable U_d denotes the wind speed at the section of the blade. The pitch angle β denotes the orientation of the cross section with respect to the longitudinal axis of the blade. It is a function of s, if the blade is twisted. The lift coefficient C_L is a function of the angle of attack $\theta = \alpha+\beta$. Typically C_L increases almost linearly to a maximum and then there is an abrupt decrease. This phenomenon is called stalling. The flow goes from laminar to turbulent flow. Analytical expressions for T and F below stalling are given in Appendix B.1. Figure 2.6 and Figure 2.7 show T and F for the WTS-3 as functions of the pitch angle at 3/4 radius ($\beta_{3/4}$) for different speeds U_0 of the oncoming wind. The expressions given in Appendix B.1 were used to calculate T and F. The implications for pitch angle control are discussed in Chapter 5.

The blade servos for pitch angle control can be electric or hydraulic. The WTS-3 has full span pitch control and the servo is designed as a position servo with a time constant of 0.4 s. However, the servo speed is limited to 4°/s (Svensson and Ulén (1982)).

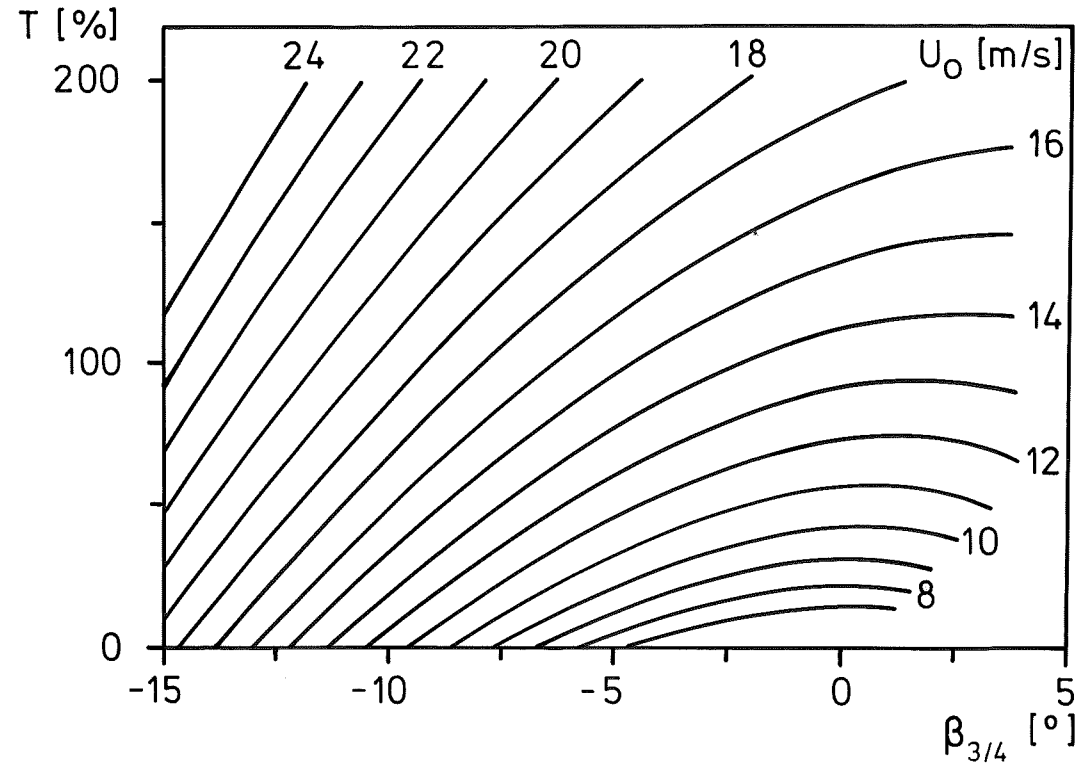

Figure 2.6: The driving aerodynamical torque T of the WTS-3 versus the pitch angle $\beta_{3/4}$ for different wind speeds U_0 at synchronous turbine speed.

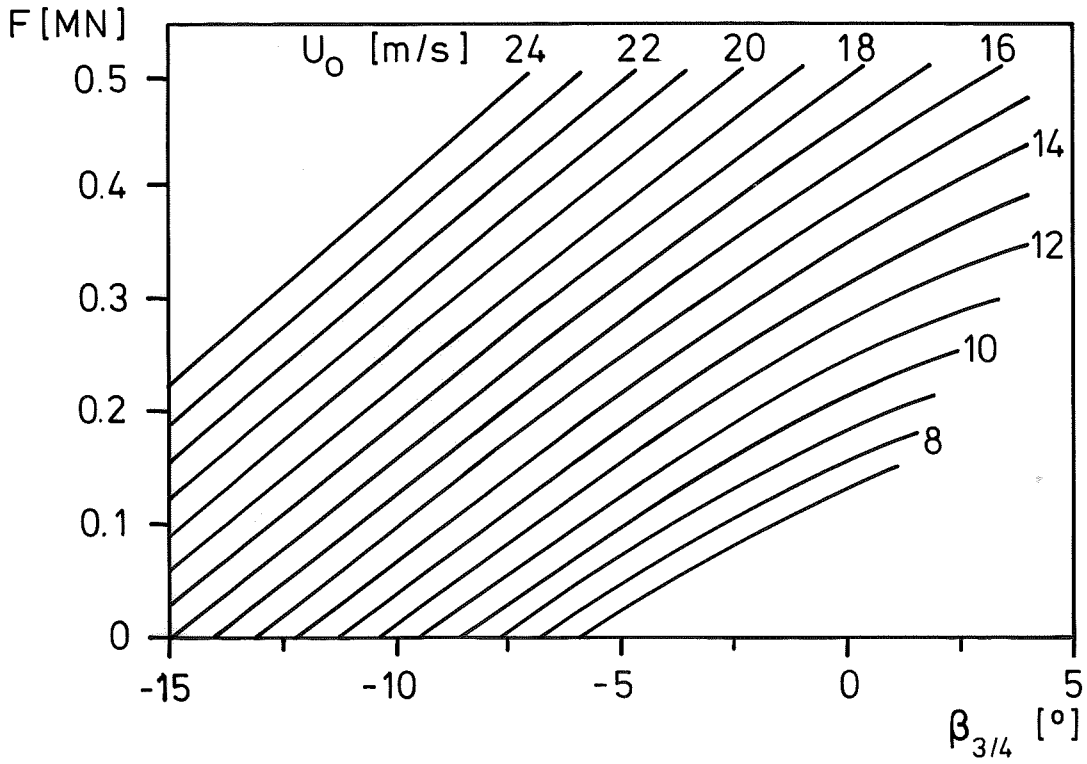

Figure 2.7: The aerodynamical thrust F of the WTS-3 versus the pitch angle $\beta_{3/4}$ for different wind speeds U_0 at synchronous turbine speed.

Orientation

A wind turbine can be designed for upwind or downwind operation. In upwind operation the rotor must be aligned against the wind by active yaw control. In downwind operation the free yaw behaviour may be stable. The WTS-3 turbine was designed for free yaw operation, but it turned out to be unstable. In free yaw operation it turns out of the wind with a yaw rate of 0.3 - 0.4°/s. The WTS-3 is now provided with an active yaw mechanism which can turn the nacelle with a maximum speed of 1.2°/s. The existing methods are deficient in their ability to predict free yaw behaviour in horizontal axis wind turbines (Thresher (1981) p. 445). Ganander and Olsson (1983) are currently considering these problems. A preliminary validation of their model shows good agreement with measured data.

The turbine axis may be tilted out of the horizontal plane. One reason is to make the turbine disc more orthogonal to the streamlines. Another reason is to increase the clearance between blades and tower so that the effect of the tower blockage is minimized. The axis of the WTS 75 is for this reason inclined 10°.

The blades can be attached to the turbine shaft in different ways. Three typical cases are

1. Hinged hub. The blades are hinged to the main shaft, so that each blade independently can move out of the plane of rotation.
2. Teeter (pendulum) hub. The blades are rigidly connected to each other and hinged to the main shaft, so that they can teeter orthogonal to the plane of rotation.
3. Rigid hub. The blades are rigidly mounted to the main shaft.

The hinged hub and teeter hub give extra degrees of freedom in orientating the rotor disc in an optimal way. It is important to decrease the loads on the blades and the hub. The heavy bending moments in the root sections of the blades are critical. The bending moments due to thrust and centrifugal forces depend on the angle between the blade and the plane of rotation, called the cone angle. Fortunately, they are in opposition and there is a specific cone angle for which they balance one another. For the hinged hub the bending moment at the blade root is zero. For the teeter and rigid hub the bending moments are substantially relieved if the angle between the blades are chosen such that the wind force and centrifugal force are in balance at the design wind speed.

Gravity, wind profile, tower blockage and turbulence generate forces and torques on the blades that vary considerably over the rotor area. A hinged or teeter hub allows the blades to yield and thus relieves them of extreme loads resulting from wind variations over the rotor area. Variations in the driving torque are also attenuated.

Hinged hubs and teeter hubs can be designed such that the blades also turn along their longitudinal axes when they move orthogonal to the plane of rotation. This introduces a local feedback by making the pitch angle vary with the angle to the plane of rotation. This feature is typically employed to reduce the motions out of the plane of rotation. It also gives flexibility in blade tuning to avoid possible structural resonances. See Perkins and Jones (1981).

Elastic motions

The bending motions of the blades have a wide nomenclature The bending motion out of plane of rotation is called flapping, flapwise, flatwise etc. and the bending in plane is called lead-lag, chordwise, edgewise etc. Table 2.2 gives some typical values of their natural frequencies. Sullivan (1981) discusses blade resonance responses. He makes the following conclusions:

1. High aerodynamical damping prevents resonance in the blade flatwise direction at all frequencies.
2. Odd harmonic excitations up to and including 5 P can cause significant blade edgewise resonance response; teetering the rotor will reduce this response substantially.

Table 2.2: Natural frequencies (in P) for some elastic blade and tower modes.

	MOD-2	WTS-3	WTS 75	Growian I
1st blade flatwise	3.3	2.6	4.2	3.5
1st blade edgewise	6.7	4.7	6.7	4.3
1st blade torsional	20	19		20
1st tower bending, thrusting direction	1.3	0.85	2.7	1.5
1st tower bending, side direction		0.90	2.6	

Table 2.2 indicates that the blades are torsionally rigid. Friedmann (1976) states that this is typical for wind turbines.

Sullivan (1981) classifies towers with first bending frequencies over 2P as "stiff" towers and those with bending frequencies between 1P and 2P as "firm" towers. He does not discuss towers with bending frequencies below 1P. Hence, Table 2.2 indicates that the tower of the WTS-3 must be considered as "soft".

When designing pitch angle control the elastic modes must be considered if their natural frequencies are close to the desired crossover frequency. The first tower bending mode must be considered when designing pitch angle control for the WTS-3, because the tower is so soft. See Section 5.3. Other elastic blade and tower modes can be neglected. The crossover frequency can be chosen lower for a plant with a generator allowing variable turbine speed. However, a plant which operates at an almost constant speed can be designed so that the rotation does not cause structural resonances. This is more difficult to obtain if the turbine speeds can vary considerably. Operation at critical speeds must be avoided. Turbines with hinged hub or teeter hub can be designed for passive load alleviation. For a rigid hub active, cyclic pitch control may be of interest. The elastic modes must then of course be considered.

2.4 Electrical Part

Synchronous Generator

From the modelling point of view all synchronous generators have similar representations. They differ only with respect to some model parameters. Modelling of the synchronous generator is covered extensively in the literature and there are many good textbooks. Elgerd (1971) gives an excellent introduction. Anderson and Fouad (1977) discuss synchronous machine modelling in detail and give many references. The excitation systems may however have quite diversified representations. Excitation systems are modelled by standard representations developed by IEEE (IEEE Committee Report (1968)). The model for the excitation system of the WTS-3 is given in Appendix B.7.

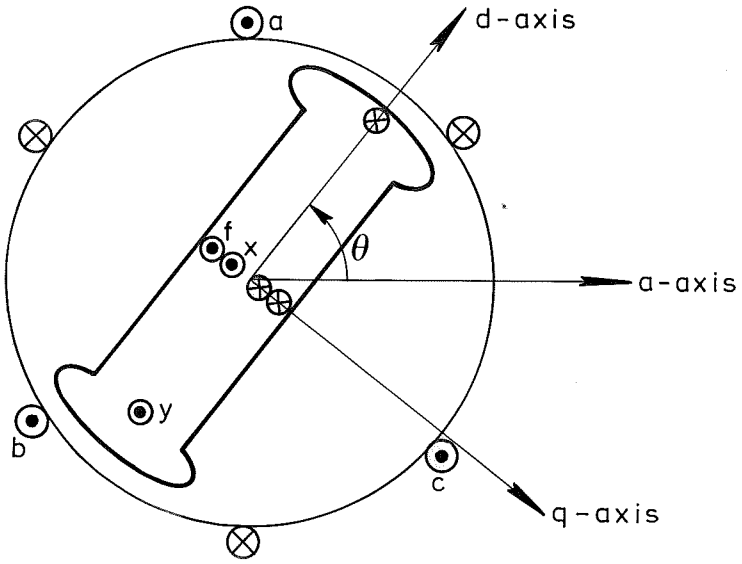

Figure 2.8: The Synchronous Generator

The basic ideas behind the modelling of the synchronous generator will now be outlined. The equations are given in Appendix B.2. The stator is considered to have three identical, symmetrically placed, lumped windings a, b and c (See Figure 2.8). On the rotor there are three windings f, x and g, placed in the direction of two orthogonal axes d (direct axis) and q (quadrature axis). The rotor winding f represents the field winding, while windings x and g are fictitious windings inserted to account for the effects of currents in the iron parts of the rotor or in damper windings. It is assumed that all self- and mutual inductances are independent of current (saturation is handled in other ways) and that they may be represented as constants plus a simple sine variation of the rotor angle θ or 2θ. The Kirchhoff's law equations and the equation of motion for the rotor (the swing equation) constitute the model.

Since the inductances depend on the rotor angle θ, Kirchhoff's equations for this model contain time-varying parameters. This complication can be avoided by using Parks transformation (Park (1929)). The idea is to express the stator flux linkages in the rotating d, q reference system (see Figure 2.8) instead of the normal stator fixed reference system. The stator windings are replaced with two fictitious windings which are fixed with respect to the rotor. One winding is chosen to coincide with the d-axis and the other with the q-axis.

The equations describing the rotor motion and the windings give a seventh order model, which contains both fast modes in the millisecond range and slow modes in the second range. The linearized model for the generator of the WTS-3 gives at zero power the following poles

$-19.6 \pm 313i, -72.8, -2.65 \pm 21.6i, -16.2, -1.16$

and at the rated operating point

$-19.6 \pm 313i, -74.5, -2.23 \pm 24.6i, -15.9, -0.64$

The two fastest poles ($-19.6 \pm 313i$) are due to the stator windings. In the literature they are referenced as the stator dynamics. The poles at -74.5 and -15.9 are due to the damper windings and the pole at -0.64 is due to the field winding. The time constant of the field winding is normally 10 to 100 times longer than the time constants of the equivalent damper time constants. The poles at $-2.23 \pm 24.6i$ give the basic oscillatory mode of the rotor motion. The zeros of the transfer function from the mechanical torque Δt_m to the electrical torque Δt_e at the rated operating point are $-9.8 \pm 313i$, -51.4, -15.7 and -0.64. In Section 2.2 the synchronous generator was modelled by the swing equation with Δt_e and Δt_{el} given by (2.14). Figure 2.9 shows that this second order model is a good approximation when studying the influence from the wind on the power generation.

The stator dynamics and the dynamics of the windings are important when electrical properties such as the response to faults in the grid are studied. Hwang and Gilbert (1978) used the seventh order model outlined above when simulating synchronization of wind power plants against an infinite bus. The implications of neglecting the stator dynamics are discussed by Olive (1968). This means that second and higher harmonics in flux linkages and stator currents are neglected.

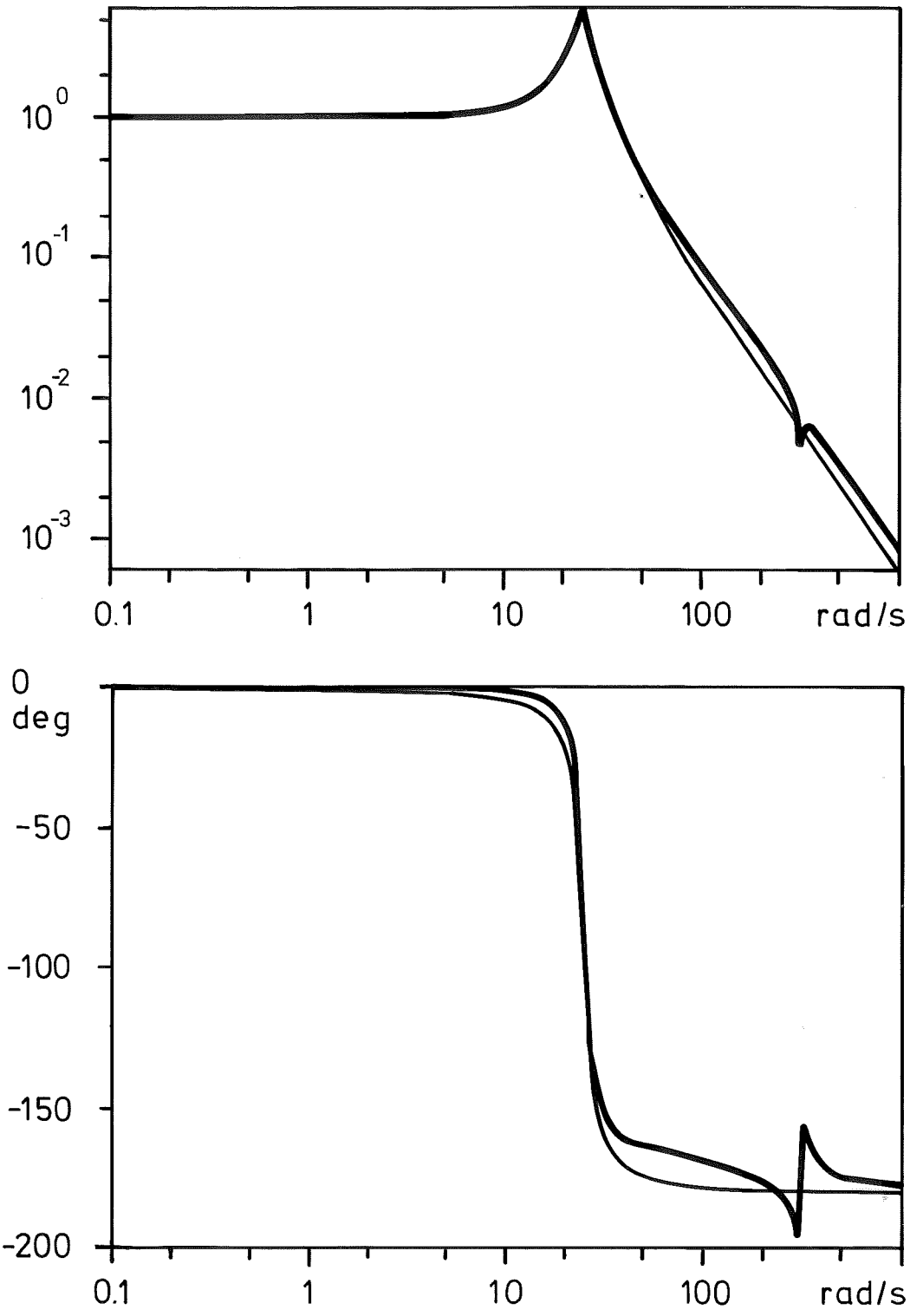

Figure 2.9: Bode plot of the transfer function from Δt_m to Δt_e for the synchronous generator of the WTS-3 at the rated operating point. The bold lines are for the seventh order model. The thin lines are for the second order model.

30

Induction Generator

The induction generator is also modelled using the Kirchhoff's law equations and the equation of motion for the rotor (for example Leonhard (1974) or Nordanlycke, Paulsson and Wredenberg (1974)). The rotor is considered to have two orthogonal windings. To make the equations time invariant, the stator quantities are transformed to a synchronous rotating system in the same way as for the synchronous generator. The rotor quantities are transformed to a rotating system with the rotational speed $\dot{\delta} - \omega_0$. The equations give a sixth order model. The complex pole pair giving the stator dynamics is of the same magnitude as in the synchronous generator case. Figure 2.10 shows that the first order model (2.20) is a good approximation when studying the influence from the wind on the power generation.

Loss of Electrical Load

Electrical faults may change the dynamic behaviour drastically. If the load is lost this corresponds to $T_e = 0$. For the WTS-3 the torsion γ_e of the drive train is 1000° at rated operation. If the load is lost, the untwisting of this spring between the turbine and the generator will accelerate the rotor of the generator. The behaviour can be estimated by the model (2.11). If damping is neglected the power angle δ can be estimated by

$$\delta(t) - \delta(0) = 1000° \cdot (1 - \cos 3.8 \cdot t) \qquad (2.27)$$

For example $\delta(0.1) - \delta(0) = 75°$. A rigorous calculation using the simulation model in Appendix B shows that synchronism is upset if the load is lost more than 0.16 s. This is also a typical value for conventional turbine generators.

If the synchronous generator is connected and the bus voltage is greater than zero during the fault, it is possible to increase the electrical torque by increasing the excitation voltage. The synchronism can be maintained, if the excitation voltage can be increased so much that the electrical torque can be restored in steady state. The dynamics of the excitation system can be made sufficiently fast. However, it is another question whether it is a good practice to deliver power to the grid when the bus voltage is low.

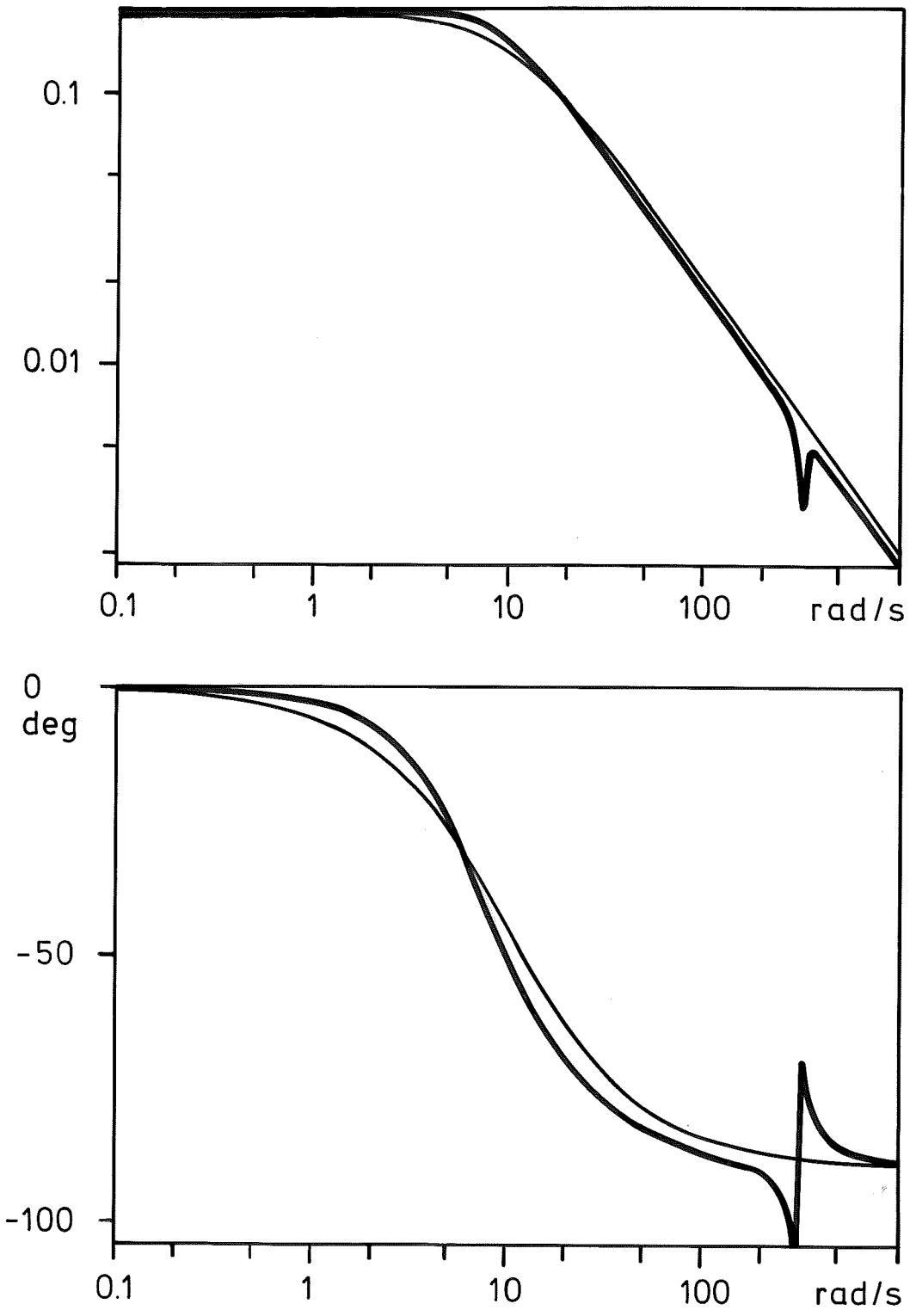

Figure 2.10: Bode plot of the transfer function from $\Delta\dot{\delta}$ [rad/s] to Δt_e for a typical induction generator. The bold lines are for the sixth order model. The thin lines are for the first order model (2.20).

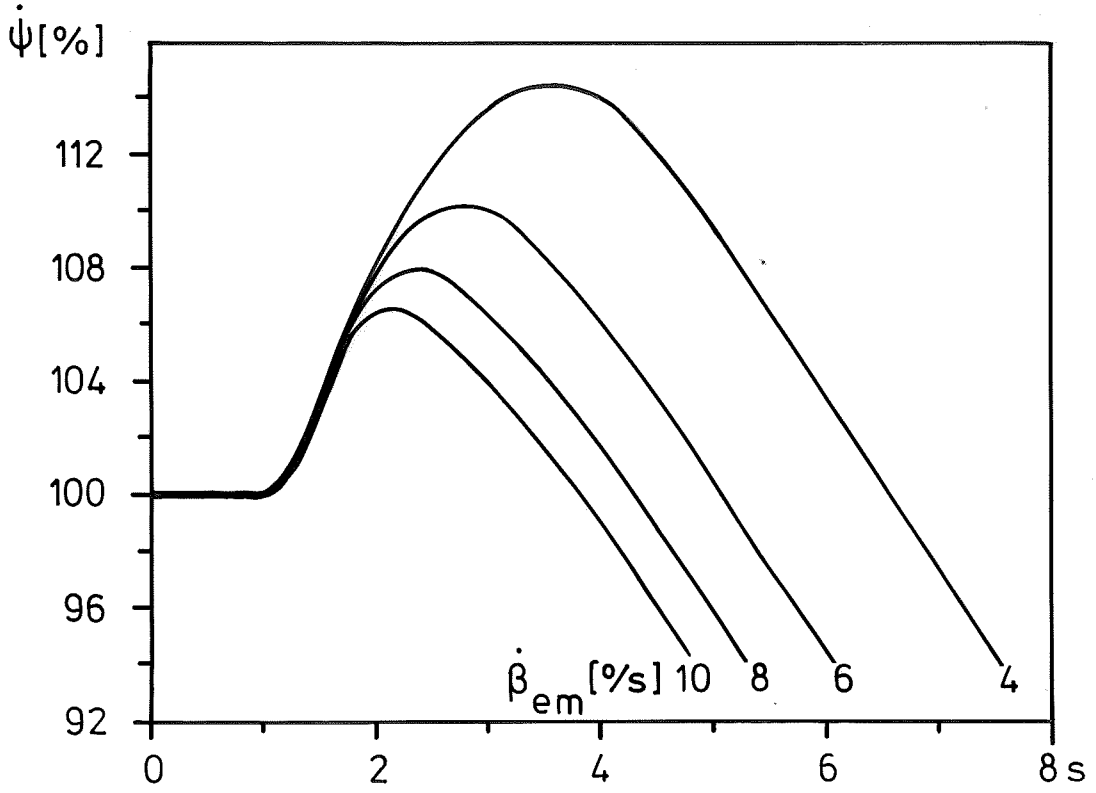

Figure 2.11: Simulated turbine speed response of the WTS-3 to a loss of load for different emergency pitch rates $\dot{\beta}_{em}$. The wind speed is constant 14 m/s and the system is operating in stationarity generating 3 MW when the generator is disconnected at the time 1 s and the emergency system is activated.

It is not possible to prevent loss of synchronism during electrical faults by controlling the pitch angle even if the shaft is stiff. Hau (1982) reports that the Growian I has received battery storage units weighing $2.5 \cdot 10^3$ kg in order to fulfil the requirement of bridging grid interruptions of up to 20 s. For the WTS-3, the blade angle must be changed more than ten degrees to obtain zero driving aerodynamical torque at rated wind speed. Figure 2.11 shows simulated turbine rotor overspeed of the WTS-3 at loss of load for different emergency pitch rates. The simulation model described in Appendix B was used.

2.5 Models for Design of Pitch Angle Control

When modelling it is important to know the purpose of the model. Here we will discuss models for design of pitch angle control. Modelling and control design are normally an iterative procedure. Control objectives and control design are discussed in Chapter 5. A basic objective of the pitch angle control is to compensate for variations in the wind.

In Section 2.2 it was found that horizontal axis wind turbines with synchronous generators or induction generators have similar basic dynamics. The transfer function from the aerodynamical torque Δt_a to the electrical torque Δt_e has two complex pole pairs and a zero at $-k_s/d_s$. The first torsional mode is important when designing pitch angle control. This mode is excited by the wind and by the blade angle changes. It acts as a low pass filter and prevents rapid disturbances in the turbine from going through the system into the utility grid. It has low damping (at least when a synchronous generator is used). Consequently, the mode indicates the crossover frequency needed for pitch angle control which should compensate for variations in generated power. It is not reasonable to chose the crossover frequency much higher than the natural frequency of the mode. Inspection of (2.16) and (2.22) shows that in the frequency range of interest for pitch angle control the relation between Δt_a and Δt_e can be approximated by

$$\Delta t_e(s) = \frac{d_s s + k_s}{p_2 s^2 + p_1 s + k_s} \Delta t_a(s) \qquad (2.28)$$

where

$$p_2 = k_s/(\sigma^2 + \omega^2)$$

$$p_1 = -2\sigma p_2$$

and $\sigma \pm i\omega$ is the pole pair associated with the first torsional mode. The static gain, the zero at $-k_s/d_s$ and the pole pair at $\sigma \pm i\omega$ are preserved. The second pole pair is neglected because of the frequency range involved. Inspection of (2.17) and (2.23) shows that in the same frequency range the relation between Δt_a and $\Delta\gamma_e$ can be approximated by

$$\Delta\gamma_e(s) = \frac{1}{p_2 s^2 + p_1 s + k_s} \Delta t_a(s) \qquad (2.29)$$

Thus in the time domain we have

$$p_2\Delta\ddot{\gamma}_e + p_1\Delta\dot{\gamma}_e + k_s\Delta\gamma_e = \Delta t_a \qquad (2.30)$$

$$\Delta t_e = d_s\Delta\dot{\gamma}_e + k_s\Delta\gamma_e \qquad (2.31)$$

Design of compensation for variations in the mean wind speed over the turbine disc results for the MOD-2, the WTS-3 and the WTS 75 in a crossover frequency of 2 - 3 rad/s for the pitch angle control. For the MOD-2 and the WTS-3 the pitch angle control must also provide damping of the first torsional mode. For these systems the soft shaft attenuates the 2P, 4P, 6P and 8P variations in the aerodynamical torque before they appear as shaft and electrical torques. The turbines are designed to withstand these variations in the aerodynamical torque and the pitch angle control is supposed to neglect the variations. The first torsional mode of the WTS 75 need not be damped, but the WTS-75 has no filtering effect for the 2P variations. Today the large 2P variations in the electrical power are accepted, but the plant is prepared for active cyclic pitch control. Compensation of the 2P disturbances means that the pitch angle control must have a higher crossover frequency.

When the electrical system allows the turbine to operate at variable speed and the power output can be controlled at the electrical system, the requirements on the blade angle control to respond to changing wind conditions may be lowered considerably. By allowing the turbine to perform limited speed excursions transient wind power is absorbed by the large turbine as kinetic energy. It is possible to keep the turbine speed variations with a high probability within 10% using a pitch angle control having a crossover frequency of less than 1 rad/s. The generator dynamics is then unimportant for pitch angle control.

When structural dynamics must be considered in the design simple inertia-stiffness models can be used. Model (2.39) below for tower bendings is an example.

The WTS-3

For convenience models for design of pitch angle control for the WTS-3 are are listed below. These models are compared with models identified from measured data from the WTS-3 in Chapter 4. The discussion of pitch angle control in Section 5.3 are for simplicity first specialized to the WTS-3. The dynamics from the aerodynamical torque to generated power is as we found above similar for systems having synchronous generators or induction generators.

The torsional mode of the WTS-3 has a simple physical interpretation as the oscillation of the turbine against the electrical system. Inspection of (2.17) and (2.18) shows that $\Delta\dot{\psi}_e \approx \Delta\dot{\gamma}_e$. Another interpretation is that the dynamics of the generator can be neglected. Hence $p_2 = j_t$ and $p_1 = d_s$. Consequently, if all quantities are reduced to the turbine axis, a model is given by

$$J_t\Delta\ddot{\gamma} + D_s\Delta\dot{\gamma} + K_s\Delta\gamma = \Delta T \tag{2.33}$$

$$\Delta P_E = \dot{\psi}_0(D_s\Delta\dot{\gamma} + K_s\Delta\gamma) \tag{2.34}$$

$$\Delta\dot{\psi} = \Delta\dot{\gamma} \tag{2.35}$$

where $\dot{\psi}_0$ is the synchronous turbine speed and P_E is the generated electrical power. In this approximation the variations in the shaft torque are proportional to the variations in the generated power.

The aerodynamical torque T and the aerodynamical thrust F are nonlinear functions of the pitch angle β, the mean speed U_0 over the rotor disc of the oncoming wind, $\dot{\psi}$ and $\dot{z}_T$. Expressions for T and F are given in Appendix B.1. The linearized expressions for ΔT and ΔF are written as

$$\Delta T = T_\beta\,\Delta\beta + T_U\,\Delta U_0 + T_{\dot{\psi}}\,\Delta\dot{\psi} + T_{\dot{z}}\,\Delta\dot{z}_T \tag{2.36}$$

$$\Delta F = F_\beta\,\Delta\beta + F_U\,\Delta U_0 + F_{\dot{\psi}}\,\Delta\dot{\psi} + F_{\dot{z}}\,\Delta\dot{z}_T \tag{2.37}$$

The dynamics of the blade servo must also be included. The blade servo of the WTS-3 is modelled by a linear, first order system. Let β_r be the control input, then

$$\dot{\beta} = (\beta_r - \beta)/T_{bs}, \quad \dot{\beta}_{min} \le \dot{\beta} \le \dot{\beta}_{max} \tag{2.38}$$

The first mode of the tower bendings can be modelled by

$$M_T\ddot{z}_T = F - D_T\dot{z}_T - K_T z_T \tag{2.39}$$

where z_T is the displacement of the nacelle in the direction perpendicular to the rotor disc and F is the aerodynamical thrust acting on the turbine in this direction. The mass M_T, the spring coefficient K_T and the damping coefficient D_T are chosen such that the model gives correct static displacement, natural frequency and damping. The models (2.33) - (2.37) and (2.39) then give the dynamics from $\Delta\beta$ and ΔU_0 to $\Delta\gamma$ in the frequency domain as

$$\begin{aligned}\{(J_t s^2 + (D_s - T_{\dot{\psi}})s + K_s)(M_T s^2 + (D_T - F_{\dot{z}})s + K_T) - T_{\dot{z}}F_{\dot{\psi}}s\}\,\Delta\gamma \\ = T_\beta\{M_T s^2 + (D_T - F_{\dot{z}} + T_{\dot{z}}F_\beta/T_\beta)s + K_T\}\,\Delta\beta \\ + T_U\{M_T s^2 + (D_T - F_{\dot{z}} + T_{\dot{z}}F_U/T_U)s + K_T\}\,\Delta U_0\end{aligned} \tag{2.40}$$

Relations (2.33) - (2.39) constitute a linear, fifth order system model. The model is good for design of pitch angle control. The single most important approximation for this use is the linearization of the expression for the aerodynamical torque ΔT.

3. WIND CHARACTERISTICS

The variation of the wind speed as function of space and time is a complex phenomenon. The wind turbulence gives it a stochastic behaviour. The power spectrum of horizontal wind speed near ground level ranges over several decades of frequencies. The spectrum has two major eddy-energy peaks in the spectrum; one peak occurs at a period of about 4 days, and a second peak occurs at a period of about 1 minute (van der Hoven (1957)). The former peak is due to wind speed fluctuations caused by migratory pressure systems of synoptic weather-map scale. The latter peak is in the micrometeorological range and is a mechanical and convective type of turbulence. Between the two peaks, a broad spectral gap is centered at a period ranging from 10 minutes and 1 hour. When considering blade angle control, it is the high frequency part that is of interest. The low frequency part gives the mean wind speed. This means that it is convenient to model a wind speed component at a point $\vec{x}$ as

$$U_i(\vec{x},t) = \bar{U}_i(\vec{x}) + \Delta U_i(\vec{x},t) \qquad (3.1)$$

where $\bar{U}_i$ is the mean value of U_i over typically 10 minutes and ΔU_i is the turbulence part having zero mean.

The properties of the wind turbulence at a fixed point are discussed in Section 3.1 as an introduction to the discussion in Section 3.2 on how a large turbine experiences the wind variations. A summary was given in Section 2.1.

3.1 Wind Turbulence at a Fixed Point

Wind turbulence is a complex and not completely understood phenomenon. An introduction can be found in Lumley and Panofsky (1964). Etkin (1972) gives a nice summary of basic concepts and relations. Engineering Sciences Data (1974) and Frost et al (1978) give detailed computational procedures.

Several analytical expressions for the power spectrum of the horizontal wind speed at a fixed point are given in the literature. They are typically of the form

$$\phi(\omega) = \frac{K \cdot |\omega|^{\gamma}}{\left[1 + (\omega T)^{\alpha}\right]^{\beta}} \qquad (3.2)$$

where K and T depend on the surface roughness, mean wind speed and height over ground level. Mathematical models and also most spectra obtained from measurements indicate that there is a range (the inertial subrange) where $\phi(\omega) \sim \omega^{-5/3}$, which means that in (3.2) $\alpha\beta - \gamma = 5/3$. Engineering Sciences Data (1974) recommends the von Karman spectrum. It has $\alpha = 2$, $\beta = 5/6$ and $\gamma = 0$. A detailed description on how to calculate K and T is given. Also many references are given. Etkin (1972) uses also the von Karman spectrum. Davenport (1961) suggests a spectrum with $\alpha = 2$, $\beta = 4/3$ and $\gamma = 1$. In the Swedish Specification for the WTS-3 a spectrum with $\alpha = 1$, $\beta = 5/3$ and $\gamma = 0$ is given. Frost et al (1978) and Spera and Richards (1980) use a spectrum with $\alpha = 5/3$, $\beta = 1$ and $\gamma = 0$. Unfortunately, these spectra are not rational and this makes it complicated to use them for control design. The Dryden spectrum, which has $\alpha = 2$, $\beta = 1$ and $\gamma = 0$, is rational. A stochastic process with the Dryden spectrum can be modelled by the output of a first order system driven by white noise.

Engineering Sciences Data (1974) states that it is reasonable in many applications to assume that wind turbulence is a Gaussian process, but in practice it contains 'patches' of a significantly non-Gaussian nature when larger gusts and longer lulls occur more frequently than indicated by the Gaussian distribution.

Spectral models are not well-suited for modelling extreme events like large gusts. Events of this kind can be modelled by discrete gust models. Powell and Connell (1980) define gusts as

> "any series of discrete velocity-time events that can be defined from a turbulence time series according to some extrinsic criterion."

For example the extrinsic criterion may be chosen as adjacent crossings of the mean value and the velocity-time events as the amplitude and duration.

A discrete gust model gives the statistics for the velocity-time events. Unfortunately, there is no good and generally accepted discrete gust model available today. Powell and Connell (1980) review a number of discrete gust

models suggested in the literature. Linde (1983) gives short descriptions of the models and presents analysis of measurements in the vertical plane at different heights. The findings show that the variations in gust intensity at different heights and under different conditions are larger than can be expected from available models. Another result is that the measurements show that positive gusts generally are more frequent than negative. This anisotropy is a function of several parameters. Linde thinks that a reasonable explanation is the existence of well ordered turbulence structures. The measurements also indicate that a gust extends to less than 60 m in the vertical direction.

3.2 How a Turbine Experiences Wind Variations

Connell (1982) gives both theoretical and experimental evidence that a point on a rotating wind turbine blade encounters turbulence whose characteristics are quite different from turbulence encountered at a fixed point. The midfrequency region is depleted and the removed energy is distributed into the high frequency end of the spectrum and the spectrum also contains narrow-band spikes of turbulence energy centered on integer multiples P. An intuitive explanation is that a rotating point chops across the eddies whereas a small fixed anemometer is totally immersed in the turbulence eddies.

It is convenient to view the wind variations experienced by the turbine as consisting of the mean value over the turbine area and of narrow-band variations at integer multiples of P. There are three major sources of the variations at the integer multiples of P: the rotational sampling of turbulence eddies, the wind profile and the tower blockage.

When designing pitch angle control it is reasonable to assume that the rotor disc is orthogonal to the mean wind direction, which means that it is the wind variations in the longitudinal direction that are of interest. To simplify the notation a cylindrical coordinate system (r,ψ,z) with the origin at the hub center and the z-axis parallel with the mean wind direction is introduced. The longitudinal wind component at the point (r,ψ,z) at time t is denoted by $U_z(r,\psi,z,t)$.

Mean Wind over the Turbine Area

Different ways to model the mean wind of an area are suggested in the literature. Davenport (1977) suggests a nonrational transfer function to account for the averaging over rectangular walls.

Holley et al (1981) gives a simple model for the mean wind $U_0(t)$ of $U_z(r,\psi,0,t)$ over a rotor disc with the radius R. Let U_0 be the sum of $\bar{U}_0$ and ΔU_0, where $\bar{U}_0$ is the mean of U_0. Let σ be the standard deviation of the turbulence at a fixed point and let $c_{zz}(\Delta z)$ be the covariance between $U_z(r,\psi,z+\Delta z,t)$ and $U_z(r,\psi,z,t)$. Introduce the integral scale L defined as

$$L = \sigma^{-2} \int_0^\infty c_{zz}(\xi)\, d\xi \qquad (3.3)$$

Intuitively, L can be interpreted to be the size of typical eddies. Their model for ΔU_0 is then given as

$$\Delta\dot{U}_0 = -\Delta U_0 / T_w + \sigma_w \sqrt{2/(r_w/T_w)}\, w \qquad (3.4)$$

where w is Gaussian white noise with zero mean and noise intensity r_w. The time constant T_w is given by

$$T_w = L/\bar{U}_0/a_* \qquad (3.5)$$

and the standard deviation σ_w of ΔU_0 is given by

$$\sigma_w = b_* \sigma \qquad (3.6)$$

Holley et al (1981) gives a_* and b_* as functions of the quotient R/L. For R = 0 we get $a_* = b_* = 1$ and the point spectrum. The functions a_* and b_* are close to one when R/L < 0.1. Thus the point spectrum and the spectrum of ΔU_0 are equal when the eddies are much larger then the disc. For R/L = 1 we get $a_* = b_* = 0.5$, which give a spectrum that differ significantly from the point spectrum.

An important issue is the possibilities of measuring U_0. From the basic relations given in Holley et al (1981) for incompressible flow and homogeneous and isotropic turbulence it is easy to calculate that the covariance between the mean wind speed $U_0(t)$ over a disc with radius R and the wind speed $U_z(0,0,0,t)$ at the center of the disc is $c_{zz}(R)$. The von Karman covariance functions imply that for R/L > 0.5, $c_{zz}(R)/\sigma^2 < 0.6$ (a plot of c_{zz} can be found in for example Frost et al

(1978)). Such poor correlation implies that it is not possible to obtain representative measurements of U_0 using an anemometer.

Rotational Sampling

Holley et al (1981) approximates ΔU_z at a point in the rotor disc with the polar coordinates (r,ψ) as

$$\Delta U_z(r,\psi,0,t) = \Delta U_0(t) + \Delta U_{zx}(t)\, r \cos\psi + \Delta U_{zy}(t)\, r \sin\psi \qquad (3.7)$$

The uniform terms ΔU_0 and the gradient terms ΔU_{zx} and ΔU_{zy} are three uncorrelated processes. The uniform term ΔU_0 is the mean value over the rotor disc and was discussed above. The gradient terms ΔU_{zx} and ΔU_{zy} are also modelled by first order systems driven by white noise. The Simnon code for this model is enclosed in Appendix B.9.

The model (3.7) gives a spectrum for a rotating point which is depleted in the midfrequency region and has a peak at the frequency of rotation, but does not reproduce an energy excess at frequencies greater than the frequency of rotation as Connell's above referenced model (Connell (1982)) has. Connell's model for the wind spectrum at a rotating point is unfortunately not given in a simple analytical form.

Wind Profile

Different analytic expressions for the variation of the mean speed with the altitude for an airflow over a horizontal and homogeneous terrain are suggested in the literature. Shepherd (1978) gives a survey. The influence of ridges and hills are discussed in Jackson and Hunt (1975) and Bradley (1980). Frost et al (1978) gives detailed computational procedures intended for fatigue strength analysis or structural strength analysis under extreme wind shear. Since it is only the wind profile over the rotor disc that is of interest, it is in many cases reasonable to assume a linear wind profile when calculating variations in power output or when designing cyclic pitch control. However, ridges and hills may cause very nonlinear wind profiles, that must be considered if active cyclic pitch control is going to be used to alleviate the loads on the blades.

Tower Blockage

The tower blocks the airflow in the rotor disc. The effect is most significant on turbines operating downwind of the tower. The wake depends critically on the aerodynamical properties of the tower. For the WTS-3 Hamilton Standard calculated a velocity defect of 30% and a wake width of 1.4 times the tower diameter in the rotor disc. This means that the major part of the driving torque on a blade is lost as it swings behind the tower. Seidel (1977) reports that the MOD-0 wind turbine (The ERDA-NASA 100 kW wind turbine near Sandusky, Ohio) momentarily loses more than 60% of the rotor torque as a blade swings behind the tower. For the WTS-75, whose turbine operates upwind of the tower, the velocity defect is about 6%.

Let the variable T_{TB} denote the defect in the aerodynamical torque caused by the tower. For a turbine with two blades the disturbance occurs with a frequency of 2P. Assume that the turbine is influenced by the tower blockage when for some integer m

$$-\alpha/2 + 2\pi m \leq 2\psi \leq \alpha/2 + 2\pi m$$

and that otherwise $T_{TB}(\psi) = 0$. Fourier analysis gives the amplitudes of the harmonics as

$$A_n = \frac{2}{\pi} \int_{-\alpha/2}^{\alpha/2} T_{TB}(\psi) \cos (n \cdot 2\psi) \, d\psi \qquad (3.8)$$

The disturbance is of short duration, because a blade is in the wake only a few per cent of the time. This means that at least 3 - 4 of the first harmonics have amplitudes of the same magnitude.

If we for the WTS-3 translate the estimation of the wake width which is 1.4 times the tower diameter to $\alpha = 10°$ and assume that a blade loses all driving torque in the wake, we get that $A_1 = 5\%$ of the mean aerodynamical torque. The soft shaft attenuates the disturbance to 0.7% in the electrical power.

4. SYSTEM IDENTIFICATION

Measurements from the WTS-3 are analysed in this chapter. Attention is focused on dynamics of interest for pitch angle control. Different models are identified and compared with the physical models listed in Section 2.5.

This chapter is organized as follows. The measurements are presented in Section 4.1. The interactive program package Idpac (Wieslander (1980a)) was used to analyse the data. The measured data are sampled and Idpac's identification procedures give discrete time input/output models. The physical models are continuous time models. The transformation of the physical models to discrete time models is discussed in Section 4.2. The identification of models for different parts starts with the servo dynamics in Section 4.3 and with the relation between turbine speed and generated power in Section 4.4. The wind speed does not enter as a direct source of the variations in the outputs of these models. This is, however, the case when we want to identify the behaviour from the blade angle to the generated power. The wind measurements are analysed in Section 4.5. The behaviour from the blade angle and the wind speed to the generated power is then identified in Section 4.6. The 2P variations in the generated power are investigated in Section 4.7. Finally, the results are summarized in Section 4.8.

4.1 Measurements

Three measurement series from the WTS-3 recorded on the 11th October 1983 are used:

Series 1. at 11:05, 240 seconds long, 24 000 data points

Series 2. at 12:52, 240 seconds long, 24 000 data points

Series 3. at 13:04, 210 seconds long, 21 000 data points

The measurements were filtered with a sixth order Bessel filter having a cut-off frequency of 25 Hz (157 rad/s). The filtered signals were then sampled with 100 Hz (628 rad/s). One difficulty is that the system may be poorly identifiable, because the data were collected when the process was in closed loop control. The power reference of the controller was switched between 2 MW and 3 MW according to a PRBS-sequence to improve the identifiability.

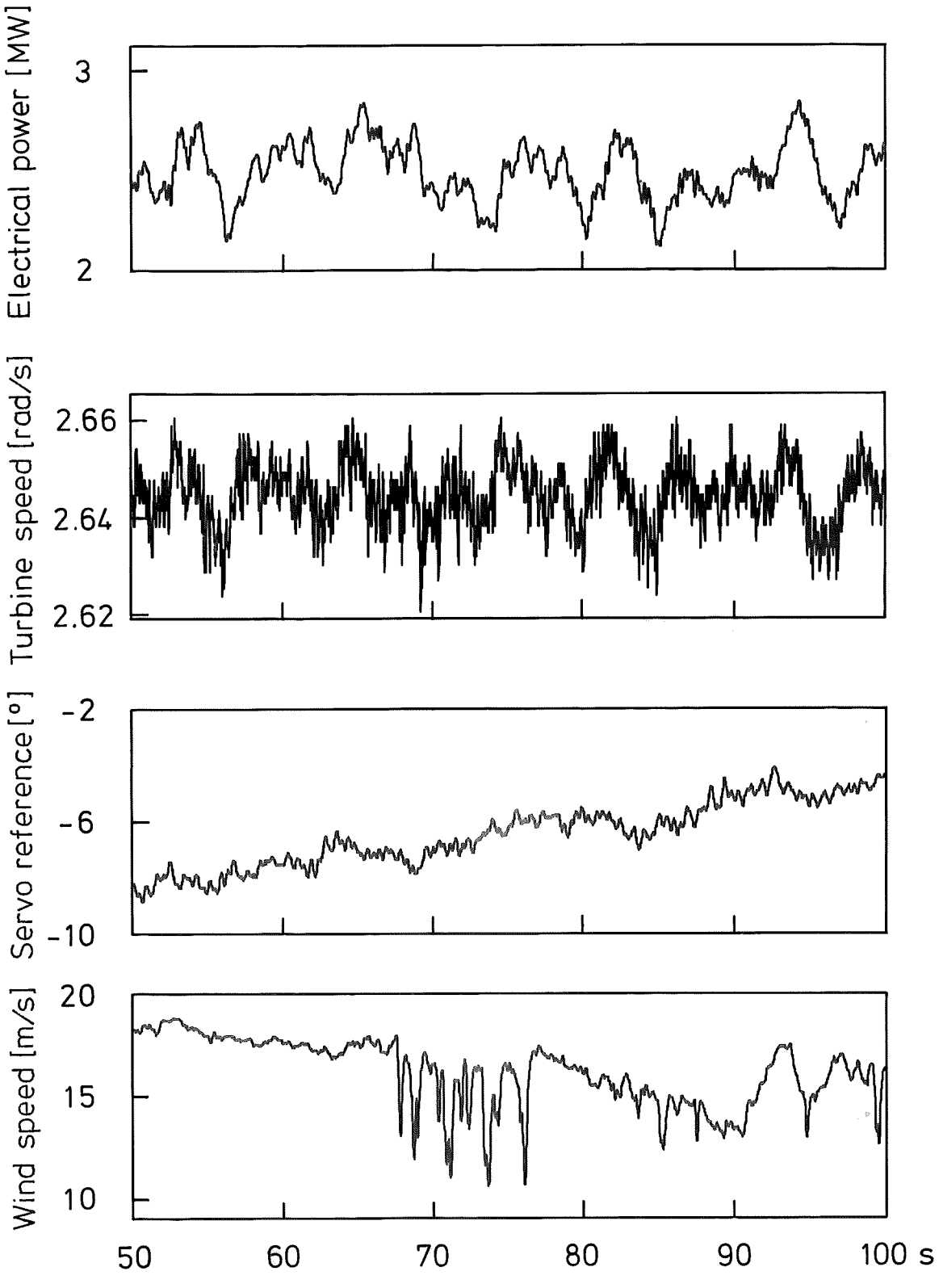

Figure 4.1: Measurements from series 3. The wind speed measurement is from an anemometer on the nacelle.

An example of measurements obtained is shown in Figure 4.1.

The measurements are analysed in Sections 4.3 - 4.6 for the purpose of identifying the plant dynamics of interest for pitch angle control. Besides the plant dynamics and the wind characteristics, the power spectra of the measurements must also be considered in the control design, because high spectral densities above the crossover frequency may cause excessive servo motions if they are neglected in the control design.

Figure 4.2 shows a power spectrum for the electrical power P_E calculated from measurement series 1. The series was split into blocks containing 2048 data points each. Discrete Fourier transform with a 4-term Blackman-Harris time window with a sidelobe level of -74 dB (Harris (1978)) was used to calculate a spectrum for each of the first ten data blocks. Figure 4.2 shows the mean of these spectra. The power spectra for the turbine speed $\dot{\psi}$ and the servo reference β_r shown in Figures 4.3 and 4.4 were calculated in the same way. The power spectra from the three different measurement series are very similar.

The power spectra for P_E and $\dot{\psi}$ have several peaks. There are large peaks at 2P (= 5.2 rad/s), 4P, 6P and 8P. These variations are caused by the spatial variation of the wind speed over the turbine area. See Section 3.2. They must be considered in the control design to avoid excessive servo motions. The controller had notch filters at these frequencies so these variations are as seen from Figure 4.4 suppressed in the servo reference. There are also peaks at odd integer multiples of P, but they are much smaller. The variations at odd integer multiples of P are smaller, because the turbine has two blades. These variations are not suppressed in the servo reference and they make the servo reference look noisy. The 2P variations in the electrical power are investigated further in Section 4.7.

If the generator inertia is included in the physical models, the calculations in Section 2.2 show that there is a torsional mode having a natural frequency of about 25 rad/s. This mode is a possible explanation for the peak at 8P (21 rad/s) being wider than those at 4P and 6P.

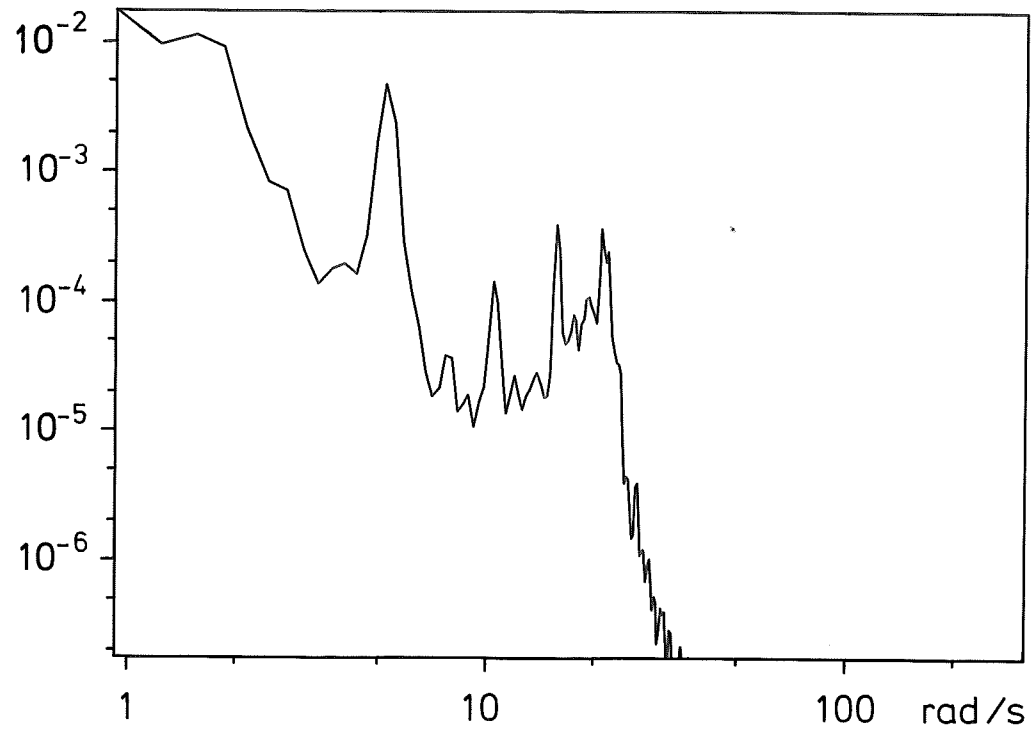

Figure 4.2: Power spectrum for the electrical power P_E [MW] from series 1.

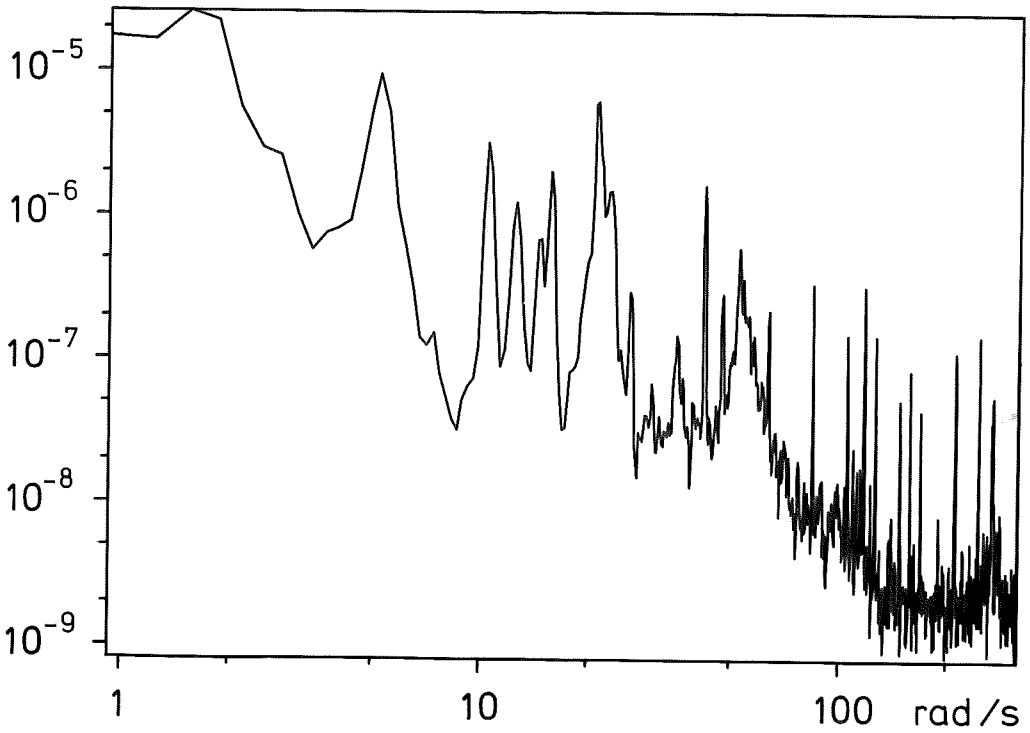

Figure 4.3: Power spectrum for the turbine speed $\dot{\psi}$ [rad/s] from series 1.

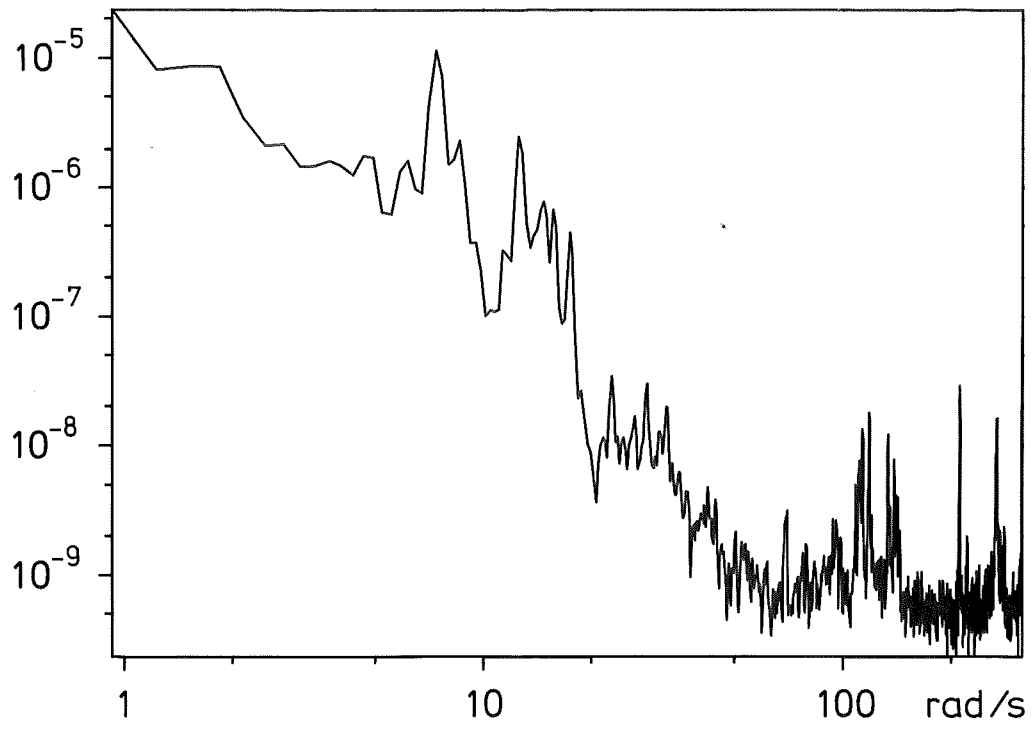

Figure 4.4: Power spectrum for the servo reference β [rad] from series 1.

4.2 Transformation to Discrete Time Input/Output Models

Idpac's identification procedures give discrete time input/output models on the form

$$A(q^{-1})y(t) = B(q^{-1})u(t) + \lambda C(q^{-1})e(t) \qquad (4.1)$$

where y is the output, u is the input of the system, e is discrete time, white noise with zero mean and variance one and q^{-1} is the delay operator, $q^{-1}x(t) = x(t-h)$, with h being the time between two sampling instances. The polynomials A, B and C are defined as

$$A(q^{-1}) = 1 + a_1 q^{-1} + \ldots + a_{na} q^{-na} \qquad (4.2)$$

$$B(q^{-1}) = b_0 + b_1 q^{-1} + \ldots + b_{nb} q^{-nb} \qquad (4.3)$$

$$C(q^{-1}) = 1 + c_1 q^{-1} + \ldots + c_{nc} q^{-nc} \qquad (4.4)$$

The model may be extended to have several inputs.

Since the physical models presented in Section 2.5 are continuous time models, they must be transformed to discrete time input/output models to compare with the experimental data. The physical models can be written as

$$\dot{x} = Fx + Gu + v \tag{4.5}$$

$$y = Hx + Du \tag{4.6}$$

with F, G, H and D being constant matrices and v being multivariable, continuous time, white noise with zero mean and the noise intensity R_1. A discrete time model with sampling interval h is then given by

$$x(t+h) = \Phi x(t) + \int_0^h e^{F(h-s)}Gu(t+s)ds + \tilde{v}(t) \tag{4.7}$$

$$y(t) = Hx(t) + Du(t) \tag{4.8}$$

with

$$\Phi = e^{Fh} \tag{4.9}$$

and $\tilde{v}$ being multivariable discrete time, white noise with zero mean and the variance

$$\tilde{R}_1 = \int_0^h e^{F(h-s)}R_1\left[e^{F(h-s)}\right]^T ds \tag{4.10}$$

To calculate the transfer function $\lambda C/A$ from e to y a spectral factorization must be performed. If we like, we can introduce white measurement noise $\tilde{e}$ with variance $\tilde{R}_2$ and uncorrelated with $\tilde{v}$;

$$y(t) = Hx(t) + Du(t) + \tilde{e}(t) \tag{4.11}$$

Let P be a symmetric, nonnegative definite solution to the discrete time, algebraic Riccati equation

$$P = \Phi P\Phi^T + \tilde{R}_1 - \Phi PH^T(HPH^T + \tilde{R}_2)^{-1}HP\Phi^T \tag{4.12}$$

Introduce K defined as

$$K = \Phi PH^T(HPH^T + \tilde{R}_2)^{-1} \tag{4.13}$$

and let I_n be an n*n unity matrix, where n is the dimension of the matrix F, then

$$\frac{C(q^{-1})}{A(q^{-1})} = 1 + H(qI_n - \Phi)^{-1}K; \quad A(q^{-1}) = q^{-n}\det(qI_n - \Phi) \tag{4.14}$$

with $n_c = n_a = n$ and

$$\lambda = (HPH^T + \tilde{R}_2)^{1/2} \tag{4.15}$$

To calculate the transfer function B/A from u to y we must evaluate the integral on the right side of (4.7). This requires knowledge of the shape of u between the sampling instances. If we can choose the representation for u, it is convenient to let it be constant between the sampling instances. This is typically the case when u is an output from a digital controller. However, in our case the inputs are analog signals. If the sampling frequency is sufficiently high it is reasonable to assume that u varies linearly between sampling instances. However, we must not choose too high a sampling frequency, since it gives an estimation problem which is badly conditioned numerically. If p is a pole of the continuous time model then e^{ph} is a pole of the discrete time model. If h is small compared to the time constants of the system, the discrete time model, thus has its poles close to one, and the calculation of the time constants of the continuous time model is ill-conditioned. It is possible to estimate the parameters directly from discrete time measurements. See Åström and Källström (1976). However, this approach requires a much greater effort, both in form of development of software and computing time.

Let t be a sampling instance. Assume that u varies between the sampling instances as

$$u(t+s) = u(t) + \alpha \cdot s/h \cdot (u(t+h)-u(t)) \text{ for } 0 \leq s < h \tag{4.16}$$

where $\alpha = 0$ gives an u that is constant between the sampling instances and $\alpha = 1$ gives an u that is continuous and varies linearly between the sampling instances. Under this assumption we get

$$x(t+h) = \Phi x(t) + \Gamma u(t) + \alpha\Gamma_1(u(t+h)-u(t)) + \tilde{v}(t) \tag{4.17}$$

with

$$\Gamma = \int_0^h e^{F(h-s)}G \, ds \tag{4.18}$$

$$\Gamma_1 = \frac{1}{h}\int_0^h s\, e^{F(h-s)}G\, ds \qquad (4.19)$$

The transfer function B/A from u to y becomes

$$\frac{B(q^{-1})}{A(q^{-1})} = D + H(qI_n - \Phi)^{-1}(\Gamma + \alpha\Gamma_1(q-1)) \qquad (4.20)$$

with $n_a = n_b = n$. In the case D = 0 and α = 0 there is no direct term ($b_0 = 0$).

4.3 Blade Servo

Sampling of the servo model (2.38) according to Section 4.2 gives

$$(1 - aq^{-1})\Delta\beta = \left[(1-a)q^{-1} + \alpha(1+(1-a)/\ln a)(1-q^{-1})\right]\Delta\beta_r \qquad (4.21)$$

where $a = \exp(-h/T_{bs})$.

For each measurement series the mean value of β_r was subtracted from β_r giving $\Delta\beta_r$. The blade angle $\Delta\beta$ was calculated in the same way. The signals $\Delta\beta_r$ and $\Delta\beta$ were filtered with a second order Butterworth filter having the cut-off frequency 10 rad/s. The signals were then resampled with h = 0.1 s. Since both $\Delta\beta_r$ and $\Delta\beta$ were filtered with the same filter, the transfer function between them remains unchanged. The filtering does of course modify the importance of the behaviour at different frequencies when estimating the models. The ML-procedure and Idpac's evaluating procedures suggest that the servo dynamics can be modelled by (2.38) with $T_{bs} = 0.65 \pm 0.05$ s. The model error, which is the difference between measured output and model output, shows that this model is good. For α = 0 as well as for α = 1 the model error of (4.21) with $T_{bs} = 0.65$ is for all three measurement series less than 0.2° and its standard deviation is 0.06°. The shape of $\Delta\beta_r$ between the sampling points turned out to be unimportant, because h is small compared to T_{bs}. A typical result is illustrated in Figure 4.5.

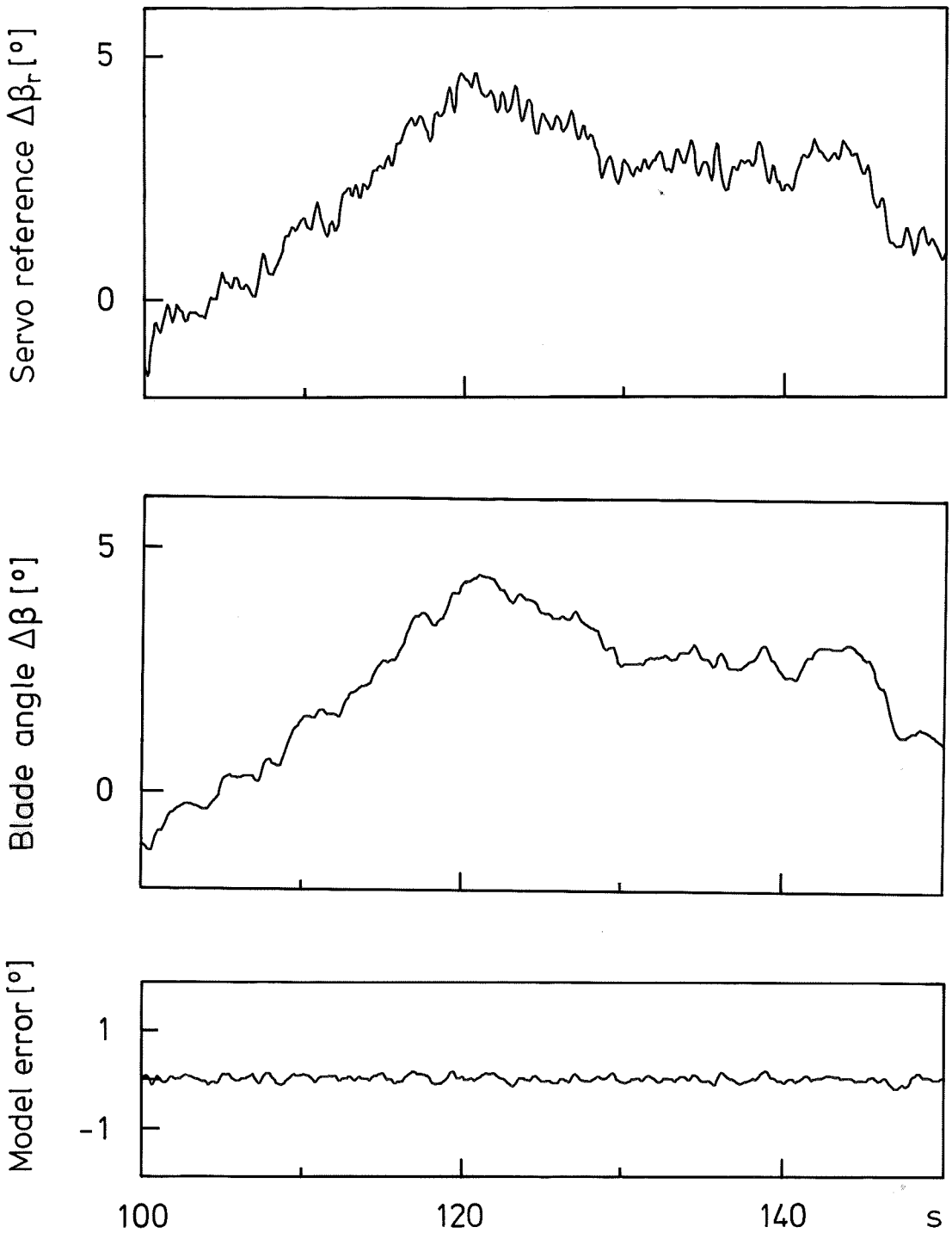

Figure 4.5: Measurements from series 2 and the model error of the model (4.21) with T_{bs} = 0.65 s and α = 1.

4.4 Turbine Speed and Electrical Power

The relations (2.34) - (2.35) imply that

$$\Delta P_E = \dot{\psi}_0 (D_s \Delta\dot{\psi} + K_s \Delta\psi) \qquad (4.22)$$

To get some insight into the validity of the relation (4.22) the coherence between turbine speed and electrical power was determined. Figure 4.6 shows that the coherence is good in the frequency range 0.5 - 5 rad/s.

Low coherence is caused by nonlinearities or other input sources. The quantization in the turbine speed measurements is a significant nonlinearity. The quantization unit is 0.0016 rad/s and the difference between minimum and maximum turbine speed for these three measurement series is less than 0.05 rad/s. This implies that the turbine speed measurement is quantized into only 30 different values. The resolution in the power measurements is better. The quantization is 0.0025 MW and the variation was 1 MW implying over 300 different values. Low resolution in the turbine speed measurements is a probable

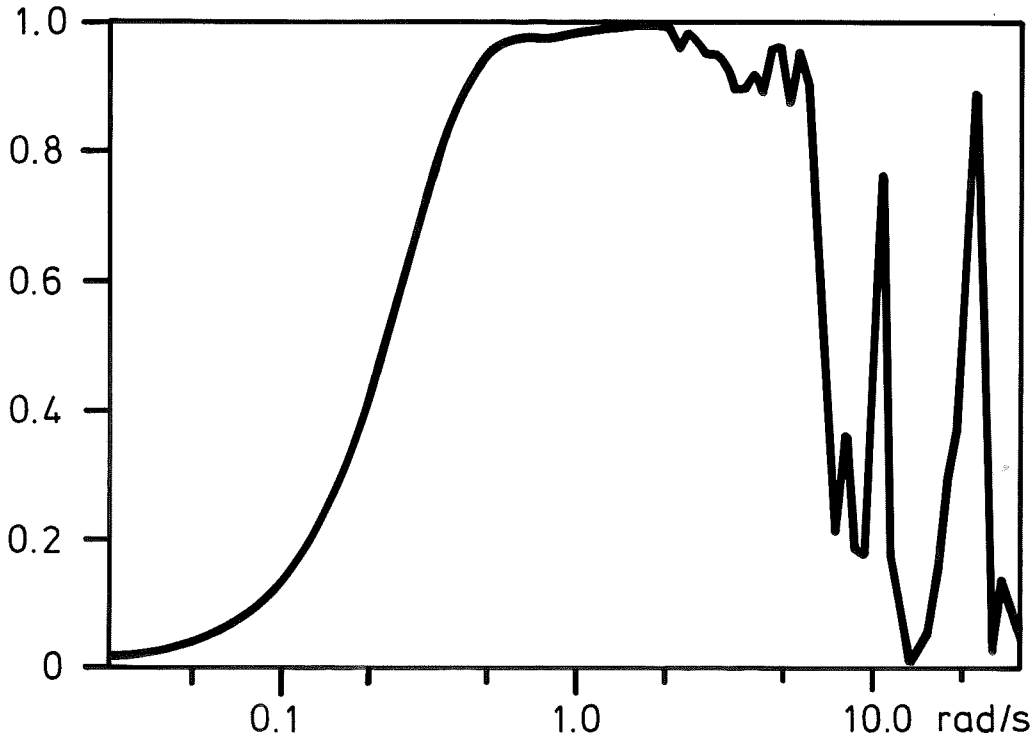

Figure 4.6: The coherence between $\dot{\psi}$ and P_E for measurement series 1.

reason for the poor correlation at high frequencies. Furthermore, Figure 4.3 shows that the spectrum of $\dot{\psi}$ has a peak at 12 - 13 rad/s, but the spectrum of P_E has no such peak. No explanation to this has been found. Artefacts in the measurement device for the turbine speed may be an explanation.

When deriving relation (4.22) it was assumed that $\Delta\dot{\psi} = \Delta\dot{\gamma}$ and hence that $\Delta\psi = \Delta\gamma$. This assumption is violated if the bus frequency varies. Low frequency variations in the bus frequency may cause a significant difference between $\Delta\gamma$ and $\Delta\psi$. This is one possible explanation for the poor coherence between turbine speed and electrical power below 0.5 rad/s. If the bus frequency is assumed to be constant, the relation (4.22) indicates that the spectral density of $\Delta\dot{\psi}$ should be small for low frequencies. Low frequency measurement disturbances when measuring the turbine speed have then large impact on the spectral properties for low frequencies and these disturbances are thus another possible explanation for the poor coherence below 0.5 rad/s.

The drive train is equipped with hydraulic dampers. Measurements made by the manufacturers show that hydraulic dampers have a pure quadratic characteristic with no linear term up to 0.03 rad/s. Above 0.03 rad/s the hydraulic dampers give a constant torque. For all three measurements series the deviation from mean turbine speed is less than 0.03 rad/s. This suggests an extension of the model (4.22) to

$$\Delta P_E = \dot{\psi}_0(D_s\Delta\dot{\psi} + D_{s2}|\Delta\dot{\psi}|\Delta\dot{\psi} + K_s\Delta\psi) \tag{4.23}$$

If $\Delta\dot{\psi}$, $\Delta\dot{\psi}|\Delta\dot{\psi}|$ and $\Delta\psi$ are viewed as inputs and ΔP_E as output, the parameters can be estimated by a least square fit. However, the values for $\Delta\psi$ are not available, but have to be calculated from $\Delta\dot{\psi}$. If it is assumed that $\Delta\dot{\psi}$ varies linearly between the sampling instances we get

$$\begin{aligned}\Delta P_E(nh)/\dot{\psi}_0 = {} & D_s\Delta\dot{\psi}(nh) + D_{s2}\left|\Delta\dot{\psi}(nh)\right|\Delta\dot{\psi}(nh) \\ & + K_s h\Big\{\sum_{i=0}^{n-1}\Delta\dot{\psi}(ih) + (\Delta\dot{\psi}(nh)-\Delta\dot{\psi}(0))/2\Big\}\end{aligned} \tag{4.24}$$

Guided by the coherence, the measured $\Delta\dot{\psi}$ and ΔP_E were processed in the following way: First they were low pass filtered with a second order Butterworth filter with the cut-off frequency 5 rad/s and resampled with h = 0.1 s. The resampled signals were then high pass filtered with a second order Butterworth filter with the cut-off frequency 0.5 rad/s. A least square fit to the model (4.24) gave the following parameter estimates K_s = 9.4 ±0.2 MNm/rad, D_s = 4.3 ±0.3 MNms/rad and $D_{s2} \approx 0$. Figure 4.7 shows a typical result of the identification. The model error in the electrical power of this model is for all three measurement series less than 0.08 MW and its standard deviation is 0.025 MW. The high pass filtering was necessary in order to obtain a good result. The model error of the above identified model has low frequency (<0.2 rad/s) components giving model errors of 0.5 MW, if the measured turbine speed and electrical power are used without being high pass filtered. Identification using signals without high pass filtering gives K_s = 2.2 MNm/rad and the same D_s and D_{s2} as above. The standard deviation of the model error is 0.13 MW.

The identification indicates that there are other sources of damping than the hydraulic dampers that are important for small oscillations. If the linear damping is eliminated from the model by setting D_s to zero, identification gives the same value for K_s and D_{s2} = 460 ± 50 MNm(s/rad)^2. The given value for the hydraulic dampers is 488 MNm(s/rad)^2. This model gives a poorer fit to the data than the linear model. The standard deviation of the model error in the electrical power is 0.034 MW.

Let us return to the linear model (4.22). We can view either $\Delta\dot{\psi}$ or ΔP_E as input and use ML-identification. It turns out that it is not possible to improve the system model by increasing the model order. It is only the noise model that is improved. Errors in the observations of the turbine speed and the electrical power are a basic problem. When using ML-identification it is assumed that the inputs are the true ones. The effects of errors in the inputs when estimating model parameters are discussed in Kendall and Stuart (1961). Nothing more can be done without a priori knowledge about the measurement noises. In summary, the relation (4.22) is at least good in the frequency range 0.5 - 5 rad/s, which is an important frequency range for pitch angle control.

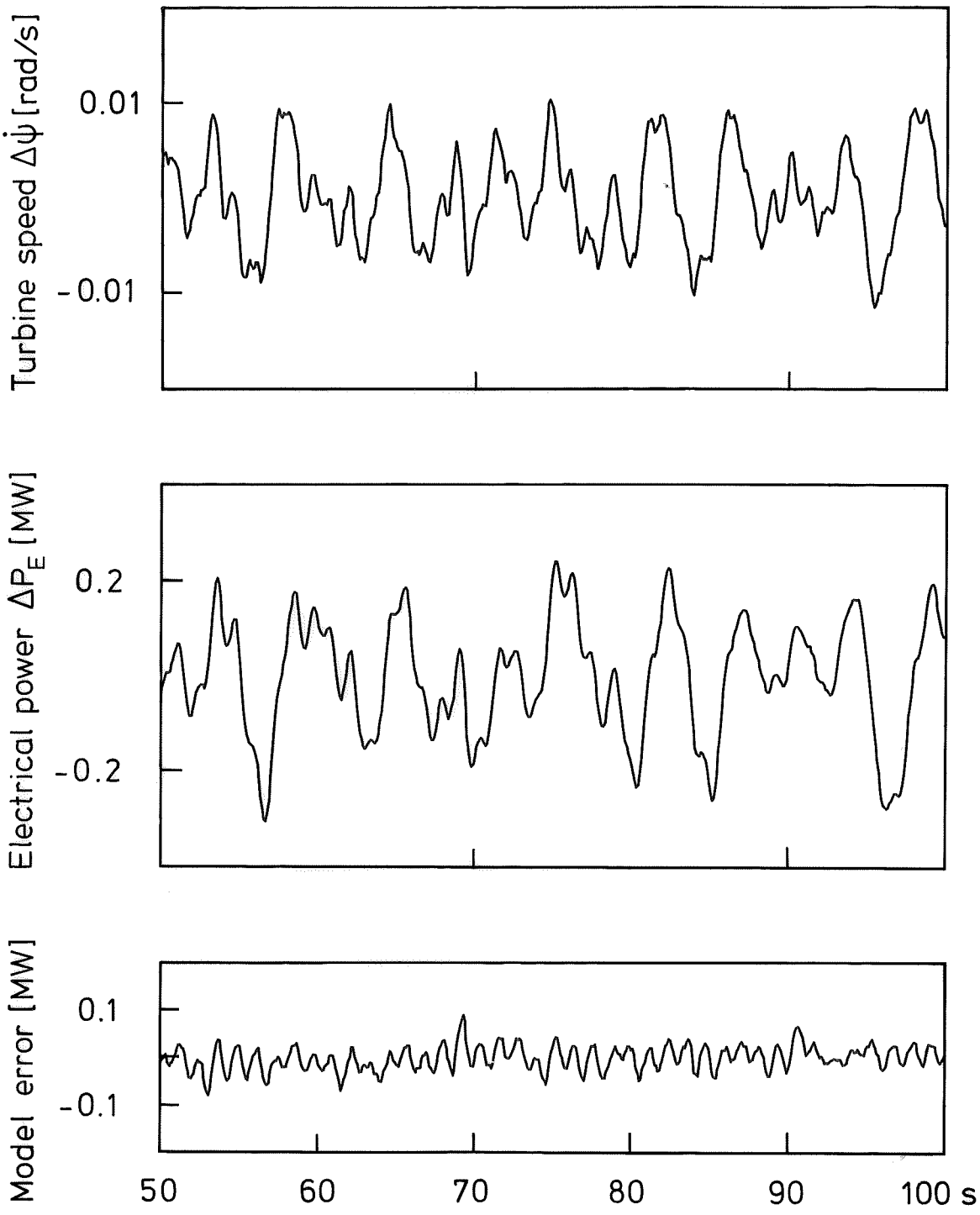

Figure 4.7: Measurements from series 3 and the model error of the model (4.24) with K_s = 9.4 MNm/rad, D_s = 4.3 MNms/rad and D_{s2} = 0. The measurements are low pass filtered with a second order Butterworth filter with the cut-off frequency 5 rad/s and high pass filtered with a second order Butterworth filter with the cut-off frequency 0.5 rad/s.

4.5 Wind Speed

The unavailability of representative wind speed measurements causes many problems. There is an anemometer on the nacelle. A few hundred meters from the plant there is a mast with several anemometers. Let U_N denote the output from the anemometer on the nacelle and U_M the output from the anemometer on the mast at an altitude of 75 m. The signal U_N is very strange. It has dips down to 8 - 10 m/s with a duration of about one second. See Figure 4.1. The signal U_M has no such dips. The plant probably induces local wind disturbances so that the anemometer on the nacelle gives bad measurements.

Measurement series 3 was used in the following, since it had the highest mean wind speed (> 16 m/s). The mean wind speed of series 1 is about 14 m/s. Measurement series 2 was collected just before measurement series 3. The wind dropped, however, to 11 - 13 m/s for a minute, while it was between 14 - 18 m/s for the rest of the time when series 2 was collected.

Measurement series 3 has the mean values $m(U_N)$ = 16.3 m/s and $m(U_M)$ = 16.7 m/s and the standard deviations $\sigma(U_N)$ = 2.07 m/s and $\sigma(U_M)$ = 0.60 m/s. From ΔU_M (sampling frequency 2 Hz) the ML-procedure gave the first order model

$$\Delta\dot{U}_M = -\Delta U_M/T_M + \sigma(U_M)\sqrt{2/(r_v T_M)}\, v \qquad (4.25)$$

with $T_M = 5 \pm 1$ s, where v is white noise with zero mean and noise intensity r_v. The model (3.4) can now be used to calculate estimates of the parameters in the wind model (2.2) for the mean wind speed ΔU_0 over the turbine disc. We get L = 84 m, $a_* = 0.63$ and $b_* = 0.73$, which gives the time constant T_w = 7.9 s and standard deviation σ_w = 0.44 m/s.

The integral scale L indicates that a typical eddy is of the same size as the rotor disc. In Section 3.2 it was pointed out that the correlation between the wind speed at the center of the disc and the mean value over the disc is about 0.6 when the eddies and the rotor disc are of the same size. This is another reason to why it is difficult to get representative measurements.

4.6 From Blade Servo and Wind To Electrical Power

We will now consider the behaviour from the blade servo and the wind speed to the electrical power. Consider first the models (2.33) - (2.39). They indicate as seen from (2.40) that the elasticity of the tower introduces a complex pole pair in the transfer function from $\Delta\beta_r$ to ΔP_E. According to Table 2.2 the natural frequency of the tower bendings is 2.2 rad/s. However, it turned out that the effect of the tower bendings could not be detected in the available measurements of β_r and P_E. The controller was designed so as not to excite the tower bendings. Furthermore, the models (2.34) and (2.40) indicate that the transfer functions from $\Delta\beta_r$ and ΔU_0 to ΔP_E have one one complex zero pair that lies close to the pole pair associated with the tower bendings. This indicates poor observability of the tower bendings in the electrical power. Consequently, it is not surprising that the pole pair associated with the tower bendings could not be detected by the identification procedure. To simplify further use of the physical models the tower bendings are neglected in the rest of this section.

The values in Table 4.1 represent our a priori knowledge of the system. The derivatives of the aerodynamical torques depend on the wind speed. They are calculated under the assumption that the mean wind speed $\bar{U}_0$ is 16.7 m/s and that the generated power P_E is 2.5 MW. The uncertainties in the calculations are indicated in the following. An increase of $\bar{U}_0$ with 1 m/s gives an increase of 10% in T_β, and an increase of 5% in T_U. An increase of P_E with 0.5 MW gives a decrease of 5% in T_β and an increase of 4% in T_U.

Table 4.1: Numerical values used in calculations with the physical models.

K_s	$7.7 \cdot 10^6$	Nm/rad	D_s	$3.0 \cdot 10^6$	Nms/rad
J_t	$5.1 \cdot 10^6$	kgm^2	T_{bs}	0.4	s
σ_w	0.44	m/s	T_w	7.9	s
T_β	$9.8 \cdot 10^6$	Nm/rad	T_U	$2.1 \cdot 10^5$	Ns
$T_{\dot{\psi}}$	$-6.0 \cdot 10^5$	Nms/rad			

If the sampling frequency was chosen to 10 Hz when identifying a model with the output ΔP_E and the inputs $\Delta\beta_r$ and ΔU_N, the ML-procedure mainly attempted to model the noise. Models for the 2P, 8P, 4P and 6P variations were obtained with increasing model order. Idpac's ML-procedure minimizes the one-step prediction error, which means that the noise characteristics are more important than the system dynamics for short sampling periods.

To eliminate the 4P, 6P and 8P variations the measured data were filtered with a second order Butterworth filter with the cut-off frequency 5 rad/s. The signals were resampled with 2 Hz. If it is assumed that $\Delta\beta_r$ varied linearly between the sampling instances the time discrete model gives a direct term. This is unfortunately not identifiable, since the controller also has a direct term. But fortunately, this is not too serious as shown by Figure 4.8. The discrete time transfer functions calculated using $\alpha = 0$ or $\alpha = 1$ have the same poles. Below 2 rad/s the difference in amplitude is less than 10% and in phase less than 25° below 2 rad/s.

The ML-procedure and Idpac's test procedures indicate that ΔU_N has low explanatory significance for variations in the electrical power. The variations are picked up in the noise model. A fifth order model is obtained if both $\Delta\beta_r$ and ΔU_N are used as input. A sixth order model is obtained if only $\Delta\beta_r$ is used as input. The fifth order model is just on the borderline for acceptance. Figure 4.9 shows that the estimated transfer functions from the white noise e to ΔP_E are similar whether ΔU_N is used as input or not. Figure 4.10 compares the noise model of the estimated sixth order model with the physical model. Note that the 2P variations are not included in the physical model. It is hard to analyse the uncertainties in the transfer function. The ML-procedure gives a covariance matrix for the uncertainties of the parameters. Idpac's RANPA-command provides a facility which can give us an idea of the uncertainties. It generates a new model by picking parameters with the random distribution given by the estimated parameters and their covariance matrix. Figure 4.11 shows the transfer functions for four such models. The physical noise model lies within the uncertainties of the estimated noise model.

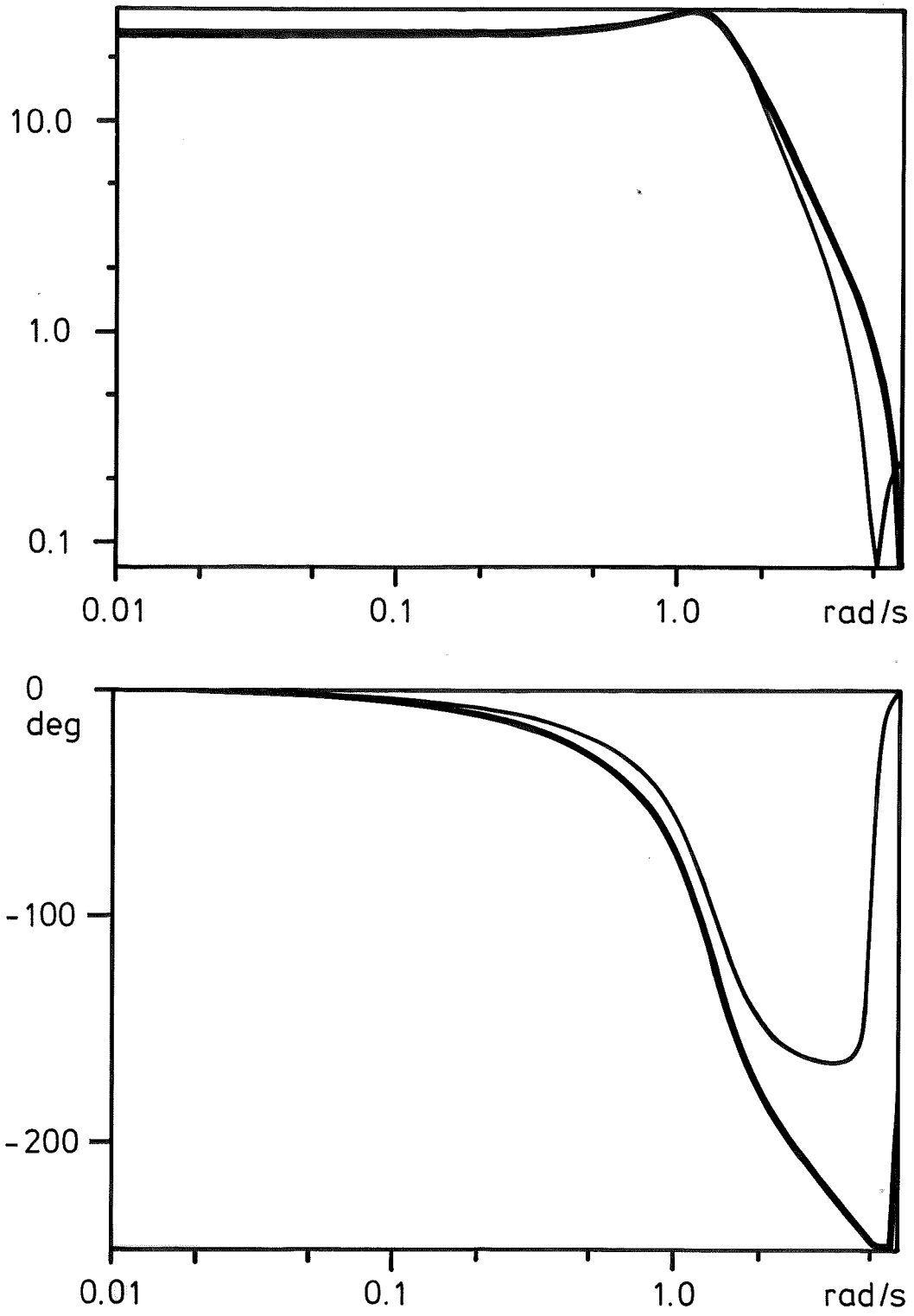

Figure 4.8: Bode plots of the transfer functions from $\Delta\beta_r$[rad] to ΔP_E [MW] calculated from models (2.33) - (2.38) using the parameter values in Table 4.1. The bold lines are for $\alpha = 0$ and the thin lines are for $\alpha = 1$.

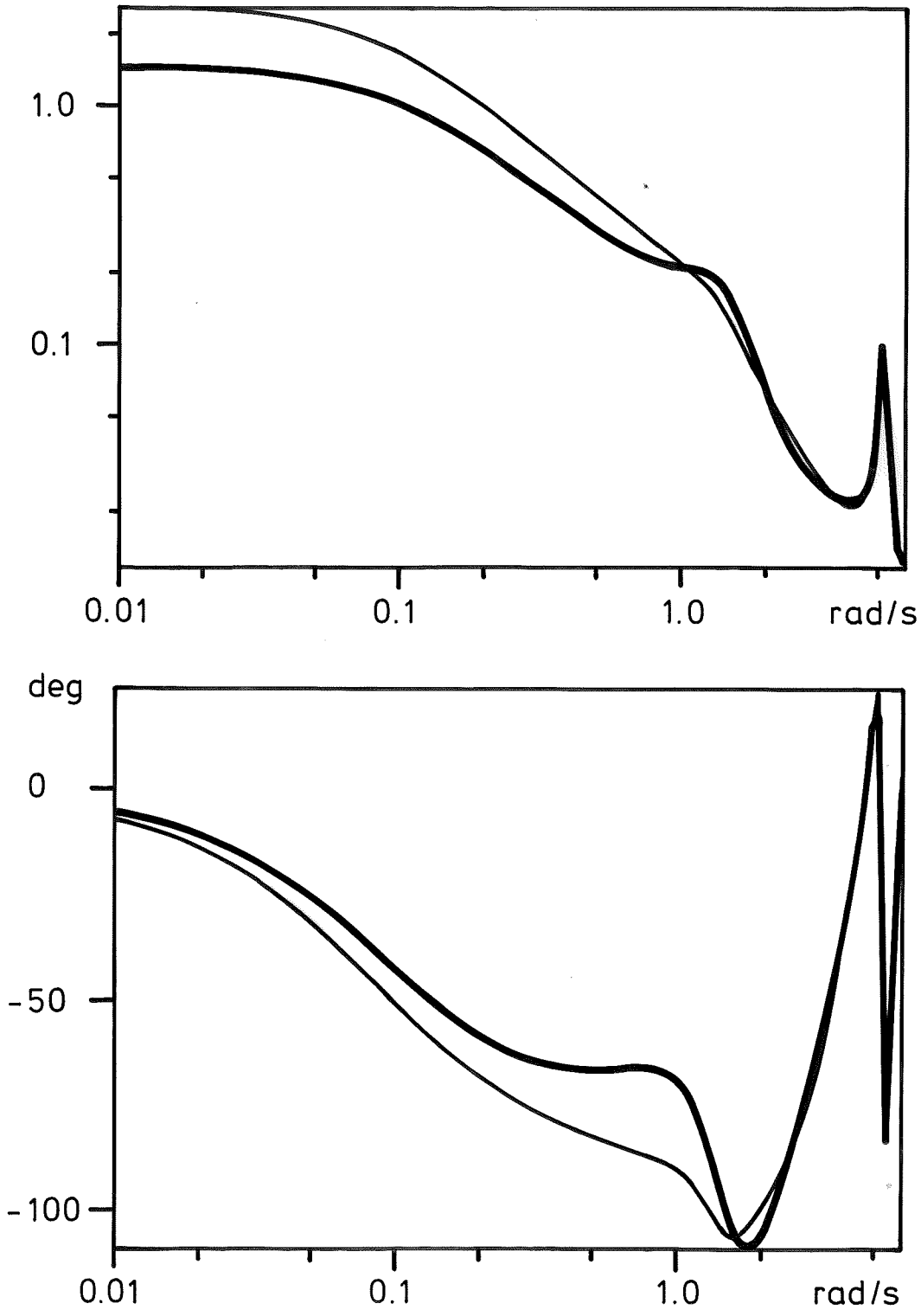

Figure 4.9: Bode plots of the transfer function from the white noise e to ΔP_E [MW]. The bold lines are for the estimated fifth order model with the inputs $\Delta\beta_r$ and ΔU_N. The thin lines are for the estimated sixth order model with the input $\Delta\beta_r$.

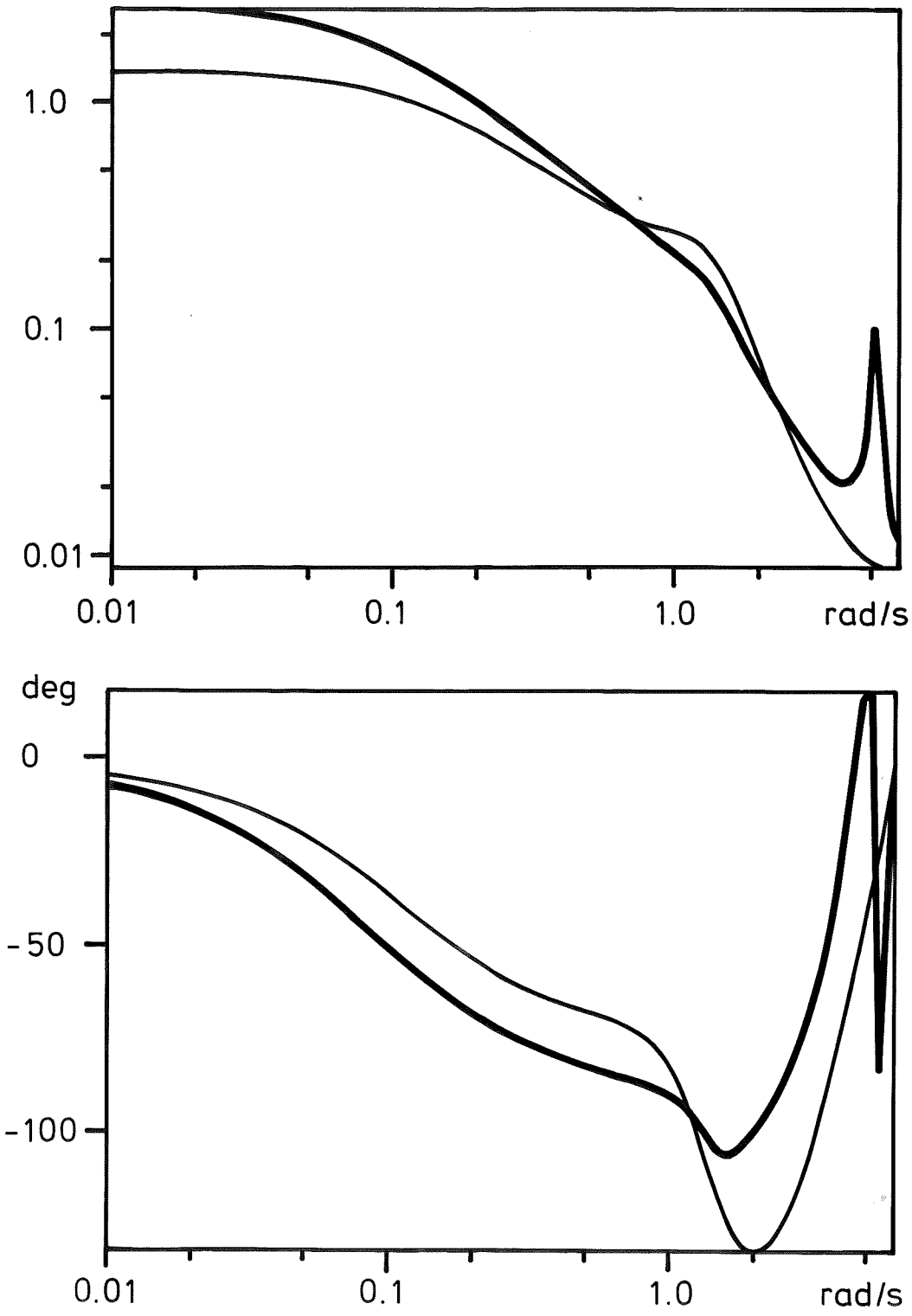

Figure 4.10: Bode plots of the transfer function from the white noise e to ΔP_E [MW]. The bold lines are for the estimated sixth order model with the input $\Delta\beta_r$. The thin lines are for the models (2.2) and (2.33) - (2.38) with the parameter values in Table 4.1.

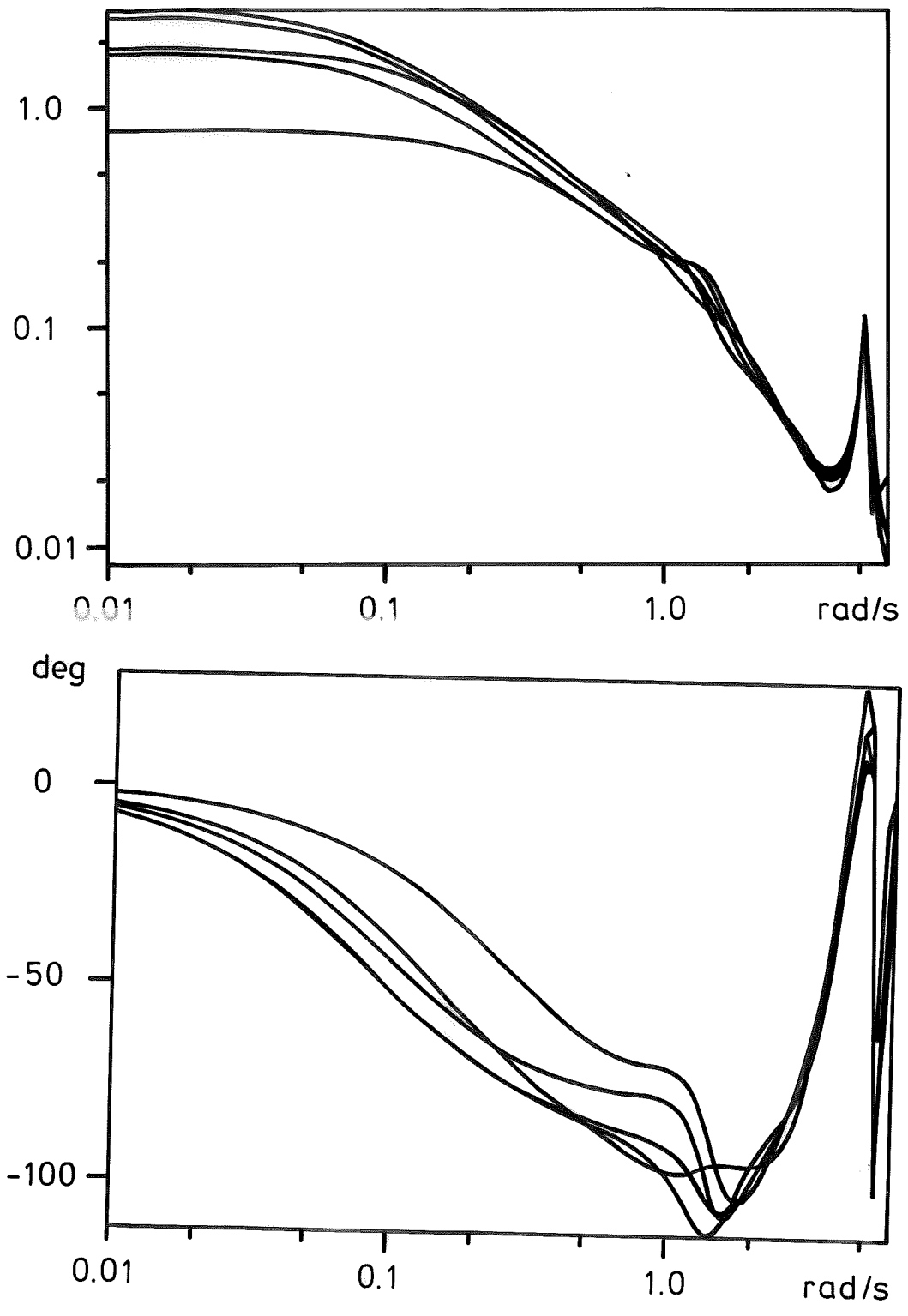

Figure 4.11: Bode plots of the transfer functions from the white noise e to ΔP_E [MW] for the estimated sixth order model and four models picked with the random distribution given by the estimated parameters and their covariance matrix.

Figure 4.12 shows the Bode plot of the transfer function from $\Delta\beta_r$ to ΔP_E for the estimated sixth order model. The poor explanatory power of ΔU_N is unfortunate, since it implies a larger statistical uncertainty. It also introduces numerical problems. The A-polynomial needs a zero close to one to model the turbulence. To eliminate that pole in the transfer function from $\Delta\beta_r$ the B-polynomial must have a zero close to one. This is hard to obtain numerically. The location of this pole is quite uncertain. It can be eliminated by using $(1-q^{-1})\Delta\beta_r$ as input and $(1-q^{-1})\Delta P_E$ as output when making ML-identification of the deterministic part. A fourth order model is then obtained. Figure 4.13 shows the Bode plot of the transfer function of that model. Figure 4.14 illustrates uncertainties. It is hard to estimate the static gain, because, as the model (2.2) indicates, the wind has a great amount of energy at low frequencies.

The estimated model has one complex pole pair corresponding to the 2P variations and one complex pole pair at 0.62 ± 0.52i, which in continuous time corresponds to -0.4 ± 1.4i. Interpretation of this pole as the pole of the soft shaft mode gives $(D_s-T_\psi^i)/J_t = 0.85\ (\text{s rad})^{-1}$ and $K_s/J_t = 2.13\ (\text{s}^2\text{rad})^{-1}$. In Section 4.4 the values K_s = 9.4 MNm/rad and D_s = 4.3 MNms/rad were estimated from the relation between turbine speed and electrical power. These values then give $J_t = (5 \pm 0.5)\cdot 10^6\ \text{kgm}^2$. A possible explanation to the absence of the servo pole is that it is hard to detect because the continuous time pole is close to the zero at $-K_s/D_s$.

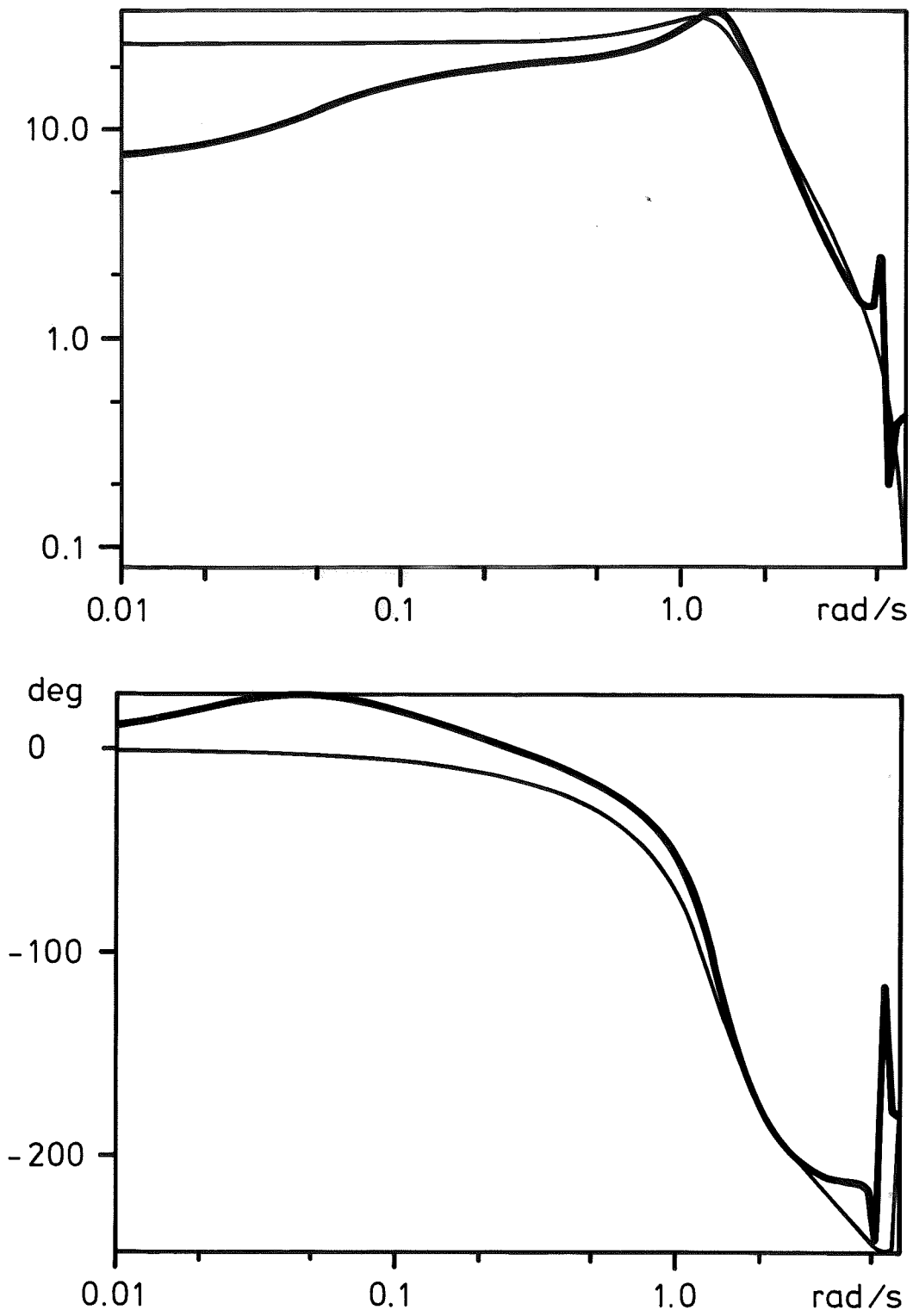

Figure 4.12: Bode plots of the transfer function from $\Delta\beta_r$ [rad] to ΔP_E [MW]. The bold lines are for the estimated sixth order model with the input $\Delta\beta_r$. The thin lines are for the models (2.33) - (2.38) with the parameter values in Table 4.1 and $\alpha = 0$.

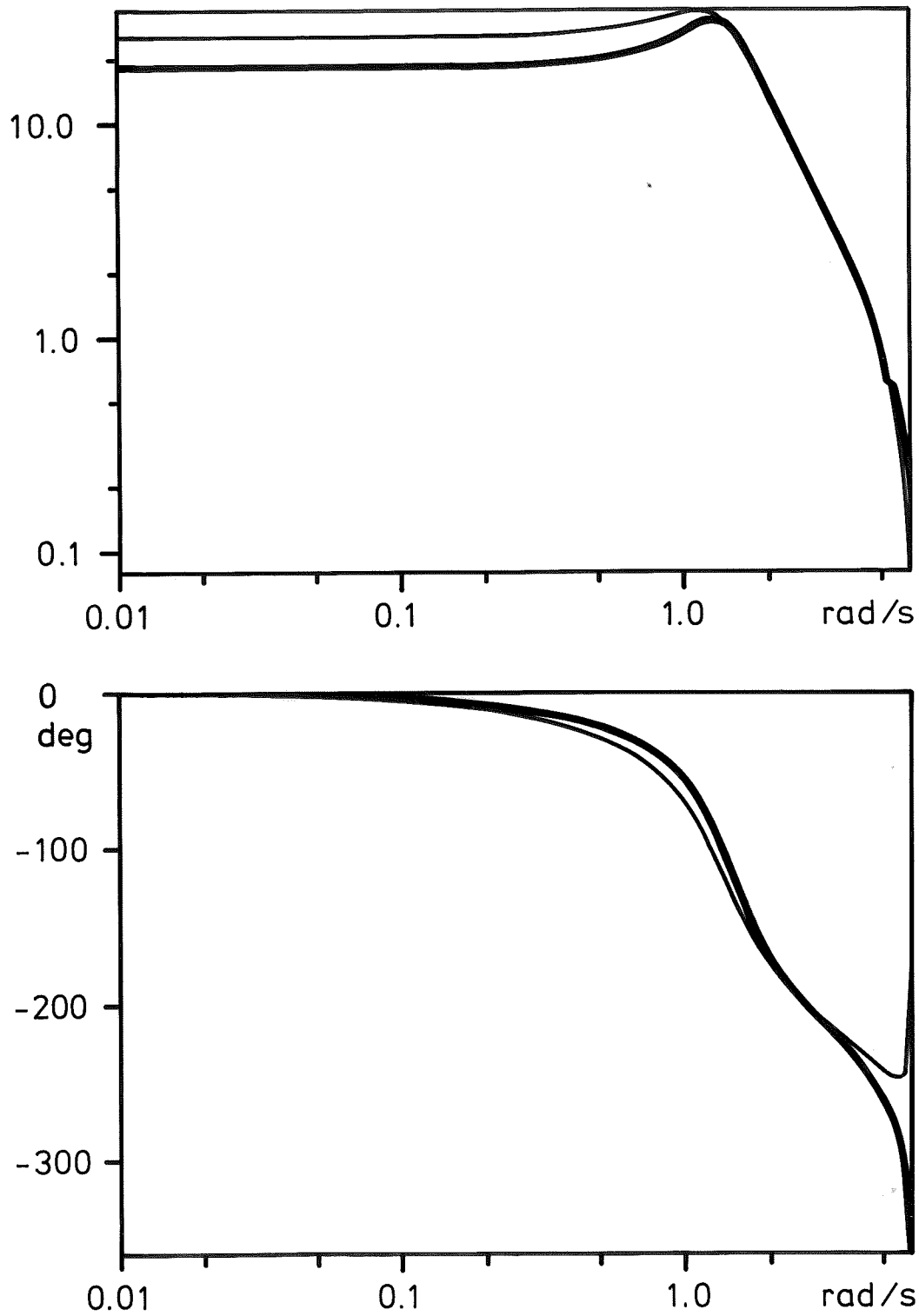

Figure 4.13: Bode plots of the transfer function from $\Delta\beta_r$ [rad] to ΔP_E [MW]. The bold lines are for the estimated fourth order model. The thin lines are for the models (2.33) - (2.38) with the parameter values in Table 4.1 and $\alpha = 0$.

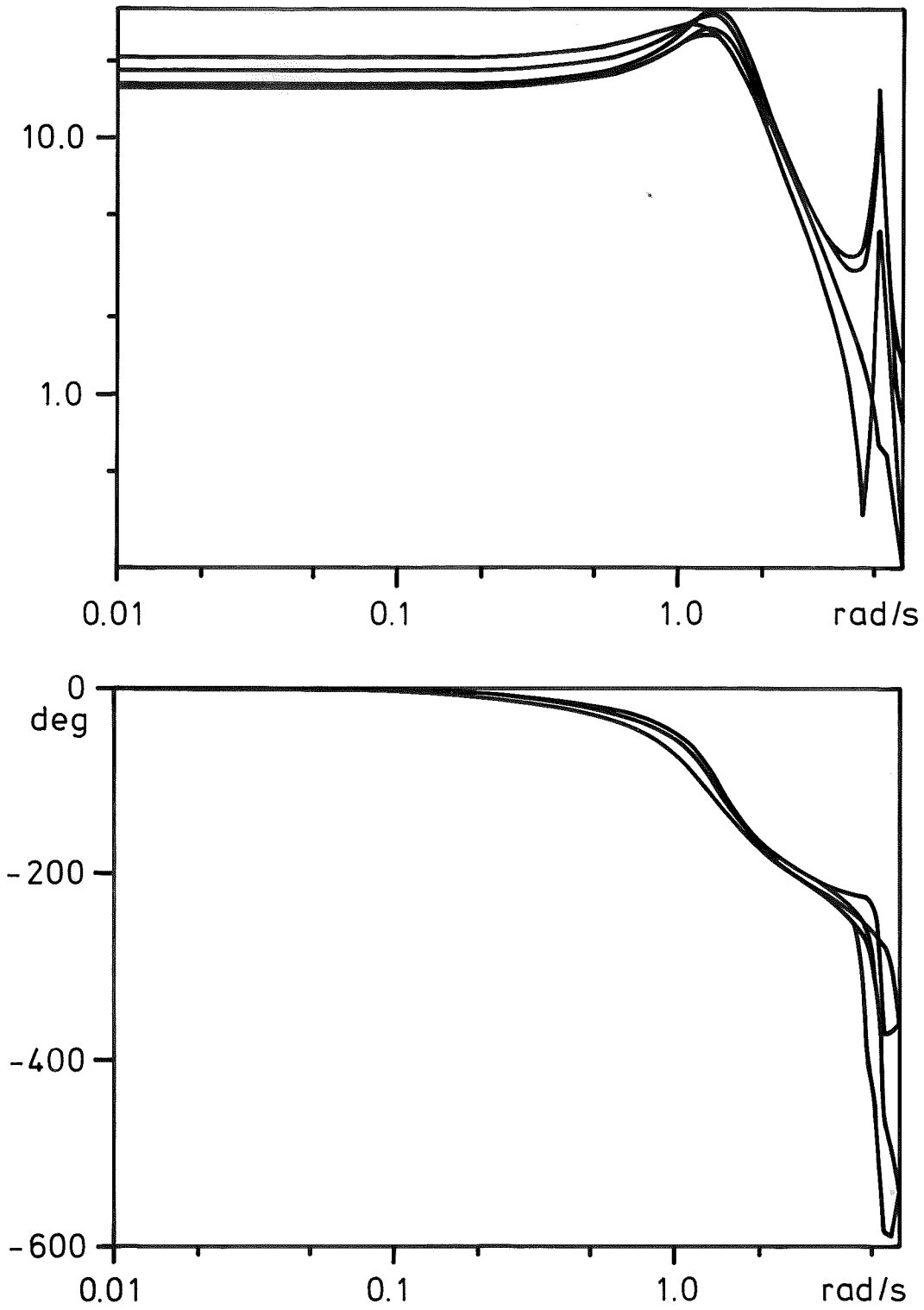

Figure 4.14: Bode plots of the transfer functions from $\Delta\beta_r$ [rad] to ΔP_E [MW] for the estimated fourth order model and four models picked with the random distribution given by the estimated parameters and their covariance matrix.

4.7 The 2P Variations in the Generated Power

We will now investigate the properties of the 2P variations in the electrical power. A possible model for them is

$$\begin{aligned} P_{E2P}(t) &= A(t)\cos(2\psi(t)+\alpha(t)) \\ &= A(t)\cos\alpha(t)\cos 2\psi(t) - A(t)\sin\alpha(t)\sin 2\psi(t) \\ &= C_1(t)\cos 2\psi(t) + C_2(t)\sin 2\psi(t) \end{aligned} \tag{4.26}$$

where the amplitude A(t) and the phase $\alpha(t)$ in some sense should vary slowly compared to the frequency 2P. Furthermore, the coordinate system is chosen such that the blades are in vertical position when $\psi = 0$.

We will use a recursive least square method with exponential weighting to estimate $C_1(t)$ and $C_2(t)$. Estimates of A(t) and $\alpha(t)$ are then calculated from $\hat{C}_1(t)$ and $\hat{C}_2(t)$. Let h denote the sampling period. Introduce $\theta(t)$ and $\varphi(t)$ as

$$\theta(t) = [C_1(t) \quad C_2(t)]^T \tag{4.27}$$

$$\varphi(t) = [\cos 2\psi(t) \quad \sin 2\psi(t)]^T \tag{4.28}$$

Hence

$$P_{E2P}(t) = \theta(t)^T\varphi(t) \tag{4.29}$$

An estimate $\hat{\theta}(t+h;t)$ of $\theta(t+h)$ based on data available up to time t is now given by the following expressions

$$\hat{\theta}(t+h;t) = \hat{\theta}(t;t-h) + P(t)\varphi(t)\varepsilon(t) \tag{4.30}$$

$$\varepsilon(t) = \Delta P_E(t) - \hat{\theta}(t;t-h)^T\varphi(t) \tag{4.31}$$

$$\begin{aligned} P(t) &= \frac{1}{\lambda}\left[P(t-h) - \frac{P(t-h)\varphi(t)\varphi(t)^T P(t-h)}{\lambda + \varphi(t)^T P(t-h)\varphi(t)}\right] \\ &= (\lambda P(t-h)^{-1} + \varphi(t)\varphi(t)^T)^{-1} \end{aligned} \tag{4.32}$$

If we start with $P(t_0)^{-1} = 0$ and $\hat{\theta}(t_0+h;t_0) = 0$ then $\hat{\theta}(t_0+nh;t_0+(n-1)h)$ minimizes the criterion

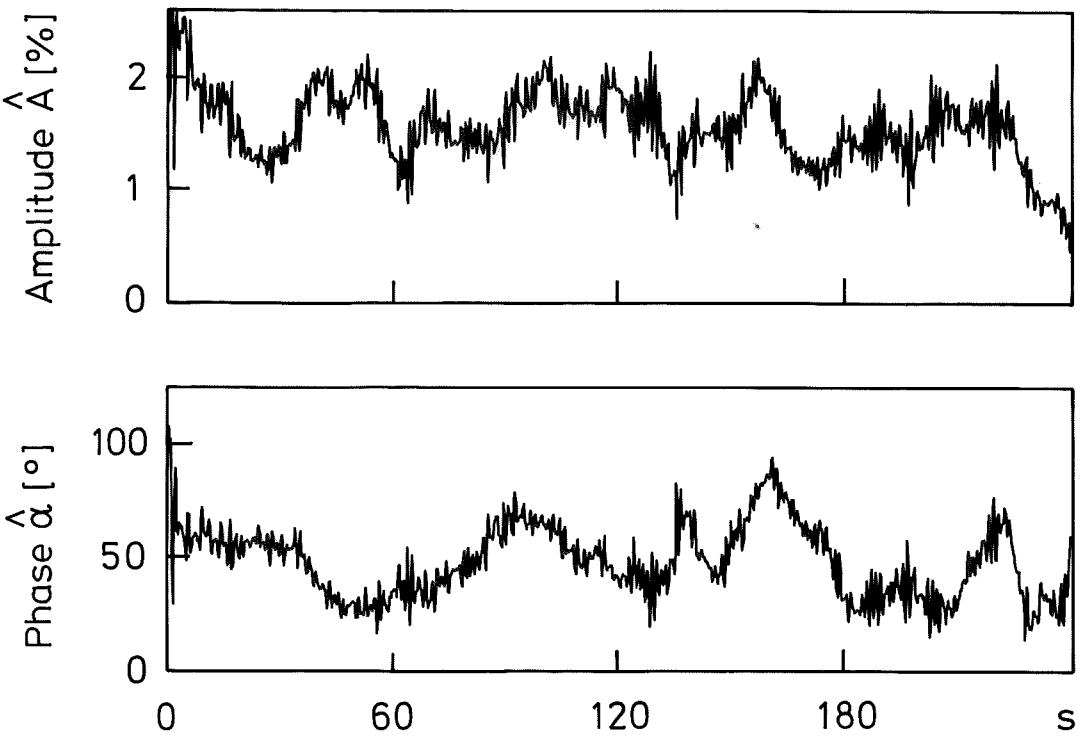

Figure 4.15: Estimates for measurement series 1. The forgetting factor λ was 0.99 and the sampling period h was 0.1 s.

$$J(\theta) = \sum_{i=1}^{n} \lambda^{2(n-i)} \left[\Delta P_E(t_0+ih) - \theta^T \varphi(t_0+ih)\right]^2 \qquad (4.33)$$

where λ is called the forgetting factor. As indicated by (4.33) it gives a possibility to discount old data.

A typical example of estimates obtained is given in Figure 4.15. The residual $\varepsilon(t)$ given by (4.31) is the difference between ΔP_E and $\hat{P}_{E2P}$. The procedure given above for calculating ε from ΔP_E and ψ can be viewed as a filter which attenuates the 2P variations. Since this filter is nonlinear, we cannot describe it with a transfer function. We can, however, calculate the power spectrum of $\varepsilon(t)$ and compare it with the power spectrum of ΔP_E. Figure 4.16 shows the power spectra of $\varepsilon(t)$ and $\Delta P_E(t)$. The spectral density is decreased in a small band around 2P. At 2P it is decreased a factor of ten. Otherwise it is almost unchanged. If the forgetting factor λ is 0.98 the spectrum of $\varepsilon(t)$ is almost similar to that for λ = 0.99, but the estimates are noisier.

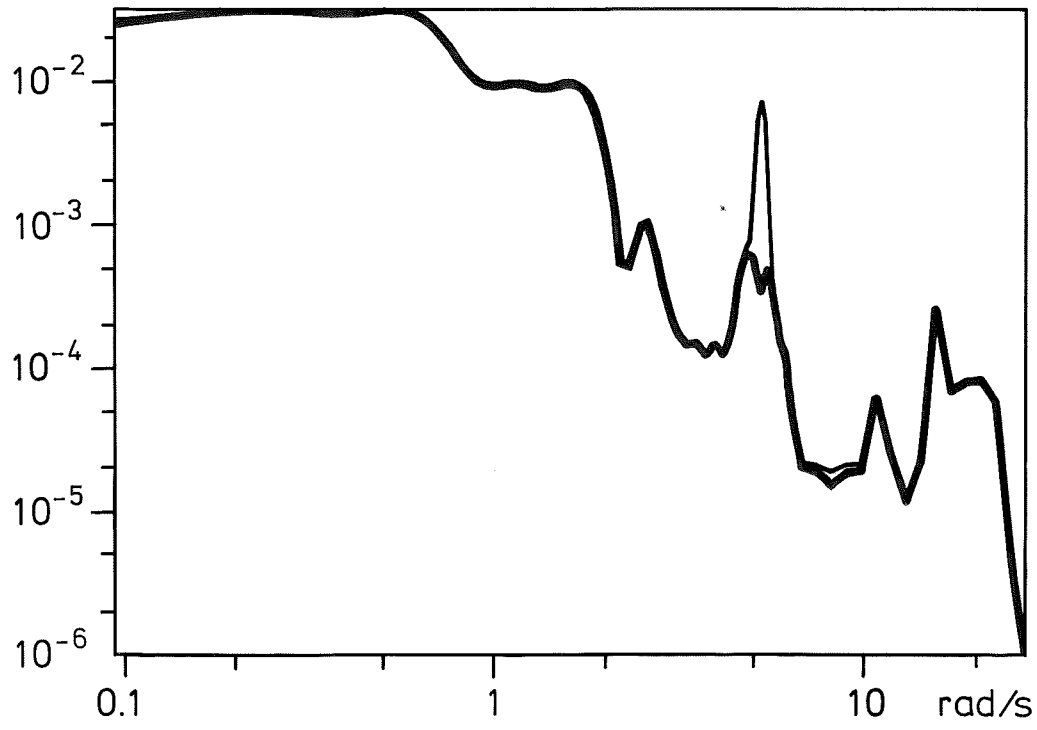

Figure 4.16: The bold line is the power spectrum of ϵ (in MW) for measurement series 1 when the forgetting factor is 0.99. The thin line is the power spectrum of P_E (in MW) for measurement series 1.

The estimated amplitude $\hat{A}$ lies within 1 - 3% of the rated power. This means that the 2P variations in the aerodynamical torque is in the range of 10 - 30% of the rated turbine torque. There are three major sources of the 2P variations in the aerodynamical torque: the wind profile, the tower blockage and the rotational sampling of the turbulence eddies. These are discussed in Section 3.2. The 2P disturbance caused by the tower blockage is there estimated to be 0.7% of rated power. This disturbance has constant phase in relation to the turbine angular position. Figure 2.1 indicates that the dynamics from aerodynamical torque to electrical power introduces a phase lag of 100 - 120°. This combined with the fact that the tower decreases the flow when $2\psi \bmod 2\pi = 0$ imply that α would be 60 - 80° if the tower blockage was the only source for the 2P variations. The mean value of $\hat{\alpha}$ seems to lie in this range, but $\hat{\alpha}$ is not constant. The estimated amplitude $\hat{A}$ is significantly greater than 0.7%. Rotational sampling of turbulent eddies is a very probable explanation to the varying phase and the larger amplitude. The integral scale L is above estimated to 84 m, which means that 'typical' eddies are of the same size as the rotor disc.

4.8 Summary

The measurements from the WTS-3 showed that the servo model (2.38) is a very good model in the frequency range up to at least 10 rad/s. The relations (2.34) - (2.35) are a good model for the relation between the turbine speed and the electrical power at least in the frequency range 0.5 - 5 rad/s. This is sufficient for pitch angle control.

The signal from the anemometer on the nacelle turned out to have poor explanatory power for the variations in the electrical power. This signal was quite different from signals from anemometers in a mast a few hundred meters from the plant. This indicates that the plant induced local disturbances so that the anemometer on the nacelle gave bad measurements. Identification using the signal from an anemometer on the mast at an altitude of 75 m gave a model of the type (2.2).

The lack of representative wind speed measurements complicated the identification of the dynamics from blade angle to electrical power, since not only blade angle variations but also wind speed variations is a source of the variations in the electrical power. The variations in the electrical power caused by wind speed variations had to be modelled by noise. This increased the statistical uncertainty. Above the frequency 2P it was not possible to identify the system dynamics due to the large disturbances at 2P, 4P, 6P and 8P. The wind speed has as indicated both by (2.2) and the identified model, high spectral density for low frequencies. This gave an uncertainty in the estimated static gain of 20 - 30%. The dynamics of the soft shaft was very significant in the identified models. The tower bendings did not appear in the models, because the controller was designed so as not to excite the tower. Furthermore, the physical model indicates poor observability of the tower bendings in the electrical power. No dynamics was found which could not be explained by the models (2.33) - (2.38) or the statistical uncertainty.

Estimation of the 2P variations in the electrical power showed that the amplitude varied between 1 - 3% of mean power. Neither the amplitude nor the phase relative to the blade position was constant. The conclusion is that aside from the disturbance caused by the tower blockage there is a random component due to the turbulence.

5. CONTROL

A wind turbine system connected to an electrical network is intended to produce power by transforming wind energy into electrical energy with an optimal overall efficiency. It is of course desirable that the plant extracts as much energy as possible, but this does not mean that a strategy that maximizes instantaneous power gives the best overall economic results. A safe and reliable operation must be guaranteed to give the system a lifetime of 20 - 30 years with low maintenance and repair costs. The limited capability of the plant to withstand mechanical stress must be considered. The operation is also constrained by demands from the environment. Some demands emanate from the desire to have a stable utility grid, but there are others like that the acoustic noise should be low. This discussion indicates that the regulator design may be viewed as a constrained dynamic optimization problem. It is, however, not obvious how such a problem should be formulated. First, there are open questions concerning energy prices and fatigue. Second, there are strong interactions between process design and regulator design, since the outcome may depend critically on constraints due to the process design. Third, constrained dynamic optimization problems are often difficult to solve. It is thus desirable to simplify the problem as much as possible. The control objectives are discussed further in Section 5.1.

The system has the following control signals: the orientation of the turbine, the pitch angle and possibly the excitation of the generator. It has many variables that may be of interest to control: orientation relative to the wind, electrical power, terminal voltage and mechanical stress in blades and tower. It is an important task to find out if the control actions have to be coordinated. The control problem is simplified considerably if the different control actions can be considered to be independent. The need for coordination is discussed further in Section 5.2.

Pitch angle control is discussed in Sections 5.3 and 5.4. The case when the system has a synchronous generator or an induction generator is discussed in Section 5.3. In this case the turbine must operate at an almost constant speed and pitch angle control is the only means of controlling generated power. This imposes severe constraints on the system. Other generator systems, which allow variable turbine speed and control of the power output at the generator, are discussed in Section 5.4.

5.1 Control Objectives

Extraction of maximum power means that generated power follows the wind variations since the plant cannot store significant amounts of energy. Holm and Lindström (1982) have studied installation of wind power in the Swedish utility grid up to 30% of the total electrical power. They conclude that, on second and minute timebases, variations of the wind do not cause any frequency control problems and do not require any extensive increase of the reserve, since the variations from different plants are not coherent.

Neither do the demands on the voltage cause any significant problems. The Swedish norm for acceptable voltage variations in a low-voltage system is based on the sensitivity of the eye to light flickering. The eye is most sensitive to variations having frequencies between 15 and 20 Hz. In this frequency range the acceptable variations are as low as 0.3%. At frequencies around 1 Hz the voltage variation may be 0.8%. For occasional voltage fluctuations such as start-ups a few times a day, the norm accepts a 2.5% voltage fluctuation.

Strain and stress limit the generated power. As pointed out in Section 2.3 the bending moments at the root sections of the blades are critical. The shaft torque are also critical. The supervisory system of the WTS-3 disconnects the generator and initiates an emergency shutdown, if the generated power exceeds 140% of rated power. The control system must not excite elastic modes in blades and tower. Fatigue is another serious problem. The parts of the turbine are typically supposed to withstand 10^8 load cycles during the plant lifetime. This is about 100 times more than for ordinary constructions. It is an open question how available data should be extrapolated and how the load cycle calculations should be done.

It is important to have a safe and reliable system so that breakdowns are avoided. The demands emanating from the mechanical parts are decisive for pitch angle control during normal operation. There are of course also basic demands like that a synchronous generator should remain in synchronism with the grid. A loss of the synchronism caused directly by the wind should not be possible. A torque in the magnitude of twice rated torque is required to pull a synchronous generator out of synchronism. Such a high power generation cannot be tolerated for safety reasons. The generator itself constrains the power output. If generated power is

greater than rated power for longer times, the generator may be overheated and damaged.

It is a difficult mathematical problem to handle load limits in the regulator design and to guarantee that they are not exceeded while at the same time maximizing the power generation. To obtain a good result, a good model for the wind gusts is required. Such models are not available today. A common control strategy is to let the controller try to extract maximum power up to a certain level P_{E0} and to keep the power generation constant above this level. The control must not excite the elastic modes of the tower and the blades. The level P_{E0} is chosen in such a way that the controller can keep the peak loads inside the design limits with a high probability. It may depend on the weather conditions. Thus the controller should try to maximize the power generation when the mechanical loads are small and it should try to achieve a smooth operation for high mechanical loads. This decreases the risks for fatigue. Furthermore, it gives a design problem that can be handled satisfactorily using existing control theory. The better the generated power can be held constant at P_{E0} the closer P_{E0} can be chosen to the design limits.

A standard technique to 'guarantee' that the limits are not exceeded is to introduce a supervisor and new 'fictitious' limits inside the 'real' limits. If one of these fictitious limits is exceeded, the system should be put in an emergency mode. In the emergency mode the objective is to avoid excess of the real limits; for example backup systems may be invoked to provide a safe shutdown.

5.2 Coordination of Control Actions

Both the orientation of the turbine rotor (the yaw control) and the pitch angle of the blades influence the driving aerodynamical torque. The purposes of the two controls are, however, different. The yaw control intends to orient the turbine correctly to achieve high efficiency and to avoid large dynamical loads caused by cross winds. The yaw control should eliminate the effects of variations in the wind direction, not the effects of variations in wind speed. The pitch angle control should take care of the variations in wind speed experienced by the turbine rotor. Since the wind speed experienced by the rotor depends on the orientation,

the pitch angle control can be more effective if the actions of the yaw controller are known. However, no coordination is necessary, since the yaw drives are slow.

As found in Section 2.2 the synchronous generators of the MOD-2 and the WTS-3 have a second torsional mode at 25 rad/s with low damping. A high frequency disturbance around 25 rad/s is needed to excite this mode. Due to the low pass filtering effect of the large turbine and the soft shaft, this mode is barely influenced by the wind variations or by the blade servo. For the WTS-3 such large and rapid disturbance as the loss of driving torque, when a blade passes behind the tower, causes only few small oscillations that die out before the next blade comes into the tower shadow. The second torsional mode may, however, be excited by the grid and also by the excitation control. Consequently, the damping and control of this mode is an internal electrical problem. It can be neglected when designing the pitch blade control. There may be a conflict between using the excitation system for voltage control and damping of the generator oscillations. It is probably a good approach to assume that pitch and excitation control can work independently in normal operation when a synchronous generator is used.

The situation is somewhat different when a variable speed generator is used. To obtain maximum power the tip speed/wind speed ratio and the pitch angle should be constant. This means that the generator should let the turbine speed vary with the wind speed. However, critical speeds causing structural resonances must be avoided. As found in Section 2.2 the allowed range for the generator speed depends on the generator. There are systems which allow the generator speed to vary in the range 4 - 130% of synchronous speed. For the Growian I the range is only 85 - 115% of synchronous speed and the possibility of varying the turbine speed is not intended to be used to maximize the generated power, but the plant is desired to operate close to synchronous speed. Here, it is natural to let the pitch angle control try to extract maximum power. The generator control can use the large inertia to improve the power quality under the constraint that the generator rotor speed should be kept inside the allowed interval. Above the power level P_{E0} it is natural to let the pitch angle control keep the turbine speed constant and let the generator control keep the shaft torque constant. It is also possible to accept variations in shaft torque and improve the power quality.

5.3 Pitch Angle Control for Constant Speed Plants

In this section pitch angle control for systems with a synchronous generator or an induction generator is discussed.

Figure 2.6 indicates that it is not difficult to obtain a good result when trying to maximize the generated power. The maxima of the aerodynamical torque are rather flat with respect to the blade angle and the maxima for different wind speeds are close to each other. It is no use to follow rapid wind variations like the 2P variations, since compared to possible power gain it gives excessive servo motions. The control can be based on nonlinear feedback from the generated power P_E and the pitch angle β in the following way. From measured P_E (possibly filtered) and β the wind speed, U_0 is calculated neglecting the dynamics. From U_0 the optimal pitch angle is calculated giving the reference value β_r to the servo. However, it is more difficult to gain the last few per cent of the available power, since it requires good knowledge of the actual wind and the actual aerodynamical characteristics of the blades. Furthermore, it is important to have a well-adjusted blade servo, so that bias does not ruin the result. If the blade angle is increased too much stalling appears and the situation becomes more complex with hysteresis. Rasmussen and Pedersen (1982) report that skew wind may cause high dynamical loads on a stalled turbine.

Figure 2.6 shows that the WTS-3 is able to produce rated power already at about a wind speed of 13.5 m/s, but the WTS-3 is not allowed to do that until the wind speed is over 14.2 m/s. Figures 2.6 and 2.7 show that the thrust increases with the wind speed when generated power is maximized. By not extracting maximum power, but keeping the thrust below a certain limit, excessive blade loads are avoided.

Note that it is difficult for pitch angle control to dampen the first torsional mode when maximizing the power output. The control authority is low, because the system then operates close to the maximum and there is $\partial T/\partial\beta$ small. Furthermore, the maxima are flat. This means that large servo motions are needed to dampen the oscillations.

Above the level P_{E0} the control objective is to keep the power output constant. One difficulty is that the system is nonlinear. The only important nonlinearity is that from the pitch angle, the wind speed and turbine speed to the driving aerodynamical torque. It makes the process gain vary with the wind speed. Transformations or gain scheduling are common ways to handle such effects.

Linear Quadratic Gaussian (LQG) control theory (for example, see Åström (1970), Anderson and Moore (1971) and Kwakernaak and Sivan (1972)) is useful for the linear design. It makes it possible to estimate the possibilities and limitations of pitch angle control and it reveals difficulties in a simple way. The separation theorem is useful. It says that the optimal control strategy can be separated into two parts: one state estimator, which gives the best estimates of the states from the observed outputs, and one linear feedback law from the estimated states. This means that the processing of the measurements and the pitch angle control can be discussed separately.

The rest of this section is organized as follows. Design of pitch angle control for the WTS-3 at a given weather condition using LQG control theory is first discussed in detail. Effects of different plant designs, weather conditions and nonlinearities are then discussed.

Models

In Section 2.5 it was found that horizontal axis wind turbines with synchronous generators or induction generators have similar basic behaviour from the aerodynamical torque T to the electrical torque T_E. To simplify the discussion we will first limit discussion to the WTS-3 and assume that the tower is rigid.

The LQG control theory assumes a linear state space model. We will use the models (2.2) and (2.33) - (2.38) to describe the deviations from the stationary operating point defined by the mean wind speed $\bar{U}_0$, the synchronous turbine speed $\dot{\psi}_0$, and the desired power level P_{E0}. This linear model can be written as

$$\begin{cases} \Delta\dot{x} = A\cdot\Delta x + B\cdot\Delta\beta_r + B_w\cdot w \\ \Delta x = \begin{bmatrix} \Delta\beta & \Delta U_0/100 & \Delta\dot{\gamma} & \Delta\gamma \end{bmatrix}^T \end{cases} \qquad (5.1)$$

where the servo reference $\Delta\beta_r$ is the control input and w is the white noise which is input to the model giving the mean wind speed U_0 over the rotor disc.

Table 5.1: Numerical values used in the design.

$\dot{\psi}_B$	2.618	rad/s	P_B	$3.0 \cdot 10^6$	W
$\dot{\psi}_0$	2.618	rad/s	P_{E0}	$3.0 \cdot 10^6$	W
J_t	$5.1 \cdot 10^6$	kgm^2	M_T	$2.1 \cdot 10^5$	kg
K_s	$7.7 \cdot 10^6$	Nm/rad	K_T	$9.4 \cdot 10^5$	N/m
D_s	$3.0 \cdot 10^6$	Nms/rad	D_T	$1.1 \cdot 10^4$	Ns/m
T_β	$1.0 \cdot 10^7$	Nm/rad	F_β	$1.8 \cdot 10^6$	N/rad
T_U	$2.4 \cdot 10^5$	Ns	F_U	$3.0 \cdot 10^4$	Ns/m
$T_{\dot{\psi}}$	$-7.6 \cdot 10^5$	Nms/rad	$F_{\dot{\psi}}$	$-4.5 \cdot 10^4$	Ns/rad
$T_{\dot{z}}$	$-2.8 \cdot 10^5$	Ns	$F_{\dot{z}}$	$-3.7 \cdot 10^4$	Ns/m
T_{bs}	0.4	s	$\bar{U}_0$	18	m/s
σ_w	1.8	m/s	T_w	20	s

The possibilities of measuring different quantities and models for measurement noise are discussed further below.

The interactive program package Synpac (Wieslander (1980b)) was used to carry out the LQG-design. The linear models for the servo, the turbine, the tower and the wind were entered in Synpac and connected together to give the total system. This structured description was useful, because it made it easy to modify parts of the system.

The design for a mean wind speed $\bar{U}_0$ around 18 m/s will now be discussed. Unless otherwise stated, the numerical values given in Table 5.1 are used. Using SI-units, we get for model (5.1):

$$A = \begin{bmatrix} -2.5 & 0 & 0 & 0 \\ 0 & -0.05 & 0 & 0 \\ 2.0 & 4.7 & -0.74 & -1.5 \\ 0 & 0 & 1 & 0 \end{bmatrix}, \quad B = \begin{bmatrix} 2.5 \\ 0 \\ 0 \\ 0 \end{bmatrix}, \quad B_w = \begin{bmatrix} 0 \\ 0.0057 \\ 0 \\ 0 \end{bmatrix} \qquad (5.2)$$

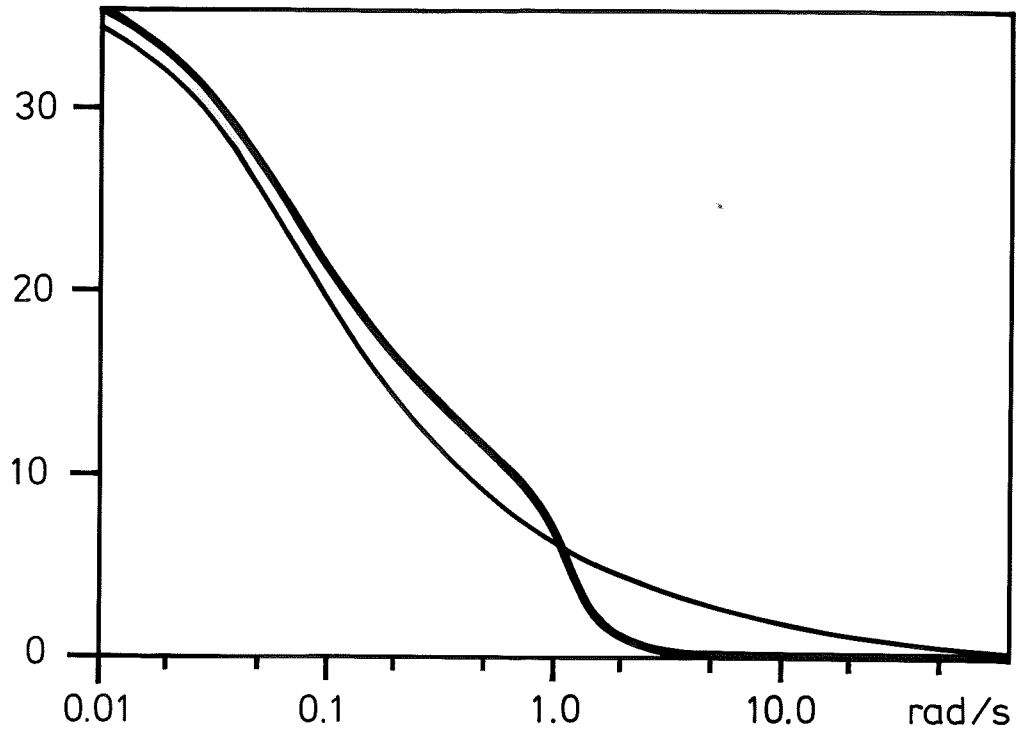

Figure 5.1: Standard deviations $\sigma(\Delta P_E,w;\omega,\infty)$ [% of P_B]. The bold line is for the open loop system. The thin line is for an open loop system with a rigid drive train.

The contribution to the standard deviation in y caused by v is denoted as $\sigma(y,v)$. The spectral properties of the disturbances are of a great interest. The contribution to $\sigma(y,v)$ in the frequency range (ω_1,ω_2) is denoted as $\sigma(y,v;\omega_1,\omega_2)$ and given by

$$\sigma(y,v,\omega_1,\omega_2) = \left\{ 2 \int_{\omega_1}^{\omega_2} \left| G_{y,v}(\omega) \right|^2 \phi_v(\omega)\, d\omega \right\}^{1/2} \qquad (5.3)$$

where $G_{y,v}(s)$ is the transfer function from v to y and $\phi_v(\omega)$ is the spectral density of v.

The quantity $\sigma(\Delta P_E,w;\omega,\infty)$ for the open loop system is shown in Figure 5.1. If the drive train is assumed to be stiff, the model above gives $\Delta P_E = \dot{\psi}_0 T_U \Delta U_0$. This case is also shown in Figure 5.1 to illustrate the effect of the soft shaft.

Loss Function and State Feedback

The LQG theory assumes that the purpose of the control is to minimize a loss function J that is a quadratic function of the state vector Δx and the control signal $\Delta\beta_r$. Since the objective is to keep the power output constant, it is natural to include ΔP_E in the loss function. To avoid excessive servo motions it also of interest to introduce a weight on the servo speed $\Delta\dot{\beta}$ $(=\dot{\beta})$. This is the same as penalizing $\Delta\beta_r - \Delta\beta$ in the loss function, since $\Delta\dot{\beta} = (\Delta\beta_r - \Delta\beta)/T_{bs}$. The objective of the pitch angle control will thus be formulated as to minimize the loss function J defined as

$$J = E\left\{\lim_{T\to\infty} \frac{1}{T} \int_0^T q^2 \Delta P_E^2 + q_\beta^2 (\Delta\beta_r - \Delta\beta)^2 \, dt\right\} \tag{5.4}$$

The design parameter q_β gives a possibility to get a proper bandwidth and reasonable servo motions. It gives also a finite control input $\Delta\beta_r$. There is no reason for penalizing $\Delta\beta_r$ further. It is only the servo reference. The variable q is a scale factor, which is arbitrarily chosen as 1 $(MW)^{-1}$.

The optimal control law is given by the state feedback

$$\Delta\beta_r = - L \cdot \Delta x \tag{5.5}$$

Rewrite the loss function (5.4) as

$$J = E\left\{\lim_{T\to\infty} \frac{1}{T} \int_0^T \Delta x^T Q_1 \Delta x + 2\Delta x^T Q_{12} \Delta\beta_r + \Delta\beta_r^T Q_2 \Delta\beta_r \, dt\right\} \tag{5.6}$$

The feedback gain matrix L then is given by

$$L = Q_2^{-1} (SB + Q_{12})^T \tag{5.7}$$

where S is a symmetric nonnegative definite solution to the algebraic Riccati equation

$$A^T S + SA + Q_1 - (SB + Q_{12}) \, Q_2^{-1} (SB + Q_{12})^T = 0 \tag{5.8}$$

In the following Lx denotes a feedback law and L_x denotes its feedback gain matrix. The following feedback gains are obtained for model (5.1) - (5.2)

$L_1 = [\ 1.46 \quad 5.85 \quad 3.85 \quad 4.83\ ]$ for $q_\beta = 3\ rad^{-1}$

$L_2 = [\ 0.936 \quad 4.60 \quad 2.39 \quad 2.54\ ]$ for $q_\beta = 5\ rad^{-1}$

$L_3 = [\ 0.379 \quad 3.26 \quad 1.21 \quad 0.954\ ]$ for $q_\beta = 10\ rad^{-1}$

$L_4 = [\ 0.113 \quad 2.62 \quad 0.790 \quad 0.487\ ]$ for $q_\beta = 15\ rad^{-1}$

$L_5 = [\ -0.261 \quad 1.73 \quad 0.348 \quad 0.103\ ]$ for $q_\beta = 30\ rad^{-1}$

Some properties of these state feedback designs are given in Table 5.2. The results indicate that the control authority with respect to the variations in U_0 is good. The feedback L gives a local proportional servo feedback l_1 where l_1 is the first element of L. Consider now just the servo in closed loop with this feedback l_1. It has then the time constant $T_{bs}/(1 + l_1)$, where T_{bs} is as before the time constant of the servo in open loop. This shows that the compensations above do not imply any excessive dynamical demands and that it is appropriate to use the simple servo model in the design at least when q_β is greater than 5 rad^{-1}.

Consider now the total system. Cut the loop after the servo but keep the local servo feedback. The crossover frequency ω_c when the loop is cut in this way is given in Table 5.2. It indicates that the simple turbine model only considering the soft shaft dynamics is appropriate for pitch angle design.

Table 5.2: Some properties of the closed loop system with different state feedbacks.

	Design				
	L1	L2	L3	L4	L5
$\sigma(P_E,w)$[% of P_B]	0.65	0.97	1.7	2.4	4.2
$\sigma(\dot{\beta},w)$ [°/s]	1.7	1.5	1.2	1.1	0.85
$\sigma(\dot{\gamma},w)$ [% of $\dot{\psi}_B$]	0.06	0.08	0.13	0.16	0.25
ω_c [rad/s]	3.2	2.7	2.1	1.8	1.3

If the elasticity of the tower is taken into account in the design, it is possible to obtain both a reasonable damping of the tower and practically the same standard deviations as those for a rigid tower. Before considering the tower bendings in more detail, the possibilities of measuring or reconstructing the states in the design model will be discussed, since the difficulties in measuring the wind speed and other quantities influence on the performance more than the tower bendings.

Measurements and Observers

The state feedback requires knowledge of the variables $\Delta\beta$, ΔU_0, $\Delta\dot{\gamma}$ and $\Delta\gamma$. According to (2.34) the variable $\Delta\gamma$ can be replaced by a linear combination of ΔP_E and $\Delta\dot{\gamma}$.

Electrical quantities like power and voltage are all easily measured. Note that the model indicates that in normal on-line operation the shaft torque, the electrical torque and the electrical power are dynamically equivalent in the frequency range of interest. Rotational speed at the primary and secondary shafts can also be measured.

The quality of the control depends also on how well the wind speed ΔU_0 is known and on how well its behaviour can be predicted. In Section 3.2 it was shown that in some weather conditions the wind speed at a point in the rotor disc is poorly correlated with the mean wind speed over the rotor disc. The plant may also itself induce local disturbances so that an anemometer gives bad measurements. This indicates that an anemometer may be of little use for feedforward compensation. However, it may be possible to use the wind turbine itself as wind gauge by measuring other quantities. The reconstruction of the wind speed from turbine speed and power measurements using Kalman filters will therefore be considered.

Assume that a linear system is written as

$$\begin{cases} \dot{x} = Ax + Bu + v \\ y = Cx + e \end{cases} \tag{5.9}$$

where u is the control inputs, y is the measured outputs and v and e are Gaussian white noise processes with zero means, $Ev(t)v(\tau)^T = R_1\delta(t-\tau)$, $Ev(t)e(\tau)^T = R_{12}\delta(t-\tau)$ and $Ee(t)e(\tau)^T = R_2\delta(t-\tau)$. Under these assumptions the

minimum variance estimate $\hat{x}$ of x is in stationarity given by the Kalman filter

$$\dot{\hat{x}} = A\hat{x} + Bu + K(y - C\hat{x}) \tag{5.10}$$

where the filter gain matrix K is given by

$$K = (PC^T + R_{12})\, R_2^{-1} \tag{5.11}$$

with P being the largest symmetric nonnegative definite solution to the algebraic Riccati equation

$$AP + PA^T + R_1 - (PC^T + R_{12})\, R_2^{-1}(PC^T + R_{12})^T = 0 \tag{5.12}$$

The matrix P is the covariance of the prediction error $\tilde{x}(t) = x(t) - \hat{x}(t)$; $P = E\,\tilde{x}(t)\tilde{x}(t)^T$.

To apply these Kalman filter equations we will in the following assume that β is known exactly and that P_E and $\dot{\psi}$ are measured with noise. Models of the measurement noises P_{Ee} and $\dot{\psi}_e$ are needed to proceed. Figures 4.2, 4.3 and 5.1 give some clues. Figure 5.1 shows for the open loop system that due to the soft shaft, the wind has negligible effect on P_E for frequencies above 5 rad/s. Consider now Figures 4.2 and 4.3 and neglect for the moment the peaks at 2P, 4P, 6P and 8P. If the measurement noises are assumed to be white, the spectral density Φ_{PEe} of the electrical power measurement noise can be estimated by $\Phi_{PEe} = 3{\cdot}10^{-5}(MW)^2/(rad/s)$ and the spectral density $\Phi_{\dot{\psi}e}$ of the rotor speed measurement noise by $\Phi_{\dot{\psi}e} = 2{\cdot}10^{-7}$ rad/s.

As seen from the servo model the pitch angle $\Delta\beta$ depends just on $\Delta\beta_r$. Since $\Delta\beta$ is known the servo dynamics can be eliminated and $\Delta\beta$ can equally be viewed as the input instead of $\Delta\beta_r$. The model (5.1) can then be reduced to

$$\begin{cases} \Delta\dot{x} = A_1 \cdot \Delta x + B_1 \cdot \Delta\beta + B_{w1} \cdot w \\ \Delta y = \left[\, \Delta P_{Em}/10^6 \quad \Delta\dot{\psi}_m \,\right]^T = C_1 \cdot \Delta x + e \\ \Delta x = \left[\, \Delta U_0/100 \quad \Delta\dot{\gamma} \quad \Delta\gamma \,\right]^T \end{cases} \tag{5.13}$$

where e is Gaussian white noise with the noise intensity matrix R_e. The measurement noise e is assumed to be uncorrelated with w. The measurement noises of the electrical power measurement and the rotor speed measurement are

assumed to be uncorrelated, which means that R_e is assumed to be diagonal with $R_e(1,1) = 2\pi\Phi_{PEe}$ and $R_e(2,2) = 2\pi\Phi_{\dot{\psi}e}$. Three cases will be considered

$$R_{e1} = \text{diag}(2{\cdot}10^{-4} \quad 1{\cdot}10^{-6})$$

$$R_{e2} = \text{diag}(2{\cdot}10^{-4} \quad 3{\cdot}10^{-6})$$

$$R_{e3} = \text{diag}(2{\cdot}10^{-4}) \quad \text{(no rotor speed measurement)}$$

In the following Kx denotes an observer and K_x denotes its filter gain matrix. Model (5.13) is transformed to the form (5.9) if the term $B_{w1}{\cdot}w$ is exchanged for v and we introduce $R_1 = B_{w1}B_{w1}^T$, $R_{12} = 0$ and R_2 as given below. The model gives the following filter gains:

$$K_1 = \begin{bmatrix} 0.212 & 0.241 & 0.060 \\ 4.75 & 4.94 & 0.464 \end{bmatrix}^T \quad \text{for } R_2 = R_{e1}$$

$$K_2 = \begin{bmatrix} 0.294 & 0.376 & 0.082 \\ 2.17 & 2.54 & 0.256 \end{bmatrix}^T \quad \text{for } R_2 = R_{e2}$$

$$K_3 = \begin{bmatrix} 0.396 & 0.552 & 0.108 \end{bmatrix}^T \quad \text{for } R_2 = R_{e3}$$

To investigate these designs consider the closed loop system when using the state feedback L3 combined with the observer K1. Compared to the result obtained for the state feedback L3, when U_0 was assumed to be known, the standard deviation $\sigma(P_E,w)$ has doubled to 3.4% of P_B. Figure 5.2 shows that the controller attenuates the variations in the electrical power caused by the wind variations up to about 2 rad/s, but above 2 rad/s they are increased. Figure 5.3 shows that this increase is not particularly harmful as far as the variations ΔU_0 in the mean wind are concerned.

The standard deviation $\sigma(\dot{\beta},w)$ is 1.3°/s implying only a slight increase compared to the value for the state feedback L3 shown in Table 5.2. However, the measurement noise increases the servo motions. The noise intensities assumed in the design give $\sigma(\dot{\beta},P_{Ee}) = 0.48°/s$ and $\sigma(\dot{\beta},\dot{\psi}_e) = 0.74°/s$. The variance $\sigma^2(\dot{\beta},w \,\&\, P_{Ee} \,\&\, \dot{\psi}_e)$ is the sum of the variances $\sigma^2(\dot{\beta},w)$, $\sigma^2(\dot{\beta},P_{Ee})$ and $\sigma^2(\dot{\beta},\dot{\psi}_e)$ since w and the measurement noises P_{Ee} and $\dot{\psi}_e$ are assumed to be uncorrelated. It gives $\sigma(\dot{\beta},w \,\&\, P_{Ee} \,\&\, \dot{\psi}_e) = 1.6°/s$. Figures 5.4 and 5.5 show the transfer

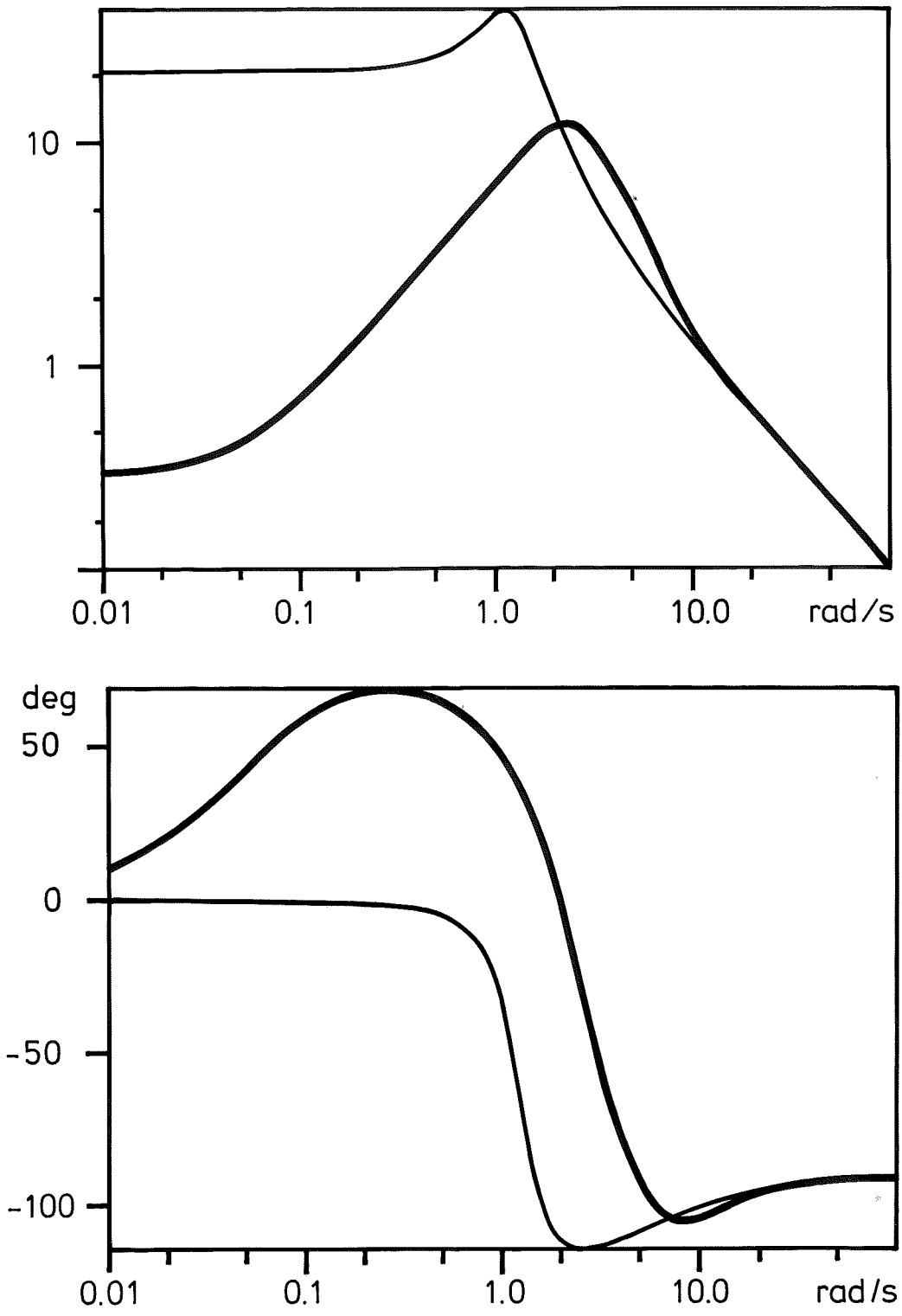

Figure 5.2: Bode plots of the transfer function from ΔU_0 [m/s] to ΔP_E [% of P_B]. The bold lines are for the closed loop system when L3 and K1 are used. The thin lines are for the open loop system.

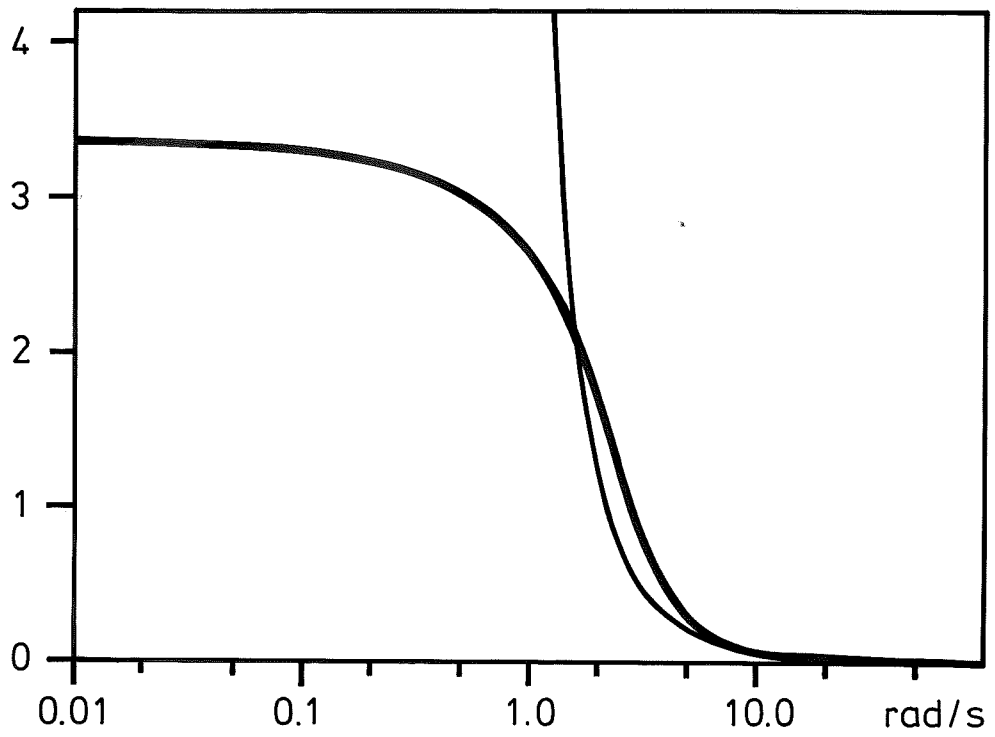

Figure 5.3: Standard deviations $\sigma(P_E,w;\omega,\infty)$ [% of P_B]. The bold line is for the closed loop system when L3 and K1 are used. The thin line is for the open loop system.

functions from P_{Ee} and $\dot{\psi}_e$ to $\Delta\dot{\beta}$. They show that the sensitivity for measurement noise increases drastically at the natural frequency of the soft shaft. This can be explained by the following argument. Figure 5.1 shows that the wind variations ΔU_0 for frequencies up to a bit above the natural frequency of the first torsional mode must be compensated for to obtain good control. To be able to do that it is important to have good estimates of ΔU_0 in this frequency interval. However, around the natural frequency of the soft shaft there is a considerable increase in the phase lag from ΔU_0 to $\Delta\dot{\psi}$ and ΔP_E. To minimize the criterion (5.4) the controller must introduce phase lead at the expense of sensitivity to measurement noise, so that the servo motions increase. The turbine dynamics decreases the influence of measurement noise on the output P_E. The standard deviation $\sigma(P_E,P_{Ee}\&\dot{\psi}_e) = 0.5\%$. Summation of the variances gives $\sigma(P_E,w\&P_{Ee}\&\dot{\psi}_e) = 3.5\%$, showing that the influence of measurement noise on P_E is negligible.

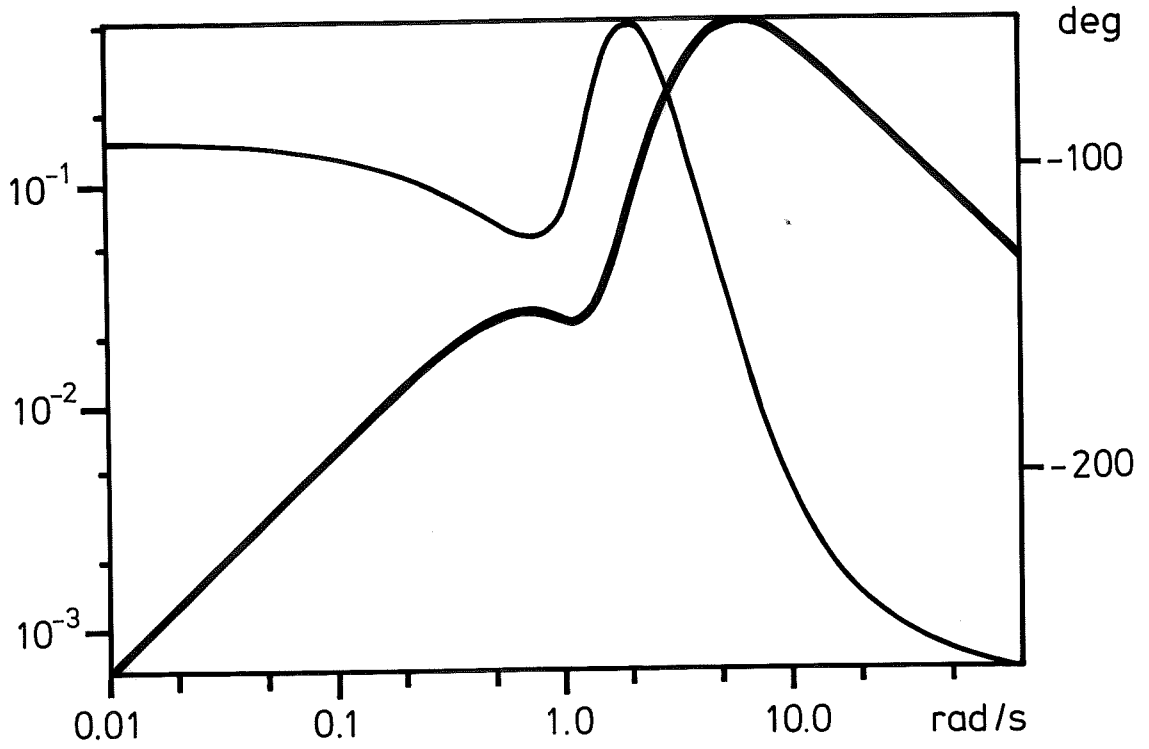

Figure 5.4: Bode plot of the transfer function from P_{Ee} [% of P_B] to $\Delta\dot{\beta}$ [°/s] for the closed loop system when L3 and K1 are used.

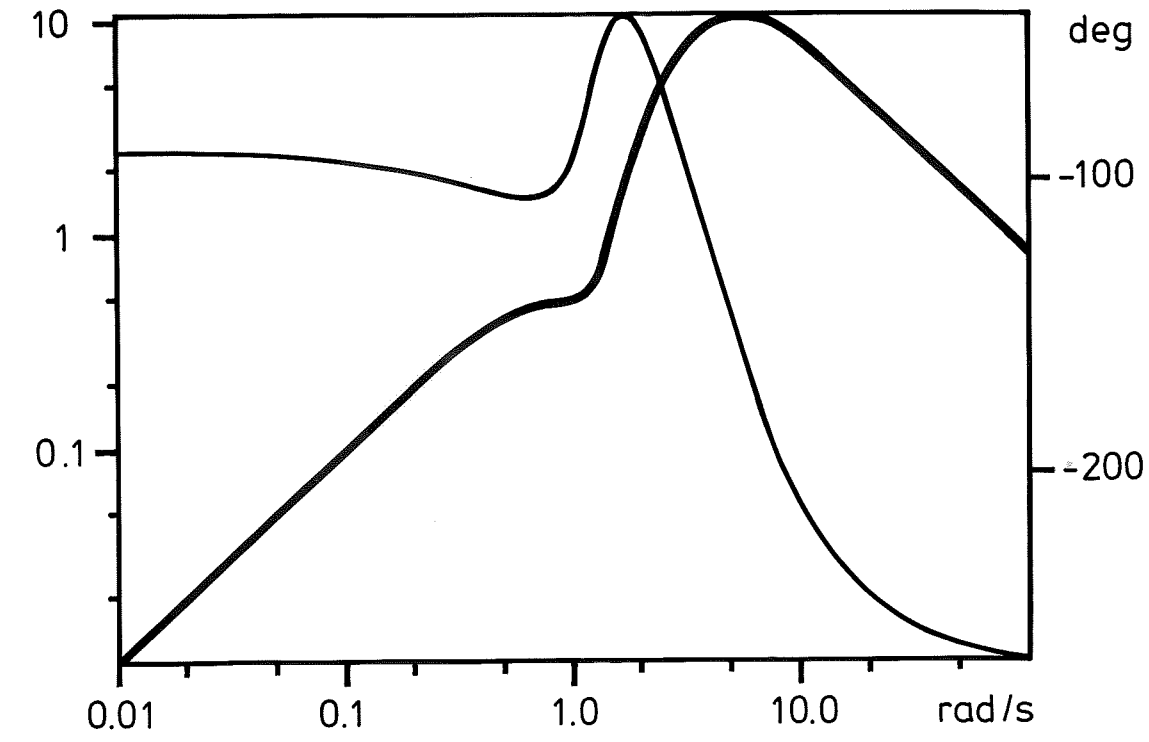

Figure 5.5: Bode plot of the transfer function from $\dot{\psi}_e$ [% of $\dot{\psi}_B$] to $\Delta\dot{\beta}$ [°/s] for the closed loop system when L3 and K1 are used.

The 2P Disturbances

Unfortunately, there are large disturbances at 2P (5.2 rad/s) as indicated in Figures 4.2 and 4.3. These disturbances cannot be neglected in the design. Figure 5.2 shows that a sinusoidal variation in the electrical power with the frequency 2P and an amplitude of 1% of P_B can for the open loop system be viewed as caused by a sinusoidal variation in the wind speed ΔU_0 with the frequency 2P and an amplitude of 0.37 m/s. We will assume that these variations in the wind speed are independent of those caused by the source w. In Section 4.7 we found that for the WTS-3 the amplitude of the 2P variations in P_E is 1 - 3% of P_B, which we thus can view as being caused by 2P variations in the wind speed with amplitudes of 0.3 - 1.1 m/s. Figure 5.2 shows that the controller with the feedback L3 and the observer K1 the 2P variations in P_E increases with a factor α_{2P} = 1.7. Figure 5.6 shows that this controller also gives excessive servo motions. The gain from ΔU_0 to $\Delta\dot{\beta}$ at 2P is g_{2P} = 5.3°/s/(m/s). This means that the control system forces the servo to oscillate at this frequency with an amplitude of 0.3 - 1° and a rate of 1.5 - 6°/s. Since the turbine speed varies and the peaks in the different spectra have finite width, we want more robust

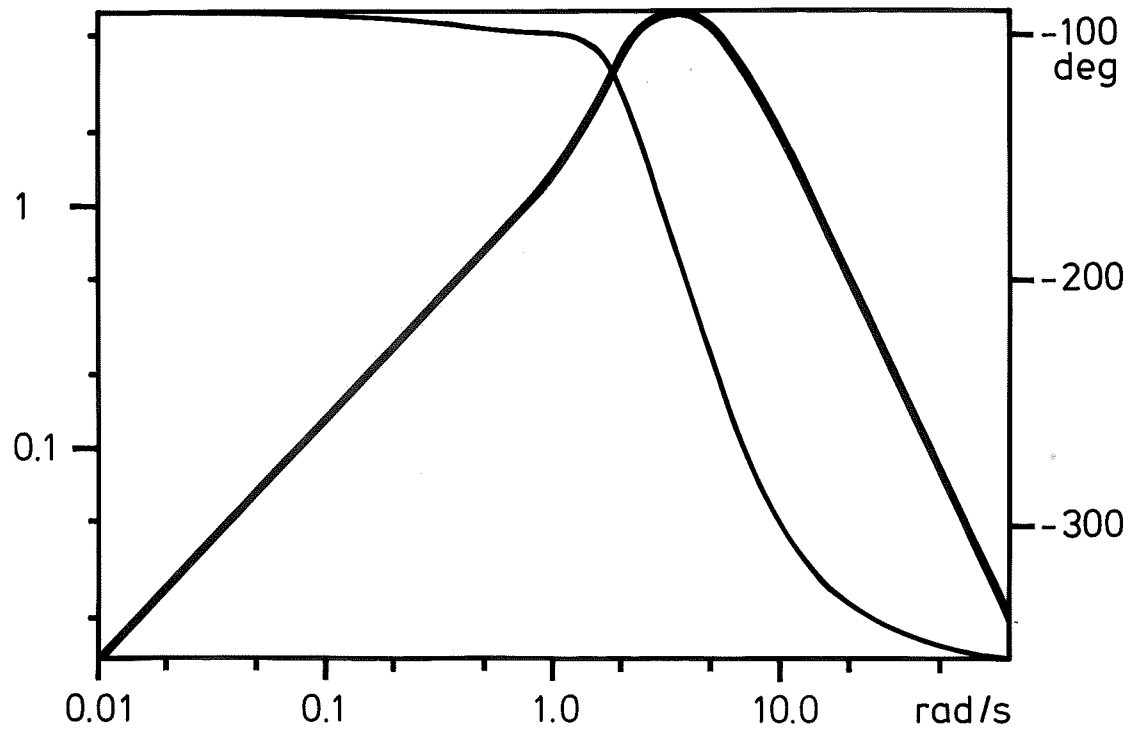

Figure 5.6: Bode plot of the transfer function from ΔU_0 [m/s] to $\Delta\dot{\beta}$ [°/s] for the closed loop system when L3 and K1 are used.

measures when evaluating the attempts to eliminate the excessive servo motions. In the following we will let g_{2P} represent the largest value of the gain from ΔU_0 to $\Delta\dot{\beta}$ in the frequency range ±1% around 2P. The variable α_{2P} is also redefined analogously.

The pitch servo is not designed to handle these 2P variations. They are instead taken care of by the teeter hub and the soft shaft. The control system should not try to eliminate these variations and more importantly they should not cause excessive servo motions. Murdoch et al (1983) state that for the MOD-5A (a 6.2 MW system under design by General Electric Co.) the steady state motion limit on the pitch actuator is 0.2°. Use of notch filters and low pass filters is a common way to reduce such variations. Low pass filters are not good alternatives in this case, since the 2P frequency is too close to the desired crossover frequency of the pitch angle control. The basic notch filter has the transfer function

$$G_N(s) = \frac{s^2 + 2\zeta_N\omega_N s + \omega_N^2}{s^2 + 2\zeta_D\omega_N s + \omega_N^2} \qquad (5.14)$$

A possible approach is to filter the feedback from $\Delta\hat{U}_0$, $\Delta\hat{\dot{\gamma}}$ and $\Delta\hat{\gamma}$ so that the spectral density around 2P is decreased to that level assumed in the observer design. Figures 4.2 and 4.3 show that the spectral densities of P_{Em} and $\dot{\psi}_m$ at 2 P are about 100 times higher than those given by white measurement noise with the noise intensity R_{e1}. This indicates that we should choose $\omega_N = 2\dot{\psi}_0$ and $|G_N(i\omega_N)|^2 = (\zeta_N/\zeta_D)^2 = 0.01$. The desire to give the filter a proper bandwidth then gives $\zeta_N = 0.03$ and $\zeta_D = 0.3$. This notch filter will be called N1 in the following. Figure 5.9 further below compares $|G_N(i\omega)|^{-2}\cdot(2\cdot10^{-4}/(2\pi))$ and the spectral density in Figure 4.2. Some properties of the closed loop system when N1 is used are given in Table 5.3. It shows that $\sigma(P_E,w)$ is greater when N1 is used.

If the loop is cut at A (See Figure 5.7) where we have the largest variations in the process gain due to the nonlinearities in the aerodynamical torque, we find that the amplitude margin A_m has decreased from 3.6 to 2.5. See Figure 5.8. Without N1 the loop gain passes -180° at 7 rad/s, but with N1 the loop gain passes -180° already at 4.2 rad/s. However, the gain of N1 is almost one at 4.2 rad/s. We face here the open question of determining how much stability margin is really needed. As we will find, the nonlinearities are not so simple that

Table 5.3: Some properties of the closed loop system for different feedbacks and different observers.

	Design					
	L3 K1	L3 K2	L3 K3	L3 K1 N1	L3 K2 N1	L3 K3 N1
$\sigma(P_E,w)$ [%]	3.4	3.8	4.2	4.4	4.7	5.1
$\sigma(\dot{\beta},w)$ [°/s]	1.3	1.3	1.3	1.3	1.3	1.3
$\sigma(\dot{\beta},P_{Ee})$ [°/s]	0.48	0.75	1.1	0.40	0.61	0.90
$\sigma(\dot{\beta},\dot{\psi}_e)$ [°/s]	0.74	0.67	-	0.63	0.55	-
$\sigma(\dot{\beta},w\&P_{Ee}\&\dot{\psi}_e)$ [°/s]	1.6	1.6	1.7	1.5	1.5	1.6
ω_c [rad/s]	2.8	2.7	2.6	2.5	2.4	2.3
A_m	3.6	3.3	2.9	2.5	2.2	2.0
φ_m [°]	37	35	34	28	27	26
α_{2P}	1.68	1.66	1.59	1.08	1.07	1.06
g_{2P} [°/s/(m/s)]	5.3	4.7	4.1	0.48	0.43	0.37

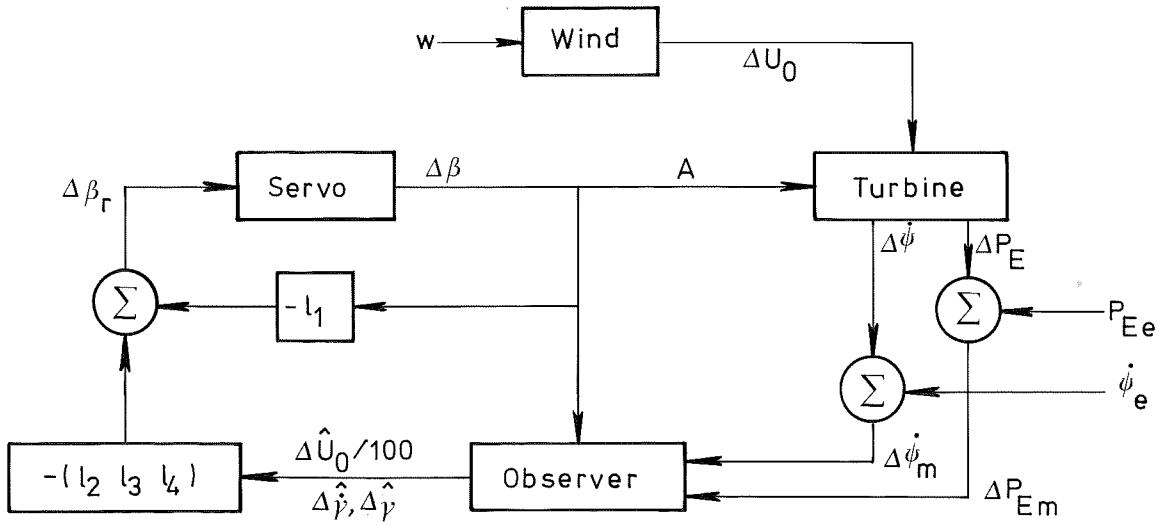

Figure 5.7: Control Configuration.

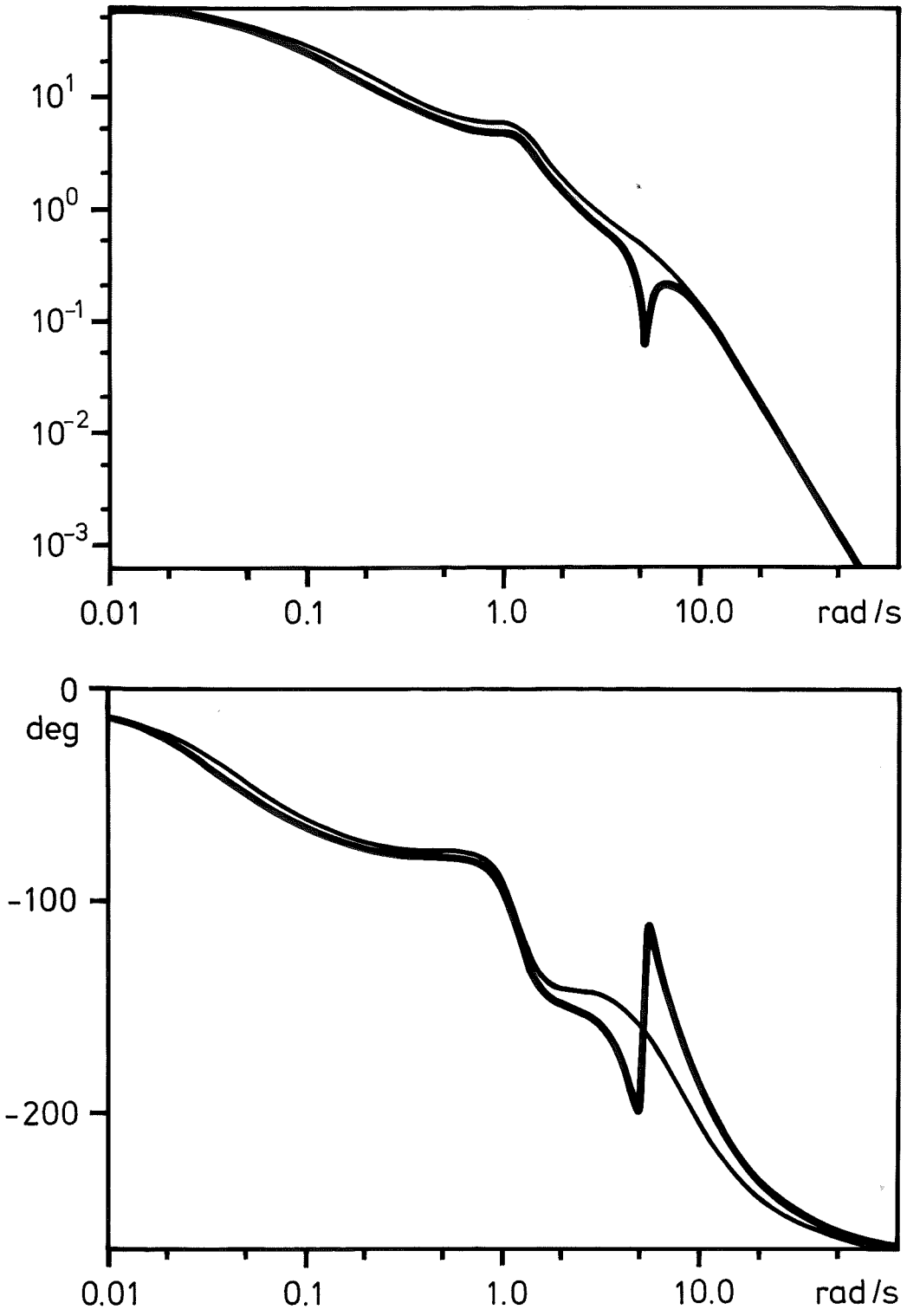

Figure 5.8: Bode plot of the loop gain at A. See Figure 5.7. The bold lines are for the case when L3, K1 and N1 are used. The thin lines are for the same case without N1.

the circle criterion can be used to establish stability. The possibilities of increasing the stability margins without deteriorating the disturbance rejection too much will be investigated in the following. Since the variations at 4P, 6P and 8P are further away from ω_c, notch filters can be used without any difficulty to prevent signals at those frequencies to generate servo motions.

One way to handle the 2P variations in the LQG design procedure is to have a frequency dependent weight on $\Delta\beta_r - \Delta\beta$ and to put a large weight at 2P in the loss function. This can be done by expanding the design model with a part that has a resonance at 2P and which input is $u_N = \Delta\beta_r - \Delta\beta$ and by letting the output y_N replace $\Delta\beta_r - \Delta\beta$ in the loss function (5.4). Here we let that part have the transfer function (5.14). On state space form this can be written as

$$\begin{cases} \dot{x}_{N1} = -2\zeta_D\omega_N x_{N1} - \omega_N x_{N2} + 2(\zeta_N - \zeta_D)\omega_N u_N \\ \dot{x}_{N2} = \omega_N x_{N1} \end{cases} \tag{5.15}$$

with

$$y_N = x_{N1} + u_N \tag{5.16}$$

Expansion of model (5.1) - (5.2) with (5.15) and choosing the state vector as

$$\Delta x = \begin{bmatrix} \Delta\beta & \Delta U_0/100 & \Delta\dot{\gamma} & \Delta\gamma & x_{N1} & x_{N2} \end{bmatrix}^T \tag{5.17}$$

and the parameters in (5.15) as $\omega_N = 2\dot{\psi}_0$, $\zeta_N = 0.3$ and $\zeta_D = 0.03$, gives the following state feedback gains

$$L_6 = \begin{bmatrix} 0.603 & 3.78 & 1.20 & 0.781 & 0.775 & 0.617 \end{bmatrix} \text{ for } q_\beta = 10 \text{ rad}^{-1}$$

$$L_7 = \begin{bmatrix} 0.262 & 2.97 & 0.771 & 0.372 & 0.853 & 0.512 \end{bmatrix} \text{ for } q_\beta = 15 \text{ rad}^{-1}$$

$$L_8 = \begin{bmatrix} -0.195 & 1.88 & 0.328 & 0.052 & 0.935 & 0.350 \end{bmatrix} \text{ for } q_\beta = 30 \text{ rad}^{-1}$$

Some properties of the closed loop systems with these feedback laws are given in Tables 5.4 and 5.5.

Doyle and Stein (1979) have proposed a method for increasing the stability margins in LQG designs. A fictitious noise e_β is added to the control input in the model for observer design. The noise intensity matrix R_1 of model (5.13) then becomes $B_{w1}B_{w1}^T + r_\beta B_1 B_1^T$. In the case with $R_2 = R_{e1}$ and $r_\beta = 5{\cdot}10^{-5}$ we get

Table 5.4: Some properties of the closed loop system for different feedbacks and observers.

	Design					
	L6 K1	L6 K3	L6 K4	L6 K5	L3 K6	L3 K7
$\sigma(P_E,w)$ [%]	4.2	5.0	5.3	5.8	4.8	5.3
$\sigma(\dot{\beta},w)$ [°/s]	1.2	1.2	1.0	1.0	1.2	1.0
$\sigma(\dot{\beta},P_{Ee})$ [°/s]	0.44	1.0	0.41	1.0	1.0	1.0
$\sigma(\dot{\beta},\dot{\psi}_e)$ [°/s]	0.70	-	0.66	-	-	-
$\sigma(\dot{\beta},w\&P_{Ee}\&\dot{\psi}_e)$ [°/s]	1.4	1.5	1.3	1.4	1.6	1.5
ω_c [rad/s]	2.5	2.4	2.3	2.2	2.4	2.3
A_m	3.0	2.2	3.6	2.9	2.1	3.0
φ_m [°]	34	31	40	40	32	40
α_{2P}	1.09	1.08	1.06	1.06	1.09	1.10
g_{2P} [°/s/(m/s)]	0.62	0.47	0.36	0.34	0.53	0.66

$$K_4 = \begin{bmatrix} 0.204 & 0.541 & 0.0602 \\ 4.71 & 12.5 & 0.476 \end{bmatrix}^T$$

The case with $R_2 = R_{e3}$ and $r_\beta = 5{\cdot}10^{-5}$ gives

$$K_5 = \begin{bmatrix} 0.390 & 1.09 & 0.113 \end{bmatrix}^T$$

Another approach to handle the 2P variations in the LQG design procedure is to view them as measurement disturbances, since they should be neglected by the controller, and model them as coloured measurement noise when designing the observer. The measured electrical power ΔP_{Em} can be viewed as the sum of ΔP_E, P_{E2P} and P_{Ee}, where ΔP_E represents the part of interest for pitch control, P_{E2P} the disturbance at 2P and P_{Ee} the remaining part. The measured turbine speed $\Delta\dot{\psi}_m$ can similarly be viewed as the sum of $\Delta\dot{\psi}$, $\dot{\psi}_{2P}$ and $\dot{\psi}_e$. Since the 2P variations have their origin at the turbine, the linearity and (2.34) - (2.35) give

Table 5.5: Some properties of the closed loop system for different feedbacks and observers.

	Design					
	L7 K1	L7 K3	L4 K6	L8 K1	L8 K3	L5 K6
$\sigma(P_E,w)$ [%]	5.1	5.9	5.7	7.2	8.1	7.8
$\sigma(\dot{\beta},w)$ [°/s]	1.0	1.0	1.1	0.79	0.79	0.81
$\sigma(\dot{\beta},P_{Ee})$ [°/s]	0.33	0.72	0.73	0.19	0.41	0.42
$\sigma(\dot{\beta},\dot{\psi}_e)$ [°/s]	0.52	-	-	0.30	-	-
$\sigma(\dot{\beta},w\&P_{Ee}\&\dot{\psi})_e$[°/s]	1.2	1.3	1.3	0.82	0.89	0.91
ω_c [rad/s]	2.3	2.1	2.2	1.8	1.7	1.8
A_m	3.1	2.4	2.3	4.0	3.1	2.9
φ_m [°]	38	36	36	49	48	47
α_{2P}	1.07	1.06	1.06	1.05	1.05	1.04
g_{2P} [°/s/(m/s)]	0.48	0.34	0.39	0.27	0.19	0.22

$$P_{E2P} = \dot{\psi}_0(D_s\dot{\psi}_{2P} + K_s\psi_{2P}) \tag{5.18}$$

Here we will only consider the case when the rotor speed is not measured. A possible model for $P_{E2P} + P_{Ee}$ is the output y_N of (5.15) - (5.16) with u_N being white noise. Figure 5.9 shows the spectral density of $P_{E2P} + P_{Ee}$ for the choice $\omega_N = 2\dot{\psi}_0$, $\zeta_N = 0.3$ and $\zeta_D = 0.03$ and when the white noise u_N has the intensity R_{e3}. The model for observer design can be written as

$$\begin{cases} \Delta\dot{x} = A_2\cdot\Delta x + B_2\cdot(\Delta\beta + e_\beta) + B_{w2}\cdot w + B_{2P}e_{2P} \\ \Delta y = \Delta P_{Em}/10^6 = C_2\cdot\Delta x + D_{2P}e_{2P} + P_{Ee} \\ \Delta x = \left[\ \Delta U_0/100 \quad \Delta\dot{\gamma} \quad \Delta\gamma \quad x_{N1} \quad x_{N2}\ \right]^T \end{cases} \tag{5.19}$$

Transformation to the form (5.9) gives the following noise intensity matrices:

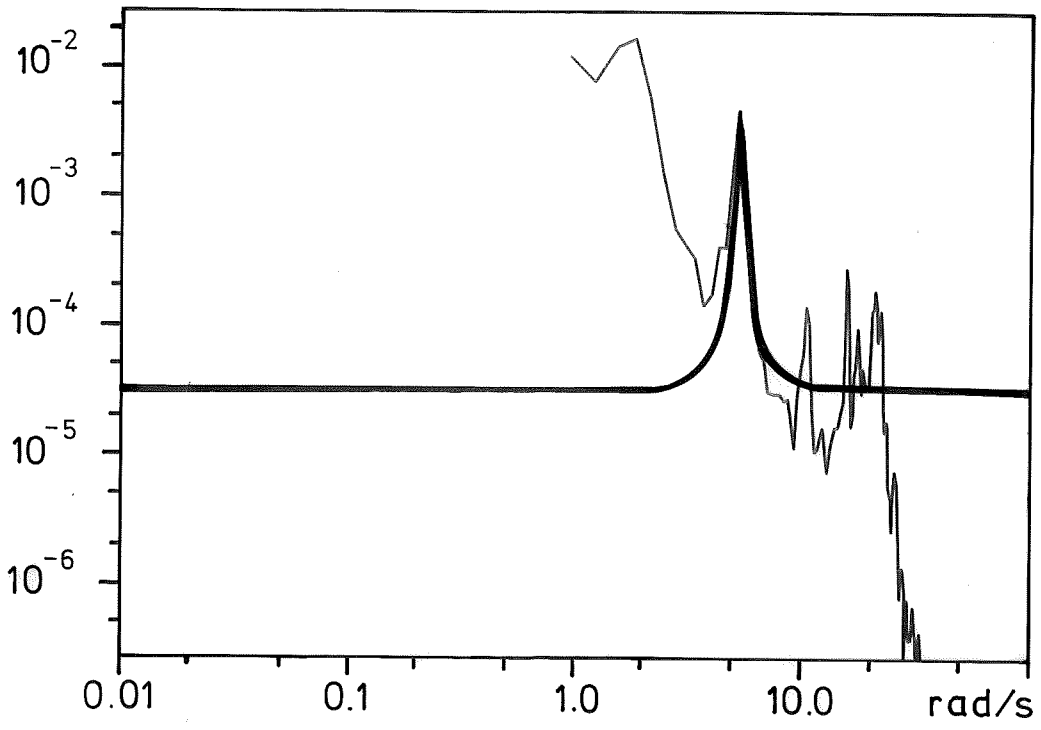

Figure 5.9: The bold line is the spectral density of the output from (5.14) with $\omega_N = 2\dot{\psi}_0$, $\varsigma_N = 0.3$ and $\varsigma_D = 0.03$ when the input is white noise with the noise intensity R_{e3}. The thin line is the spectral density of the electrical power given in Figure 4.2.

$$\begin{cases} R_1 = B_{w2}B_{w2}^T + B_{2P}B_{2P}^T + r_\beta B_2 B_2^T \\ R_{12} = B_{2P}D_{2P}^T \\ R_2 = R_{e3} + D_{2P}D_{2P}^T \end{cases}$$

With the above given parameter values and $r_\beta = 0$ we get the following filter gains

$$K_6 = \begin{bmatrix} 0.379 & 0.639 & 0.155 & 0.789 & -2.56 \end{bmatrix}^T$$

With $r_\beta = 5{\cdot}10^{-5}$ we get

$$K_7 = \begin{bmatrix} 0.389 & 1.12 & 0.161 & 0.288 & -2.45 \end{bmatrix}^T$$

In the designs above we have assumed that the 2P variations are caused by a small-banded stochastic noise. If this assumption is true, Tables 5.3 - 5.5 show that the desire to avoid excessive servo motions is in conflict with the desire to keep the power output constant. The model of the 2P variations as small-banded noise may seem somewhat conservative. A large part of the disturbance is due to the tower blockage which is much more 'deterministic' than the small-banded noise model indicates. There are, however, also random disturbances like the effects of rotational sampling. The investigation in Section 4.7 using recursive LS-estimation was initiated to see if the phase or the amplitude was constant. If this was true it would be possible to design a better filter to attenuate the 2P variations in the control output β_r. The investigation in Section 4.7 shows that neither the phase nor the amplitude is constant. See Figure 4.15. Figure 4.16 shows the effect of the LS-estimator viewed as a filter to attenuate the 2P variations. The notch filters discussed above decrease further the spectral density around 2P a factor of 4 - 5 times. Moreover, the LS-estimator needs a measurement of the turbine position ψ or some other kind of synchronization input to be effective. The 2P variations have a random component and when trying to attenuate the 2P variation efficiently in the servo reference β_r notch filters appear in some way or other. The designer must balance excessive servo motions against variations in the shaft torque and the generated electrical power.

Different Plant Designs

The process designer can influence the parameter values in the basic relation given by (2.28). We will now study how the control result depends on these parameters. As a starting point three different cases will be studied. The plant given by model (5.1) - (5.2) will continue to serve as a reference and will be referenced as Plant 1. Table 2.1 shows that the torsional damping coefficient D_s of the drive train is much lower for the MOD-2 than for the WTS-3. To investigate the effect of this parameter variation Plant 2 is chosen identical to Plant 1, but with D_s a five times smaller, which gives $D_s = 0.6 \cdot 10^6$ Nms/rad. Plant 3 is chosen to be the WTS-75. The complex pole pair $\sigma \pm i\omega$ of (2.27) is chosen as $-3 \pm 5i$ and K_s and D_s are chosen as $K_s = 6.5 \cdot 10^8$ Nm/rad and $D_s = 0$. All the three plants are assumed to have a rigid tower. We thus have

Plant 1: The plant given by model (5.1) - (5.2) ($\sigma = -0.37$ and $\omega = 1.17$).

Plant 2: As Plant 1, but with $D_s = 0.6 \cdot 10^6$ Nms/rad ($\sigma = -0.13$ and $\omega = 1.22$).

Plant 3: As Plant 1, but with $\sigma = -3$, $\omega = 5$, $K_s = 6.5 \cdot 10^8$ Nm/rad and $D_s = 0$.

With the design parameter q_β = 10 rad^{-1} the following feedbacks are obtained:

L_{P1} = [0.379 3.26 1.21 0.954] for Plant 1

L_{P2} = [0.433 3.39 1.31 0.912] for Plant 2

L_{P3} = [1.06 4.90 10.2 36.1] for Plant 3

Some properties of the closed loop system for these state feedbacks are given in Table 5.6. The table shows that almost the same results are obtained for Plants 1 and 2. The pitch angle control introduces damping of the torsional mode and moves the pole pair to -1.23 ± 2.06i for Plant 1 and to -0.97 ± 2.05i for Plant 2. The first torsional mode of Plant 3 is much better damped and the pitch angle control need not dampen this mode. The feedback LP3 moves the pole pair from -3 ± 5i to -3.3 ± 6.1i, which means a lower relative damping. The loop gain at A in Figure 5.7 is less than 0.3 for all frequencies, indicating that the feedback from $\Delta\dot{\gamma}$ and $\Delta\gamma$ is small in spite of the feedback coefficients for $\Delta\dot{\gamma}$ and $\Delta\gamma$ being ten times greater than those for Plants 1 and 2. The control relies on feedforward from ΔU_0 and a fast servo. The first element of L_{P1}, L_{P2} and L_{P3} shows that the local servo feedback from $\Delta\beta$ is greater for Plant 3 than for Plants 1 and 2. This local servo feedback for Plant 3 halves the servo response time. For a given control energy $\sigma(\dot{\beta},w)$ the standard deviation $\sigma(P_E,w)$ is greater because Plant 3 has less filtering effect for high frequency disturbances than Plants 1 and 2. Control of high frequency disturbances gives a large $\sigma(\dot{\beta},w)$.

Table 5.6: Some properties of the closed loop system with state feedback for the three different plants.

	Plant/Feedback		
	1 LP1	2 LP2	3 LP3
$\sigma(P_E,w)$ [% of P_B]	1.7	1.6	2.5
$\sigma(\dot{\beta},w)$ [°/s]	1.2	1.3	1.4
$\sigma(\dot{\gamma},w)$ [% of $\dot{\psi}_B$]	0.13	0.14	0.0076
ω_c [rad/s]	2.1	2.2	-

Consider now the design of observers. Model (5.13) with $R_2 = R_{e1}$ for observer design gives the following filter gains:

$$K_{P1A} = \begin{bmatrix} 0.212 & 0.241 & 0.060 \\ 4.75 & 4.94 & 0.464 \end{bmatrix} \quad \text{for Plant 1}$$

$$K_{P2A} = \begin{bmatrix} 0.079 & 0.132 & 0.069 \\ 5.50 & 6.51 & 0.798 \end{bmatrix} \quad \text{for Plant 2}$$

$$K_{P3A} = \begin{bmatrix} 0.396 & 0.042 & 0.007 \\ 0.563 & 0.059 & 0.005 \end{bmatrix} \quad \text{for Plant 3}$$

With $R_2 = R_{e3}$ we get

$$K_{P1B} = \begin{bmatrix} 0.396 & 0.552 & 0.108 \end{bmatrix} \quad \text{for Plant 1}$$

$$K_{P2B} = \begin{bmatrix} 0.392 & 0.846 & 0.240 \end{bmatrix} \quad \text{for Plant 2}$$

$$K_{P3B} = \begin{bmatrix} 0.398 & 0.043 & 0.007 \end{bmatrix} \quad \text{for Plant 3}$$

Some properties of the closed loop system when these observers are used are given in Table 5.7.

To obtain a good control result it is important to have a good estimate of ΔU_0 in the frequency interval where the filtering effect of the dynamics from ΔU_0 to ΔP_E is low. Phase lag in the dynamics from ΔU_0 to the measurements makes the reconstruction of ΔU_0 more difficult. Around the natural frequency of the first torsional mode there is low filtering effect, but a considerable increase in phase lag. To minimize the loss function (5.4) the controller must introduce phase lead at the expense of sensitivity to noise. Since ΔP_E is proportional to $D_s\Delta\dot{\gamma} + K_s\Delta\gamma$ there is less phase lag in $\Delta\dot{\gamma}$ than in ΔP_E. However, the variations in the electrical power are relatively larger and are easier to measure. If measured per unit, the variations in ΔP_E are more than ten times higher than those in $\Delta\dot{\gamma}$.

Table 5.7 shows that the results for Plants 1 and 2 are rather similar when $\Delta\dot{\gamma}$ and ΔP_E are measured, but different when only ΔP_E is measured. The table and the Kalman filter gains K_{P1A} and K_{P2A} show that the measurements are used differently. The control of Plant 2 relies more on the measurement of $\Delta\dot{\gamma}$ than Plant 1 does. The damping coefficient D_s of Plant 2 is small so in the frequency range of interest for pitch angle control the variations in ΔP_E is almost 90° after

Table 5.7: Some properties of the closed loop system when observers are used to reconstruct the wind speed for the three different plants.

	Plant/Feedback/Observer					
	1 LP1 KP1A	1 LP1 KP1B	2 LP2 KP2A	2 LP2 KP2B	3 LP3 KP3A	3 LP3 KP3B
$\sigma(P_E,w)$ [%]	3.4	4.2	3.5	5.8	5.5	5.5
$\sigma(\dot{\beta},w)$ [°/s]	1.3	1.3	1.4	1.5	1.2	1.2
$\sigma(\dot{\beta},P_{Ee})$ [°/s]	0.48	1.1	0.22	1.6	0.92	0.93
$\sigma(\dot{\beta},\dot{\psi}_e)$ [°/s]	0.74	-	0.98	-	0.11	-
$\sigma(\dot{\beta},w\&P_{Ee}\&\dot{\psi}_e)$ [°/s]	1.6	1.7	1.7	2.2	1.5	1.5
ω_c [rad/s]	2.8	2.6	2.8	2.4	2.9	2.9
A_m	3.6	2.9	3.3	2.2	2.7	2.7
φ_m [°]	37	34	32	23	71	71
α_{2P}	1.68	1.59	1.74	1.33	1.30	1.30
g_{2P} [°/s/(m/s)]	5.3	4.1	5.5	2.9	6.1	6.1

those in $\Delta\dot{\gamma}$. The damping coefficient D_s of Plant 1 is greater so the phase difference is considerably less than 90°.

A stiffer drive train gives less variations in $\Delta\dot{\gamma}$. This means that speed measurements must be very accurate to be useful for Plant 3. The accuracy of the turbine speed measurements of the WTS-3 is as good as the normal measurements for large power plants. However, here we are interested in reconstructing the state of a rapidly varying power source.

The possibility of simplifying the measurement and reconstruction task by having dampers in the drive train is worth considering if the damping of the first torsional mode is small, since there are also other reasons for having damping in the drive train. In the beginning of this section we noted that when the controller maximizes the power output the control authority is low and it is difficult to

dampen the oscillations by pitch angle control. Damping in the drive train is also good for the generator. The second torsional mode is the oscillation of the generator against the grid. Damping in the drive train also provides damping of this mode. As an example, the drive train of the WTS-3 is equipped with dampers giving the first torsional mode of the open loop system a relative damping of 0.25. The dampers double the relative damping of the second mode to 0.20. The energy loss is small, only a few hundred watts.

The filtering properties at 2P are different for the three systems. The gain for the open loop system from ΔU_0 to ΔP_E for Plants 1-3 is 2.74, 1.31 and 22.2 (% of P_B)/(m/s). Consequently, the 2P variations in the driving aerodynamical torque cause large variations in the shaft torque for Plant 3. To reduce these variations active cyclic pitch control is needed. Liebst (1980, 1981) discusses alleviation of cyclic loads by active pitch control. Sensors like accelerometers and strain gauges are needed to measure blade motions and blade loads. It must be possible to control the blade angles individually. Liebst (1981) states that preliminary investigations for the MOD-2 showed that pitch rates of the order of 12°/s would be necessary to obtain significant vibration reductions. It seems more robust to design the turbine to have passive load alleviation as discussed in Section 2.3.

A soft shaft is a nice way to attenuate the 2P variations in the shaft torque. However, it is not quite easy to design a torsionally soft shaft that can stand the bending torques. A soft suspension of the planetary gearbox as used in the WTS-3 is one solution to the problem. Another quite different approach to attenuate the variations in the shaft torque is to use generator systems which allow variable turbine speed and control of the power output at the generator.

Tower Bendings

Let us now consider the tower bendings by using the models (2.33) - (2.39) and the numerical values in Table 5.1. The tower damping coefficient D_T in Table 5.1 is calculated under the assumption that the structural damping of the tower is 2%. To force the control system to dampen the tower bendings, the loss function (5.4) is modified by adding the new term $q_z^2 \Delta \dot{z}_T^2$ to the integral. With the state vector

$$\Delta \dot{x} = \left[\Delta\beta \quad \Delta U_0/100 \quad \Delta\dot{\gamma} \quad \Delta\gamma \quad \Delta\dot{z}_T/10 \quad \Delta z_T/10 \right] \tag{5.20}$$

Table 5.8: Some properties of the closed loop system with state feedback. For the open loop system we have the relative tower damping ς_{To} = 5.4% and $\sigma(\dot{z}_T,w)$ = 0.055 m/s.

	Design				
	L3	LA	LB	LC	LD
$\sigma(P_E,w)$[% of P_B]	2.1	1.8	1.8	1.8	1.8
$\sigma(\dot{\beta},w)$ [°/s]	1.2	1.3	1.3	1.3	1.3
$\sigma(\dot{z}_T,w)$[m/s]	0.083	0.078	0.060	0.045	0.035
ς_{Tc} [%]	1.9	2.6	4.3	7.3	11.5

the following feedback gains are obtained for q_β = 10 rad^{-1}:

L_A = [0.336 3.26 1.20 0.883 -0.144 0.705] for q_z = 0.0 s/m

L_B = [0.364 3.34 1.19 0.844 -0.121 0.821] for q_z = 0.3 s/m

L_C = [0.414 3.48 1.77 0.779 0.227 0.999] for q_z = 0.6 s/m

L_D = [0.485 3.68 1.15 0.694 0.581 1.21] for q_z = 1.0 s/m

Some properties of the closed loop system when using these state feedbacks are given in Table 5.8. The variable ς_{Tc} denotes the resulting relative damping of the tower bendings for the closed loop system. The results show that it is possible to increase the tower damping and decrease the tower oscillations without deteriorating the control of the power output.

Assume that $\Delta\dot{z}_T$ is measured. For the observers discussed above, the tower bendings enter only in the calculation of the aerodynamical torque as given by expression (2.36). If $\Delta\dot{z}_T$ is viewed as an input like $\Delta\beta$, it is easy to modify the observers to include the tower bendings. It is just to extend the observer with an input for $\Delta\dot{z}_T$ and add a new term in the calculation of ΔT. Let K7T denote K7 extended in this way. When LC and K7T are used, then the results are very close to those given in Table 5.4 for L3 and K7. Figure 5.10 shows the Bode plot of the

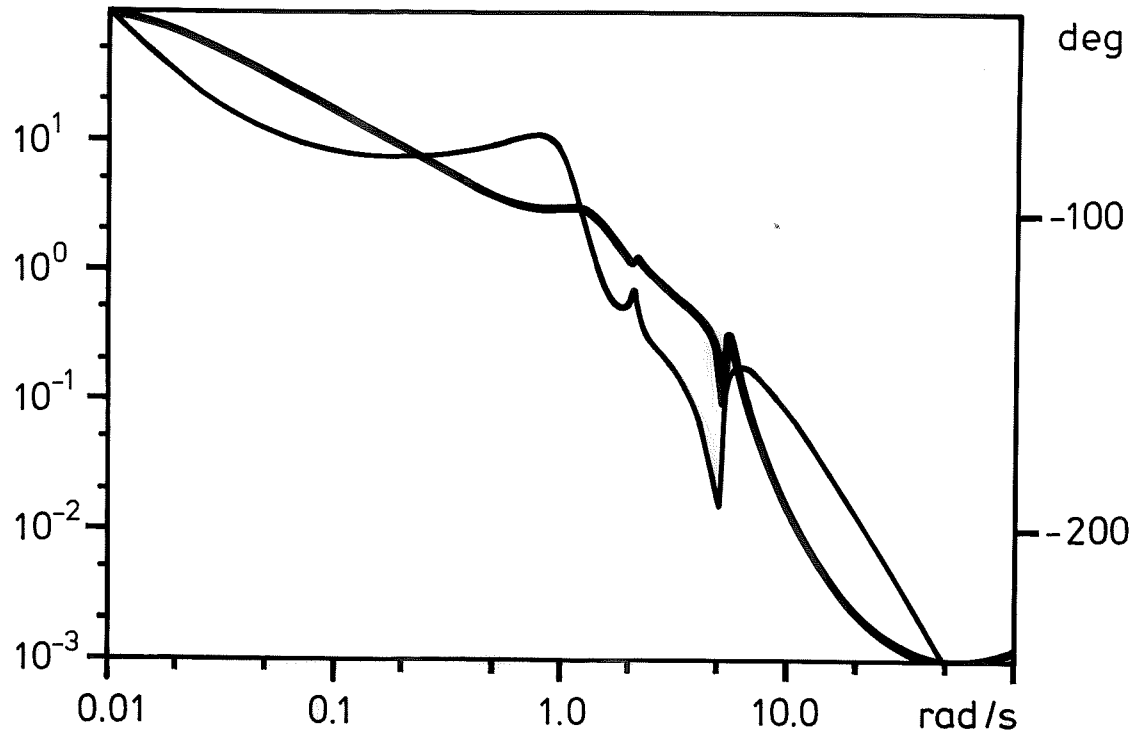

Figure 5.10: Bode plot of the loop gain at A when LC and K7T are used.

loop gain. For the tower we get ζ_{Tc} = 7.3%, $\sigma(\dot{z}_T,w)$ = 0.082 m/s and $\sigma(\dot{z}_T,P_{Ee})$ = 0.015 m/s. If we make a state feedback design similar to L6 but with q_z = 0.6 s/m and extend the observer K1, then the properties of the closed loop system are very close to those given in Table 5.4 for L6 and K1. For the tower we get ζ_{Tc} = 7.3% and $\sigma(\dot{z}_T,w)$ = 0.086 m/s. For these designs the standard deviations $\sigma(\dot{z}_T,w)$ are unfortunately greater than for the open loop system. The tower has its resonance at 2.1 rad/s. Figure 5.2 shows that the control is poor at this frequency even if the tower is assumed to be rigid. The phase lag in the reconstruction of ΔU_0 caused by the observer eliminates the feedforward effect from ΔU_0. A more systematic approach should exploit the information of the wind in the measurements of $\dot{z}_T$ by including the tower model in the observer. This approach requires a model for the measurement noise and will not be discussed here.

Design attempts show that it is unrealistic to reconstruct $\Delta\dot{z}_T$ from turbine speed and power measurements and use the feedback laws discussed above, and still have a robust closed loop system. The demands on ΔP_E must be lowered considerably. The elastic tower introduces one poorly damped complex pole pair

(See (2.40)) into the frequency range close to the desired crossover frequency. The transfer functions from $\Delta\beta$ to $\Delta\dot{\gamma}$ and ΔP_E have also one complex zero pair to the right of the pole pair. This dynamics is too complex to be handled only by dynamic output feedback from $\Delta\dot{\gamma}$ and ΔP_E, if high performance is desired.

Table 2.2 shows that the resonance frequency of the tower of the WTS-3 is low. It is about twice as high for the Growian I. If we analyse the properties of such a tower by increasing the value of K_T in Table 5.1 four times to $37 \cdot 10^6$ N/m and assuming that the structural damping is 2%, we find that we can manage without tower measurements. The properties in Tables 5.4 and 5.5 apply almost unchanged for this plant. For the tower we get the following properties. The open loop system has the relative tower damping $\varsigma_{To} = 3.3\%$ and the standard deviation $\sigma(\dot{z}_T,w) = 0.026$ m/s. For example the closed loop system with the feedback L6 and the observer K1 has $\varsigma_{Tc} = 4.0\%$ and $\sigma(\dot{z}_T,w) = 0.048$ m/s. The closed loop system with the feedback L3 and the observer K7 has $\varsigma_{Tc} = 5.5\%$ and $\sigma(\dot{z}_T,w) = 0.040$ m/s.

Different Weather Conditions and Different Operating Points

So far the design has been carried out for a wind with a mean speed $\bar{U}_0 = 18$ m/s, a standard deviation $\sigma_w = 1.8$ m/s and a time constant $T_w = 20$ s. We will now consider how the design should be extended to handle different weather conditions. Changes in the weather conditions are much slower than the system dynamics so we can separate the control design into two parts. First we can consider design for different but constant weather conditions and then we can consider how the controller should adapt to changing weather conditions, since this adaptation can be slow. This is a common approach in adaptive control.

Let us now first consider the design of pitch angle control for different but constant weather conditions. For simplicity it first will be assumed that the tower is rigid. The mean wind speed $\bar{U}_0$, the synchronous turbine speed $\dot{\psi}_0$ and the desired power level P_{E0} define a stationary operating point. We will as above use the linear models (2.2) and (2.33) - (2.38) to describe the deviations from this point.

The largest variations in the system dynamics are caused by the nonlinear function $T(\beta,U,\dot{\psi})$. The partial derivative T_β varies significantly with $\bar{U}_0$. The influence of the wind turbulence also varies since it is proportional to T_U. The aerodynamical damping is small compared to the desired damping so variations in $T_{\dot{\psi}}$ can be neglected. Let $\beta_0(P_E,U_0)$ denote the blade angle giving P_E at U_0. If P_E cannot be obtained at U_0, let it denote the blade angle giving maximum power. The dependence on $\dot{\psi}_0$ is left out for convenience. It is practical to use the values in Table 5.1 as nominal values and introduce the relative variations k_β and k_U defined as

$$k_\beta(P_E,U_0) = \frac{T_\beta(\beta_0(P_E,U_0),U_0)}{T_\beta(\beta_0(P_n,U_n),U_n)} \tag{5.22}$$

$$k_U(P_E,U_0) = \frac{T_U(\beta_0(P_E,U_0),U_0)}{T_U(\beta_0(P_n,U_n),U_n)} \tag{5.23}$$

with P_n = 3 MW and U_n = 18 m/s. Figures 5.11 and 5.12 show k_β and k_U.

We will now consider the possibilities of isolating and factoring out these variations in the control design. The partial derivatives T_β and T_U enter the linearized model only in the calculation of ΔT, which is basically the sum of the two terms $T_\beta\Delta\beta$ and $T_U\Delta U_0$. Some of the variations are isolated if $T_\beta\Delta\beta$ or the scaled version $k_\beta\Delta\beta$ is viewed as the quantity of interest instead of $\Delta\beta$ itself. Similarly it is sometimes more convenient to consider the quantity $k_U\Delta U_0$ than ΔU_0.

The A and B matrices of model (5.1) which were used for the state feedback design are independent of σ_w. If the second state $\Delta U_0/100$ of this model is changed to $k_U\Delta U_0/100$, the A and B matrices of the model will be independent of T_U. This means that with this modification the resulting state feedback matrix L for a given loss function (5.4) is independent of σ_w and T_U. The matrix L is also rather insensitive to variations in the time constant T_w of the wind model. If T_w varies from ten seconds to 'infinity', the elements of L vary only with a few per cent.

The change of the state $\Delta U_0/100$ to $k_U\Delta U_0/100$ also implies that the observer is independent of σ_w and T_U when the filter gain K is given. The observer becomes independent of T_β if the input $\Delta\beta$ to the observer is changed to $k_\beta\Delta\beta$.

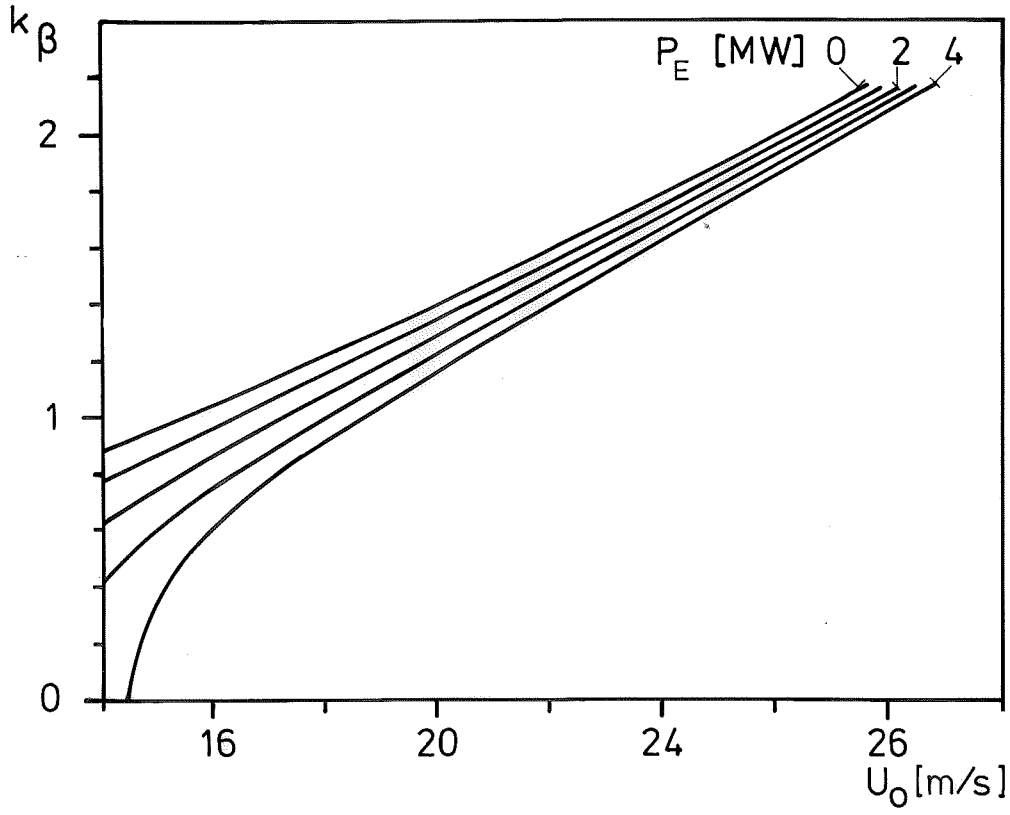

Figure 5.11: $k_\beta(P_E,U_0)$

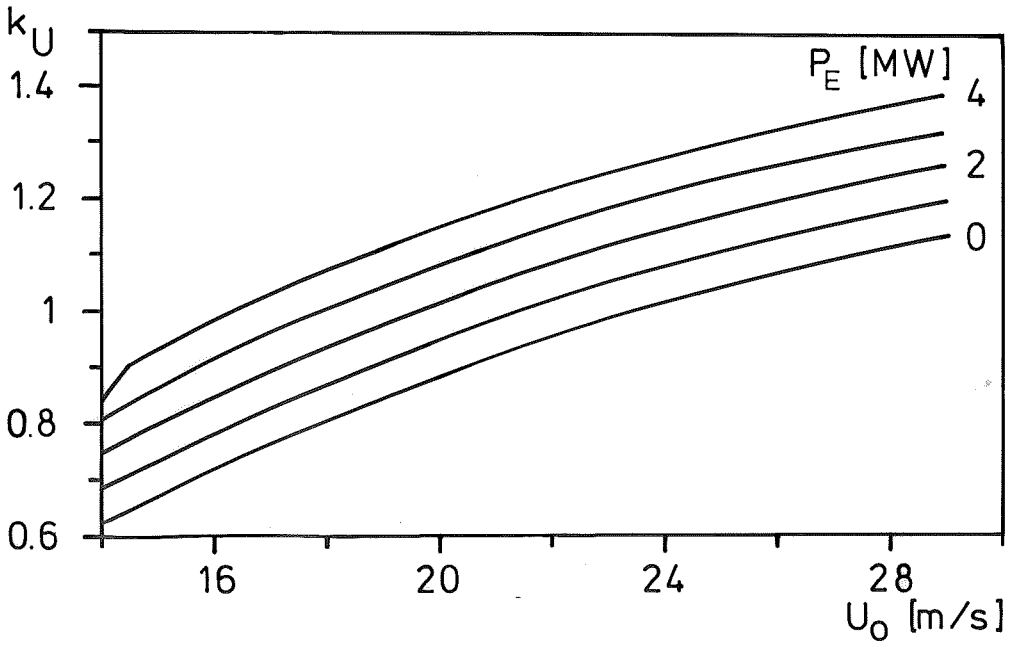

Figure 5.12: $k_U(P_E,U_0)$

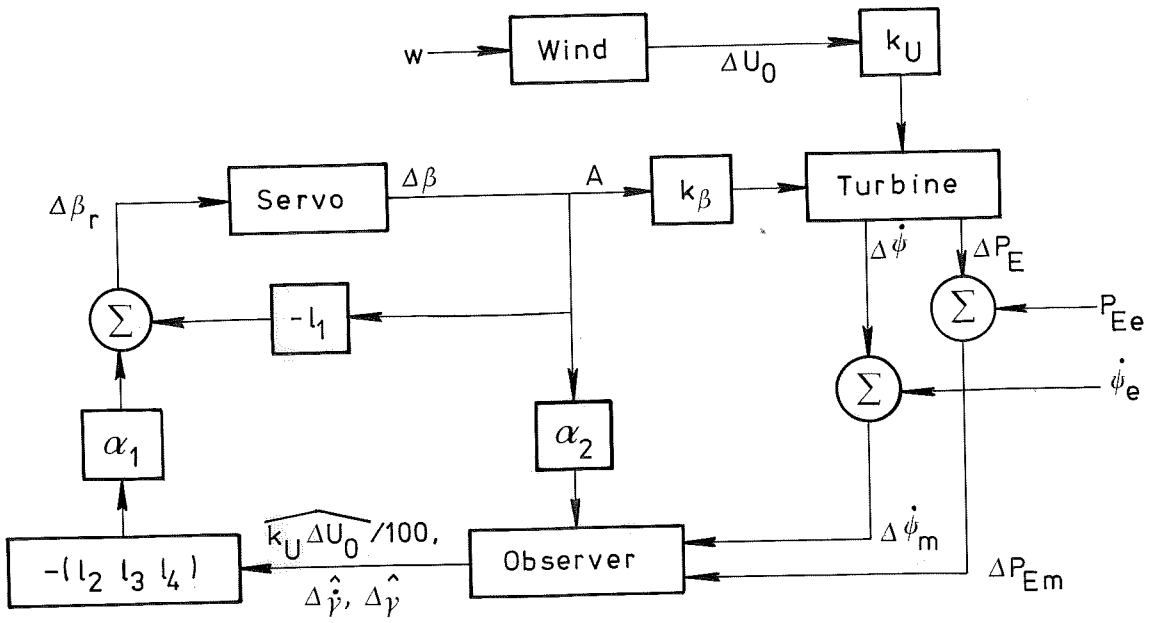

Figure 5.13: Control Configuration (the tower is assumed to be rigid).

Consider Figure 5.13. Assume that the observer has constant A, B and L matrices and that it is designed for the nominal weather condition. Figure 5.13 then shows for a constant feedback L that variations in k_β cause changes in the magnitude of the loop gain when the loop is cut at A. We found above that the possibilities of keeping the power output constant critically depend on the possibilities of measuring or reconstructing ΔT. Variations in k_β do not influence these possibilities to any large extent. From this point of view it thus seems reasonable to try to keep the loop gain constant. The variations in loop gain are eliminated if we choose $\alpha_1 = k_\beta$ and $\alpha_2 = k_\beta^{-1}$. A minimum wind speed $U_0(P_{E0})$ is needed to obtain a certain power level P_{E0}. At this wind speed k_β is zero and then increases as shown by Figure 5.11. This indicates that the regulator gain α_2 becomes large when $\bar{U}_0$ is close to $U_0(P_{E0})$.

For the designs discussed above, the major parts (>80%) of $\sigma(P_E,w)$ and $\sigma(\dot{\beta},w)$ lie within the frequency range above 0.5 rad/s. Since T_w >> 2 s, the spectral density $\Phi_{U0}(\omega)$ of the wind turbulence over the turbine disc given by (2.3) can be approximated by

$$\Phi_{U0}(\omega) \approx \sigma_w^2/(\pi T_w \omega^2) \quad \text{for } \omega >> 1/T_w \tag{5.24}$$

This gives

$$\sigma(U_0,w;\omega_1,\infty) \approx \sigma_w\sqrt{2/(\pi T_w\omega_1)} \quad \text{for } \omega_1 >> 1/T_w \tag{5.25}$$

Model (3.4) can be used to relate σ_w and T_w to the properties of the spectrum for the wind speed at a fixed point. It gives

$$\sigma(U_0,w;\omega_1,\infty) \approx \sigma\cdot b_*\sqrt{2a_*/(\pi L\omega_1)\cdot\bar{U}_0} = \sigma\cdot\sigma_*\bar{U}_0^{0.5} \tag{5.26}$$

where σ is the standard deviation of the point turbulence and L is the integral scale defined by (3.3). The variables a_* and b_* are functions of the ratio R/L. For L > 10 R = 380 m we have $a_* = b_* = 1$ and $\sigma_* = c_*(10R/L)^{0.5}$. The variable c_* is only a function of ω_1. For L = 200 m we have $\sigma_* = 1.18c_*$ and for L = 100 m we get $\sigma_* = 1.28c_*$.

If the loop gain is kept constant for different $\bar{U}_0$, the standard deviation $\sigma(P_E, w)$ is proportional to $\sigma\sigma_* k_U\bar{U}_0^{0.5}$ and $\sigma(\dot{\beta}, w)$ is proportional to $\sigma\sigma_* k_U\bar{U}_0^{0.5}/k_\beta$. We can write these relations as

$$\sigma(P_E,w)\,|_{P_{E0},\bar{U}_0} = c_1\sigma\sigma_*\cdot g_U(P_{E0},\bar{U}_0)/\bar{U}_0^{0.5} \tag{5.27}$$

$$\sigma(\dot{\beta},w)\,|_{P_{E0},\bar{U}_0} = c_2\sigma\sigma_*\cdot g_\beta(P_{E0},\bar{U}_0)/\bar{U}_0^{0.5} \tag{5.28}$$

where c_1 and c_2 are constants and

$$g_U(P_{E0},\bar{U}_0) = (\bar{U}_0/U_n)\cdot k_U(P_{E0},\bar{U}_0),\ U_n = 18\ \text{m/s} \tag{5.29}$$

$$g_\beta(P_{E0},\bar{U}_0) = g_U(P_{E0},\bar{U}_0)/k_\beta(P_{E0},\bar{U}_0) \tag{5.30}$$

Figure 5.14 and 5.15 show g_U and g_β. Figure 5.15 shows that g_β is almost independent of $\bar{U}_0$, when $\bar{U}_0$ is sufficiently larger than $U_0(P_{E0})$. Figure 5.14 shows that g_U is affine in U_0 for a given P_{E0}. The possibility of keeping the output constant depends critically on the measurements as concluded above. When $k_\beta > 1$ this means that the gain from the measurement noises and the 2P variations to $\Delta\dot{\beta}$ is less than in the nominal design.

At mean wind speeds $\bar{U}_0$ close to $U_0(P_{E0})$, a strategy which keeps the loop gain constant would be disastrous. The parameter α_2 must be limited. The choice $\alpha_1 = k_\beta$ means that the physical interpretation of the observer states are maintained. The choice $\alpha_1 = \alpha_2^{-1}$ means that the phase and the shape of the

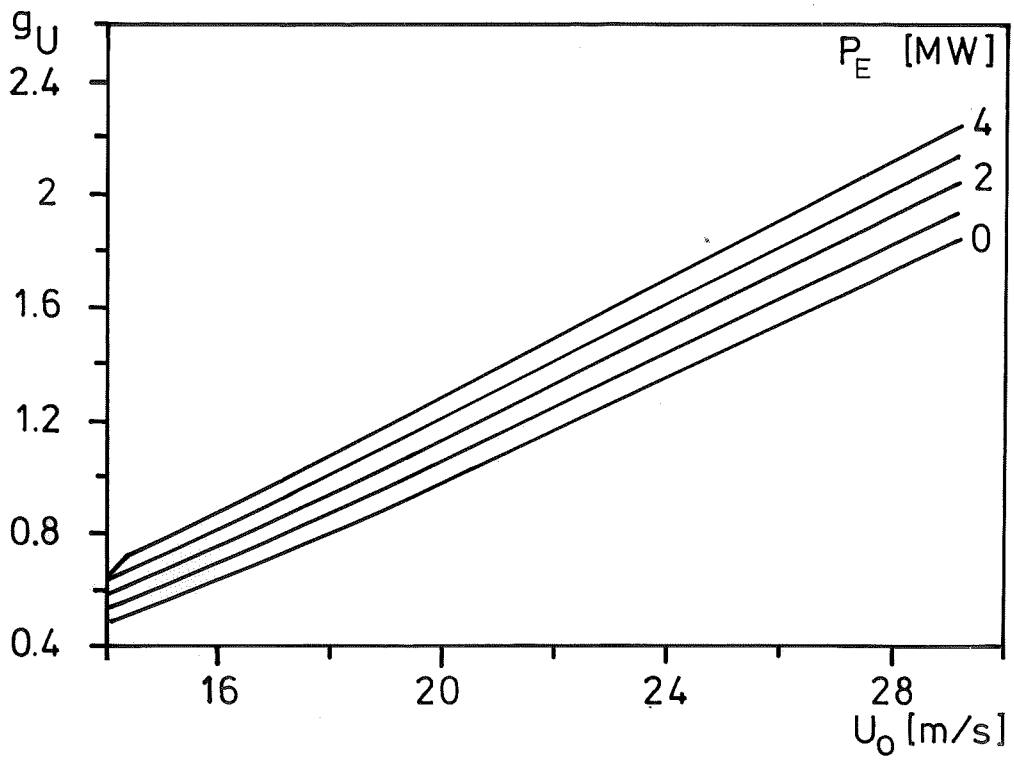

Figure 5.14: $g_U(P_E,U_0)$

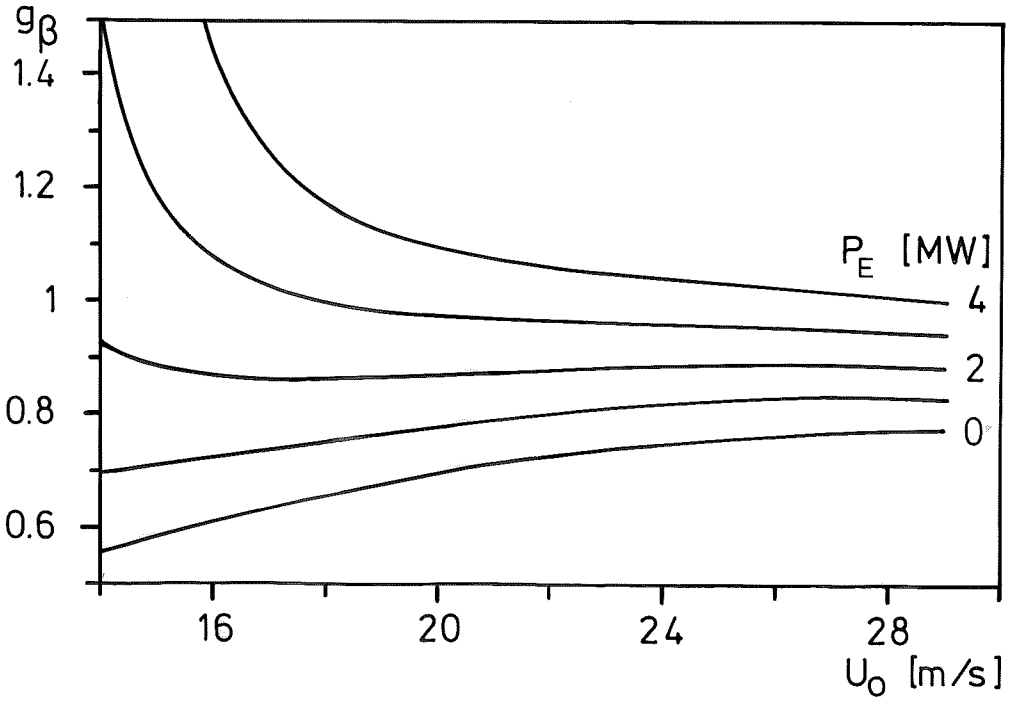

Figure 5.15: $g_\beta(P_E,U_0)$

amplitude curve of the loop gain is maintained. At $\bar{U}_0$ = 15 m/s, σ_w = 1.5 m/s and T_w = 20 s the controller with LC, K7 and α_2 = 1 and $\alpha_1 = \alpha_2^{-1}$ gives the standard deviations $\sigma(P_E,w)$ = 5.5% of P_B and $\sigma(\dot{\beta},w)$ = 0.84 °/s, the relative tower damping ζ_{Tc} = 8.8%, crossover frequency ω_c = 1.8 rad/s and the stability margins φ_m = 48° and A_m = 4.5. The choice α_2 = 1 and $\alpha_1 = k_\beta$ gives $\sigma(P_E,w)$ = 8.5 %, which is worse. It is of course possible to use more sophisticated schemes, but we will not elaborate this problem further.

The scheme discussed above can easily be modified to handle the tower bendings, if $\Delta\dot{z}_T$ is measured. Extend the observer with an input for $\Delta\dot{z}_T$. The coefficient T_z in the observer can be kept constant. Scale the feedback from $\Delta\dot{z}_T$ and Δz_T with α_2. At $\bar{U}_0$ = 25 m/s we have α_2 = 0.56 and for example the controller with LC and K7T gives ζ_{Tc} = 5.4%, φ_m = 46° and A_m = 3.1.

The controller must be able to calculate $\Delta\beta$, ΔP_{Em}, $\Delta\dot{\psi}_m$, $\Delta\dot{z}_T$ and Δz_T from β, P_{Em}, $\dot{\psi}_m$ and $\dot{z}_{Tm}$. The desired power level P_{E0} should be chosen such that the controller can keep the loads inside tolerable limits with a high probability. It can for example be chosen constant or it may be adjusted using estimates of $\sigma(P_E)$. A simple way to estimate β_0 is to use a low pass filtered value of β;

$$\dot{\beta}_0 = (\beta - \beta_0)/T_{b0} \tag{5.31}$$

This introduces integral action. In stationarity the mean values $m(\beta_r)$, $m(\beta)$ and $m(\beta_0)$ are equal, which means that $m(\Delta\beta_r)$ = 0 and $m(\Delta\beta_r)$ = 0. In stationarity our control laws give that $m(\Delta\beta_r)$ is a linear combination of $m(\Delta\beta)$ (=0), $m(\Delta P_{Em})$, $m(\Delta\dot{\psi}_m)$, $m(\Delta\dot{z}_{Tm})$ and $m(\Delta z_{Tm})$. Consequently, if $m(\Delta\dot{\psi}_m)$, $m(\Delta\dot{z}_{Tm})$ and $m(\Delta z_{Tm})$ all are zero, this gives $m(\Delta P_{Em})$ = 0.

If $\Delta\dot{\psi}_m$ is estimated by high pass filtering $\dot{\psi}_m$, we have $m(\Delta\dot{\psi}_m)$ = 0. Since $\Delta\dot{z}_T = \dot{z}_T$ and $m(\dot{z}_T)$ = 0 in stationarity, $m(\Delta\dot{z}_{Tm})$ = 0 in stationarity, if $\dot{z}_T$ is measured without bias. Bias in the $\dot{z}_T$ measurement can be eliminated by high pass filtering, so that $m(\dot{z}_{Tm})$ = 0. In the calculations above the estimate $\Delta\hat{z}_T$ given by

$$\frac{d}{dt}\Delta\hat{z}_T = \dot{z}_{Tm} - \Delta\hat{z}_T/T_{IzT} \tag{5.32}$$

with T_{IzT} = 10 s was used. If $m(\dot{z}_{Tm})$ = 0 then also $m(\Delta\hat{z}_T)$ = 0.

The time constant T_{b0} should be chosen larger than the time constants of the design model, in order not to interfere with that design. In the following we will use T_{b0} = 20 s. The adaption of α_1 and α_2 to changing weather conditions can be based on P_{E0} and β_0. An estimate of $\bar{U}_0$ can be calculated from these values, giving an estimate of k_β.

The controller must also be able to switch between the two operating modes "generate maximum power" and "keep generated power constant" according to the wind variations. A simple way to do this is to have a controller for each mode and run them in parallel and select the smallest output from these two as β_r. The proposed controller for the mode "generate maximum power" is static and thus stable. The proposed controllers for the mode "keep generated power constant" are also stable and the proposed way of introducing integral action avoids wind-up.

Nonlinearities

The variation of the process gain with the wind speed is the most important nonlinearity. If we neglect the variations in turbine speed and the tower bendings, we get

$$\Delta T(\beta,U_0) = [T(\beta,U_0)-T(\beta_0,U_0)] + [T(\beta_0,U_0)-T(\beta_0,\bar{U}_0)] \tag{5.33}$$

The linearized expression

$$\Delta T(\beta,U_0) \approx T_\beta(\beta_0,\bar{U}_0)(\beta - \beta_0) + T_U(\beta_0,\bar{U}_0)(U_0 - \bar{U}_0) \tag{5.34}$$

was used in the design. The second term on the left of hand of both (5.33) and (5.34) is independent of β and can be viewed as the disturbance. The first term describes how the dependence on β varies with the wind speed. The quotient α_β between the nonlinear gain and the linearized gain at the stationary operating point is given by

$$\alpha_\beta(\beta,U_0,\beta_0,\bar{U}_0) = \begin{cases} \dfrac{T(\beta,U_0) - T(\beta_0,U_0)}{T_\beta(\beta_0,\bar{U}_0)(\beta - \beta_0)} & \text{for } \beta \neq \beta_0 \\ T_\beta(\beta_0,U_0)/T_\beta(\beta_0,\bar{U}_0) & \text{for } \beta = \beta_0 \end{cases} \tag{5.35}$$

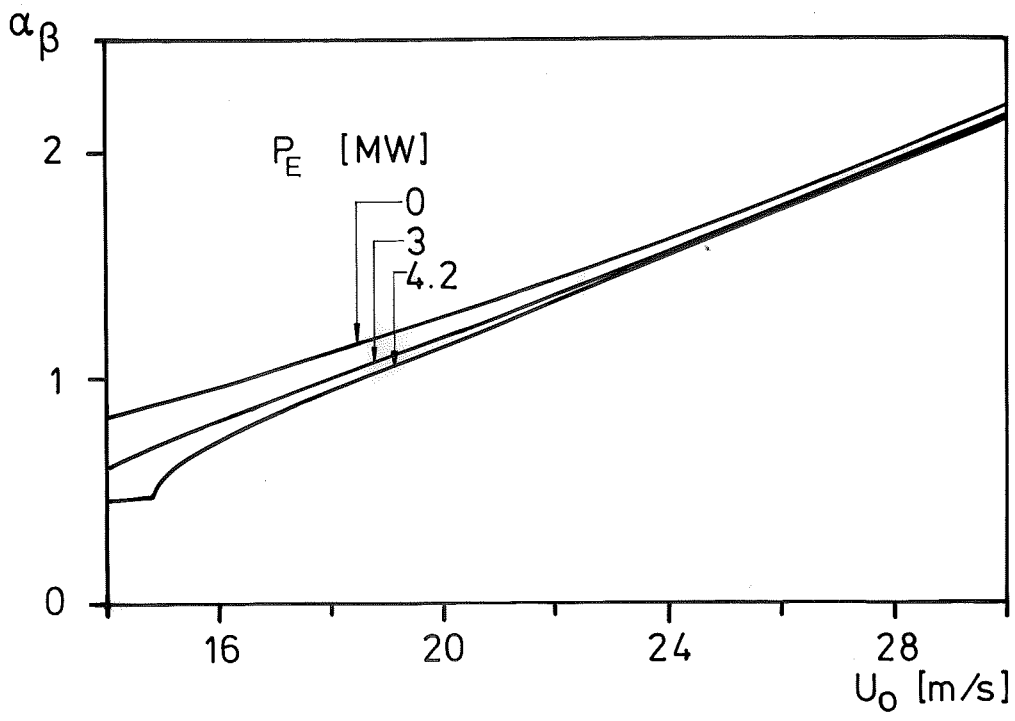

Figure 5.16: $\alpha_\beta(\beta_0(P_E,U_0), U_0, \beta_0(P_n,U_n),U_n))$ for P_n = 3 MW and U_n = 18 m/s.

Since the supervisor will disconnect the generator if $P_E > 4.2$ MW or $P_E < 0$ for longer times, we need only to study α_β for those blade angles which give $0 < P_E < 4.2$ MW. The variable α_β is plotted in Figure 5.16.

The controller for the operating mode "generate maximum power" introduces other nonlinearities so that stability cannot be established simply by use of the circle criterion even if the tower is assumed to be rigid and the nonlinearities introduced by the adaption of α_1 and α_2 are neglected.

Simulations

The behaviour of the system with the controllers suggested above has been simulated using the nonlinear simulation model given in Appendix B. Three typical simulation results will be shown. The controller based on LC and K7T with schedules of operating point and gains as given above was used in these simulations. The controller was also extended with notch filters (5.14) with $\zeta_N = 0.01$ and $\zeta_D = 0.1$ for the 4P, 6P and 8P variations. The Simnon code for this controller is given in Appendix B.9. For excitation control the voltage

controller described in Appendix B.7 was used. No measurement noise was introduced but exact measurements were assumed.

Figure 5.17 shows the behaviour in the weather condition assumed for the base design. The behaviour is consistent with the calculations above. Figure 5.17 also shows that the variations in the terminal voltage V_{gen} are small.

Linde (1983) has calculated average gusts from turbulence measurements. In one case he used a measurement series from Maglarp at the level 84 m. The mean wind speed was 18.1 m/s and the standard deviation was 1.6 m/s. In the simulation presented in Figure 5.18 the mean wind speed U_0 over the turbine disc was chosen as the average gust of this measurement series. This choice is probably pessimistic since Linde (1983) found that the measurements indicated the extent of a gust in the vertical direction is less than 60 m. The figure shows that the response in the electrical power is well damped. Also the tower response is satisfactory. The small and rapid variations in P_E, $\hat{U}_0$, $\dot{\beta}$ etc are caused by the tower blockage. This disturbance does not cause excessive servo motions as shown by the figure. Figure 5.18 also illustrates the lag in the estimation of U_0. The loss of measured U_0 limits the performance considerably. The maximum value of P_E is just below 130%. If U_0 had been available then the feedback LC extended with notch filtering at the frequencies 2P, 4P, 6P and 8P of the feedback from $\Delta\dot{\psi}$, ΔP_E, $\Delta\dot{z}_T$ and Δz_T would have kept P_E below 111% with almost the same control effort.

Figure 5.19 shows the behaviour around the rated wind speed when the controller switches operating mode back and forth. A simple schedule based on generated power was used for the operating mode "generate maximum power".

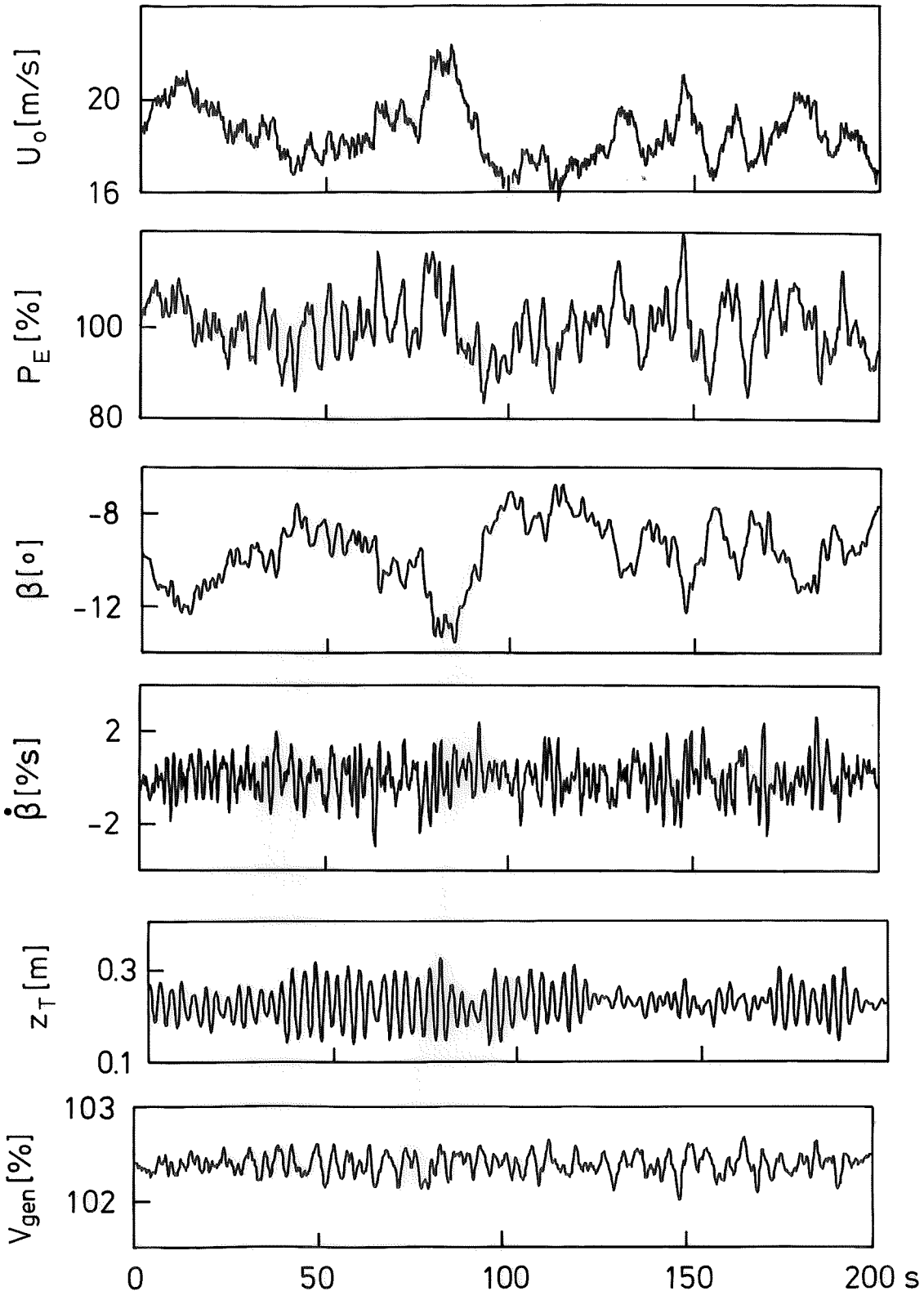

Figure 5.17: Simulated response to turbulent wind around 18 m/s when the controller based on LC and K7T is used.

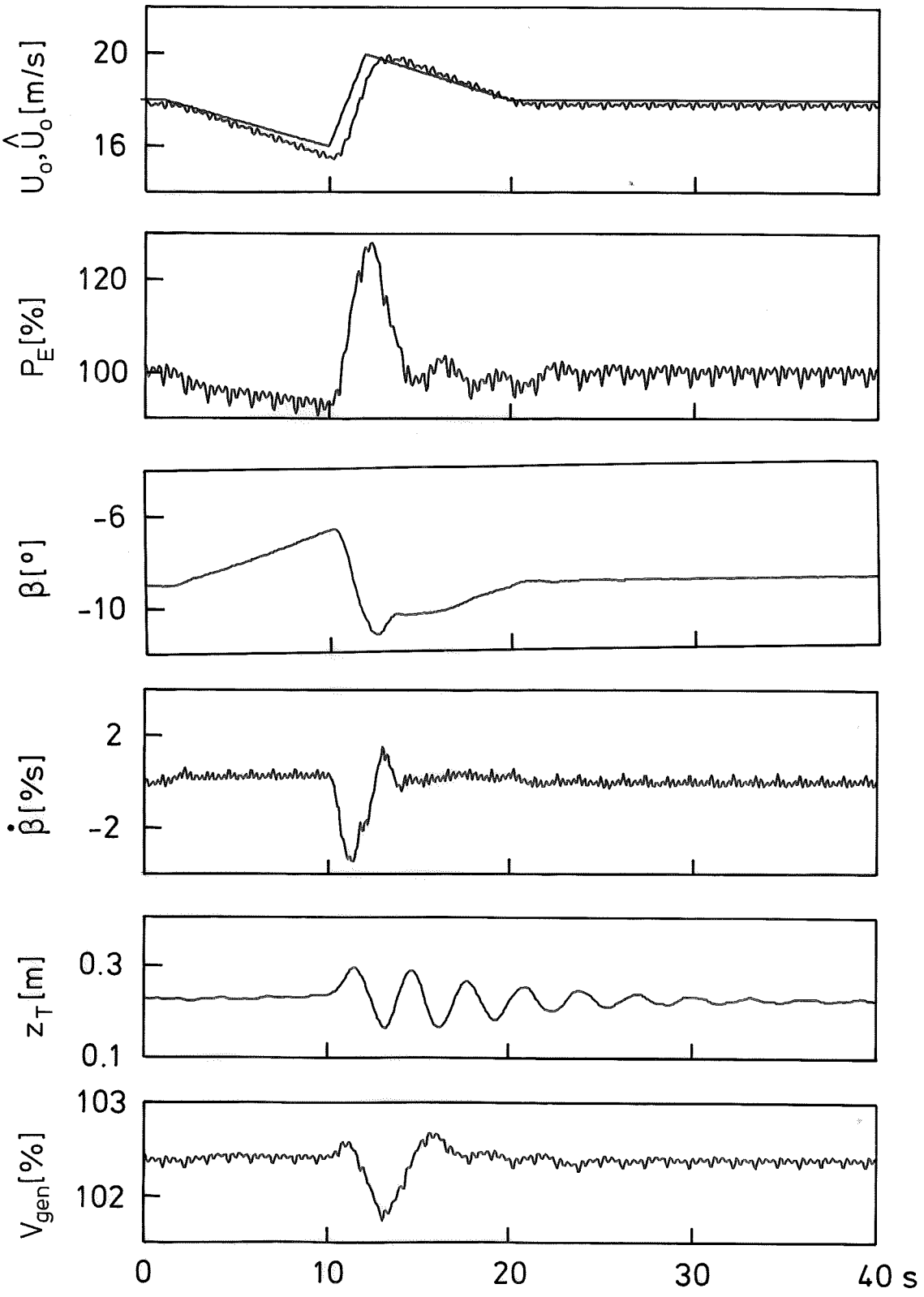

Figure 5.18: Simulated response to a large gust when the controller based on LC and K7T is used.

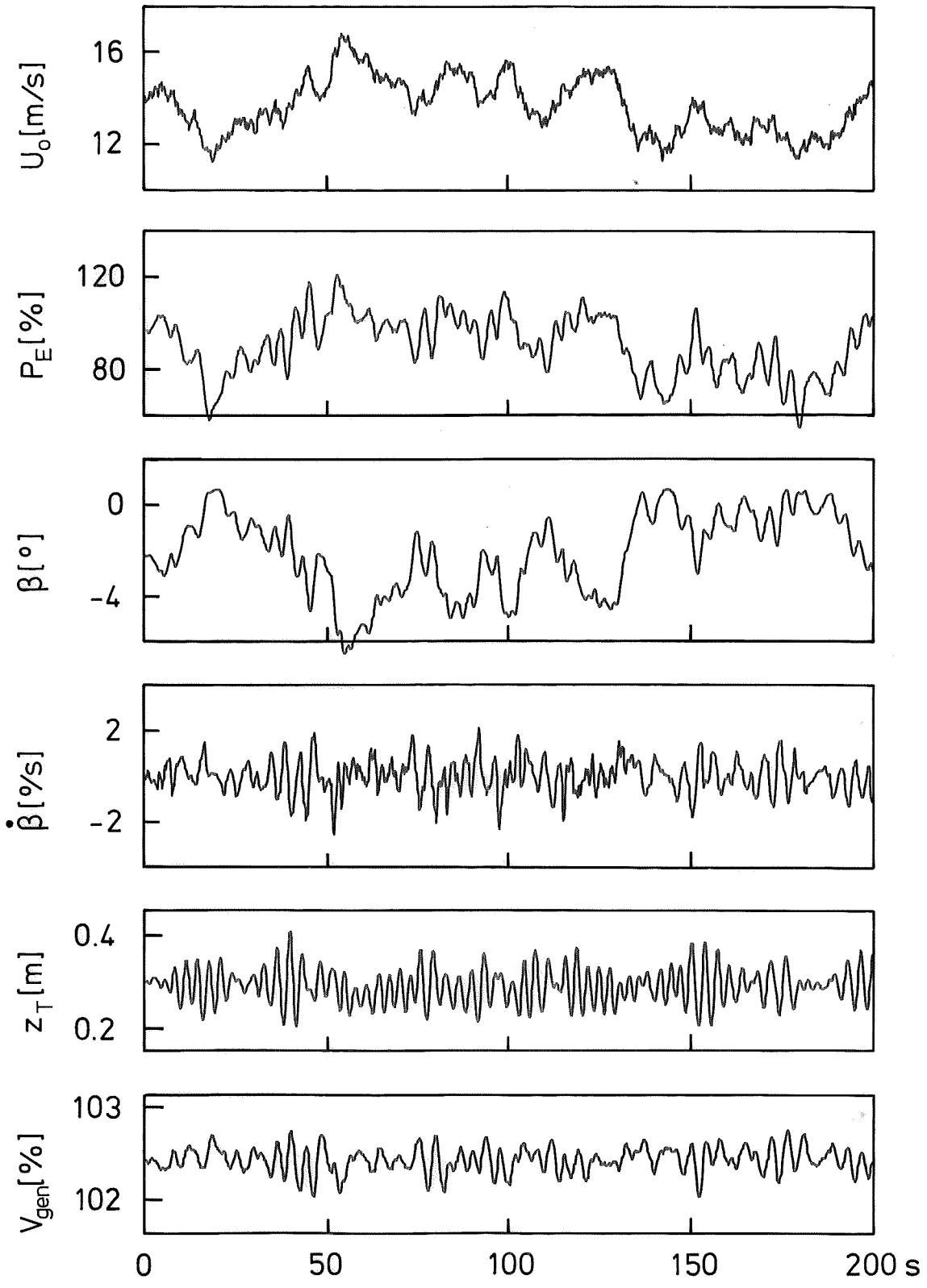

Figure 5.19: Simulated response to turbulent wind around 14 m/s when the controller based on LC and K7T is used.

Summary

In this section design of pitch angle control for plants having synchronous or induction generators has been discussed. It was found that it was easy to obtain a good result for the operating mode "generate maximum power". The mode "keep generated power constant" was more difficult.

When designing pitch angle control for keeping the power output constant, attention was focused on the variations caused by the mean wind speed U_0 over the turbine disc. Cyclic pitch control was not considered. It was assumed that the 2P variations were properly attenuated by a soft shaft or could be neglected.

In the mode "keep generated power constant", it is the difficulties in measuring the wind speed U_0 experienced by the turbine that limit the performance. The control authority is good. Feedforward from U_0 is a key to good performance. If U_0 is known it is possible for a system like the WTS-3 to keep the generated power output constant within 10 - 15% with a high probability and with a maximum servo speed of 5°/s. Unfortunately, it is not possible to obtain representative measurements of U_0 using an anemometer. When only turbine speed measurements and power measurements are available the measurement noise are important. To obtain a good performance the controller must introduce phase lead which means that measurement noise is amplified generating excessive servo motions. Even if the turbine speed measurements and power measurements are improved they still contain the 2P variations. These can be viewed as measurement disturbances since they should be neglected by the pitch angle controller. To avoid excessive servo motions and to get a robust control variations in the generated power up to 30 - 40% must be accepted.

Normally the first tower bending mode is the only structural mode that may have to be considered when designing compensators for the variations caused by U_0. It can be neglected if its natural frequency is greater than twice the crossover frequency of the pitch angle control. If the frequencies are closer together, it is possible to get an adequate damping of the tower bendings without deteriorating the control of the power output if the speed of the tower bendings is measured. Without measurements of the tower bendings greater variations in the generated power must be accepted.

5.4 Pitch Angle Control for Variable Speed Plants

In this section pitch angle control for systems with variable speed generators is discussed. The important differences in comparison to systems with synchronous generators or induction generators are that the the generated power also can be controlled at the generator and that the large turbine inertia can be used to store kinetic energy.

If we want to extract maximum power the pitch angle should be kept constant and the generator should control the turbine speed so that the tip speed/wind speed ratio is constant. The critical turbine speeds causing structural resonances must of course be avoided. As found in Section 2.2 there are systems which allow the generator speed to vary in the range 4 - 130% of synchronous speed. For the Growian I the range is only 85 - 115% of synchronous speed and the possibility of varying the turbine speed is not intended to be used to maximize the generated power, but the plant is desired to operate close to synchronous speed. Here, it is natural to use the pitch angle control to extract maximum power. The generator control can make use of the large inertia to improve the power quality under the constraint that the generator rotor speed be inside the allowed interval.

When reconstructing the wind speed U_0 for calculation of the optimal control, the generator dynamics and the generator losses can be neglected. The wind speed can be estimated from turbine speed and power measurements using the equation of motion for the turbine

$$J_t\ddot{\psi} = T - P_E/\dot{\psi} \qquad (5.36)$$

The problems with measurement noise are not serious, since the demands on the bandwidth are moderate.

The pitch angle control problem above the power level P_{E0} is simpler when a variable speed generator is used. The bandwidth of the control loop can be made lower, since the large turbine can be used to store kinetic energy. The objective of the pitch angle control is to keep the deviation $\Delta\dot{\psi}$ of the turbine speed from synchronous speed $\dot{\psi}_0$ within tolerable limits. A plant which operates at an almost constant turbine speed can be designed so that the rotation does not cause structural resonances. When the turbine speed can vary, operation at the critical

speeds of the system must be avoided. One way to do this is to keep the turbine speed variations small.

We will not discuss the control problem in such detail as for the case when a synchronous or induction generator is used. Let it suffice to show the adequacy of the simple PI-controller with a low pass filter

$$\Delta\beta_r(s) = K\left[1 + \frac{1}{sT_I}\right] / (sT_F + 1)\ \Delta\dot{\psi}(s) \qquad (5.37)$$

The low pass filter is included to protect the servo from high frequency noise.

Above the power level P_{E0}, the objective of the generator control can be to keep the shaft torque or the generated power constant. We will study the case when the generator keeps the generated power constant. In this case it is somewhat more difficult to keep the turbine speed constant by pitch angle control, because of the shaft torque decrease with increasing turbine speed. Since the resulting crossover frequency ω_c can be kept below 1 rad/s, it is reasonable to make the simplifying assumption that the dynamics of the generator can be neglected and that the generated power is kept constant at P_{E0} by the generator control system. Note that these assumptions hold for any generator when it is disconnected. Consequently, this discussion also considers the possibilities of keeping the turbine speed constant when synchronizing a synchronous generator against the grid.

The assumptions for (5.36) are fulfilled. Linearization around the stationary operating point $\bar{U}_0$, $\dot{\psi}_0$ and P_{E0} assuming constant generated power gives

$$J_t\ddot{\psi} - (P_{E0}/\dot{\psi}_0^2 + T_{\dot{\psi}})\Delta\dot{\psi} = T_\beta\Delta\beta + T_U\Delta U_0 + T_{\dot{z}}\Delta\dot{z}_T \qquad (5.38)$$

The models (2.2), (2.36) - (2.39), (5.38) and the values in Table 5.1 give $\sigma(\dot{\psi},w)$ = 38.3% of $\dot{\psi}_0$ for the open loop system. The controller (5.37) with K = 0.5 rad/(rad/s), T_I = 10 s and T_F = 0.5 s gives the standard deviation of the output $\sigma(\dot{\psi},w)$ = 2.1% of $\dot{\psi}_0$ and of the input $\sigma(\dot{\beta},w)$ = 0.66°/s. For the tower we get the standard deviation $\sigma(\dot{z}_T,w)$ = 0.076 m/s and the relative damping ζ_{Tc} = 7.4%. The crossover frequency ω_c = 0.9 rad/s and the stability margins A_m = 2.8 and φ_m = 42°. The influences of the measurement noise are low. If we assume that the measurement noise of the turbine speed is as given by R_{e1} we get $\sigma(\dot{\psi},\dot{\psi}_e)$ = 0.04% of $\dot{\psi}_B$ and $\sigma(\dot{\beta},\dot{\psi}_e)$ = 0.054°/s. Since the turbine speed varies, it is

not quite correct to speak about 2P disturbances. Nevertheless, the tower blockage, the wind profile and the rotational sampling generate disturbances. A sinusoidal variation in the aerodynamical torque with the frequency 5.2 rad/s and the amplitude 10% cause for fixed pitch angle a variation in the turbine speed of 0.2%. The increase in the gain from ΔU_0 to $\Delta\dot{\psi}$ for the closed loop system compared with the open loop system above 4.5 rad/s is less than 4%. The gain from ΔU_0 to $\Delta\dot{\beta}$ above 4.5 rad/s is less than 0.3°/s/(m/s) and the value of g_{2P} = 0.21°/s/(m/s).

6. CONCLUSIONS

To make wind power competitive in a large utility grid it is important that the wind power plants are cheap and reliable. It is a nontrivial design problem to make the best choice. The objective of this thesis has been to give a global picture of the control problem of large horizontal axis wind power plants. The system dynamics has been discussed and explained. Measured data have been analysed and models have been identified. Comparisons between mathematical models and identified models showed good agreement. The possibilities and limitations of pitch angle control as well as the interaction between control design and process design have been discussed.

This investigation has also resulted in a modular simulation model. The model, which is programmed in a high level language, is easy to use. It is valuable both for further research and education. A design procedure for pitch angle control based on the LQG framework is proposed. The design procedure considers wind properties and measurement noise explicitly. Pitch angle control has been discussed in a number of papers: Kos (1978), Wasynczuk et al (1981), Liebst (1980, 1981), Murdoch et al (1983) and Hinrichsen (1984). It is remarkable that all these papers and reports except Liebst (1981) overlook measurement noise and do not consider the wind properties explicitly. The measurement noise is very important. Svensson and Ulén (1982) found when testing the control system of the WTS-3 that measurement noise was a limiting factor. The control proposed by Liebst (1981) is a complex cyclic pitch control for load alleviation on wind turbines. He proposes accelerometers on the blades as measurement devices and gives the design procedure for design of Kalman filters. However, he does not discuss or analyse how measurement noise influences the result.

The results of the investigation are summarized in Section 6.1 and some aspects of more general interests are given in Section 6.2.

6.1 A Global Picture of the Control Problem

Wind Characteristics

The variations in the wind speed are large, rapid and random. For control design the variations in the mean wind speed over the turbine disc can be modelled as the output of a first order system driven by white noise with a time constant of the order of 5 - 30 seconds. The standard deviation is approximately 5 - 20% of the mean wind speed. Wind profile, tower blockage and wind turbulence cause spatial variations in the wind speed over the turbine disc. These spatial variations give fluctuations in torque with frequencies being multiples of the rotational frequency of the turbine. For a turbine with two blades the largest component has a frequency twice the rotational frequency (2P) of the turbine. Without compensation the amplitude of the variation in the driving aerodynamical torque is typically 10 - 30% of mean torque.

Control objectives

Reduction of the peak loads caused by the varying wind speed is a basic control objective, since it is expensive to build plants that can withstand large loads. The drive train, the gearbox and the root sections of the blades are critical parts. The demands on voltage and power quality are not critical. A reasonable strategy is to let the controller try to extract maximum power up to a certain level and to keep power generation constant above this level. This means that the controller should try to maximize generated power when the mechanical loads are small and that it should try to achieve a smooth operation for high mechanical loads. This approach gives a design problem that can be handled satisfactorily using existing control theory.

Basic Plant Characteristics

The driving aerodynamical torque, which forces the turbine to rotate, is a function of the oncoming wind, the blade angle and the turbine speed. Consequently, the power generation can be controlled by turning the blades or parts of them along their longitudinal axes. The torsional dynamics of the turbine, the drive train, the generator and the coupling to the grid are a key to understanding the basic dynamics of horizontal axis wind power plant.

A wind turbine has a very high per unit inertia. The low energy density of wind requires a large turbine diameter. To achieve good efficiency the turbine speed/wind speed ratio must lie within a narrow range giving turbine speeds between 15 and 50 rpm. Typically the per unit inertias of wind turbines are about ten times greater than those of typical hydro or steam turbines. The large turbine inertia can be used to store kinetic energy if the turbine speed is allowed to vary on-line operation. This facilitates the control of the plant. It is thus natural to divide plants into the two groups

1. Constant speed plants

   The plants have a synchronous generator or induction generator so that the turbine speed is almost constant. Pitch control is the only means of controlling the power generation.

2. Variable speed plants

   The plants have a generator that can operate at variable speed so that the turbine speed may vary. The power output can also be controlled at the generator.

Possibilities with Constant Speed Plants

It is easy to achieve a good result when trying to maximize generated power. The maxima for different wind speeds are rather flat with respect to the blade angle. A simple and adequate strategy is to make the servo reference a function of the generated electrical power and the blade angle.

Feedforward from the mean wind speed sensed by the turbine is a key to good results when trying to keep the power output constant If the turbine speed, the electrical power and the wind speed sensed by the turbine are known, it is possible to design a controller which for a system like the WTS-3 keeps the generated power constant within 10 - 15% of the rated value with a high probability and with a maximum servo speed of 5°/s. Unfortunately, it is not possible to obtain representative measurements of wind speed using an anemometer. The wind speed at a point is in some weather conditions poorly correlated with the wind speed experienced by the turbine. The plant may also induce local disturbances so that an anemometer gives bad measurements. The inadequacy of wind measurements makes it impossible to keep the generated power within 10% of the rated value; 30 - 40% is a more realistic goal.

The dynamics of interest for pitch angle control is given by the first torsional mode of the turbine, the drive train, the generator and the coupling to the grid. The behaviour from the aerodynamical torque T to the torsion γ of the drive train can be approximated by the transfer function

$$\Delta\gamma(s) = \frac{1}{p_2 s^2 + p_1 s + K_s} \Delta T(s) \qquad (6.1)$$

where K_s is the torsional spring coefficient of the drive train. The coefficients p_1 and p_2 are such that model (6.1) preserves the pole pair related to the first torsional mode. For the generated power P_E we have

$$\Delta P_E(s) = \dot{\psi}_0 (D_s s + K_s) \Delta\gamma(s) \qquad (6.2)$$

where $\dot{\psi}_0$ is the synchronous turbine speed and D_s is the damping coefficient of the drive train. In this approximation the variations in the shaft torque is proportional to the variations in generated power.

The relations (6.1) and (6.2) are important and fundamental for pitch angle control. They show that the variations in the aerodynamical torque above the natural frequency ω_1 of the first torsional mode are attenuated when they appear as shaft torques and generated power. The natural frequency ω_1 is in the interval 1 - 10 rad/s. The torsional stiffness of the drive train is the major design parameter for choosing ω_1. The spring coefficient K_s can be varied in a range of two decades.

When a synchronous generator is used, the damping is given by the drive train and is in general low. The aerodynamical damping of the turbine is low, because the blades are designed to give minimum losses. The controller must dampen the mode. The natural frequency ω_1 and thus K_s influence the crossover frequency needed for pitch angle control. There is no sense in choosing it much higher than ω_1 when trying to keep the generated power constant, due to the filtering effect of the dynamics. When an induction generator is used the first torsional mode is much better damped since the coupling to the grid basically acts as a damper. The relative damping increases with increasing ω_1 and the pitch angle control need not dampen the mode if ω_1 is large.

The designers of the MOD-2 and the WTS-3 have taken advantage of the low pass dynamics and deliberately designed the drive train to be torsionally soft. The MOD-2 has ω_1 = 0.9 rad/s and the WTS-3 has ω_1 = 1.4 rad/s. An important disturbance is the 2P variations in the aerodynamical torque. The turbine speeds of MOD-2 and WTS-3 are 25 rpm. This implies that the 2P variations have a frequency of 5.2 rad/s. This means that the 2P variations in the aerodynamical torque are attenuated more than eight times when they appear as shaft torques. The turbines are designed to withstand the variations in the aerodynamical torque. Consequently, the pitch angle control system does not have to take care of the 2P variations.

To obtain a good control result it is important to have a good estimate of the wind speed in the frequency interval where the filtering effect of the dynamics from the wind speed to generated power is low. However, the dynamics also introduce a phase lag from the wind speed to the measurements. This makes the reconstruction of the wind speed difficult. Around the natural frequency ω_1 of the first torsional mode there is low filtering effect, but a considerable increase in phase lag. The controller must compensate for the phase lag by introducing phase lead which means that measurement noise is amplified generating excessive servo motions. Relation (6.2) indicates that there is less phase lag in $\dot{\gamma}$ than in P_E. However, if the variations in P_E are kept within 10% of rated value the variations in $\dot{\gamma}$ for a soft shaft is less than 1% of synchronous turbine speed. A stiffer drive train gives less variations in $\dot{\gamma}$. This means that speed measurements must be very accurate. Note that (6.2) also indicates that an increase of D_s gives a decrease in phase lag of P_E. Recall that in the frequency range of interest for pitch angle control the dynamics from aerodynamical torque to shaft torque and to electrical power are similar, so it is of no use to measure the shaft torque.

Even if the measurements of turbine speed and electrical power are improved they still contain 2P variations. The 2P variations can in this case be viewed as measurement disturbances since they should be neglected by the pitch angle controller. Unfortunately, the 2P frequency lies near the desired crossover frequency (2 - 3 rad/s) of the pitch angle control. If the 2P variations are neglected when designing the pitch angle control the controller obtained will introduce high gain in this frequency range. The result will be an oscillation of the servo with a rate amplitude of several degrees per second. Notch filters must be used so that excessive servo motions are avoided. The notch filters degrade

the performance. Analysis of measurements indicates that the 2P variations have a random component. Neither the amplitude nor the phase is constant. The effect of rotational sampling of the turbulence is a possible explanation. It seems impossible to design better filters.

The filter properties at 2P depends on ω_1. If ω_1 is close to or larger then 2P the 2P variations in the driving aerodynamical torque cause large variations in the shaft torque. To reduce these variations servo speeds of several degrees per second are needed. A soft shaft is a nice way to attenuate the 2P variations in the shaft torque. However, it is not quite easy to design a torsionally soft shaft that can stand the bending torques. A soft suspension of the planetary gearbox as done in the WTS-3 is one solution to the problem. Another quite different approach to attenuate the variations in the shaft torque is to use a variable speed generator.

Possibilities with Variable Speed Plants

The problem of keeping the shaft torque or the generated power constant is simpler when a variable speed generator is used. The large turbine can be used to store kinetic energy and the generated power can also be controlled at the generator. The generator control determines the variations in the shaft torque and the generated power. The standard deviation of turbine speed variations can be kept below a few per cent of the rated speed with a pitch angle control having a crossover frequency below 1 rad/s and with a maximum servo speed of 5°/s. Note that these figures also apply for any system which is is not connected to the grid. Thus it is not difficult to synchronize a generator against the grid.

Structural Dynamics

The control system must not excite structural modes of the tower and the blades. It is the first tower bending mode that may interfere with the pitch angle control and cause problems. Normally the first tower bending mode is the structural mode with the lowest natural frequency. If the natural frequency of the mode is sufficiently (say a factor of two) larger than the crossover frequency of the pitch angle control, the tower bendings can be neglected when designing the pitch angle control. When the frequencies are closer together, it is possible to get an adequate damping without deteriorating the control of the power output, if the speed of the tower bendings is measured. Greater variations in the torques must

be accepted without measurements of the tower motions. Consequently, the designer must consider the cost of an additional sensor when reducing weight of the tower. Note also that pitch angle control for variable speed plants in general has lower crossover frequencies than those for constant speed plants. However, a plant which operates at an almost constant turbine speed can be designed so that the rotation does not cause structural resonances. When the turbine speed can vary, operation at the critical speeds of the system must be avoided.

The turbine can be designed to withstand variations in the aerodynamical torque. This seems more robust than to alleviate the blade loads by having active cyclic pitch control. Sensors like accelerometers and strain gauges are then needed to measure blade motions and blade loads. It must be possible to control the blade angles individually. High servo speeds in the order of 12°/s are also needed.

6.2 General Aspects

This thesis has dealt with a specific problem. Hence we may also ask what we have learned that can be of more general interest.

Since the main objective of the work was to give a global picture of the control problem, we had to gain understanding for a complex physical process. Mathematical models were compiled from the literature. The behaviour of different models was simulated, analysed and evaluated. Measurements from the WTS-3 were analysed and dynamical models were identified and compared with models derived from first principles. Control systems were designed. Their properties were investigated as well as the interaction with the system design. These steps involve lots of calculations. Unfortunately, only a very few of them can be carried out analytically. Most of them must be done numerically by a computer. For professional use, methods which are not supported with good software are of small value. The numerics must be robust and reliable. The user should not be forced to numerically scale his problem. The programs for analysis and design should of course warn the user when the result is sensitive to variations in the input data. Furthermore, many methods for analyse and design involve steps of trial and error. A good interactive man-machine interface is then of great value. The user should be able to control the steps in a simple way. He should be able

to examine the results using for example good graphics. With a computer it is rather easy to calculate a number of cases under different assumptions and to generate lots of results. However, it is impossible to keep in mind how the different results were obtained. Automatic documentation is needed. Let us now consider the different steps.

Modelling, Simulation and Analysis of the System Dynamics

This work was started with a more modest objective in mind than giving a global picture of the control problem. The work was initiated during the design of the WTS-3 by request of Sydkraft AB (the South Swedish Power Company Ltd.). They wanted a simulation model for design verification and failure investigation. They also wanted a model suitable for educational purposes and for future design of new controllers. This resulted in a simulation model and a number of simulation studies. The latest version of the simulation model is given in Appendix B. The interactive simulation package Simnon (Elmqvist (1975)) was used. Simnon allows good structuring and programming in a high level language.

The model in Appendix B is modular. Modularization gives many advantages. It simplifies the modelling, it makes the model more flexible and easier to adapt and manage. Technical systems are often built in a modular way composed of standard components. Their behaviour may be well-known. Even good, generally accepted models may already exist. A synchronous generator is an example of such a standard component. We can build and use libraries of models. Modularization makes the model easier to adapt for different simulations. Two conceptually different needs of adaptability can be identified: adaptability with respect to different plant designs and adaptability with respect to model complexity. During the design of a system the model has to be updated as the design proceeds. Questions of the type "What happens if we modify the design in this way?" arise frequently in simulation projects. It is impossible to make a model which can simulate all aspects of a given plant. Models of different complexity must be used for simulation of different events. For example, if we want to simulate how a power plant behaves at electrical faults in the grid, a complex generator model is needed. The complex model contains fast modes which requires a lot of computations. Fortunately, these events are short and we are only interested in simulating a few seconds. If we want to simulate the behaviour in turbulent wind we are interested in simulating over a couple of minutes. The fast modes are not excited and can thus be neglected. The improvement in computational speed is

considerable. It may be improved a factor of 10 - 50. Modularization facilitates testing. It is difficult to verify that a simulation program implements the intended mathematical model. Use of a high level language facilitates the programming and the documentation and makes the program more readable. With a modular approach we split the problem into smaller parts. We can start with simple models and use them as references when testing the more complex ones.

The analysis presented in Chapter 2 is the result of a number of simulation studies including several revisions of the models. The aim was to gain a more profound understanding of the system dynamics. The simulation studies had given an insight in the dynamics based on available equations. However, the mathematical simulation model is a complex description composed of models for the different parts. It is not apparent what the basic dynamics for the total system is. It is difficult to analyse nonlinear systems. The simulation model was used for empirical studies concurrently with the mathematical analysis. The possibilities in Simnon to include and exclude different features in the model by changing the model for one part or by making parameter changes were useful when studying their importance. To have some success with the analysis we are more or less forced to work mainly with linear models and to estimate the effects of nonlinearities. Linearization is tedious to do with paper and pen. A good formula manipulation program which takes the nonlinear equations and outputs the linearized ones would be a real time-saver. If there also was a program that took the linear model and intervals for the parameters and made proper approximations, the analysis would be even simpler to carry out. A nice thing with linear models is that they can be transformed into the frequency domain where many dynamical properties are easier to understand. When analysing a system it is also useful to have different viewpoints and possibilities to transform back and forth between different representations.

System Identification

The analysis of measurements from the WTS-3 presented in Chapter 4 and the control design presented in Chapter 5 were done concurrently. The analysis of measurements and the identification of dynamic models involve a lot of trial and error. We have to try different filtering of data, different sampling frequencies and different model structures. Consequently, we generate many versions of the measurements which are filtered or processed in other ways. A database manager that keeps track of the different versions is thus of great value.

We also faced the problem of system identification using analog inputs. A low sampling frequency facilitates the identification, but the shape of the inputs between the sampling instances becomes more important. A high sampling frequency makes it more difficult for the identification procedure and makes the transformation from discrete time model to continuous time model more ill-conditioned. New approaches to system identification so that continuous time models can be identified directly from data sampled with high frequency are desirable.

Control Design

The simple models obtained from the analysis of the system dynamics were used for control design. They gave a possibility to gain a good understanding of the possibilities for pitch angle control and the interaction with process design. Caution is needed when using simple models. The model must be valid for frequencies a bit over the crossover frequency. It must be verified that unmodelled dynamics is not harmful. If it is difficult to estimate the crossover frequency in advance, one possibility is to use a more complex design model. If the controller then is considered to be too complex try to simplify it afterwards. The frequency range of interest is then known.

The control design and the analysis of its interaction with process design implied that many cases had to be considered. Modularization of the models gave also here many advantages. The interactive program package Synpac (Wieslander (1980b)) was used. In Synpac linear models can be entered and connected together to give the total system.

A way to check a result is to calculate it in two different ways. The package CTRL-C (1983) was used in this way to check some of the results. Synpac and CTRL-C are so different that the programming has to be done in quite different ways.

7. ACKNOWLEDGEMENTS

It is a great pleasure for me to thank my supervisor Professor Karl Johan Åström for his encouraging support and guidance throughout the work.

I would like to thank all my colleagues at the Department of Automatic Control for a lovely time and for a most stimulating atmosphere. In particular, I would like to thank Per Hagander, Björn Wittenmark and Craig Elevitch for their valuable criticism of the manuscript. Many thanks also to Leif Andersson for his excellent document programs, and to Britt-Marie Carlsson and Doris Nilsson for careful preparation of the figures.

This work has drawn upon results and experiences from a number of projects in the wind energy area since 1980. I would like to express my sincere gratitude for the valuable discussions I have had during this time with manufacturers of wind power plants, the Swedish utilities, the Aeronautical Research Institute of Sweden and the Swedish National Defence Research Institute.

Especially, I would like to thank Sten Bergman. He was with Sydkraft AB during the major part of this work. I am grateful for his assistance in providing information about wind power plants and for many stimulating discussions.

Finally, the financial support given by the National Swedish Board for Energy Source Development (NE) and Sydkraft AB is gratefully acknowledged.

8. REFERENCES

Anderson, B.D.O. and Moore, J.B. (1971). Linear Optimal Control. Prentice-Hall, Inc., Englewood Cliffs, New Jersey.

Anderson, P.M. and Fouad, A.A. (1977). Power Systems Stability and Control. Iowa State University Press.

ASEA (1980). Karlskronavarvet AB WTS-System Studies, Final Report. ASEA ref FKG 9519.2003, ASEA, Västerås, Sweden.

Åström, K.J. (1970). Introduction to Stochastic Control Theory. Academic Press.

Åström, K.J. and Källström, C.G. (1976). Identification of Ship Steering Dynamics. Automatica, Vol. 12, Pergamon Press, 1976, pp. 9-22.

Bergman, S., Mattsson, S.E. and Östberg, A.B. (1981). A Modular Simulation Model for a Wind Turbine System. AIAA-81-2558. AIAA 2nd Terrestrial Energy Systems Conference, December 1-3, 1981/Colorado Springs, Colorado or Journal of Energy, Vol. 7, No. 4, July-August 1983, pp. 319-324.

Bergman, S. and Mattsson, S.E. (1983). Wind Power Plant Modelling and Simulation. The Fifth Power Plant Dynamics, Control and Testing Symposium, March 21-23, 1983, Knoxville, Tennessee. pp. 7.1-7.27.

Bradley, E.F. (1980). An Experimental Study of the Profiles of Wind-Speed, Shearing Stress and Turbulence at a Crest of a Large Hill. Quart. J. Roy. Met. Soc. 106, pp. 101-123.

Connell, J.G. (1982). The Spectrum of Wind Speed Fluctuations Encountered by a Rotating Blade of a Wind Energy Conversion System. Solar Energy, Vol. 29, No. 5, pp. 363-375.

CTRL-C (1983). CTRL-C User's Guide. Systems Control Technology, Inc., Palo Alto, California, USA.

Davenport, A.G. (1961). The Spectrum of Horizontal Gustiness Near the Ground in High Winds. Quarterly J. Roy. Met. Soc., Vol 87, pp. 194-211.

Davenport, A.G. (1977). The Prediction of the Response of Structures to Gusty Winds. International Research Seminar on Safety of Structures under Dynamic Loading.

Doyle, J.C. and Stein, G. (1979). Robustness with Observers. IEEE Trans. Automatic Control, Vol. AC-24, No. 4, August 1979, pp. 607-611.

Elgerd, O.I. (1971). Electric Energy Systems Theory, An Introduction. Mc Graw-Hill, Inc.

Elmqvist, H. (1975). SIMNON - User's Manual. Department of Automatic Control, Lund Institute of Technology, Sweden, Rept. TFRT-3091.

Engineering Sciences Data (1974). Characteristics of atmospheric turbulence near the ground. Part II: single point data for strong winds (neutral atmosphere), Item No. 74031, London.

Etkin, B. (1972). Dynamics of Atmospheric Flight. Wiley, New York.

Friedman, P.R. (1976). Aeroelastic Modeling of Large Wind Turbines. J. Am Helicopter Soc. 21(4), 17-27.

Frost, W., Long, B.H. and Turner, R.E. (1978). Engineering Handbook on the Atmospheric Environmental Guidelines for Use in Wind Turbine Generator Development. NASA Technical Paper 1359.

Ganander, H. and Olsson, B. (1983). Inverkan av vindriktningsvariationer på horisontalaxlade vindkraftaggregat (Influences of variations of winddirections on horizontal axis windturbines. In Swedish with summary in English). VIND-83/34. National Energy Administration, Stockholm, Sweden.

Harris, F.J. (1978). On the Use of Windows for Harmonic Analysis with the Discrete Fourier Transform. Proc. of the IEEE, Vol. 66, No. 1, January 1978, pp. 51-83.

Hau, E. (1982). GROWIAN, design manufacturing, latest state of the project. 4th International Symposium on Wind Energy Systems, Sweden (September 21 - 24, 1982). Organized by BHRA Fluid Engineering, Cranfield, Bedford, England. Vol. 1, pp. 317-335.

Hinrichsen, E.N. and Nolan, P.J. (1980). MOD-2 Wind Turbine Stability Study, DOE/NASA/0134-1, NASA CR-165156. A summary is given in Dynamics and Stability of Wind Turbine Generators. IEEE Trans. on Power Apparatus and Systems, Vol. PAS-101, August 1982, pp. 2640-2648.

Hinrichsen, E.N. (1981). Discussion of the paper 'Methods of resynchronizing wind turbine generators' by Krause P.C. and Wasynczuk O. IEEE Trans. on Power Apparatus and Systems, Vol. PAS-100, October 1981, p. 4308.

Hinrichsen, E.N. (1984). Controls for Variable Pitch Wind Turbine Generators. IEEE Trans. on Power Apparatus and Systems, Vol. PAS-103, April 1984, p. 886-892.

Holley, W.E., Thresher, R.W. and Lin, S-R. (1981). Wind Turbulence Inputs for Horizontal Axis Wind Turbines. In Thresher (1981), pp. 101-112.

Holm, J.O. and Linström, P.O. (1982). Analysis of the Spontaneous Variations in Wind Power and Necessary Continuous Regulation of Hydro-Electric and Thermal Power, Related to a Future Swedish Power System. 4th International Symposium on Wind Energy Systems, Sweden (September 21 - 24, 1982). Organized by BHRA Fluid Engineering, Cranfield, Bedford, England. Vol. 2, pp. 273-295.

van der Hoven, I. (1957). Power spectrum of horizontal wind speed in the frequency range from 0.0007 to 900 cycles per hour. J. Meteoral., 14 pp. 160-164.

Hultgren, L.S. (1979). Torsional Oscillations of the Rotor Disc for Horizontal Axis Wind Turbines with Hinged or Teetered Blades. Technical Note AU-1499 part 12, The Aeronautical Research Institute of Sweden, Stockholm, Sweden.

Hwang, H.H. and Gilbert, L.J. (1978). Synchronization of Wind Turbine Generators Against an Infinite Bus under Gusting Wind Conditions. IEEE Trans. on Power Apparatus and Systems, Vol. PAS-97, March/April 1978, pp. 536-544.

IEEE Committee Report (1968). Computer Representation of Excitation Systems. IEEE Trans. on Power Apparatus and Systems, Vol. PAS-87, June 1968, pp. 1460-1464.

Jackson, P.S. and Hunt, J.C.R. (1975). Turbulent Wind Flow Over a Low Hill. Quart. J. Roy. Met. Soc. 101, pp. 929-955.

Kendall, G. and Stuart, A. (1961). The Advanced Theory of Statistics, Volume 2. Charles Griffin & Company Limited, London.

Koeppl, G.W. (1982). Putnam's Power from the Wind, Second Edition. Van Nostrand Reinhold Company, New York.

Kos, J.M. (1978). On-Line Control of Large Horizontal Axis Energy Conversion System and Its Performance in a Turbulent Wind Environment. Proceedings of the 13th Intersociety Energy Conversion Engineering Conference, August 1978, pp. 2064-2073.

Krause, P.C., Nozari F., Skvarenina T.L. and Olive D.W. (1979). The Theory of Neglecting Stator Transients. IEEE Trans. on Power Apparatus and Systems, Vol. PAS-98, Jan/Feb 1979, pp. 141-146.

Krause, P.C. and Man, D.T. (1981). Transient Behavior of a Class of Wind Turbine Generators during Electrical Disturbances. IEEE Trans. on Power Apparatus and Systems, Vol. PAS-100, May 1981, pp. 2204-2210.

Kwakernaak, H. and Sivan, R. (1972). Linear Optimal Control Systems. Wiley-Interscience, New York.

Leonhard, W. (1974). Regelung in der elektrischen Antriebstechnik. Teubner.

Leonhard, W. (1979). Field Oriented Control of a Variable Speed Alternator Connected to the Constant Frequency Line. Implementing Agreement for Co-Operation in the Development of Large Scale Wind Energy Conversion Systems, Second Meeting of Experts - Control of LS-WECS and Adaptation to the Network, July 1979, pp. 121-125. Zentralbibliothek der Kernforschungsanlage Julich GmbH, Julich, West Germany.

Liebst, B.S. (1980). Optimized Pitch Controller for Load Alleviation on Wind Turbines. Technical Note HU-2189 part 1, The Aeronautical Research Institute of Sweden, Stockholm, Sweden.

Liebst, B.S. (1981). A Pitch Control System for Large Scale Wind Turbines. Technical Note HU-2262 part 6, The Aeronautical Research Institute of Sweden, Stockholm, Sweden.

Linde, M. (1983). Gust Structure and Gust Statistics. Results from an Analysis of Atmospheric Turbulence Measurements by Using Conditional Sampling Technique. FFA TN 1983-28, The Aeronautical Research Institute of Sweden, Stockholm, Sweden.

Lumley, J.L. and Panofsky, H.A. (1964). The Structure of Atmospheric Turbulence. John Wiley & Sons, Inc.

Mattsson, S.E. (1982). Development of a Modular Simulation Model for a Wind Turbine System. Department of Automatic Control, Lund Institute of Technology, Lund, Sweden. CODEN: LUTFD2/(TFRT-7239)/1-033/(1982)

Mets, V. and Hermansson, O. (1983). Status and Experience with the 2 MW WTS 75 at Näsudden, Gotland. KaMeWa AB, Box 1010, S-681 01 Kristinehamn, Sweden.

Miller, D.R. (1978). Wind Turbines Structural Dynamics. NASA-CP-2034, A workshop held at Lewis Research Center, Cleveland, Ohio, Nov 15-17, 1977.

Murdoch, A., Winkelman, J.R., Javid, S.H. and Burton, R.S. (1983). Control Design and Performance Analysis of a 6 MW Wind Turbine-Generator. IEEE Trans on Power Apparatus and Systems, Vol. PAS-102, No. 5, May 1983, pp. 1340-1347.

NE (1982). The National Swedish Wind Energy Program. NE, The National Swedish Board for Energy Source Development, Stockholm, Sweden.

Nordanlycke, I., Paulsson, E. and Wredenberg, L. (1974). Solution Methods of Power System Dynamics. The Royal Institute of Technology, Power Systems Research Group, Sweden.

Nygren, I., Grop, S. and Pettersson, B. (1981). Vindkraftverk med lågvarvig generator (Wind power plant with low speed generator). NE/WIND 81/7. NE, The National Swedish Board for Energy Source Development, Stockholm, Sweden.

Olive, D.W. (1968). Digital Simulation of Synchronous Machine Transients. IEEE Trans. on Power Apparatus and Systems, Vol. PAS-87, August 1968, pp. 1669-1675.

Park, R.H. (1929). Two-Reaction Theory of Synchronous Machines, Generalized Method of Analysis, pt. I. AIEE Trans., vol 48, July 1929, pp. 716-730; pt. II. AIEE Trans., vol 52, June 1933, pp. 352-355.

Perkins, F.W. and Jones, R. (1981). The Effect of δ_3 on a Yawing HAWT Blade and on Yaw Dynamics. In Thresher (1981), pp. 295-304.

Powell, D.C and Connell, J.R. (1980). Definition of Gust Model Concepts and Review of Gust Models. PNL-3138, Pacific Northwest Laboratory, Richland, Washington.

Raina, G. and Malik, O.P. (1983). Wind Energy Conversion Using a Self-Excited Induction Generator. IEEE Trans. on Power Apparatus and Systems, Vol. PAS-102, December 1983, pp. 3933-3936.

Rasmussen, F. and Pedersen, T.F. (1982). Measurements and calculations of forces on the blades of a stall regulated HAWT. 4th International Symposium on Wind Energy Systems, Sweden (September 21 - 24, 1982). Organized by BHRA Fluid Engineering, Cranfield, Bedford, England. Vol. 2, pp. 59-69.

Schweickardt, H. and Suchanek, V. (1982). Converter-Fed Synchronous Generator Systems for Wind Power Plants. Brown Boveri Rev. 3, 1982, pp. 57-64.

Seidel, R.C. (1977). Power Oscillation of the Mod-0 Wind Turbine. NASA-CP-2034, for a Workshop: Wind Turbine Structural Dynamics held at NASA Lewis Research Center, Cleveland, Ohio, Nov 15-17, 1977, In Miller (1978), pp. 151-156.

Shepherd, D.G. (1978). Wind Power. In Auer, P.: Advances in Energy Systems and Technology, Vol 1. Academic Press, pp. 1-124.

Spera, D.A. and Richards, T.R. (1980). Wind Gust Analysis for Wind Turbine Design. Appendix A in Powell and Connell (1980).

Stoddard, F.S. (1978). Structural Dynamics and Control of High Aspect Ratio Wind Turbines. Energy Alternatives Program, University of Massachusetts, Amherst, Massachusetts.

Sullivan, T.L. (1981). A Review of Resonance in Large, Horizontal-Axis Wind Turbines. In Thresher (1981), pp. 235-244. Also in Solar Energy, Vol. 29, No. 5, pp. 377-383, 1982.

Svensson, J.E. and Ulén, E. (1982). The Control System of WTS-3, instrumentation and testing. 4th International Symposium on Wind Energy Systems, Sweden (September 21 - 24, 1982). Organized by BHRA Fluid Engineering, Cranfield, Bedford, England. Vol. 2, pp. 195-215.

Swedyards (1981). Swedish wind power. Swedyards Wind Turbine Systems Corp., Göteborg, Sweden.

Swedyards (1982). A milestone for wind power. Swedyards Wind Turbine Systems Corp., Göteborg, Sweden. March/April 1982.

Thresher, R.W. (1981). Wind Turbine Dynamics. NASA-CP-2185, DOE CONF-810226, A workshop held at Cleveland State University, Cleveland, Ohio, February 24-26, 1981.

Wasynczuk, G., Man, D.T. and Sullivan, J.P. (1981). Dynamic Behavior of Wind Turbine Generators during Random Wind Fluctuations. IEEE Trans. on Power Apparatus and Systems, Vol. PAS-100, June 1981, pp. 2837-2845.

Wieslander, J. (1980a). Idpac Commands - User's Guide. Department of Automatic Control, Lund Institute of Technology, Lund, Sweden.
CODEN: LUTFD2/(TFRT-3157)/1-108/(1980)

Wieslander, J. (1980b). Synpac Commands - User's Guide. Department of Automatic Control, Lund Institute of Technology, Lund, Sweden.
CODEN: LUTFD2/(TFRT-3159)/1-130/(1980)

APPENDIX A

CHARACTERISTICS OF SOME WIND POWER PLANTS

Some characteristics of the MOD-2, the WTS-3, the WTS 75 and the Growian I are listed in Table A.1 of this appendix. References to reports and papers containing descriptions, simulation models, simulation plots and experiences are also given. All of these four wind power systems are described in Koeppl (1982).

The MOD-2

The MOD-2 was designed by Boeing Engineering and Construction Company for DOE-NASA. Three plants have been installed at Goodnoe Hills, Washington. They are operated by the Bonneville Power Administration. References are Hinrichsen and Nolan (1980), Krause and Man (1981), Sullivan (1981) and Wasynczuk, Man and Sullivan (1981).

The WTS-3

The WTS-3 was designed by Karlskronavarvet AB, Sweden, and Hamilton Standard, a division of United Technologies Inc, USA, for the National Swedish Board for Energy Source Development (NE). Karlskronavarvet AB is a part of Swedyard Group. One plant is installed at Maglarp, near the city of Trelleborg, in southern Sweden. Sydkraft AB (The South Swedish Power Company Ltd.) operates this plant. A 4 MW plant (the WTS-4) of the same design is installed in Medicine Bow, Wyoming, USA. References are Kos (1978), Swedyards (1981, 1982), Svensson and Ulén (1982), NE (1982), Bergman, Mattsson, and Östberg (1981), Mattsson (1982) and Bergman and Mattsson (1983).

The WTS 75

The WTS 75 was designed by KaMeWa AB, Sweden, for the National Swedish Board for Energy Source Development (NE). A plant is installed at Näsudden in the south-west of Gotland, Sweden. Statens Vattenfallsverk (The Swedish State Power Board) operates the plant. References are NE (1982) and Mets and Hermansson (1983).

The Growian I

The Growian I (Grosse Windenergie Anlage) was designed by Mashienenfabrik Augsburg-Nurnberg Aktiengesellschaft (MAN-Neue Technologie) for the West German Ministry for Research and Technology. A plant is installed at Kaiser-Wilhelm-Koog which is located at the mouth of the river Elbe near the North Sea. References are Hau (1982) and Leonhard (1979).

Table A.1: Major Characteristics

	MOD-2	WTS-3	WTS 75	Growian I
Rated power [MW]	2.5	3	2	3
Wind speeds				
cut-in [m/s]		7.2	6	5.4
rated [m/s]	12.3	14.2	12.5	12.0
cut-out [m/s]	20	27.2	21	24
Rotor				
blades	2	2	2	2
	steel	GRP-Epoxy*)	steel 1)	steel 2)
location	upwind	downwind	upwind	downwind
yaw control	hydraulic	hydraulic	hydraulic	el.-mech
max rate [°/s]	0.25	1.2		0.5
hub type	teetered	teetered	rigid	teetered
hub height [m]	100	80	80	100
diameter [m]	100	78	75	100
speed [rpm]	17.5	25	25	18.5±15%
pitch control	hydraulic outer 30%	hydraulic full span	hydraulic full span	el.-mech full span 3)
Generator	synch	synch	induction	asynch
speed [rpm]	1800	1500	1500	1500
frequency [Hz]	60	50	50	50
Tower	cyl steel shell	cyl steel shell	reinforced concrete	cyl steel shell

*) Glass-Fibre Reinforced Plastic
1) with GRP-Epoxy leading and trailing edges
2) with a GRP-shell
3) doubly-fed

APPENDIX B

A MODULAR SIMULATION MODEL

A mathematical simulation model for a large horizontal axis wind turbine system is presented. Older versions are presented in Mattsson (1982), as well as in Bergman, Mattsson and Östberg (1981) and Bergman and Mattsson (1983)). The two last papers also contain simulation plots.

The model is intended to be a framework for simulation of the system behaviour in different situations such as synchronization of the wind turbine generator against the utility grid, normal operation under different wind conditions and emergencies caused by faults in the plant or in the electrical network. The model can for example be used for education, design verification, failure investigation and when designing new controllers.

When developing a model for a complex system it is important to use a modular and well structured approach. Particular attention has been given to the modularization. The model is divided into subsystems to make it easy to modify the model and adapt the complexity of a subsystem to the case to be simulated. The interactive simulation package Simnon (Elmqvist (1975)) has been used. Simnon allows good structuring and programming in a high level language.

The simulation model is adapted to the WTS-3. However, the modularization and use of a high level language make it easy to adapt the model to other systems of similar type.

To make the model manageable and not unnecessarily complicated some simplifying assumptions of importance for the modularization are made.

Assumption B.1:

The synchronous generator is connected via an impedance to an infinite bus.

This means that the bus voltage and bus frequency are not affected by the wind turbine system. The system is designed to supply power in parallel with other electrical generators to a large utility grid. Consequently, the power

supplied by the wind turbine system will only constitute a small portion. By making the bus frequency and bus voltage time varying, it is possible to model a large utility grid in both normal operation and during faults.

Assumption B.2:

The moment of inertia of the gearbox and shafts can be neglected.

If the moment of inertia of the gearbox is reduced to the generator side, it is less than 10 % of the moment of inertia of the generator and, if it is reduced to the turbine side, it is less than 2 % of the moment of inertia of the wind turbine rotor. Simulations performed by ASEA (1980) show that this is a very good approximation. This assumption means that, disregarding the gearing, the drive train between the turbine and the generator can be modelled as one spring with a damper.

Assumption B.3:

The nacelle is aligned in the direction of the wind.

The WTS-3 has an active yaw mechanism, but yawing will not be modelled here.

Assumption B.4:

The blades are torsionally rigid and the pitch servo is not affected by the wind.

Friedmann (1976) states that the blades of typical wind turbine are torsionally rigid. The first frequency of torsional mode is high (for the WTS-3 about 37 rad/s).

Assumptions B.1 - B.4 make it possible to draw a simple block diagram (Figure B.1) that can be directly translated to a Simnon program. The block diagram only defines which outputs each subsystem must provide and which inputs are available. To increase the flexibility, the inputs and outputs of the subsystems are chosen as unscaled, physical quantities. SI-units are used. However, to improve the numerics scaled quantities are used inside the subsystems. Models for the different subsystems in Figure B.1 are discussed below. The Simnon code for these models is given at the end of this appendix.

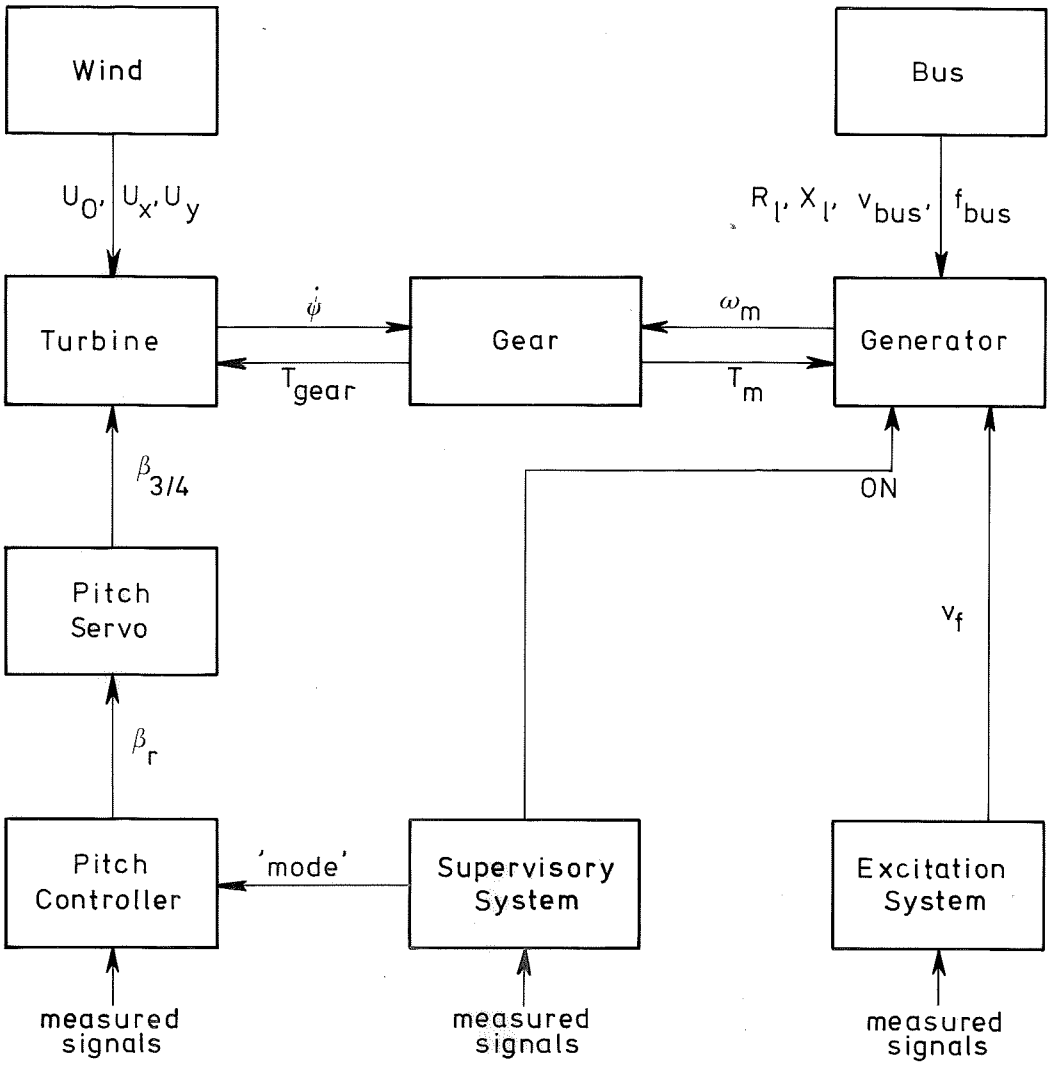

Figure B.1: Model structure.

Other mathematical simulation models for the complete system can be found in for example Hwang and Gilbert (1978), Kos (1978), Hinrichsen and Nolan (1980), Krause and Man (1981) (also in Wasynczuk, Krause and Man (1981)). These reports and papers also contain simulation plots. These models are similar to that given here. The differences are mainly in the aerodynamical part. Yawing is not considered in any of these models. Unfortunately, none of the authors describes how their models are programmed. The advantages with the model presented here is that this model is modularized and programmed in a high-level modelling language which makes the model flexible, readable and easy to modify and use.

B.1 Wind Turbine

The wind turbine is considered in Section 2.3. Here the equations of motion for a turbine with a teeter hub are given as well as analytical expressions for the aerodynamical torques and thrust are given. Yawing is neglected and it is assumed that the nacelle is aligned in the direction of the wind (Assumption B.3).

Equations of Motion

For a wind turbine with teeter hub the blades are rigidly mounted to each other hinged to the main shaft by means of a teeter pin. This means that the flapping angles satisfy (See Figure B.2)

$$\varphi_1 + \varphi_2 = 2\varphi_0 = \text{constant} \tag{B.1.1}$$

so the motion around the teeter pin can be described by one variable,

$$\varphi = (\varphi_1 - \varphi_2)/2 \tag{B.1.2}$$

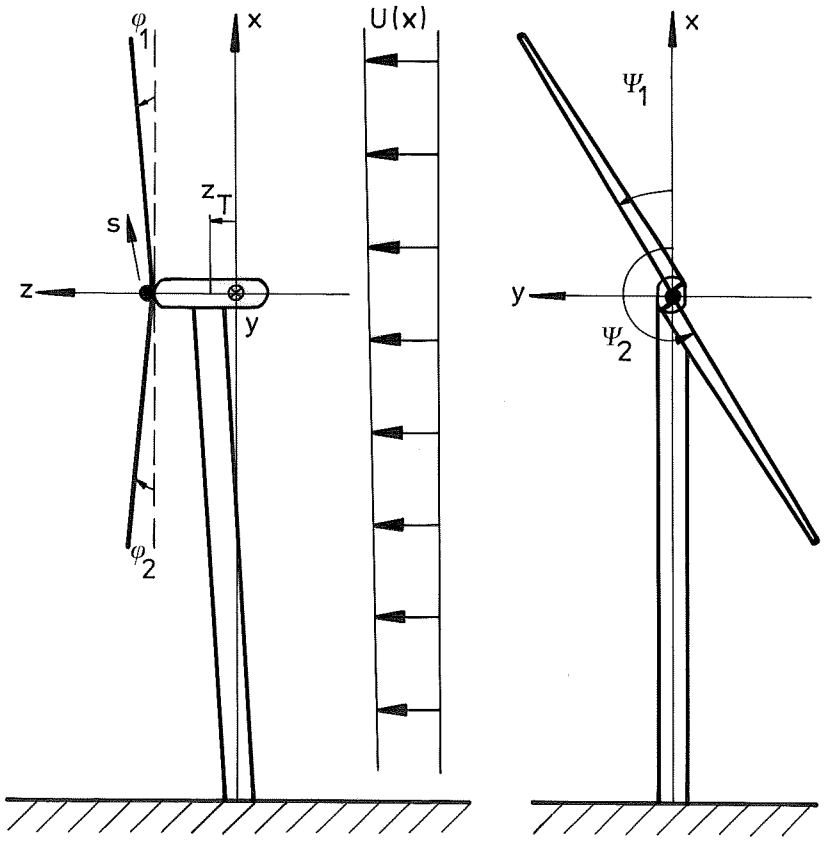

Figure B.2: Wind turbine geometry.

The first lead-lag oscillations (bending motions of the blades in the plane of rotation) are modelled by viewing the turbine as a three mass system (hub and two blades) connected by springs and dampers. Values for the equivalent blade inertia J_{eB}, hub inertia J_{eH} and blade stiffness K_{eB} are chosen so that correct rigid hub first edgewise frequency ω_{er} and operational first edgewise frequency ω_{el} are achieved (Kos (1978))

$$J_{eH} = (J_H + 2J_B)\omega_{er}^2/\omega_{el}^2 \tag{B.1.3}$$

$$J_{eB} = \{(J_H + 2J_B) - J_{eH}\}/2 \tag{B.1.4}$$

$$K_{eB} = J_{eB}\omega_{er}^2 \tag{B.1.5}$$

The first mode of the tower bendings perpendicular to the plane of rotation is modelled. The influence of the tower on the nacelle is modelled as a spring with damper

$$F_T = -(D_T\dot{z}_T + K_T z_T) \tag{B.1.6}$$

Consider Figure B.2. The motion in the ψ and φ directions assuming a rigid tower is modelled by Hultgren (1979). His model, extended with the z_T-motion, will be used. Applications of Lagrange's equations yield the following equations of motion

$$(J_{eB}\cos^2\varphi_i)\,\ddot{\psi}_i - 2J_B\dot{\varphi}_i\dot{\psi}_i\sin\varphi_i\cos\varphi_i + D_{eB}(\dot{\psi}_i - \dot{\psi}) - 2gS_B\cos\varphi_i\sin\psi_i + K_{eB}(\psi_i - \psi + (i-1)\pi) = T_{\psi i} \qquad i = 1, 2 \tag{B.1.7}$$

$$J_{eH}\ddot{\psi} - D_{eB}(\dot{\psi}_1 + \dot{\psi}_2 - 2\dot{\psi}) - K_{eB}(\psi_1 + \psi_2 - 2\psi + \pi) = -T_{gear} \tag{B.1.8}$$

$$2J_B\ddot{\varphi} + S_B(\cos\varphi_1 - \cos\varphi_2)\,\ddot{z}_T + (J_B\dot{\psi}_1^2\cos\varphi_1 - gS_B\sin\psi_1)\sin\varphi_1 - (J_B\dot{\psi}_2^2\cos\varphi_2 - gS_B\sin\psi_2)\sin\varphi_2 = T_{\varphi 1} - T_{\varphi 2} \tag{B.1.9}$$

$$S_B(\cos\varphi_1 - \cos\varphi_2)\,\ddot{\varphi} + M_T\ddot{z}_T - S_B(\dot{\varphi}_1^2\sin\varphi_1 + \dot{\varphi}_2^2\sin\varphi_2) = F_{z1} + F_{z2} + F_T \tag{B.1.10}$$

where

g	Gravitational acceleration
ψ	Azimuth angle of hub
ψ_1, ψ_2	Azimuth angles of blades
S_B	Static moment of one blade
M_T	Mass of the nacelle
$T_{\psi i}$, $T_{\varphi i}$	Aerodynamical torques
F_{zi}	Aerodynamical thrust
T_{gear}	Driving torque to the gearbox
F_T	Reaction thrust from the tower

Aerodynamical Thrust and Torques

The aerodynamical thrust and torques can be obtained by applying static and two-dimensional airfoil theory to each cross section of the blades.

It is assumed that over the rotor disc the wind speed $U(r,\psi,t)$ of the oncoming undisturbed wind (as if there was no wind power plant) can be written as

$$U(r,\psi,t) = U_0(t) + U_x(t)\ r\ \cos\psi + U_y(t)\ r\ \sin\psi \qquad (B.1.11)$$

It is also assumed that $U(r,\psi,t)$ and the wind speed $U_d(r,\psi,t)$ at the rotor disc are related as

$$U_d(r,\psi,t) = (1-a(t))\ U(r,\psi,t) \qquad (B.1.12)$$

where $a(t)$ is the interference factor.

The tower has a significant effect on the flow especially for turbines downwind of the tower. The wake depends critically on the aerodynamical properties of the tower and is difficult to model. However, the form of the wake is probably not critical for the intended use of this model. A common modification for the wind at the i:th blade is given by the factor

$$q_i(\psi_i) = \begin{cases} 1 - C\cos\left(\frac{\pi}{2}\,\frac{\tilde{\psi}_i - \pi}{\alpha}\right), & |\tilde{\psi}_i - \pi| < \alpha \\ 1 & \text{otherwise} \end{cases} \qquad (B.1.13)$$

where $\tilde{\psi}_i = \psi_i \bmod 2\pi$.

The pitch distribution of the blades is assumed to be of the form

$$\beta(s) = \beta_1 + \frac{R}{s}\beta_2 \qquad \text{(B.1.14)}$$

The profile lift increment is assumed to depend linearly on the angle of attack. The profile drag increment is assumed to be independent of the angle of attack. Consequently, stalling is not modelled. Introduce

$$\lambda_i = (1-a)U_0/(R\dot{\psi}_i) \qquad \text{(B.1.15)}$$

$$u_i = R(U_x\cos\psi_i + U_y\sin\psi_i)/U_0 \qquad \text{(B.1.16)}$$

Lengthy calculations, ignoring terms of the orders $O(\lambda_i^4)$ and $O(\lambda_i^3\dot{\varphi}_i)$ and nonlinear terms in u_i, $\dot{\varphi}_i$ and $\dot{z}_T$ give (Hultgren (1979) extended with the motion in the z_T direction)

$$T_{\psi i} = \tfrac{1}{2}R^3\dot{\psi}_i^2\cos^3\varphi_i\{(A_2\beta_1+A_1\beta_2)\Lambda_i + A_1\Lambda_i^2 + \tfrac{1}{2}(A_0\beta_1+A_{-1}\beta_2)\Lambda_i^3 - B_3\}$$

$$- \tfrac{1}{2}R^2\dot{\psi}_i\cos^2\varphi_i\{\{(A_3\beta_1+A_2\beta_2) + 2A_2\Lambda_i + \tfrac{3}{2}(A_1\beta_1+A_0\beta_2)\Lambda_i^2\}\dot{\Phi}$$

$$+ \{(A_2\beta_1+A_1\beta_2) + 2A_1\Lambda_i + \tfrac{3}{2}(A_0\beta_1+A_{-1}\beta_2)\Lambda_i^2\}\dot{z}_T\cos\varphi_i\},$$

$$i = 1, 2 \qquad \text{(B.1.17)}$$

$$T_{\varphi i} = \tfrac{1}{2}R^3\dot{\psi}_i^2\cos^2\varphi_i\{(A_3\beta_1+A_2\beta_2) + (A_2+B_2)\Lambda_i + \tfrac{1}{2}(A_1\beta_1+A_0\beta_2)\Lambda_i^2 + \tfrac{1}{6}A_0\Lambda_i^3\}$$

$$- \tfrac{1}{2}R^2\dot{\psi}_i\cos\varphi_i\{\{(A_3+B_3) + (A_2\beta_1+A_1\beta_2)\Lambda_i + \tfrac{1}{2}A_1\Lambda_i^2\}\dot{\Phi}_i$$

$$+ \{(A_2+B_2) + (A_1\beta_1+A_0\beta_2)\Lambda_i + \tfrac{1}{2}A_0\Lambda_i^2\}\dot{z}_T\cos\varphi_i\},$$

$$i = 1, 2 \qquad \text{(B.1.18)}$$

$$F_{zi} = \tfrac{1}{2}R^2\dot{\psi}_i^2\cos^3\varphi_i\{(A_2\beta_1+A_1\beta_2) + (A_1+B_1)\Lambda_i + \tfrac{1}{2}(A_0\beta_1+A_{-1}\beta_2)\Lambda_i^2 + \tfrac{1}{6}A_{-1}\Lambda_i^3\}$$

$$- \tfrac{1}{2}R\dot{\psi}_i\cos^2\varphi_i\{\{(A_2+B_2) + (A_1\beta_1+A_0\beta_2)\Lambda_i + \tfrac{1}{2}A_0\Lambda_i^2\}\dot{\Phi}_i$$

$$+ \{(A_1+B_1) + (A_0\beta_1+A_{-1}\beta_2)\Lambda_i + \tfrac{1}{2}A_{-1}\Lambda_i^2\}\dot{z}_T\cos\varphi_i\},$$

$$i = 1, 2 \qquad \text{(B.1.19)}$$

where

$$\Lambda_i = q_i\lambda_i \qquad \text{(B.1.20)}$$

$$\dot{\Phi}_i = R\dot{\varphi}_i - q_i R\cos^2\varphi_i (1-a)(U_x \cos\psi_i + U_y \sin\psi_i) \qquad (B.1.22)$$

The blade constants A_{-1}, A_0, A_1, A_2, A_3, B_1, B_2 and B_3 are defined as

$$A_\alpha = \varrho_a R^{-\alpha} \int_0^R ca s^\alpha \, ds \qquad (B.1.23)$$

$$B_\alpha = \varrho_a R^{-\alpha} \int_0^R cC_D s^\alpha \, ds \qquad (B.1.24)$$

where ϱ_a is the density of air, c the local chord length, a the lift curve slope of the blade section and C_D the profile drag coefficient of the section.

The interference factor a(t) can be calculated by using momentum theory (e.g. Shepherd (1978)). The generated power is

$$P = n_P \, 2\varrho_a \pi R^2 \, a(1-a)^2 \, U_0^3 \qquad (B.1.26)$$

where n_P is the degree of power efficiency of the blades. The relations (B.1.17), (B.1.26) and

$$P = \dot{\psi}_1 T_{\psi 1} + \dot{\psi}_2 T_{\psi 2} \qquad (B.1.27)$$

give (neglecting the effects of wind profile, teetering, tower motions, tower shadow and lead-lag oscillations)

$$\left\{n_P \, 2\varrho_a \pi R^2 + \tfrac{1}{2}(A_0\beta_1 + A_{-1}\beta_2)\right\} \lambda^3 - \left\{n_P \, 2\varrho_a \pi R^2 \, U_0/(R\dot{\psi}) - A_1\right\} \lambda^2 + (A_2\beta_1 + A_1\beta_2)\,\lambda - B_3 = 0 \qquad (B.1.28)$$

where $\lambda = (1-a)U_0/(R\dot{\psi})$

Representation of the Azimuth Angle ψ

From the equations (B.1.1) - (B.1.28), it can be seen that the azimuth angle ψ enter the model only as sin ψ, cos ψ and ψ mod 2π (c.f. the discussion in B.3). Since ψ is increasing with time, it is better numerically to calculate ψ from the equations

$$\dot{x}_1 = -\dot{\psi} x_2 + \alpha x_1 (1 - x_1^2 - x_2^2) \qquad (B.1.29)$$

$$\dot{x}_2 = \dot{\psi} x_1 + \alpha x_2 (1 - x_1^2 - x_2^2) \qquad (B.1.30)$$

with the interpretation $\cos\psi = x_1$ and $\sin\psi = x_2$. For $\alpha > 0$ the second term in the right hand of (B.1.29) and the second term in the right hand of (B.1.30) guarantee amplitude stability so that $x_1^2 + x_2^2$ is kept close to one;

$$\frac{d}{dt}(x_1^2 + x_2^2) = \alpha(x_1^2 + x_2^2)(1 - x_1^2 - x_2^2) \qquad \text{(B.1.31)}$$

B.2 Synchronous Generator

The basic idea behind standard models for synchronous generators is presented in Chapter 2.4 together with references. It has become a common practice to use a standard set of parameters and state variables when modelling synchronous generators. This standard will be used. To simplify the model and to improve its numerical properties, the voltages, currents and impedances are in per unit based upon the machine rating.

Synchronous Machine Equations

Kirchhoff's law equations give for the rotor circuits f, x and y (See Figure 2.8)

$$\dot{e}'_q = \left(v_f - \frac{X_d - X''_d}{X'_d - X''_d} e'_q + \frac{X_d - X'_d}{X'_d - X''_d} e''_q\right) / T'_{d0} \qquad \text{(B.2.1)}$$

$$\dot{e}''_d = -(e''_d - (X_q - X''_q)\, i_q) / T''_{q0} \qquad \text{(B.2.2)}$$

$$\dot{e}''_q = (e'_q - e''_q - (X'_d - X''_d)\, i_d) / T''_{d0} \qquad \text{(B.2.3)}$$

and for the stator circuits

$$v_d = -R_a i_d + (e''_d + X''_q i_q)\frac{\omega}{\omega_0} + \dot{\lambda}_d \qquad \text{(B.2.4)}$$

$$v_q = -R_a i_q + (e''_q - X''_d i_d)\frac{\omega}{\omega_0} + \dot{\lambda}_q \qquad \text{(B.2.5)}$$

$$\lambda_d = (e''_q - X''_d i_d)/\omega_0 \qquad \text{(B.2.6)}$$

$$\lambda_q = -(e''_d + X''_q i_q)/\omega_0 \qquad \text{(B.2.7)}$$

where

ω_0	synchronous circular frequency
λ_d	d-axis stator flux linkages
λ_q	q-axis stator flux linkages
e'_q	voltage behind transient reactance (proportional to the field flux linkage λ_f of the field circuit f)
v_f	generator field voltage
e''_d, e''_q	d-axis and q-axis components of voltage behind subtransient reactance (proportional to the flux linkages λ_y and λ_x of the circuits y and x).
X_d, X_q	d-axis and q-axis synchronous reactances
X'_d	d-axis transient reactance
X''_d, X''_q	d-axis and q-axis subtransient reactances
T'_{d0}	d-axis transient open circuit time constant
T''_{d0}, T''_{q0}	d-axis and q-axis subtransient open circuit time constants
R_a	armature resistance

The armature voltage and current of phase a are given by

$$v_a = v_d \cos\theta - v_q \sin\theta \qquad \text{(B.2.8)}$$

$$i_a = i_d \cos\theta - i_q \sin\theta \qquad \text{(B.2.9)}$$

where θ is the electrical position of the rotor and

$$\dot{\theta} = \omega \qquad \text{(B.2.10)}$$

The generator is assumed to be connected to an infinite bus through a line and a transformer with the impedance $R_l + jX_l$ (Assumption B.1). The bus voltage of phase a is assumed to be $v_{bus}\cos\theta_{bus}$. Kirchhoff's law equations describing this connection are

$$X_l \dot{i}_d = \omega_0(v_d - v_{bus}\sin\delta) - \omega R_l i_d + \omega X_l i_q \qquad \text{(B.2.11)}$$

$$X_l \dot{i}_q = \omega_0(v_q - v_{bus}\cos\delta) - \omega X_l i_d - \omega R_l i_q \qquad \text{(B.2.12)}$$

where δ is the power angle defined as

$$\delta = \theta - \theta_{bus} \qquad \text{(B.2.13)}$$

The equations are rearranged, because (B.2.4), (B.2.6) and (B.2.11) and (B.2.5), (B.2.7) and (B.2.12) contain algebraic loops. Eliminating λ_d and λ_q and solving for v_d, v_q, $\dot{i}_d$ and $\dot{i}_q$ give

$$v_d = \{(e''_d + X''_q i_q)\omega + \dot{e}''_q - X''_d \dot{i}_d\} / \omega_0 - R_a i_d \qquad (B.2.14)$$

$$v_q = \{(e''_q - X''_d i_d)\omega - \dot{e}''_d + X''_q \dot{i}_q\} / \omega_0 - R_a i_q \qquad (B.2.15)$$

$$\dot{i}_d = \{\omega[e''_d+(X''_q+X_l)i_q] - \omega_0[(R_a+R_l)i_d+v_{bus}\sin\delta] + \dot{e}''_q\}/(X''_d+X_l) \qquad (B.2.16)$$

$$\dot{i}_q = \{\omega[e''_q-(X''_d+X_l)i_d] - \omega_0[(R_a+R_l)i_q+v_{bus}\cos\delta] - \dot{e}''_d\}/(X''_q+X_l) \qquad (B.2.17)$$

Equation of Motion

The mechanical angular speed of the rotor is

$$\omega_m = \omega/(p/2) \qquad (B.2.18)$$

where p is the number of poles. Differentiation of (B.2.13) gives

$$\dot{\delta} = \frac{p}{2}\omega_m - \omega_{bus} \qquad (B.2.19)$$

The equation of motion, or swing equation is

$$\dot{\omega}_m = (T_m - D_m\omega_m - \frac{p}{2}T_e) / J_{gen} \qquad (B.2.20)$$

$$T_e = \frac{S_{base}}{\omega_0}(e''_q i_q + e''_d i_d - (X''_d - X''_q) i_d i_q) \qquad (B.2.21)$$

where T_m is the mechanical torque driving the generator, $D_m\omega_m$ represents constant friction torque, T_e is the torque developed by the generator (in SI-units) and J_{gen} is the moment of inertia of the generator.

Disconnection

When the generator is disconnected, the currents i_d and i_q should be reduced to zero. This is done by assigning constant values to their derivatives so that they are reduced to a small value within a few milliseconds. When the generator is disconnected from the grid, δ may increase. Since it is only δ mod 2π that are interest cos δ and sin δ can be used as states instead of δ itself as done in (B.1.29) and (B.1.30).

Model Simplification

The generator model given above contains as shown in Chapter 2.4 both fast modes (in the millisecond range) and slow modes (in the second range) which makes the model computationally slow. The fast modes are only of interest if the behaviour of the electrical variables are studied. If only the mechanical oscillations are investigated, the fast modes can be neglected The improvement in computational speed is considerable. Janischewskyj and Prabhashankar reports in the discussion of Olive's paper (1968) that in a particular study it was possible to increase the step size 50 times (from 1 ms to 50 ms), if the $\dot{\lambda}_d$ and $\dot{\lambda}_q$ terms in (B.2.4) and (B.2.5) were neglected. This means that (B.2.4) and (B.2.5) do not depend on $\dot{i}_d$ and $\dot{i}_q$. The algebraic loops have disappeared and only (B.2.11) and (B.2.12) have terms dependent on $\dot{i}_d$ and $\dot{i}_q$. If X_l is small, these derivatives can be eliminated from the model. Further assuming $\omega = \omega_0$ in (B.2.4), (B.2.5), (B.2.11) and (B.2.12) gives

$$v_d = e''_d + X''_q i_q - R_a i_d \qquad \text{(B.2.22)}$$

$$v_q = e''_q - X''_d i_d - R_a i_q \qquad \text{(B.2.23)}$$

$$i_d = \{(R_a+R_l)(e''_d - v_{bus}\sin\delta) + (X''_q+X_l)(e''_q - v_{bus}\cos\delta)\}/\Sigma \qquad \text{(B.2.24)}$$

$$i_q = \{(R_a+R_l)(e''_q - v_{bus}\cos\delta) - (X''_d+X_l)(e''_d - v_{bus}\sin\delta)\}/\Sigma \qquad \text{(B.2.25)}$$

$$\Sigma = (R_a+R_l)^2 + (X''_d+X_l)(X''_q+X_l) \qquad \text{(B.2.26)}$$

The equations (B.2.1) - (B.2.3), (B.2.8) - (B.2.10), (B.2.13) and (B.2.18) - (B.2.26) constitute a simplified model. Krause, Nozari, Skvarenia and Olive (1979) discuss the implications of these approximations.

B.3 Drive Train and Gearbox

The wind turbine is connected to the synchronous generator through a multi-stage planetary step-up gearbox. The gearbox is not rigidly mounted but suspended with springs and hydraulic dampers. According to Assumption B.2, the drive train can be modelled as a spring and a damper. The torsion γ of the spring viewed from the wind turbine side is

$$\gamma = (\psi - \theta_m/N_g)/(1 - 1/N_g) \qquad \text{(B.3.1)}$$

where ψ is the azimuth angle of the wind turbine, θ_m is the the mechanical position of the rotor of the generator and N_g is the step-up gear ratio. However, (B.3.1) causes numerical difficulties, since ψ and ω_m/N_g are increasing and of the same size. The difficulties are avoided if the relation is expressed as

$$\dot{\gamma} = (\dot{\psi} - \omega_m/N_g)/(1 - 1/N_g) \tag{B.3.2}$$

Torque and energy balance give

$$T_{gear} = -T_\gamma/(1 - 1/N_g) \tag{B.3.3}$$

$$T_m = -T_\gamma/(N_g - 1) \tag{B.3.4}$$

where T_{gear} is the driving torque from the wind turbine, T_m is the torque driving the generator and T_γ is the reaction torque of the gearbox suspension. The suspension consists of springs and hydraulic dampers thus giving T_γ as

$$T_\gamma = T_{sp} + T_d \tag{B.3.5}$$

where T_{sp} is the reaction torque from the springs and T_d is the reaction torque from the dampers. The suspension is soft in the interval $\gamma_{min} < \gamma < \gamma_{max}$ and outside this it is much stiffer so that

$$T_{sp} = \begin{cases} -K_{g0}\gamma_{min} - K_{g1}(\gamma - \gamma_{min}), & \gamma < \gamma_{min} \\ -K_{g0}\gamma, & \gamma_{min} < \gamma < \gamma_{max} \\ -K_{g0}\gamma_{max} - K_{g1}(\gamma - \gamma_{max}), & \gamma_{max} < \gamma \end{cases} \tag{B.3.6}$$

Two models for T_d are given. The hydraulic dampers can be modelled to have either a linear characteristic

$$T_d = -\max(-T_{dmax}, \min(T_{dmax}, D_{g1}\dot{\gamma})) \tag{B.3.7}$$

or a quadratic characteristic

$$T_d = -\max(-T_{dmax}, \min(T_{dmax}, D_{g2}|\dot{\gamma}|\dot{\gamma})) \tag{B.3.8}$$

B.4 Pitch Servo

The pitch angles of the blades can be controlled by changing the pitch angle reference signal to the hydraulic pitch change mechanism. The dynamics from the servo reference β_r to the pitch angle of blade at 3/4 radius $\beta_{3/4}$ (convention of Hamilton Standard) of the WTS-3 is modelled as a first order system with limits on the rate:

$$\dot{\beta}_{3/4} = \min(\dot{\beta}_{max}, \max(\dot{\beta}_{min}, (\beta_r - \beta_{3/4})/T_{bs})) \qquad (B.4.1)$$

where T_{bs} is the time constant of the pitch servo and $\dot{\beta}_{max}$ and $\dot{\beta}_{min}$ are the maximum and minimum rate limits.

B.5 Wind

It is possible to use measured wind data sequences when simulating the system behaviour in Simnon. It is also a simple task to write a subsystem that simulates discrete wind gusts of a given shape. The turbulence models suggested in the literature can be simulated by using random number generators provided by Simnon. As an example a subsystem simulating the longitudinal turbulence according to the model suggested by Holley et al (1981) is enclosed. See Section 3.2, model (3.7).

B.6 Bus

The generator is assumed to be connected to an infinite bus via an impedance $R_l + jX_l$ (Assumption B.1). This means that the bus voltage and bus frequency are not affected by the wind turbine system. By making the bus frequency and bus voltage time varying it is possible to model a large utility grid in both normal operation and during faults. Consider the following example.

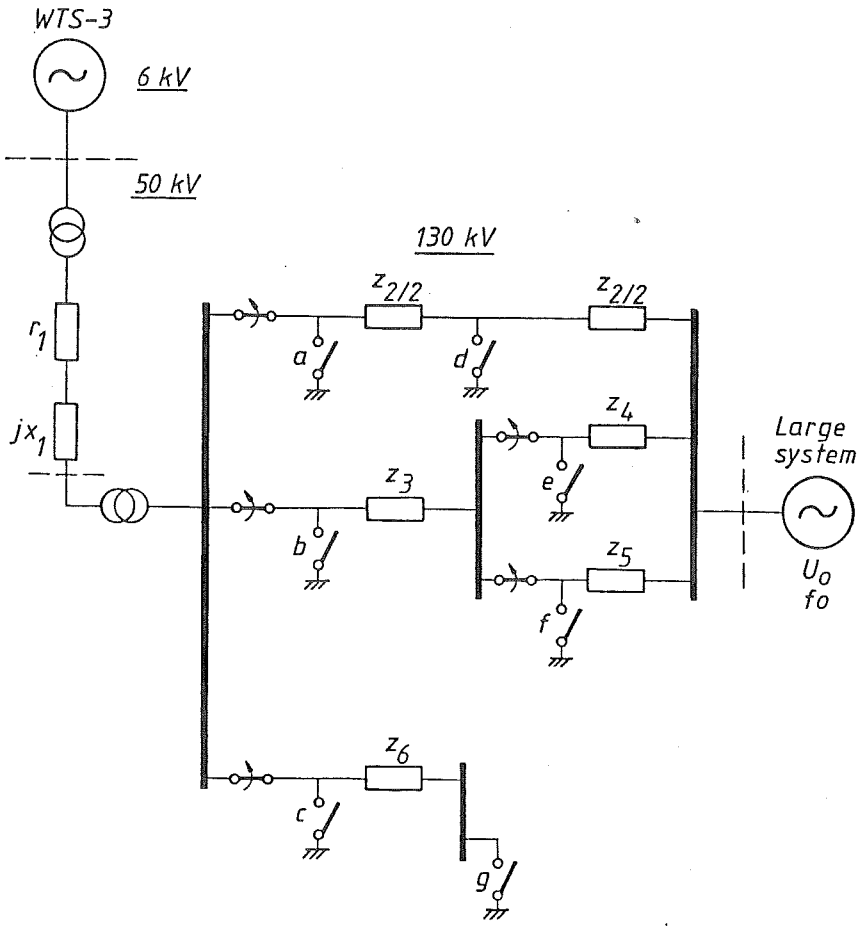

Figure B.3: Simplified bus model for transient stability simulations.

The integration of the WTS-3 prototype into the local electrical grid in southern Sweden is of great interest. A simple model was developed for the grid. See Figure B.3. A 3-phase fault in different locations (a-g) can be modelled by reducing the faults to step-changes in the bus voltage. Impedance variations are very small due to the transformers and can be neglected. The enclosed bus model simulates 3-phase faults by changing the bus voltage to a given level at a given point of time. After a given time the bus voltage is reset to normal level, simulating breaker action in the line where the fault was applied. The system also models stochastic variations in the bus frequency.

B.7 Excitation System and Voltage Controller

The excitation system of the generator of the WTS-3 use an AC alternator and a rotating rectifier to produce the direct current needed for the generator field. A Type 1 standard IEEE representation (IEEE Committee Report (1968)) including non-linear saturation effects is used to model the excitation system and voltage controller. See Figure B.4.

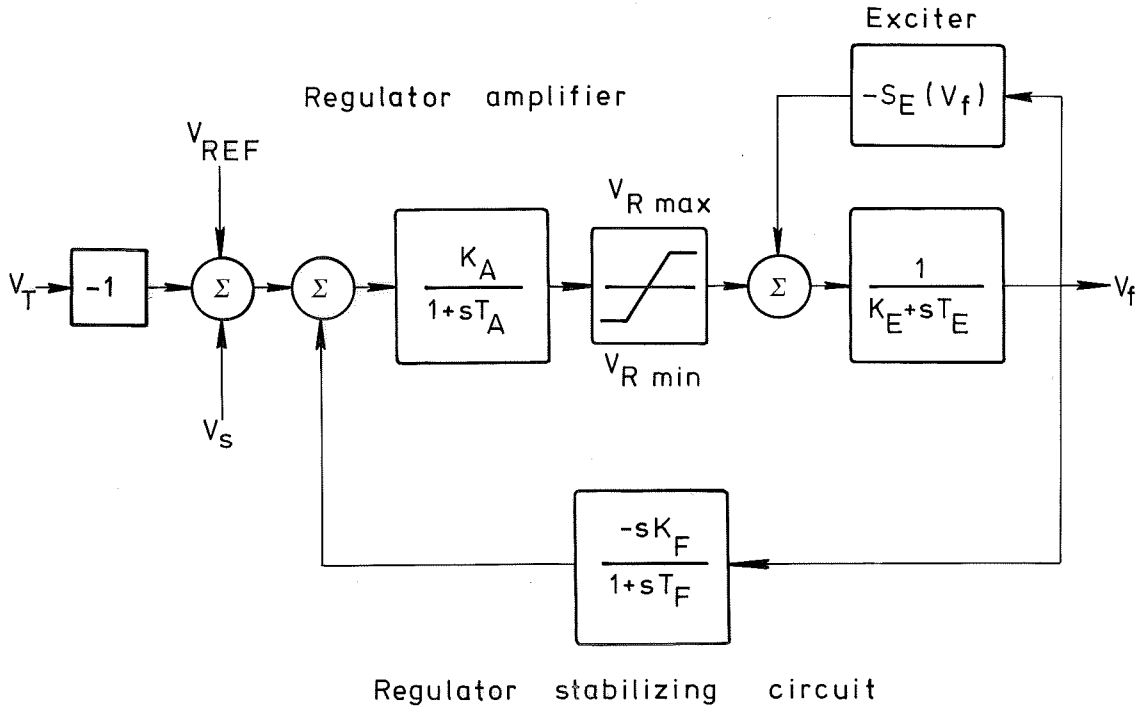

Figure B.4: IEEE Type 1 excitation system representation for a continuously acting regulator and exciter without input filter.

B.8 Pitch Angle Controller

The Simnon code for the pitch angle controller used in Section 5.3 for the simulations shown in Figures 5.17 - 5.19 is given as an example in Section B.9.

B.9 Simnon Code

The Simnon code for the models presented above is given below as follows:

```
CONTINUOUS SYSTEM TURBINE

"File: TURB6
"
"Version: 1984-02-17
"
"Author: Sven Erik Mattsson
"        Department of Automatic Control
"        Lund Institute of Technology, Sweden
"
"Description:
"  Models a horizontal axis, variable pitch downwind
"  turbine with two blades mounted on a teetered hub.
"  The teeter motion is modelled.
"  The blades, the nacelle and the tower are modelled as
"  rigid bodies. However, the first edgewise blade
"  motions can be modelled (see parameter leadlag)
"  as well as the first tower mode (see parameter tbend).
"  The nacelle is assumed to be aligned in the direction
"  of the wind. Consequently, yawing is not modelled.
"  It is assumed that over the rotor disc the speed
"  U(r, psi, t) of the oncoming, undisturbed wind (as
"  if there was no wind power plant) can be written as
"
"  U(r,psi,t) = U0 + Ux rcos(psi) + Uy rsin(psi)
"
"  The aerodynamical torques are calculated under the
"  assumption that the inflow ratio
"  lambda = U0/(R*psidot) is small (0.05 < lambda < 0.2).
"  Stalling is not modelled.
"
"References:
"  Hultgren L S (1979): Torsional Oscillations of the
"    Rotor Disc for Horizontal Axis Wind Turbines with
"    Hinged or Teetered Blades. Technical Note AU-1499
"    part 12, The Aeronautical Research Institute of
"    Sweden.

INPUT beta75 Tgear U0 Ux Uy

OUTPUT zT zTdot

STATE psidot  cospsi  sinpsi  fi  fidot  xzT  xzTdot
STATE delpsi1  delp1dot  delpsi2 delp2dot

DER  Dpsidot Dcospsi Dsinpsi Dfi Dfidot DxzT DxzTdot
DER  Ddelpsi1 Ddep1dot  Ddelpsi2 Ddep2dot

"Inputs:
"   beta75   pitch angle of blade at 3/4 radius [rad]
"   Tgear    torque to drive the gearbox [Nm]
"   U0       mean wind speed [m/s] over the rotor disc
"   Ux       measure of the wind speed variation [1/s]
"            over the rotor disc in vertical direction
"   Uy       measure of the wind speed variation [1/s]
```

```
"            over the rotor disc in horizontal direction
"
"Outputs:
"   zT       nacelle displacement [m] and
"   zTdot    nacelle velocity [m/s] in thrusting direction
"
"States:
"   psidot   angular velocity of hub [rad/s]
"   cospsi   cos(psi) and
"   sinpsi   sin(psi), where psi is the azimuth angle
"            (for psi = 0 blade #1 is pointing upwards)
"   fi       flapping angle [rad]
"   fidot    angular flapping velocity [rad/s]
"   xzT      nacelle displacement [m] and
"   xzTdot   nacelle velocity [m/s] in thrusting direction
"            if the tower bendings are modelled
"            (see parameter tbend)
"   delpsi1  lead/lag position [rad] of blade #1; angular
"            position of the blade is psi+delpsi1
"   delpsi2  ditto, but blade #2
"   delp1dot lead/lag velocity [rad/s] of blade #1; angular
"            velocity of the blade is psidot+delp1dot
"   delp2dot ditto, but blade #2

  c0 = (4/3)*beta2
beta1 = beta75 - c0
beta11 = beta1 "for blade #1
beta12 = beta1 "for blade #2
psi = atan2(sinpsi, cospsi)
psi1 = if leadlag then psi      + delpsi1 else psi
psi2 = if leadlag then psi - pi + delpsi2 else psi - pi
psi1dot = if leadlag then psidot + delp1dot else psidot
psi2dot = if leadlag then psidot + delp2dot else psidot
fi1 = fi0 + fi
fi2 = fi0 - fi
todeg = 180/pi
fi1deg = todeg*fi1
fi1dot = fidot
fi2dot = -fidot
zT    = if tbend then xzT    else 0
zTdot = if tbend then xzTdot else 0

" Calculate the aerodynamical torques and thrust

A1pB1 = A1+B1
A2pB2 = A2+B2
A3pB3 = A3+B3

Am1b2 = Am1*beta2
A0b2 = A0*beta2
A1b2 = A1*beta2
A2b2 = A2*beta2

A0b1  = A0*beta1  + Am1b2
A0b11 = A0*beta11 + Am1b2
```

```
A0b12 = A0*beta12 + Am1b2
A1b11 = A1*beta11 + A0b2
A1b12 = A1*beta12 + A0b2
A2b1  = A2*beta1  + A1b2
A2b11 = A2*beta11 + A1b2
A2b12 = A2*beta12 + A1b2
A3b11 = A3*beta11 + A2b2
A3b12 = A3*beta12 + A2b2

"      Calculate the interference factor a

  c01 = np*2*rair*pi*R*R
lambda0 = U0/(R*psidot)
  b13 = c01 + 0.5*A0b1
  b12 = A1 - c01*lambda0
  b11 = A2b1
  b10 = -B3
  v01 = -0.5*b12/b13
y0 = v01 + sqrt(v01*v01 - b11/b13)
  v02 = (3*b13*y0 + 2*b12)*y0 + b11
y1 = y0 - b10/v02
  v03 = ((b13*y1 + b12)*y1 + b11)*y1 + b10
  v04 = (3*b13*y1 + 2*b12)*y1 + b11
y2 = y1 - v03/v04
  v05 = ((b13*y2 + b12)*y2 + b11)*y2 + b10
  v06 = (3*b13*y2 + 2*b12)*y2 + b11
lambda = y2 - v05/v06
b = lambda/lambda0  " b = 1-a

"       Tower blockage

psi1mpi = if psi1<0 then psi1+pi else psi1-pi
psi2mpi = if psi2<0 then psi2+pi else psi2-pi
  c1 = pi/2/span
q1 = if abs(psi1mpi)<span then 1-amp*cos(c1*psi1mpi) else 1
q2 = if abs(psi2mpi)<span then 1-amp*cos(c1*psi2mpi) else 1
lq1 = q1*b*U0/(R*psi1dot)
lq2 = q2*b*U0/(R*psi2dot)

v1b1 = ((0.5*A0b11*lq1+A1)*lq1+A2b11)*lq1-B3
v1b2 = ((0.5*A0b12*lq2+A1)*lq2+A2b12)*lq2-B3
v2b1 =  (1.5*A1b11*lq1+2*A2)*lq1+A3b11
v2b2 =  (1.5*A1b12*lq2+2*A2)*lq2+A3b12
v3b1 =  (1.5*A0b11*lq1+2*A1)*lq1+A2b11
v3b2 =  (1.5*A0b12*lq2+2*A1)*lq2+A2b12
v4b1 = ((A0/6.0*lq1+0.5*A1b11)*lq1+A2pB2)*lq1+A3b11
v4b2 = ((A0/6.0*lq2+0.5*A1b12)*lq2+A2pB2)*lq2+A3b12
v5b1 =  (0.5*A1*lq1+A2b11)*lq1+A3pB3
v5b2 =  (0.5*A1*lq2+A2b12)*lq2+A3pB3
v6b1 =  (0.5*A0*lq1+A1b11)*lq1+A2pB2
v6b2 =  (0.5*A0*lq2+A1b12)*lq2+A2pB2
v7b1 = ((Am1/6.0*lq1+0.5*A0b11)*lq1+A1pB1)*lq1+A2b11
v7b2 = ((Am1/6.0*lq2+0.5*A0b12)*lq2+A1pB1)*lq2+A2b12
v8b1 = v6b1
v8b2 = v6b2
```

```
v9b1 =  (0.5*Am1*lq1+A0b11)*lq1+A1pB1
v9b2 =  (0.5*Am1*lq2+A0b12)*lq2+A1pB1

cosfi1 = cos(fi1)
cosfi2 = cos(fi2)
v20b1 = R*psi1dot*cosfi1
v20b2 = R*psi2dot*cosfi2
v21b1 = 0.5*R*cosfi1*v20b1
v21b2 = 0.5*R*cosfi2*v20b2
v22b1 = 0.5*R*v20b1
v22b2 = 0.5*R*v20b2
v23b1 = 0.5*cosfi1*v20b1
v23b2 = 0.5*cosfi2*v20b2

v31b1a = Ux*cos(psi1)+Uy*sin(psi1)
v31b2a = Ux*cos(psi2)+Uy*sin(psi2)
v31b1 = R*(fi1dot - q1*cosfi1*cosfi1*b*v31b1a)
v31b2 = R*(fi2dot - q2*cosfi2*cosfi2*b*v31b2a)
v32b1 = zTdot*cosfi1
v32b2 = zTdot*cosfi2

Tpsi1 = v21b1*(v20b1*v1b1-(v2b1*v31b1+v3b1*v32b1))
Tpsi2 = v21b2*(v20b2*v1b2-(v2b2*v31b2+v3b2*v32b2))
Tpsi = Tpsi1 + Tpsi2
Tpsip = 100.0*Tpsi/Tpsirat
Tfi1 =  v22b1*(v20b1*v4b1-(v5b1*v31b1+v6b1*v32b1))
Tfi2 =  v22b2*(v20b2*v4b2-(v5b2*v31b2+v6b2*v32b2))
Tfi = Tfi1 - Tfi2
FzT1 =  v23b1*(v20b1*v7b1-(v8b1*v31b1+v9b1*v32b1))
FzT2 =  v23b2*(v20b2*v7b2-(v8b2*v31b2+v9b2*v32b2))
FzT = FzT1 + FzT2

" The equations of motion

TBpsi1 = KBpsi*delpsi1 + DBpsi*delp1dot
TBpsi2 = KBpsi*delpsi2 + DBpsi*delp2dot
v41 = 1.0 - sinpsi*sinpsi - cospsi*cospsi
v42 = TBpsi1 + TBpsi2 - Tgear
v43b1 = g*SB*sin(psi1) + 2*JB*psi1dot*fi1dot*sinfi1
v43b2 = g*SB*sin(psi2) + 2*JB*psi2dot*fi2dot*sinfi2
v44 = v43b1*cosfi1 - TBpsi1 + Tpsi1
v45 = v43b2*cosfi2 - TBpsi2 + Tpsi2
Jtot = 2*JeB+JeH

Dcospsi = -psidot*sinpsi + v41*cospsi
Dsinpsi =  psidot*cospsi + v41*sinpsi
Dpsidot =  if leadlag then v42/JeH else (v42+v44+v45)/Jtot
Ddelpsi1 = if leadlag then delp1dot else 0
Ddelpsi2 = if leadlag then delp2dot else 0
Dpsi1dot = if leadlag then v44/JeB else Dpsidot
Dpsi2dot = if leadlag then v45/JeB else Dpsidot
Ddep1dot = Dpsi1dot - Dpsidot
Ddep2dot = Dpsi2dot - Dpsidot
sinfi1 = sin(fi1)
sinfi2 = sin(fi2)
```

```
FT = KT*zT + DT*zTdot
  v51 = SB*fidot*fidot*(sinfi1+sinfi2) - FT + FzT
  v52b1 = JB*psi1dot*psi1dot*cosfi1 - g*SB*cos(psi1)
  v52b2 = JB*psi2dot*psi2dot*cosfi2 - g*SB*cos(psi2)
  v52 = -v52b1*sinfi1 + v52b2*sinfi2 + Tfi
  c41 = 2*JB
  v53 = SB*(cosfi1-cosfi2)
  v54 = MT*c41 - v53*v53
Dfi = fidot
Dfidot =  if tbend then (MT*v52 - v53*v51)/v54  else v52/c41
DxzT =    if tbend then zTdot                   else 0
DxzTdot = if tbend then (c41*v51 - v53*v52)/v54 else 0

"Parameters:
pi:          3.14159265
g:           9.81    "gravitational acceleration [m/s^2]
rair:        1.3     "density of air [kg/m^3]
R:          39.08    "length of blade [m]
np:          0.70    "degree of power efficiency of the blades
Am1:      3126       "aerodynamic integral [kg/m]
A0:        759       "                     [kg/m]
A1:        362       "                     [kg/m]
A2:        211       "                     [kg/m]
A3:        142       "                     [kg/m]
B1:          0.417   "                     [kg/m]
B2:          0.236   "                     [kg/m]
B3:          0.158   "                     [kg/m]
beta2:      -0.0506  "twist angle of blade [rad]
fi0:         0.10472"steady coning angle [rad]
JB:          2.50E6  "moment of inertia of blade
                     "in fi-direction [kgm^2]
SB:          1.16E5  "static moment of blade [kgm]
amp:         0.3     "maximal velocity defect in the rotor
                     "disc due to the tower blockage
span:        0.1     "when abs(psii-pi)<span [rad] the wind
                     "at blade #i is modified by the factor
                     " 1-amp*cos(pi/2*(psii-pi)/span)
leadlag:     1.0     "if true the first edgewise blade
                     "mode is modelled
DBpsi:       1.48E6  "equiv. eff. damping of blade
                     "in psi-direction [Nms/rad]
KBpsi:       1.45E8  "equiv. eff. stiffness of blade
                     "in psi-direction [Nm/rad]
JeB:         9.25E5  "equiv. eff. moment of inertia of
                     "blade in psi-direction [kgm^2]
JeH:         3.2E6   "equiv. eff. moment of inertia of
                     "hub in psi-direction [kgm^2]
tbend:       1.0     "if true the first tower mode is modelled
MT:          2.14E5  "equiv. eff. mass of nacelle [kg]
KT:          9.38E5  "equiv. eff. stiffness of tower [N/m]
DT:          1.1E4   "structural damping coefficient of
                     "tower [Ns/m]
Tpsirat:     1.146E6"rated turbine torque [Nm]
END
```

```
CONTINUOUS SYSTEM GEN

"File: GEN12
"
"Version: 1984-02-23
"
"Author: Sven Erik Mattsson
"        Department of Automatic Control
"        Lund Institute of Technology, Sweden
"
"Description:
"  Models a synchronous generator connected to an infinte
"  bus through an external impedance. The model is a Park
"  model. Besides the field winding two fictitious
"  windings (one in the direct axis and the other in the
"  quadrature axis) are inserted to account for the
"  effects of currents in the iron parts of the rotor
"  or in damper windings. The stator dynamics can be
"  included in the model (see parameter statdyn).
"  Saturation is not modelled. Symmetrical load is assumed.
"
"References:
"  Olive D W (1968): Digital Simulation of Synchronous
"    Machine Transients. IEEE Trans. on Power Apparatus
"    and Systems, Vol. PAS-87, August 1968, 1669-1675.

INPUT Tm fbus vbus vf Rl Xl ON

OUTPUT wm Pe vd vq id iq

STATE delta  wmrel  eqp  edpp  eqpp  xidpu  xiqpu

DER  Ddelta Dwmrel Deqp Dedpp Deqpp Dxidpu Dxiqpu

"Inputs:
"   Tm       input torque [Nm]
"   fbus     bus frequency [rad]
"   vbus     bus voltage [V]
"   vf       generator field voltage [V]
"   Rl       line resistance [ohm]
"   Xl       line reactance [ohm]
"   ON       if true the generator is connected
"
"Outputs:
"   wm       mechanical angular velocity of rotor [rad/s]
"   Pe       generator power [W]
"   vd       d-axis component of armature voltage [V]
"   vq       q-axis component of armature voltage [V]
"   id       d-axis component of armature current [A]
"   iq       q-axis component of armature current [A]
"
"States:
"   delta    power angle [rad]
"   wmrel    relative mechanical angular velocity of rotor
"   eqp      voltage behind transient reactance [pu]
```

```
"   edpp      d-axis component of voltage behind
"             subtransient reactance [pu]
"   eqpp      q-axis component of voltage behind
"             subtransient reactance [pu]
"   xidpu     d-axis component of armature current [pu]
"             if the stator dynamics is modelled
"   xiqpu     q-axis component of armature current [pu]
"             if the stator dynamics is modelled

twopi = 2*pi
w0 = twopi*f0
pdiv2 = p/2
wm0 = w0/pdiv2
wm = wm0*wmrel
w = w0*wmrel
sind = sin(delta)
cosd = cos(delta)
Tbase = Sbase/w0
vbuspu = vbus/Vbase
Rlpu = Rl/Zbase
Xlpu = Xl/Zbase

Ddelta = w - twopi*fbus
  c52 = Xdpp-Xqpp
Tepu = eqpp*iqpu + edpp*idpu - c52*idpu*iqpu
Te   = Tbase*Tepu
  c54 = 100*w0/Penom
Tep = c54*Te
  c53 = wm0*Jgen
Dwmrel = (Tm - Dm*wm - pdiv2*Te)/c53
  c61 = (Xd-Xdpp)/(Xdp-Xdpp)
  c62 = (Xd-Xdp)/(Xdp-Xdpp)
Deqp = (vf/Vbase - c61*eqp + c62*eqpp)/Td0p
  c7 = Xq-Xqpp
Dedpp = (c7*iqpu - edpp)/Tq0pp
  c8 = Xdp-Xdpp
Deqpp = (eqp - eqpp - c8*idpu)/Td0pp
  c91 = Xdpp+Xlpu
  c92 = Xqpp+Xlpu
  c93 = Ra + Rlpu
  c94 = c93*c93 + c91*c92
  v41 = edpp + c92*iqpu
  v42 = c93*idpu + vbuspu*sind
  v43 = if abs(idpu)<eps then 0 else -Dioff*sign(idpu)
  v44 = edpp - vbuspu*sind
  v45 = eqpp - vbuspu*cosd
Dxidpu1 = if ON then (w*v41-w0*v42+Deqpp)/c91 else v43
Dxidpu = if statdyn then Dxidpu1 else 0
idpustat = if ON then (c93*v44 + c92*v45)/c94 else 0
idpu = if statdyn then xidpu else idpustat
  v51 = eqpp - c91*idpu
  v52 = c93*iqpu + vbuspu*cosd
  v53 = if abs(iqpu)<eps then 0 else -Dioff*sign(iqpu)
Dxiqpu1 = if ON then (w*v51-w0*v52-Dedpp)/c92 else v53
Dxiqpu = if statdyn then Dxiqpu1 else 0
```

```
iqpustat = if ON then (c93*v45 - c91*v44)/c94 else 0
iqpu = if statdyn then xiqpu else iqpustat

  v1 = edpp + Xqpp*iqpu
vdpu1 = if statdyn then (w*v1+Deqpp-Xdpp*Dxidpu)/w0 else v1
vdpu = vdpu1 - Ra*idpu
  v2 = eqpp - Xdpp*idpu
vqpu1 = if statdyn then (w*v2-Dedpp+Xqpp*Dxiqpu)/w0 else v2
vqpu = vqpu1 - Ra*iqpu
vpu = sqrt(vdpu*vdpu + vqpu*vqpu)
ipu = sqrt(idpu*idpu + idpu*idpu)
id = Ibase*idpu
iq = Ibase*iqpu
vd = Vbase*vdpu
vq = Vbase*vqpu
Ppu = vdpu*idpu + vqpu*iqpu
Qpu = vqpu*idpu - vdpu*iqpu
Spu = sqrt((vdpu*vdpu+vqpu*vqpu)*(idpu*idpu+iqpu*iqpu))
cosfi = if Spu>eps then Ppu/Spu else 1
sinfi = if Spu>eps then Qpu/Spu else 0
Pe = Sbase*Ppu
Q = Sbase*Qpu

"Parameters:
pi:          3.14159265
f0:         50.0     "synchronous frequency [1/s]
p:           4       "number of poles
Dm:          0       "constant friction torque [Nms/rad]
Jgen:      160.0     "moment of inertia of generator [kgm^2]
Penom:       3.0E6   "rated power [W]
Sbase:       3.33E6  "base power [VA]
Vbase:    6600       "base voltage [V]
Ibase:     292       "base current [A]
TdOp:        2.34    "d-axis transient open circuit
                     "time constant [s]
TdOpp:       0.163   "d-axis subtransient open circuit
                     "time constant [s]
TqOpp:       0.03    "q-axis subtransient open circuit
                     "time constant [s]
Zbase:      13.2     "base impedance [ohm]
Ra:          0.0     "armature resistance [pu]
Xd:          1.8     "d-axis synchronous reactance [pu]
Xdp:         0.274   "d-axis transient reactance [pu]
Xdpp:        0.202   "d-axis subtransient reactance [pu]
Xq:          0.78    "q-axis synchronous reactance [pu]
Xqpp:        0.30    "q-axis subtransient reactance [pu]
statdyn:     1.0     "if true the stator dynamics is modelled
Dioff:     500       "current decrease rate when disconnecting
                     "the generator [pu/s]
eps:         1.E-3   "test quantity for off-line

END
```

```
CONTINUOUS SYSTEM GEAR

"File: GEAR4
"
"Version: 1984-02-23
"
"Author: Sven Erik Mattsson
"        Department of Automatic Control
"        Lund Institute of Technology, Sweden
"
"Description:
"  Models the drive train and the gearbox as a
"  nonlinear spring and a hydraulic damper with
"  either a linear or quadratic characteristic.

INPUT psidot wm

OUTPUT Tgear Tm

STATE gamma

DER  Dgamma

"Inputs:
"   psidot   angular velocity of wind turbine [rad/s]
"   wm       mechanical angular velocity of generator
"            [rad/s]
"
"Outputs:
"   Tgear    driving torque from the turbine [Nm]
"   Tm       input torque to generator [Nm]
"
"States:
"   gamma    torsion angle [rad]

Dgamma = (psidot - wm/Ng)/(1-1/Ng)

Tgear = -Tgamma/(1-1/Ng)
Tm = -Tgamma/(Ng-1)
Tgamma = Tsp + Td

  c1 = -Kg0*gmin
  c2 = -Kg0*gmax
Tsp0 = -Kg0*gamma
Tsp1 = if gamma<gmin then c1-Kg1*(gamma-gmin) else Tsp0
Tsp = if gamma<gmax then Tsp1 else c2-Kg1*(gamma-gmax)

Td1 = -Dg1*Dgamma
Td2 = -Dg2*Dgamma*abs(Dgamma)
Tdul = if LIN then Td1 else Td2
Td = max(-Tdmax, ( min(Tdmax,Tdul) ) )
Pdamp = -Dgamma*Td
Tdp = 100*Td/Tdmax
```

```
"Parameters:
Ng:        60.0        "gear ratio between generator side
                       "and turbine side
Kg0:        7.7E6      "lower spring coefficient (ref. to
                       "the turbine side) [Nm/rad]
Kg1:        7.7E8      "higher spring coefficient (ref. to
                       "the turbine side) [Nm/rad]
LIN:        1.0        "if true the damper characteristic
                       "is linear else quadratic
Dg1:        3.0E6      "linear hydraulic damping torque
                       "coefficient [Nms/rad]
Dg2:        4.88E8     "quadratic hydraulic damping torque
                       "coefficient (ref. to the turbine
                       "side) [Nm(s/rad)^2]
Tdmax:      3.8E5      "maximum damper torque [Nm]
gmax:       0.35       "upper limit of torsion angle [rad]
gmin:      -0.05       "lower limit of torsion angle [rad]

END
```

164

```
CONTINUOUS SYSTEM SERVO

"File: SERV01
"
"Version: 1984-02-23
"
"Author: Sven Erik Mattsson
"        Department of Automatic Control
"        Lund Institute of Technology, Sweden
"
"Description:
"  Models the pitch servo as a first order system with
"  limits on the rate.

INPUT betaref

OUTPUT betadot

STATE beta75

DER  Dbeta75

"Inputs:
"   betaref  reference to pitch servo [rad]
"
"Outputs:
"   betadot  pitch servo speed [rad/s]
"
"States:
"   beta75   pitch angle of blade at 3/4 radius [rad]

  v1 = (betaref-beta75)/Tbs
Dbeta75 = min(hratelim ,max(lratelim ,v1) )
betadot = Dbeta75

"Parameters:
Tbs:       0.4     "time constant [s]
hratelim:  0.056   "maximum rate limit [rad/s]
lratelim: -0.070   "minimum rate limit [rad/s]

END
```

```
CONTINUOUS SYSTEM WIND

"File: HOLLEY1
"
"Version: 1984-02-16
"
"Author: Sven Erik Mattsson
"        Department of Automatic Control,
"        Lund Institute of Technology, Sweden
"
"Description:
"  Models the longitudinal wind velocity over the rotor
"  disc as
"
"  U(r,psi,t) = U0 + Ux rcos(psi) + Uy rsin(psi)
"
"References:
"  Holley W.E., Thresher R.W. and Lin S-R.:
"  Wind Turbulence Inputs for Horizontal Axis Wind
"  Turbines. NASA-CP-2185, DOE CONF-810226, A workshop
"  held at Cleveland State University, Cleveland, Ohio,
"  February 24-26, 1981, pp. 101-112.
"
"WARNING:
"  The value of the parameter Ts must be equal to the
"  sampling time of the random number generator.

INPUT U0mean Uxmean Uymean e0 ex ey

OUTPUT U0 Ux Uy

STATE xU0  xUx  xUy

DER  DxU0 DxUx DxUy

"Inputs:
"  U0mean  Mean value of U0 [m/s]
"  Uxmean  Mean value of Ux [1/s]
"  Uymean  Mean value of Uy [1/s]
"  ez      White noise N(0,1)
"  ex      White noise N(0,1)
"  ey      White noise N(0,1)
"          e0, ex and ey should be uncorrelated
"
"Outputs:
"  U0      Mean wind speed [m/s] over the rotor disc
"  Ux      [1/s] See formula above.
"  Uy      [1/s] See formula above.
"
"States:
"  xU0     Turbulence part of U0 (U0=U0mean+xU0) [m/s]
"  xUx     Turbulence part of Ux (Ux=Uxmean+xUx) [1/s]
"  xUy     Turbulence part of Uy (Uy=Uymean+xUy) [1/s]
```

```
U0 = U0mean + xU0
Ux = Uxmean + xUx
Uy = Uymean + xUy

DxU0 = b0*e0 - a0*xU0
DxUx = bx*ex - ax*xUx
DxUy = by*ey - ay*xUy

  v1 = U0mean/L
a0 = v1*a00
ax = v1*ax0
ay = v1*ay0
  v2 = sigma*sqrt(v1/Ts)
b0 = v2*b00
  v3 = v2/R
bx = v3*bx0
by = v3*by0

RL =R/L
lRL = log(RL)
a00 = if RL<0.1 then 1.0 else 10^(log(0.5)*(lRL+1))
  cb00 = -(0.24*lRL*lRL + 0.66*lRL + 0.28)
b00 = if RL<0.1 then 1.414 else 10^cb00
  cax01 = -(0.9*lRL + 0.3)
  cax02 = -(0.7*lRL + 0.1)
ax0 = if RL<0.1 then 10^cax01 else 10^cax02
  cbx01 = -(0.18*lRL + 0.15)
  cbx02 = -(0.25*lRL + 0.175)
bx0 = if RL<0.5 then 10^cbx01 else 10^cbx02
ay0 = ax0
by0 = bx0

"Parameters:
pi:       3.14159265
sigma:    1.8      "standard deviation [m/s]
Ts:       0.2      "sampling interval of noise [s]
R:       38        "rotor radius [m]
L:      400        "integral length scale of turbulence [m]
END
```

```
CONTINUOUS SYSTEM BUS

"File: BUS2
"
"Version: 1984-02-23
"
"Author: Sven Erik Mattsson
"        Department of Automatic Control
"        Lund Institute of Technology, Sweden
"
"Description:
"  Models a simplified network according to type B for
"  simulation SV/SK.
"  3-phase faults is simulated by changing the bus
"  voltage to a given level at a given point of time.
"  After a given time the bus voltage is reset to normal
"  level, simulating breaker action in the line where
"  the fault was applied. Impedance variations are very
"  small due to the transformers and are neglected.
"  The system also models stochastic variations in the
"  bus frequency.
"
"WARNING:
"  The value of the parameter Ts must be equal to the
"  sampling time of the noise generator.

TIME t

INPUT fnois

OUTPUT fbus vbus Rl Xl

STATE ff

DER  dff

"Input:
"  fnois      white noise N(0,1)
"
"Outputs:
"   fbus      bus frequency [Hz]
"   vbus      bus voltage [V]
"   Rl        total line resistance [ohm]
"   Xl        total line reactance [ohm]
"
"States:
"   ff        filter state for modelling frequency
"             deviation [Hz] from nominal value

  c1 = sigma*sqrt(2*Tc/Ts)
dff = if t<t3 then -ff/Tc else (c1*fnois - ff)/Tc
fbus = f0 + ff

vbus=if (t>t1 and  t<t2 ) then UB else U0bus
```

```
Rl = Rl1 + Rt
Xl = Xl1 + Xt

"Parameters:
f0:          50.0   "synchronous frequency [1/s]
Ts:          0.01   "sampling interval of noise [s]
sigma:       0.03   "standard deviation of bus frequency [Hz]
Tc:          5      "time constant of filter producing
                    "frequency noise from white noise [s]
t3:          0      "start time for frequency noise [s]
U0bus:     6600     "nominal bus voltage [V]
Rl1:         0.20   "line resistance [ohm]
Xl1:         1.05   "line reactance [ohm]
Rt:          0.05   "transformer resistance [ohm]
Xt:          0.99   "transformer reactance [ohm]
UB:          0.0    "bus voltage during fault [V]
t1:       2000.0    "fault start time [s]
t2:       2000.0    "fault stop time  [s]

END
```

```
CONTINUOUS SYSTEM VOLTCONT

"File: VOLTC1
"
"Version: 1984-02-23
"
"Author: Sven Erik Mattsson
"        Department of Automatic Control
"        Lund Institute of Technology, Sweden
"
"Description:
"  IEEE Type 1 excitation system representation including
"  nonlinear saturation effects for a continuously acting
"  regulator and exciter without input filter.
"
"Reference:
"  IEEE Committee Report (1968): Computer Representation
"  of Excitation Systems. IEEE Trans. on Power Apparatus
"  and Systems, Vol. PAS-87, June 1968, pp. 1460-1464.

INPUT vt vs

OUTPUT vf

STATE xA  xF  xE

DER  dxA dxF dxE

"Inputs:
"   vt     terminal voltage [V]
"   vs     auxiliary input signal [V]

"Outputs:
"   vf     generator field voltage [V]

"States:
"   xA     rectifier voltage  [pu]
"   xF     internal state in feedback loop [pu]
"   xE     generator field voltage [pu]

Verr = (Vref - vt + vs)/Vnorm
dxA1 = (KA*(Verr+yF) - xA)/TA
dxA2 = if (xA>VRmax and dxA1>0) then 0 else dxA1
dxA  = if (xA<VRmin and dxA2<0) then 0 else dxA2

SE = 0.17*xE*abs(xE)
dxE = (xA - SE - KE*xE)/TE
vf = Vnorm*xE

bF = KF/TF
dxF = (bF*xE - xF)/TF
yF = xF - bF*xE
```

```
"Parameters:
Vref:   6800.      "reference voltage [V]
Vnorm:  6600.      "base voltage [V]
KA:      400.      "regulator gain
TA:        0.02    "regulator amplifier time constant [s]
VRmax:     7.3     "maximum rectifier voltage [pu]
VRmin:    -7.3     "minimum rectifier voltage [pu]
KE:        1.0     "exciter constant
TE:        0.8     "exciter time constant [s]
KF:        0.03    "regulator stabilizing circuit gain [s]
TF:        1.0     "regulator stabilizing circuit time
                   "constant [s]
END
```

```
CONTINUOUS SYSTEM PITCHREG

"File: PITCHR2.T
"
"Version: 1984-03-27
"
"Author: Sven Erik Mattsson
"        Department of Automatic Control
"        Lund Institute of Technology, Sweden
"
"Description:
"  Pitch angle controller based on the state feedback LC
"  and the observer K7T with gain scheduling as described
"  in Section 5.3 of Mattsson, S.E.: Modelling and Control
"  of Large Horizontol Axis Wind Power Plants.

INPUT  PEm beta75 zTdot

OUTPUT betaref

STATE  beta750  edDgam  edgam  xekUdU0  x2P1  x2P2  edzT
DER    Dbeta750 DedDgam Dedgam DxekUdU0 Dx2P1 Dx2P2 DedzT

STATE  x4P1  x4P2  x6P1  x6P2  x8P1  x8P2
DER    Dx4P1 Dx4P2 Dx6P1 Dx6P2 Dx8P1 Dx8P2

TIME t

"Inputs:
"  PEm      measured electrical power [W]
"  beta75   measured pitch angle at 3/4 radius [rad]
"  zTdot    measured tower speed [m/s] in thrusting direction
"
"Outputs:
"  betaref  reference to pitch servo [rad]
"
"States:
"  beta750  estimated mean pitch angle [rad]
"  xekUdU0  observer state describing the wind and the
"           aerodynamical torque
"  edDgam   estimated gearbox torsion speed [rad/s]
"  edgam    estimated gearbox torsion angle deviation
"           from rated value [rad]
"  x2P1     state in the 2P-disturbance model
"  x2P2     state in the 2P-disturbance model
"  edzT     estimated nacelle displacement from mean
"           value [m]

" Estimation of mean pitch angle

dbeta75 = beta75 - beta750
Dbeta750 = dbeta75/Tb750
"
Tb750:    20.0  "time constant [s] when calculating beta750
```

```
" The observer

dPEm = PEm - PE0
edTE = Ds*edDgam + Ks*edgam
edPE = psidotn*edTE
w2p = 2*psidotn
ePe2PMW = x2P1
ePe2P = 1.0E6*ePe2PMW
edPEtot = edPE + ePE2P
diffPE   = dPEm - edPEtot
diffPEMW = diffPE/1.0E6 "MW
edDpsi = edDgam
ekUdU0 = CekUdU0*xekUdU0
edT = alfa*Tbeta0*dbeta75 + TU0*ekUdU0 + Tpsi0*edDpsi + Tz0*zTdot
DxekUdU0 = -xekUdU0/Tw + Kp1*diffPEMW
DedDgam = (edT - edTE)/Jt + Kp2*diffPEMW
Dedgam = edDgam + Kp3*diffPEMW
Dx2P1 = -w2P*(2*z2P*x2P1 + x2P2) + Kp4*diffPEMW
Dx2P2 = w2P*x2P1 + Kp5*diffPEMW
DedzT = -edzT/TizT + zTdot
"
psidotn:    2.6180     "synchronous turbine speed [rad/s]
PE0:        3.0e6      "rated power [W]
Tw:        20.0        "time constant in the wind model [s]
CekUdU0:  100.0        "ekUdU0 = CekUdU0*xekUdU0
Jt:         5.05E6     "turbine inertia [kgm^3]
Ks:         7.7E6      "gearbox spring coefficient [Nm/rad]
Ds:         3.0E6      "damping coefficient [Nm/(rad/s)]
Tbeta0:    10.6E6      "derivative of driving aerodynamical
                       "torque with respect to pitch angle
                       "[Nm/rad] at U0=18m/s and PE=3MW
TU0:        2.3E5      "ditto, but with respect to U0 [N/s]
Tz0:       -2.8E5      "ditto, but with respect to zTdot [N/s]
Tpsi0:     -7.6E5      "ditto, but with respect to turbine
                       "speed [Nm/(rad/s)]
z2P:        0.03       "relative damping in the 2P-notch filter
                       "Observer gains from electrical
Kp1:        0.389      "power (in MW) (K7) to edDgam
Kp2:        1.12       "                   to xeTUdU0
Kp3:        0.161      "                   to edgam
Kp4:        0.288      "                   to x2P1
Kp5:       -2.45       "                   to x2P2
TizT:      10.0        "time constant [s] when estimating edzT
                       "from zTdot
" betamax

c1max = (bmax2-bmax1)/(PE2-PE1)
c2max = (bmax3-bmax2)/(PE3-PE2)
b1max = bmax1+c1max*(PEm-PE1)
b2max = bmax2+c2max*(PEm-PE2)
betamax = if PEm<PE2 then b1max else b2max
"
bmax1:      0.0        "linear interpolation and extrapolation
bmax2:      0.012      "using the points (PE1, bmax1),
bmax3:     -0.045      "(PE2, bmax2) and (PE3, bmax3) [W, rad]
```

```
PE1:        1.0E6
PE2:        2.0E6
PE3:        3.0E6

" betaref

  v1 = L1*dbeta75 + L2*xekUdU0 + L3*edDgam + L4*edgam
  v2 = L5/CzTdot*zTdot + L6/CzT*edzT
betaref1 = beta750 - L1*dbeta75 - (v1 + v2)/alfa
betaref2 = min(betamax, betaref1)
" Feedback gains to betaref (LC)
L1:         0.414      "    from beta75
L2:         3.43       "    from ekUdU0/CekUdU0
L3:         1.18       "    from edDgam
L4:         0.779      "    from edgam
L5:         0.227      "    from zTdot/CzTdot
L6:         1.0        "    from edzT/CzT
CzTdot:    10.0
CzT:       10.0

" Notch filters for 4P, 6P and 8P variations

  w4P = 4*psidotn
  b4P = 2.0*(0.01-0.1)*w4P
  a4P = -2*0.1*w4P
Dx4P1 = a4P*x4P1 - w4P*x4P2 + b4P*betaref2
Dx4P2 = w4P*x4P1
betaref3 = x4P1 + betaref2
  w6P = 6*psidotn
  b6P = 2.0*(0.01-0.1)*w6P
  a6P = -2*0.1*w6P
Dx6P1 = a6P*x6P1 - w6P*x6P2 + b6P*betaref3
Dx6P2 = w6P*x6P1
betaref4 = x6P1 + betaref3
  w8P = 8*psidotn
  b8P = 2.0*(0.01-0.1)*w8P
  a8P = -2*0.1*w8P
Dx8P1 = a8P*x8P1 - w8P*x8P2 + b8P*betaref4
Dx8P2 = w4P*x8P1
betaref  = if notch then x8P1 + betaref4 else betaref2
"
notch:  1.0          "if true the notch filters are included

" Gain scheduling; alfa

  c0 = (4/3)*beta2
beta10 = beta750 - c0
  c01 = np*2*rair*pi*R*R
  c101 = R*psidotn
  c102 = c101*c101
  c103 = c101*c102
Am1b2 = Am1*beta2
A1b2 = A1*beta2
A0b10 = A0*beta10 + Am1b2
A2b10 = A2*beta10 + A1b2
```

```
  ba3 = 0.5*A0b10
  ba2 = A1
  ba1 = A2b10
  ba0 = -B3 - PE0/c103
ya1 = 0.15
  va1a = ((ba3*ya1 + ba2)*ya1 + ba1)*ya1 + ba0
  va1b = (3*ba3*ya1 + 2*ba2)*ya1 + ba1
ya2 = ya1 - va1a/va1b
  va2a = ((ba3*ya2 + ba2)*ya2 + ba1)*ya2 + ba0
  va2b = (3*ba3*ya2 + 2*ba2)*ya2 + ba1
ya3 = ya2 - va2a/va2b
  va3a = ((ba3*ya3 + ba2)*ya3 + ba1)*ya3 + ba0
  va3b = (3*ba3*ya3 + 2*ba2)*ya3 + ba1
la = ya3 - va3a/va3b
lasqr = la*la
lacub = la*lasqr
bd3 = c01 + 0.5*A0b10
bd2 = A1 - c01*la
vd1 = (3*bd3*la + 2*bd2)*la + A2b10
  s0 = (0.5*A0*lasqr + A2)*la
dldb1 = -s0/vd1
dTd1 = c102*R*((1.5*A0b10*la + 2*A1)*la + A2b10)
dTdb1 = dTd1*dldb1 + c102*R*s0
kb = dTdb1/Tbeta0
alfa = max(kb, kb0)
"
kb0:          1.0       "minimum kb that are compensated
pi:           3.14159
rair:         1.3       "density of air [kg/m^3]
Am1:       3126         "aerodynamic integral [kg/m]
A0:         759         "                     [kg/m]
A1:         362         "                     [kg/m]
A2:         211         "                     [kg/m]
A3:         142         "                     [kg/m]
B1:           0.417     "                     [kg/m]
B2:           0.236     "                     [kg/m]
B3:           0.158     "                     [kg/m]
beta2:       -0.0506    "twist angle of blade [rad]
R:           39.08      "length of blade [m]
np:           0.70      "degree of power efficiency of the blades

" Some Variables for Plotting

  c201 = c01*c102
U0m = PE0/(c201*lasqr) + c101*la
dldU0 = c01*lacub/U0m/vd1
dTdU0 = dTd1*dldU0
kU = dTdU0/TU0
edU0 = ekUdU0/kU
eU0 = edU0 + U0m
ePE = edPE + PE0
epsidot = edDpsi + psidotn
gamma0 = PE0/psidotn/Ks
egamma = edgam + gamma0
END
```

```
CONNECTING SYSTEM REGGEN

"File: REGGEN1
"
"Version: 1984-03-27
"
"Author: Sven Erik Mattsson
"        Department of Automatic Control,
"        Lund Institute of Technology, Sweden
"
"Description:
"  Connecting system for simulating on-line operation.

TIME t

betaref[servo] = if rotc then betaref[pitchreg] else bopen

U0[turbine] = U0[wind] + Ugust
Ux[turbine] = Ux[wind]
Uy[turbine] = Uy[wind]
Tgear[turbine] = Tgear[gear]
beta75[turbine] = beta75[servo]

psidot[gear] = psidot[turbine]
wm[gear] = wm[gen]

tm[gen] = tm[gear]
fbus[gen] = fbus[bus]
vbus[gen] = vbus[bus]
vf[gen] = if voltc then vf[voltcont] else vfopen
Rl[gen] = Rl[bus]
Xl[gen] = Xl[bus]
ON[gen] = 1.0

vt[voltcont] = sqrt(vd[gen]*vd[gen] + vq[gen]*vq[gen])
vs[voltcont] = 0.0

PEm[pitchreg] = Pe[gen]
beta75[pitchreg] = beta75[servo]
zTdot[pitchreg] = zTdot[turbine]

fnois[bus] = E4[noise1]
" noise1 is a standard system generating random numbers
U0mean[wind] = if (t>tpst and t<tpend) then vmnp else vmn
Uxmean[wind] = Ux0
Uymean[wind] = Uy0
e0[wind] = if t < tvel then 0 else E1[noise1]
ex[wind] = if t < tvel then 0 else E2[noise1]
ey[wind] = if t < tvel then 0 else E3[noise1]
  c1 = Ug2/(tg3-tg2)
Ug4v = if (t<tg3 and t>tg2) then c1*(tg3-t) else 0.0
  c2 = (Ug2-Ug1)/(tg2-tg1)
Ug3v = if (t<tg2 and t>tg1) then Ug1+c2*(t-tg1) else Ug4v
  c3 = Ug1/(tg1-tg0)
Ug2v = if (t<tg1 and t>tg0) then c3*(t-tg0) else Ug3v
```

```
Ugust = if t<tg0 then 0 else Ug2v

" Scaling of some variables

todeg = 180/pi
torpm = 60/(2*pi)
betadeg = todeg*beta75[servo]
psidotrp = torpm*psidot[turbine]
Psidotp = 100*Psidot[turbine]/psidotn
Tnomp = PErat/psidotn/100
Tgearp = tgear[gear]/Tnomp
Dbetadeg = todeg*betadot[servo]
wmrpm = torpm*wm[gen]
Pep = 100.0*Pe[gen]/PErat
gamdeg = todeg*gamma[gear]
deltadeg = todeg*delta[gen]
Vvel = U0[wind] + Ugust

"Parameters:
pi:          3.14159265
PErat:       3.0E6   "rated power [W]
psidotn:     2.618   "rated turbine speed [rad/s]
vmn:        18.0     "mean wind velocity [m/s]
vmnp:       18.0     "mean wind velocity [m/s] during
                     "wind pulse
tpst:      200.0     "start time for wind pulse [s]
tpend:     200.0     "stop time for wind pulse [s]
tg0:  2000.0         "when tg0<t<tg4 Ugust is given by
tg1:  10.0           " linear interpolation between the points
tg2:  12.0           " (tg0, 0), (tg1, Ug1), (tg2, Ug2) and
tg3:  20.0           " (tg3, 0) [s, m/s] otherwise Ugust = 0
Ug1:  -2.0
Ug2:   2.0

tvel:        0       "start time of turbulent wind
Ux0:         0.027   "measure of wind shear [1/s]
Uy0:         0.0     "measure of wind shear [1/s]
rotc:        1.0     "if true then the rotor controller is
                     "used else the loop is open and the
                     "pitch servo reference is bopen
bopen:       0       "see under rotc [rad]
voltc:       1.0     "if true then the voltage controller
                     "is used else the generator field
                     "voltage is vfopen
vfopen:  12000       "see under voltc [V]

END
```